

---

# MICROBIAL POLYHYDROXYALKANOATES: CONVERTING RENEWABLE RESOURCES INTO BIOPLASTICS

---

Iolanda Corrado

Dottorato in Biotecnologie – XXXIII ciclo

Università di Napoli Federico II





Dottorato in Biotecnologie – XXXIII ciclo

Università di Napoli Federico II



---

**MICROBIAL  
POLYHYDROXYALKANOATES:  
CONVERTING RENEWABLE  
RESOURCES INTO BIOPLASTICS**

---

Iolanda Corrado

Dottorando: Iolanda Corrado  
Relatore: Prof. Giovanni Sanna  
Correlatore: Dr. Cinzia Pezzella  
Coordinatore: Prof. Marco Moracci

Settore Scientifico Disciplinare BIO/11



# INDEX

<b><u>RIASSUNTO</u></b>	<b><u>I</u></b>
<b><u>SUMMARY</u></b>	<b><u>VII</u></b>
<b><u>INTRODUCTION</u></b>	<b><u>1</u></b>
<b>BIOPLASTIC: AN ECO-FRIENDLY ALTERNATIVE TO CONVENTIONAL PLASTIC</b>	<b>2</b>
<b>POLYHYDROXYALKANOATES</b>	<b>4</b>
<b>AIM OF THESIS</b>	<b>10</b>
<b><u>CHAPTER 1 PHA PRODUCTION FROM WASTE MATERIALS: INULIN-RICH FEEDSTOCKS AS CARBON SOURCE FOR PHA PRODUCTION</u></b>	<b><u>15</u></b>
<b>1.1 OPTIMIZATION OF INULIN HYDROLYSIS BY <i>PENICILLIUM LANOSOCOERULEUM</i> INULINASES AND EFFICIENT CONVERSION INTO POLYHYDROXYALKANOATES</b>	<b>19</b>
<b>1.2 THE POWER OF TWO: AN ARTIFICIAL MICROBIAL CONSORTIUM FOR THE CONVERSION OF INULIN INTO POLYHYDROXYALKANOATES</b>	<b>41</b>
<b><u>CHAPTER 2 POLYMER APPLICATION</u></b>	<b><u>73</u></b>
<b>2.1 DESIGN AND CHARACTERIZATION OF POLY (3-HYDROXYBUTYRATE-CO-HYDROXYHEXANOATE) NANOPARTICLES AND THEIR GRAFTING IN WHEY PROTEIN-BASED NANOCOMPOSITES</b>	<b>77</b>
<b>2.2 POLYHYDROXYALKANOATES-BASED NANOPARTICLES AS ESSENTIAL OIL DELIVERY CARRIERS</b>	<b>84</b>
<b><u>CONCLUDING REMARKS</u></b>	<b><u>95</u></b>
<b><u>APPENDIX</u></b>	<b><u>98</u></b>

# **RIASSUNTO**

I polidrossilcanoati (PHA) sono poliesteri termoplastici biodegradabili e biocompatibili, prodotti da diversi microrganismi come riserva energetica intracellulare. I principali tipi di PHA finora identificati sono poliesteri lineari testa-coda, composti da monomeri appartenenti al gruppo dei  $\beta/3$  (R-) idrossiacidi. Il gruppo laterale R in posizione  $\beta$  (3) è un alchile con un numero di atomi di carbonio che va da 1 a 15 e può essere lineare o ramificato, saturo o insaturo. In base al numero di atomi di carbonio dei monomeri costituenti il polimero, i PHA vengono classificati in tre gruppi: PHA a catena corta (short chain length-PHA, scl-PHA) da 3 a 5 atomi di carbonio; PHA a catena media (medium chain length-PHA, mcl-PHA) dai 6 ai 14 atomi di carbonio; PHA a catena lunga (long chain length-PHA, lcl-PHA) con oltre 14 unità di carbonio. La composizione monomerica del polimero dipende da diversi fattori, tra cui il microrganismo che lo produce e la fonte di carbonio utilizzata per la crescita microbica. In natura più di 150 (R-) idrossiacidi sono stati identificati come varianti di monomeri che possono costituire il polimero, questa eterogeneità si riflette in polimeri con proprietà chimico-fisiche e termo-meccaniche uniche. Nonostante la potenzialità di questi polimeri, gli esempi di produzione su scala industriale sono pochi e con limitate capacità produttive (che vanno da 1.000 a 10.000 tonnellate/anno) (Pakalapati *et al* 2018). Il principale ostacolo alla commercializzazione dei PHA è il costo associato al processo produttivo stimato pari a 8-11 USD per kg di cui il 50% circa è dovuto alla fonte di carbonio utilizzata per la fermentazione. In questo scenario l'utilizzo di fonti di carbonio a basso costo e rinnovabili, come le biomasse residue delle industrie alimentari, costituisce una valida e sostenibile alternativa che contribuisce alla riduzione dei costi senza dare luogo ad alcun tipo di competizione con le filiere alimentari. L'utilizzo di prodotti di scarto contribuisce alla realizzazione di un processo che acquisisce una sostenibilità non solo economica ma anche ambientale. Un approccio di questo tipo, che mira ad un utilizzo completo delle bio-risorse, è perfettamente in linea con il concetto alla base delle moderne bioraffinerie: industrie che integrano processi produttivi per la conversione di biomasse per la produzione di biocarburanti, energia, prodotti chimici e materiali. L'ottimizzazione del processo produttivo, oltre che alla scelta di fonti di carbonio a basso impatto ambientale, coinvolge la scelta di

microrganismi iper-produttori, molto spesso sistemi ingegnerizzati che permettono, oltretutto, di modulare la composizione monomerica del polimero prodotto. Negli ultimi anni alle colture pure si sono affiancate le cosiddette colture microbiche miste (MMC) che non richiedono sterilizzazione, hanno una grossa capacità adattativa dovuta alla diversità microbica e rendono possibile l'utilizzo di substrati rinnovabili.

Il presente lavoro di tesi ha come scopo principale quello di illustrare diverse strategie per la **produzione di PHA a partire da materie prime a basso costo** (Capitolo 1) e **l'applicazione di tali polimeri sotto forma di nanoparticelle per la modulazione delle proprietà meccaniche di film di natura proteica o come carrier di molecole bioattive** (Capitolo 2).

L'attività di ricerca si è focalizzata sull'utilizzo dell'inulina, il più abbondante carboidrato presente in natura dopo l'amido e prodotto come riserva di carbonio da diverse specie vegetali, tra cui il cardo (*Cynara cardunculus*). Quest'ultima è una pianta erbacea perenne appartenente alla famiglia delle *Asteraceae* che presenta una spiccata adattabilità all'ambiente mediterraneo. Il cardo è stato rivalutato dagli anni '90 come pianta per la produzione di grandi quantità di biomassa da destinare alla produzione di energia; impianti poliennali permettono di produrne fino a 25t/ha. Il 50% della biomassa recuperata è rappresentato dalle radici da cui è possibile estrarre l'inulina.

Quest'ultima è un polimero lineare composto da molecole di D-fruttofuranosio legate da legami  $\beta$ -2,1-glicosidici con un residuo di glucosio legato all'estremità riducente del polimero attraverso un legame  $1\alpha$ -2 $\beta$ -glicosidico, caratteristico del saccarosio.

La possibilità da parte di microrganismi di utilizzare l'inulina come fonte di carbonio dipende dall'azione delle inulinasi, enzimi appartenenti alla famiglia delle glicosil idrolasi (famiglia GH32) che catalizzano l'idrolisi dei fruttani. In base alla differente attività idrolitica si distinguono le eso-inulinasi che agiscono rimuovendo monomeri di fruttosio dall'estremità non riducente del polisaccaride ed endo-inulinasi che agiscono sul legame  $\beta$ -2-1 glicosidico della molecola rilasciando frutto-oligosaccaridi (FOS). In natura esistono pochi microrganismi che hanno la duplice capacità di idrolizzare l'inulina e convertire gli zuccheri rilasciati in prodotti dall'alto valore aggiunto.

Alcuni esempi sono riportati per la produzione di acido lattico, etanolo e acido poli- $\gamma$ -glutammico. Esempi di microrganismi capaci di idrolizzare l'inulina e di produrre PHA non sono riportati; di fatto, tutti i bioprocessi sviluppati sinora prevedono una fase di saccarificazione e la successiva fermentazione degli zuccheri da parte di microrganismi produttori di PHA (Haas et al, 2015).

Nel presente lavoro di tesi sono presentate due strategie per la conversione dell'inulina in biopolimeri da parte di *Cupriavidus necator*, noto produttore di Poli 3-idrossibutirrato (P3HB) ma che manca della capacità di produrre enzimi capaci di idrolizzare l'inulina. A tale scopo ci si è focalizzati sia sulla ricerca di microrganismi in grado di produrre esoinulinasi sia sulla messa a punto del processo fermentativo (Capitolo 1).

Lo screening per la selezione di microrganismi produttori di inulinasi è stato fatto su una collezione di venti fughi. Dallo screening *Penicillium lanosocoeruleum* è stato selezionato ed è stato oggetto di studio. Le condizioni di produzione della miscela enzimatica (*Plal*) sono state ottimizzate valutando diversi aspetti, tra cui la fonte di carbonio usata per la crescita, l'apporto di ossigeno e il tempo di crescita. Nelle condizioni ottimizzate sono state prodotte 28 U mL<sup>-1</sup> al quarto giorno di crescita. Una volta prodotta, *Plal* è stata caratterizzata sia in termini di attività in funzione del pH e della temperatura sia da un punto di vista di composizione isoenzimatica attraverso un approccio proteomico. La miscela ha mostrato un massimo di attività a 50°C, mantenendo comunque più del 70% di attività tra i 30 e i 60 °C. Per quanto riguarda il pH, l'attività massima è stata riscontrata a pH 5 mentre più del 50% di attività è mantenuta in un intervallo di pH tra 4.5 e 7. Questi valori sono perfettamente in linea con quanto riportato per la maggior parte delle inulinasi purificate da funghi. Un altro aspetto investigato è stato la termostabilità della miscela enzimatica. La miscela ha mostrato un'ottima stabilità a 40°C conservando la sua attività fino a tre giorni di incubazione.

La messa a punto e l'ottimizzazione delle condizioni di idrolisi dell'inulina da parte di *Plal* è stata condotta con un approccio statistico mediante Central Composite Rotatable Design (CCRD). Il disegno sperimentale ha permesso investigare le interazioni dei fattori coinvolti nell'idrolisi (pH, temperatura, concentrazione di inulina e unità

enzimatiche per g di substrato) e definire un modello matematico che descrive il processo. Nelle condizioni ottimizzate ( $T=45.5\text{ }^{\circ}\text{C}$ ;  $\text{pH}=5.1$ ; concentrazione di inulina =  $60\text{ g L}^{-1}$ ; quantità di enzima per g di substrato =  $50\text{ U g}_{\text{substrato}}^{-1}$ ) è stato raggiunto il 97% di conversione del substrato in 20 h. L'idrolizzato ottenuto, caratterizzato da alte concentrazioni di fruttosio è stato utilizzato per complementare il terreno di crescita di *C. necator* DSM 428 (SHF). Con questo approccio è stato possibile ottenere un accumulo di P3HB pari al 70% ( $\text{g}_{\text{polimero}}/\text{g}_{\text{peso secco cellulare}}$ ), corrispondente a  $2\text{ g L}^{-1}$  dopo 120 h di fermentazione. Oltre all'SHF è stato messo a punto anche un processo di simultanea saccarificazione e fermentazione (SSF). In tale approccio la miscela enzimatica è stata aggiunta direttamente al brodo di coltura e in questo caso è stato raggiunto l'80% ( $\text{g}_{\text{polimero}}/\text{g}_{\text{peso secco cellulare}}$ ) di accumulo di P3HB, corrispondente a  $3.2\text{ g L}^{-1}$  di polimero, dopo 120 h. L'SSF rappresenta il primo esempio di bioprocesso di simultanea saccarificazione e fermentazione per la conversione di inulina in PHA.

Accanto alla possibilità di utilizzare una miscela enzimatica, un'altra strategia investigata è stata quella di compensare l'incapacità idrolitica di *C. necator* allestendo delle co-colture con un microrganismo in grado di produrre inulinasi. A tale scopo una collezione di microrganismi isolati dalla rizosfera del parco naturale de Ses Salines d'Eivissa (§1.2) è stata sottoposta allo screening e *Bacillus gibsonii* (RHF15) è stato selezionato. La messa a punto delle condizioni di co-coltura dei batteri in termini di accumulo di biomassa e produzione del polimero è stata fatta mediante un disegno sperimentale (CCRD) investigando l'effetto di quattro variabili: la concentrazione di inoculo di ciascuno dei due microrganismi, la concentrazione della fonte di carbonio (inulina) e la concentrazione di azoto. Il disegno sperimentale ha permesso di determinare i valori delle suddette variabili che permettono di ottenere  $1.9\text{ g L}^{-1}$  di PHB dopo 96 h di fermentazione, corrispondente al 78.8% di accumulo e una produttività di  $0.02\text{ g L}^{-1}\text{ h}^{-1}$ .

Accanto alle strategie per la valorizzazione di biomasse a basso costo per la produzione dei PHA, oggetto di studio è stata la loro applicabilità nell'ambito delle nanotecnologie. Nel capitolo 2 sono

presentate due diverse applicazioni di nanoparticelle di PHA: 1) modulazione delle proprietà meccaniche di film di natura proteica, 2) veicolazione di molecole bioattive.

La preparazione di materiali nanocompositi, ovvero materiali composti da particelle con dimensioni dell'ordine dei nanometri conferisce ai materiali nuove proprietà chimiche, fisiche, meccaniche e funzionali. Nel presente lavoro di tesi questa strategia è stata applicata a film di natura proteica inglobando nanoparticelle di poli (3 idrobutirrato-co-3 idrossiesanoato) (P(3HB-co-3HHx) (NPs-PHA) (§2.1). La metodologia scelta per la preparazione delle NPs è stata quella dell'evaporazione del solvente. Nelle condizioni ottimizzate sono state prodotte NPs-PHA con un diametro medio di 80 nm e un valore di potenziale-Z di -40 mV, indice di nanoparticelle stabili. L'aggiunta delle suddette NPs a film prodotti a partire da proteine del siero di latte (Whey protein-WP) ha permesso di ottenere film con proprietà meccaniche e di barriera migliorate: i film sono risultati essere più elastici e con ridotta permeabilità all'O<sub>2</sub>, caratteristiche che li rendono applicabili per l'imballaggio alimentare specialmente per quei prodotti facilmente ossidabili.

Accanto alla possibilità di utilizzare le NPs come additivi nella preparazione di film, è stata valutata la possibilità di un loro utilizzo come vettori di molecole bioattive. Nel caso di studio (§2.2), è stato messo a punto il protocollo di incapsulamento di oli essenziali estratti da piante di origano in nanoparticelle di PHA. Il protocollo di incapsulamento è stato ottimizzato su due classi di polimeri: scl-PHA (P3HB) e copolimero poli 3-idrossibutirrato- 3-idrossiesanoato (P(3HB-co-3HHx)). I sistemi sviluppati sono risultati essere vantaggiosi nel rilascio delle molecole bioattive, nel prevenire la loro volatilità con un miglioramento dell'attività antimicrobica.

## **SUMMARY**

This thesis is focused on microbial Polyhydroxyalkanoates (PHA): polyesters produced by a wide range of microorganisms as intracellular carbon and energy reserve. In this PhD thesis the valorisation of inulin-rich biomasses for PHA production was investigated. The use of inulin as carbon source for polymer production requires the integration of inulinases production, its hydrolysis and microbial fermentation step. *Penicillium lanosocoeruleum* was identified as inulinase producer. Hydrolytic enzymes production by the selected fungus, was optimized reaching up to 28 U mL<sup>-1</sup> after 4<sup>th</sup> day of growth. The enzymatic mixture *Plal* was characterized in terms of isoenzymatic composition, stability, and activity profile. Optimization of inulin hydrolysis by *Plal* was performed through a statistical approach using a Central Composite Rotatable Design (CCRD). In the optimized condition (T=45.5 °C, pH=5.1, substrate concentration=60 g L<sup>-1</sup>, enzyme loading=50 U g<sub>substrate</sub><sup>-1</sup>) up to 97% of inulin conversion in fructose was achieved in 20 h. The integration of *Plal* in a process for the conversion of inulin into PHA by *Cupriavidus necator* pursued two process strategies: Separated Hydrolysis and Fermentation (SHF) and Simultaneous Saccharification and Fermentation (SSF). A maximum of 2.2 and 3.2 g L<sup>-1</sup> of PHB accumulation, corresponding to 60% and 82% polymer content, was achieved in the SHF and SSF processes, respectively. Another strategy for PHA production from inulin involved the use of a microbial “substrate facilitator” consortium (SFC). *Bacillus gibsonii* (RHF15) was selected as inulinases producer (15U/mL after 15 h of growth). RHF15 was co-cultured with *C. necator* DSM 428. Optimization of co-culture growth was carried out through response surface methodology and led to a production of 1.9 g L<sup>-1</sup> of PHB after 96 h of growth. Another part of this work was focused on the production of PHA-based nanoparticles (NPs-PHA) to be used as additive for protein-based films. Addition of PHBHHx-NPs to WP-based FFSs resulted in a plasticizing effect on the biobased material, producing a resistant and more extensible biofilm, characterized by an enhanced barrier property towards O<sub>2</sub>. A second approach for NPs-PHA application involved the encapsulation of oregano essential oils into NPs. The encapsulation protocol was optimized on two classes of polymers: PHB and P(PHBHHx). Both formulations of NPs, showed better or comparable properties to inactivate the tested microorganism

respect to free EOs, preventing their volatility, stability issues and poor water solubility, increasing their bioavailability and thus their antimicrobial activity.

# **Introduction**

**Bioplastic: an eco-friendly alternative to conventional plastic**

The term plastic is used to address a class of synthetic materials made from a wide range of organic polymers that have the capability of being moulded and shaped while soft, and then set into a rigid or slightly elastic form. These materials are characterized by different chemical and physical properties, making them versatile and suitable for a wide range of applications. One main consequence of the massive development and spread of plastic, a material that, when discovered, was supposed to simplify human's life, is pollution, the most visible example of human damage to the planet.

The boom of plastic industries blew up in the 1950s, with an exponential growth, which is still going on (Hannah Ritchie and Max Roser, 2018). The worldwide annual production of plastics exceeds 300 million tons, with about 3% end up every year in rivers, seas and oceans. Only 9% of all plastic waste ever produced is recycled. About 12% is incinerated, while the remaining 79% is accumulated in landfills, dumps, or the natural environment. Warring data, about recycling, refer to the more advanced areas of the world, with recycling figures too low to be sustainable (The United Nations Environment Programme (UNEP) Homepage. <https://www.unenvironment.org/interactive/beat-plastic-pollution>).

In EU 62 million tons of plastic are produced each year, however less than 30% of this plastic is recycled, and approximately 70% goes in landfills or incinerators (European Commission, 2018). The Great Pacific Garbage Patch is a physical representation of plastic pollution at global scale (Sohn et al., 2020). It is one of the five patches formed due to oceanic currents, covers an area of around 1.6 million km<sup>2</sup> and is expanding rapidly (Statistical Review of World Energy, 2018). The patches have plastic soup consistency and are mainly composed of plastic particles (Choi et al., 2020). Particles bigger than 5 mm account for 87% of the weight of this plastic waste (Eriksen et al., 2014). By contrast microplastics (particles with less than 5 mm in diameter) account for about 13.2% of plastic waste by mass and concerns regarding health-related problems are increasing due to their entry into the food chain (Eriksen et al., 2014). As a fact, food from marine sources, such as fish, bivalves, and crustaceans, has been reported to contain ingested microplastics.

The durability and degradation resistance that make plastics so useful, make them nearly impossible for nature to completely break down. Moreover, the environmental problems linked to plastic are not only associated to its end-life but involve each stage of the plastic lifecycle, hence their complexity and variety. In this scenario the need to either reduce plastic use or replace nondegradable plastic with sustainably produced and biodegradable plastics is imperative.

Bioplastics are plastic material that are biobased or can be biodegradable or both (Bioplastics, n.d.) and they can be considered as an alternative to conventional plastics.

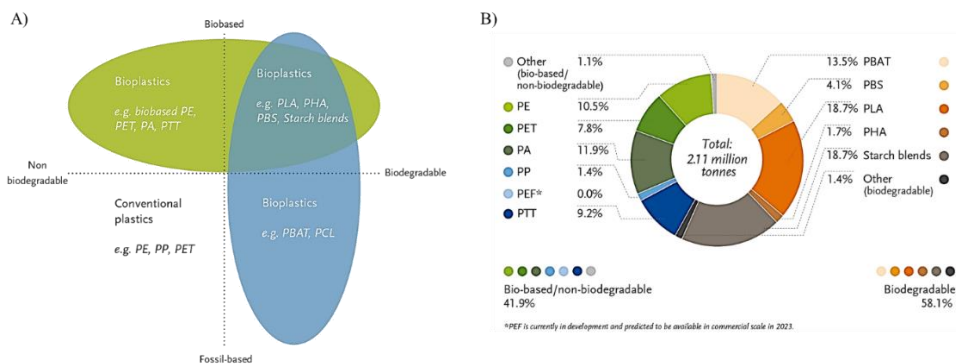


**Figure 1.** Bioplastics classification and global production capacities (2019). (Source: European Bioplastics)

Bioplastics represent about one percent of the about 368 million tonnes of plastic produced annually. Its capacity is set to increase from 2.11 million tonnes in 2020 to 2.87 million tonnes in 2025. This effect is due to the emergence of increasingly sophisticated biopolymers that expand their application fields.

Among bio-based/non-biodegradable plastics there are PE (polyethylene) and bio-based PET (polyethylene terephthalate), as well as bio-based PA (polyamides). These all together represents 41.9% of world global production capacities. In addition, a new polymer that is expected to enter in the market in 2023 is PEF (polyethylene furanoate), that is comparable to PET, with superior barrier and thermal properties, making it an ideal material for packaging of drinks, food and non-food products.

On the other hand, among bio-based and biodegradable plastics there are PLA (polylactic acid), PHA (Polyhydroxyalkanoates), cellulose or starch-based materials that all together account for over 43% of the global bioplastics production capacities.

Bio-based plastics contribute to increased efficiency resource use through a closed resource cycle; they can be designed to be either totally biodegradable to CO<sub>2</sub> and water in few months or years (Rutkowska et al., 2002), or contribute to carbon capture and storage through integration into nondegradable long-term infrastructure, including plastic-based municipal water and sewer piping, building and roofing materials, and road surfaces. The highest relative growth rates of bio-plastic production are associated to bio-based PP (polypropylene) and PHAs (polyhydroxyalkanoates).

### **Polyhydroxyalkanoates**

Polyhydroxyalkanoates (PHA) are key biopolymers that have the potential to replace the conventional petrochemical based plastics (Sabapathy et al., 2020; Sohn et al., 2020). They are a class of polyesters of R-hydroxyalkanoic acids that are both biodegradable and bio-based produced as carbon and energy storage in granular form by both Gram-positive and Gram-negative bacteria. Many of these microorganisms require, to produce PHA, nutrient limitation such as nitrogen, oxygen or magnesium while they do not accumulate PHAs during the growth phase (Nikodinovic-Runic et al., 2013). *Ralstonia eutropha* and *Pseudomonas putida* belong to this group. Other microorganisms, such as recombinant *Escherichia coli*, do not require any nutrient limitation for accumulating PHAs during the growth phase (Muhammadi et al., 2015). According to the number of carbon units in their monomers, PHAs can be divided into three groups. Short-chain-length PHAs (scl-PHAs), composed of monomers ranging from 4 to 5 carbon atoms, like 3-hydroxybutyrate (3HB) and 3-hydroxyvalerate (3HV); medium-chain-length PHAs (mcl-PHAs) which contain monomeric units with 6 to 14 carbon atoms. PHAs containing more than 14 carbon atoms in their monomers are classified as long chain PHAs (lcl-PHAs) (Raza et al., 2019). In addition, depending on the variety of monomers, PHAs can be classified into homo- and co-polymers. An example of hybrid polymers comprising both short-chain and medium-chain monomers is poly(3-hydroxybutyrate-co-3-

hydroxyhexanoate) (Castilho et al., 2009). Since the first identification of PHA accumulation in *Bacillus megaterium* by Lemoigne in 1926, over 90 PHA producing species and about 150 (R)-hydroxyalkanoic acids, as monomer constituents of natural PHAs, have been discovered (Ojumu et al., 2004).

PHA intracellular granules are coated with a monolayer of phospholipids and proteins, typically 0.2  $\mu\text{m}$  in diameter, and are visible using a phase contrast light microscopy or using specific dyes, like Nile Blue A (Khanna et al., 2005). Moreover, Licciardello et al. reported new bacterial strains, *Pseudomonas corrugata* and *Pseudomonas mediterranea* able to produce PHAs extracellularly (Licciardello et al., 2019).

Insolubility in water, good resistance to hydrolytic attack, but poor resistance to acids and bases, resistance to UV, sinking in water, that eases anaerobic biodegradation in sediments, and solubility in chloroform and other chlorate solvents are common properties to all PHAs polymers. Moreover, they are non-toxic and biocompatible, and hence suitable for medical applications (Bugnicourt et al., 2014). Structural variation in monomeric composition widely affects hydrophobicity, melting point (from 40 to 180°C), glass transition temperature (from -50 to 4°C) and degree of crystallinity. The Young's module can vary from 0.008 MPa per mcl-PHA to a peak of  $3.5 \times 10^3$  MPa per scl-PHA, elongation at break varies from a 2% to a 1,000%, while tensile strength can assume values between 8.8 and 104 MPa (Rai et al., 2011).

### *PHA biosynthesis*

Microbial PHA are produced as a form of reserve carbon or as a stress resistance mechanism (Sudesh et al., 2000). Three main pathways regulate their biosynthesis *in vivo* (Choi et al., 2020). The biosynthetic routes to PHA monomers, which are strictly interconnected with the central metabolic pathways, compete with and/or rely on tricarboxylic acid (TCA) cycle and fatty acid biosynthesis and degradation (Figure 2).

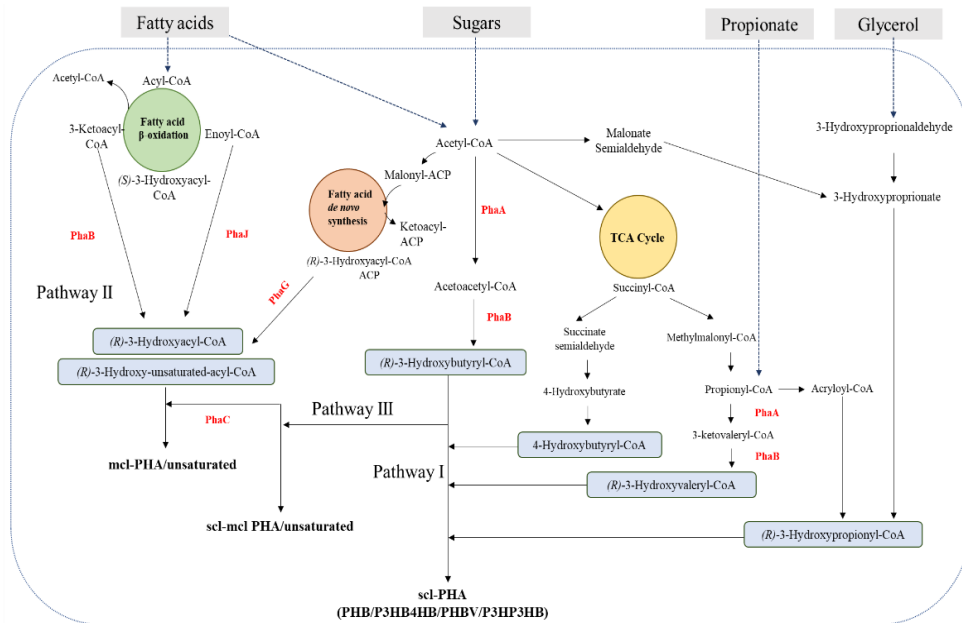


**Figure 2.** Biochemical pathways for PHAs production from different carbon sources. Abbreviation: **mcl**, medium-chain-length; **scl**, short chain length; **PhaB**, Acetoacetyl-CoA reductase; **PhaJ**, Enoyl-CoA hydratase; **PhaG**, 3-hydroxyacyl-acyl carrier protein-coenzyme A transferase; **PhaA**, Acetyl-CoA acetyltransferase ( $\beta$ -ketothiolase); **PhaC**, PHA synthase; **PHB**, polyhydroxybutyrate; **P3HB4HB**, Poly(3-hydroxybutyrate-co-4-hydroxybutyrate); **PHBV**, poly(3-hydroxybutyrate-co-hydroxyvalerate); **P3HP3HB**, poly(3-hydroxypropionate-co-3-hydroxybutyrate)

When sugars are supplied as carbon source, pathways I and III are activated, and scl-PHAs and mcl-PHAs are produced, respectively. These carbon sources are defined **unrelated** since their structure is different from that of PHA monomers. If carbon sources, such as fatty acids, are supplied, pathway II is activated, and mcl-PHAs are produced (**related** carbon source). Both pathway II and III can also lead to the production of PHA copolymers (Verlinden et al., 2007).

A key enzyme responsible for chain polymerization is PHA synthase (PhaC). Based on substrate specificity and subunit composition, there are four classes of PhaCs (Rehm, 2003). Classes I and II synthase consist of only one subunit with a molecular mass of 60-73 kDa. They are represented by *Ralstonia Eutropha* (*Cupriavidus necator*) and

*Pseudomonas oleovorans* enzymes, respectively. Class I polymerizes scl-PHA monomers, whereas class II mcl-PHA monomers. Class III and IV of PHA synthases, are represented by the *Allochromatium vinosum* and *Bacillus megaterium* enzymes, respectively. They are composed of two heterosubunits. The catalytic subunit PhaC has a molecular mass of 40 kDa and requires a secondary subunit for being active (PhaE 40 kDa for Class I and PhaR 20 kDa for Class IV) (Tsuge, 2016). Both classes of enzymes synthesise PHAs using scl-RHA-CoAs as substrate. In some exceptions, some class I PhaC can produce scl-mcl-PHA with low medium-chain-length monomers incorporation, albeit inefficiently (Sudesh et al., 2000).

PHA monomeric composition and mechanical properties are, therefore, strictly depending by the supplied carbon source, the activated pathway, the properties of the enzymes involved, as well as by growth and operating conditions (Favaro et al., 2019). The complex metabolic network that drives PHA biosynthesis *in vivo* makes every microorganism unique in its producing abilities. This scenario leave room to metabolic engineering to channel precursors into preferred routes in order to control PHA composition (G. Q. Chen and Jiang 2017; Y. Lee *et al.*, 2019). At the same time, since the incorporation of specific precursors is linked to substrate specificity of the PHA synthetic enzymes, protein engineering can be applied to PHA biosynthetic enzymes, especially PHA synthases (PhaCs), to modulate the abundance of a specific monomer into the synthesized polymers(Lee et al., 2019; Turco et al., 2021).

#### *In vivo PHA production*

PHA is currently produced by pure culture systems (wild-type or engineered microorganisms) that can be divided into two main groups:

1. Non-growth associated: bacteria that require nutrient limitation to accumulate PHA such as *C. necator* and *Pseudomonas* species. Biomass growth and PHA accumulation are typically performed in two separate stages: the first stage is associated with biomass growth due to the availability of nutrients. In the second stage, due to the limitation or depletion of one nutrient PHA production prevails.
2. Growth associated: bacteria that do not require nutrient limitation and PHA accumulation and growth occur simultaneously; among

them *Alcaligenes latus* and recombinant *Escherichia coli*. Since cell growth and PHA synthesis occur at the same time, a correct feeding strategy is essential for obtaining high PHA production yields.

In addition to the pure cultures systems an emerging and promising strategy involves the use of Mixed microbial cultures (MMCs) reducing the high costs related to aeration, media and equipment sterilization (Fradinho et al., 2019; Mannina et al., 2020). Three main processes are used to produce PHA from MMC system (Kaur et al., 2017):

1. Anaerobic-aerobic (AN/AE), a three steps process: i) culture enrichment through Activated Sludge Treatment Plant (ASTP); ii) acidogenesis into substrate containing Volatile Fatty Acids (VFAs); iii) using of VFAs for PHA production.
2. Aerobic Dynamic Feeding (ADF) system (feast and famine): long periods of substrate shortage (famine period) are alternated with short periods of substrate excess (feast period) in an aerobic reactor.
3. Fed-batch process under nutrient growth limitation: fermentation through acidogenesis into substrate containing VFAs which are used for PHA production in a fed-batch process.

MMCs have shown several advantages over pure cultures, among them the possibility of using a wide range of substrates and the ability to degrade recalcitrant compounds due to the heterogeneity and synergies of microbial species. Further advantage of MMCs-based processes is its integration in waste treatment plants (Kourmentza et al., 2017). Besides these advantages, the use of MMCs also presents major challenges which must be addressed, for examples: i) the balance between microorganisms involved in the community, ii) the definition of specific environmental and operative conditions to promote the relevant microbial community to produce the targeted biopolymers, as well as the improvement in the extraction technologies due to the higher resistance of cells to hydrolysis with respect to pure cultures (Mannina et al., 2020; Samorì et al., 2015).

#### *PHA applicability*

PHAs main properties, such as biocompatibility and biodegradability make this polymer an important biological material with diverse applications in numerous fields. The polymers can be used as biofuels (hydroxyalkanoates methyl ester), through transesterification with

methanol in the presence of catalysts (Gao et al., 2011; Kargbo, 2010; Zhang et al., 2009), packaging materials, cosmetic containers, sanitary products, carriers for long term release of herbicides or insecticides production of pharmaceutical and biomedical devices (Mozejko & Ciesielski, 2014; Tan et al., 2021). PHAs can also be applied to produce ultra-strong fibers for fisheries industry (Bugnicourt et al., 2014).

Packaging, food service, agriculture and medical products can be taken as some of the most evident examples of PHAs product development. Nevertheless, several undesirable physical properties that involve both scl and mcl PHA limit their application. These disadvantages include poor mechanical properties, limited functionalities, incompatibility with conventional thermal processing techniques and susceptibility to thermal degradation. On the other hand, these limits can be overcome by blending PHA with other polymers, like poly-lactic acid (PLA) or poly-caprolactone (PCL), or by chemical modification, such as graft or block copolymerization (Li et al., 2016).

PHA production costs are estimated to be 5-10 times higher than that of conventional plastics such as PE. In 2018 PHB price was around \$3.5/kg, while PP and PE prices were around \$1.2-\$1.3/kg (Aramvash et al., 2018). The major factors affecting production costs include carbon source, cost of fermentation, productivity, and yields (g of product/g of substrate) of production processes, and downstream processing. In particular, cost of substrates used to feed the microbial growth was estimated to account for more than 50% of the production costs (Koller et al., 2017; G. D. Saratale et al., 2020; R. G. Saratale et al., 2020). This makes the whole process not cost-efficient when compared with petroleum-based plastics and has encouraged the use of inexpensive waste biomasses to reduce the economic impact of supplying of raw material (Kourmentza et al., 2017; Sabapathy et al., 2017; Sirohi et al., 2020). The selection of a hyper productive microorganisms is equally important. For example, the average USD/kg cost of PHB production were reported to be 2.6, 5.37 and 6.69 for *Alcaligenes latus*, *E. coli* and *Mathylobacterium organophilum* (Raza et al., 2018).

## Aim of thesis

Aim of this thesis has been the development of new strategies to produce Polyhydroxyalkanoates and the assessment of new approaches for their applicability.

This work is part of the “CARDOn valorisation by inteGrAted biorefiNery (CARDIGAN)” project (Italian Minister of Research, National projects of relevant interest (PRIN), 2017). In this project Cardoon was chosen as feedstock for PHA production. Inulin, the major component of Cardoon roots, was tested as substrate for PHA production through three different approaches: a two-step process, including enzymatic hydrolysis of inulin from cardoon roots, followed by the conversion of the obtained fermentable sugars by native bacterial strain (Chapter 1, § 1.1); a one-step process, in which inulin hydrolysis and PHA production occur simultaneously (Chapter 1, § 1.1); construction of an “artificial microbial consortium” to address PHA production from inulin, by complementing *Cupriavidus necator* enzymatic deficiency with a properly isolated inulin-hydrolysing microorganism (Chapter 1, § 1.2).

To enlarge the application fields of PHAs, the preparation of a nano-biocomposite material based on the use of poly-3-hydroxybutyrate-co-hydroxyhexanoate nanoparticles (PHBHHx-NPs) within a scaffold of whey protein (WP) based films was carried out (Chapter 2, §2.1). Additionally, a protocol for encapsulation of bioactive compound into nanoparticles of PHA was set up. As a fact, PHA-NPs were used as delivering system of essential oil with antioxidant and antimicrobial activity (Chapter 2, §2.2).

Aramvash, A., Moazzeni Zavareh, F., & Gholami Banadkuki, N. (2018). Comparison of different solvents for extraction of polyhydroxybutyrate from *Cupriavidus necator*. *Engineering in Life Sciences*, 18(1), 20–28. <https://doi.org/10.1002/elsc.201700102>

Bioplastics, E. (n.d.). *European bioplastics*. <https://www.european-bioplastics.org/>

Bugnicourt, E., Cinelli, P., Lazzeri, A., & Alvarez, V. (2014). Polyhydroxyalkanoate (PHA): Review of synthesis, characteristics, processing and potential applications in packaging. *Express Polymer Letters*, 8(11), 791–808. <https://doi.org/10.3144/expresspolymlett.2014.82>

Castilho, L. R., Mitchell, D. A., & Freire, D. M. G. (2009). Production of polyhydroxyalkanoates (PHAs) from waste materials and by-products by submerged and solid-state fermentation. *Bioresource Technology*, 100(23), 5996–6009. <https://doi.org/10.1016/j.biortech.2009.03.088>

- Chen, G. Q., & Jiang, X. R. (2017). Engineering bacteria for enhanced polyhydroxyalkanoates (PHA) biosynthesis. *Synthetic and Systems Biotechnology*, 2(3), 192–197. <https://doi.org/10.1016/j.synbio.2017.09.001>
- Choi, S. Y., Rhie, M. N., Kim, H. T., Joo, J. C., Cho, I. J., Son, J., Jo, S. Y., Sohn, Y. J., Baritugo, K. A., Pyo, J., Lee, Y., Lee, S. Y., & Park, S. J. (2020). Metabolic engineering for the synthesis of polyesters: A 100-year journey from polyhydroxyalkanoates to non-natural microbial polyesters. *Metabolic Engineering*, 58(February), 47–81. <https://doi.org/10.1016/j.ymben.2019.05.009>
- Eriksen, M., Lebreton, L. C. M., Carson, H. S., Thiel, M., Moore, C. J., Borerro, J. C., Galgani, F., Ryan, P. G., & Reisser, J. (2014). Plastic Pollution in the World's Oceans: More than 5 Trillion Plastic Pieces Weighing over 250,000 Tons Afloat at Sea. *PLoS ONE*, 9(12), 1–15. <https://doi.org/10.1371/journal.pone.0111913>
- Favaro, L., Basaglia, M., & Casella, S. (2019). Improving polyhydroxyalkanoate production from inexpensive carbon sources by genetic approaches: a review. *Biofuels, Bioproducts and Biorefining*, 13(1), 208–227. <https://doi.org/10.1002/bbb.1944>
- Fradinho, J. C., Oehmen, A., & Reis, M. A. M. (2019). Improving polyhydroxyalkanoates production in phototrophic mixed cultures by optimizing accumulator reactor operating conditions. *International Journal of Biological Macromolecules*, 126, 1085–1092. <https://doi.org/10.1016/j.ijbiomac.2018.12.270>
- Gao, X., Chen, J. C., Wu, Q., & Chen, G. Q. (2011). Polyhydroxyalkanoates as a source of chemicals, polymers, and biofuels. *Current Opinion in Biotechnology*, 22(6), 768–774. <https://doi.org/10.1016/j.copbio.2011.06.005>
- Hannah Ritchie and Max Roser. (2018). *Plastic Pollution*. Our World in Data. <https://ourworldindata.org/plastic-pollution>
- Kargbo, D. M. (2010). Biodiesel production from municipal sewage sludges. *Energy and Fuels*, 24(5), 2791–2794. <https://doi.org/10.1021/ef1001106>
- Kaur, L., Khajuria, R., Parihar, L., & Dimpal Singh, G. (2017). Polyhydroxyalkanoates: Biosynthesis to commercial production- A review. *Journal of Microbiology, Biotechnology and Food Sciences*, 6(4), 1098–1106. <https://doi.org/10.15414/jmbfs.2017.6.4.1098-1106>
- Koller, M., Maršálek, L., de Sousa Dias, M. M., & Braunnegg, G. (2017). Producing microbial polyhydroxyalkanoate (PHA) biopolyesters in a sustainable manner. *New Biotechnology*, 37, 24–38. <https://doi.org/10.1016/j.nbt.2016.05.001>
- Kourmentza, C., Plácido, J., Venetsaneas, N., Burniol-Figols, A., Varrone, C., Gavala, H. N., & Reis, M. A. M. (2017). Recent advances and challenges towards sustainable polyhydroxyalkanoate (PHA) production. *Bioengineering*, 4(2), 1–43. <https://doi.org/10.3390/bioengineering4020055>
- Lee, Y., Cho, I. J., Choi, S. Y., & Lee, S. Y. (2019). Systems Metabolic Engineering Strategies for Non-Natural Microbial Polyester Production. *Biotechnology Journal*, 14(9), 1800426. <https://doi.org/10.1002/biot.201800426>
- Li, Z., Yang, J., & Loh, X. J. (2016). Polyhydroxyalkanoates: Opening doors for a sustainable future. *NPG Asia Materials*, 8(4), 1–20.

- <https://doi.org/10.1038/am.2016.48>
- Licciardello, G., Catara, A. F., & Catara, V. (2019). Production of polyhydroxyalkanoates and extracellular products using *Pseudomonas corrugata* and *P. mediterranea*: A review. *Bioengineering*, 6(4). <https://doi.org/10.3390/bioengineering6040105>
- Mannina, G., Presti, D., Montiel-Jarillo, G., Carrera, J., & Suárez-Ojeda, M. E. (2020). Recovery of polyhydroxyalkanoates (PHAs) from wastewater: A review. *Bioresource Technology*, 297(October 2019), 122478. <https://doi.org/10.1016/j.biortech.2019.122478>
- Mozejko, J., & Ciesielski, S. (2014). Pulsed feeding strategy is more favorable to medium-chain-length polyhydroxyalkanoates production from waste rapeseed oil. *Biotechnology Progress*, 30(5), 1243–1246. <https://doi.org/10.1002/btpr.1914>
- Muhammadi, Shabina, Afzal, M., & Hameed, S. (2015). *Green Chemistry Letters and Reviews Bacterial polyhydroxyalkanoates-eco-friendly next generation plastic : Production , biocompatibility , biodegradation , physical properties and applications*. 8253. <https://doi.org/10.1080/17518253.2015.1109715>
- Nikodinovic-Runic, J., Guzik, M., Kenny, S. T., Babu, R., Werker, A., & O'Connor, K. E. (2013). Carbon-rich wastes as feedstocks for biodegradable polymer (polyhydroxyalkanoate) production using bacteria. In *Advances in Applied Microbiology* (Vol. 84). <https://doi.org/10.1016/B978-0-12-407673-0.00004-7>
- Ojumu, T. V., Yu, J., & Solomon, B. O. (2004). Production of Polyhydroxyalkanoates, a bacterial biodegradable polymer. *African Journal of Biotechnology*, 3(1), 18–24. <https://doi.org/10.5897/AJB2004.000-2004>
- Rai, R., Keshavarz, T., Roether, J. A., Boccaccini, A. R., & Roy, I. (2011). Medium chain length polyhydroxyalkanoates, promising new biomedical materials for the future. *Materials Science and Engineering R: Reports*, 72(3), 29–47. <https://doi.org/10.1016/j.mser.2010.11.002>
- Raza, Z. A., Abid, S., & Banat, I. M. (2018). Polyhydroxyalkanoates: Characteristics, production, recent developments and applications. *International Biodeterioration and Biodegradation*, 126(September 2017), 45–56. <https://doi.org/10.1016/j.ibiod.2017.10.001>
- Raza, Z. A., Tariq, M. R., Majeed, M. I., & Banat, I. M. (2019). Recent developments in bioreactor scale production of bacterial polyhydroxyalkanoates. *Bioprocess and Biosystems Engineering*, 42(6), 901–919. <https://doi.org/10.1007/s00449-019-02093-x>
- Rehm, B. H. A. (2003). Polyester synthases: Natural catalysts for plastics. *Biochemical Journal*, 376(1), 15–33. <https://doi.org/10.1042/BJ20031254>
- Rutkowska, M., Krasowska, K., Heimowska, A., Steinka, I., Janik, H., Haponiuk, J., & Karlsson, S. (2002). Biodegradation of Modified Poly( $\epsilon$ -caprolactone) in Different Environments. *Polish Journal of Environmental Studies*, 11(4), 413–420.
- Sabapathy, P. C., Devaraj, S., & Kathirvel, P. (2017). Parthenium hysterophorus: Low cost substrate for the production of polyhydroxyalkanoates. *Current Science*, 112(10), 2106–2111. <https://doi.org/10.18520/cs/v112/i10/2106-2111>

- Sabapathy, P. C., Devaraj, S., Meixner, K., Anburajan, P., Kathirvel, P., Ravikumar, Y., & Zayed, H. M. (2020). Bioresource Technology Recent developments in Polyhydroxyalkanoates ( PHAs ) production – A review. *Bioresource Technology*, 306(January), 123132. <https://doi.org/10.1016/j.biortech.2020.123132>
- Samori, C., Basaglia, M., Casella, S., Favaro, L., Galletti, P., Giorgini, L., Marchi, D., Mazzocchetti, L., Torri, C., & Tagliavini, E. (2015). Dimethyl carbonate and switchable anionic surfactants: Two effective tools for the extraction of polyhydroxyalkanoates from microbial biomass. *Green Chemistry*, 17(2), 1047–1056. <https://doi.org/10.1039/c4gc01821d>
- Saratale, G. D., Rijuta, G. R., Varjani, S., Cho, S., Ghodake, G. S., Kadam, A., Mulla, S. I., Bharagava, R. N., Kim, D., & Shin, H. S. (2020). Industrial Crops & Products Development of ultrasound aided chemical pretreatment methods to enrich sacchari fi cation of wheat waste biomass for polyhydroxybutyrate production and its characterization. *Industrial Crops & Products*, 150(April), 112425. <https://doi.org/10.1016/j.indcrop.2020.112425>
- Saratale, R. G., Cho, S., Ghodake, G. S., Shin, H., Saratale, G. D., Park, Y., Lee, H., Bharagava, R. N., & Kim, D. (2020). Utilization of Noxious Weed Water Hyacinth Biomass as a Potential Feedstock for Biopolymers Production: *Polymers*, 12. <https://doi.org/10.3390/polym12081704>
- Sirohi, R., Prakash Pandey, J., Kumar Gaur, V., Gnansounou, E., & Sindhu, R. (2020). Critical overview of biomass feedstocks as sustainable substrates for the production of polyhydroxybutyrate (PHB). *Bioresource Technology*, 311(May), 123536. <https://doi.org/10.1016/j.biortech.2020.123536>
- Sohn, Y. J., Kim, H. T., Baritugo, K., Jo, S. Y., Song, H. M., Park, S. Y., Park, S. K., Pyo, J., Cha, H. G., Kim, H., Na, J., Park, C., Choi, J., Joo, J. C., & Park, S. J. (2020). Recent Advances in Sustainable Plastic Upcycling and Biopolymers. *Biotechnology Journal*, 1900489, 1–16. <https://doi.org/10.1002/biot.201900489>
- Sudesh, K., Abe, H., & Doi, Y. (2000). Synthesis, structure and properties of polyhydroxyalkanoates: Biological polyesters. *Progress in Polymer Science (Oxford)*, 25(10), 1503–1555. [https://doi.org/10.1016/S0079-6700\(00\)00035-6](https://doi.org/10.1016/S0079-6700(00)00035-6)
- Tan, D., Wang, Y., Tong, Y., & Chen, G. Q. (2021). Grand Challenges for Industrializing Polyhydroxyalkanoates (PHAs). *Trends in Biotechnology*, 1–11. <https://doi.org/10.1016/j.tibtech.2020.11.010>
- Tsuge, T. (2016). Fundamental factors determining the molecular weight of polyhydroxyalkanoate during biosynthesis. *Polymer Journal*, 48(11), 1051–1057. <https://doi.org/10.1038/pj.2016.78>
- Turco, R., Santagata, G., Corrado, I., Pezzella, C., & Di Serio, M. (2021). In vivo and Post-synthesis Strategies to Enhance the Properties of PHB-Based Materials: A Review. *Frontiers in Bioengineering and Biotechnology*, 8. <https://doi.org/10.3389/fbioe.2020.619266>
- Verlinden, R. A. J., Hill, D. J., Kenward, M. A., Williams, C. D., & Radecka, I. (2007). Bacterial synthesis of biodegradable polyhydroxyalkanoates. *Journal of Applied Microbiology*, 102(6), 1437–1449. <https://doi.org/10.1111/j.1365-2672.2007.03335.x>

Zhang, L., Shi, Z. Y., Wu, Q., & Chen, G. Q. (2009). Microbial production of 4-hydroxybutyrate, poly-4-hydroxybutyrate, and poly(3-hydroxybutyrate-co-4-hydroxybutyrate) by recombinant microorganisms. *Applied Microbiology and Biotechnology*, 84(5), 909–916. <https://doi.org/10.1007/s00253-009-2023-7>

**Chapter 1**  
**PHA Production from waste materials:**  
**inulin-rich feedstocks as carbon source for**  
**PHA production**

In this chapter, two parallel approaches for sustainable conversion of renewable inulin-rich biomasses into PHA are presented. Inulin-rich biomasses represent inexpensive, renewable, and abundant feedstock (Hughes et al., 2017; Li et al., 2013). Inulin is a linear polysaccharide ( $\beta$ -2,1-linked d-fructose residues terminated by a glucose residue) accumulated as a storage carbohydrate in plants such as chicory, dahlia, and more interestingly, in low-requirement crops, such as *Jerusalem artichoke* and *Cynara cardunculus* (Hughes et al., 2017). Growing well in non-fertile and harsh lands, these inulin-containing biomasses do not compete with grain crops for arable land and have received attention as renewable resource for the production of several bio-based products, such as PHA, through microbial bioprocesses (Chi et al., 2011; Qiu et al., 2019a). On the other hand, the use of low-cost substrates as starting feedstock for microbial fermentation represents a key aspect to promote a cost-effective and sustainable exploitation of this class of biopolymers (Kumar et al., 2019; Tsang et al., 2019; Vastano et al., 2019). Inulin hydrolysis into fermentable monosaccharides is a prerequisite for its utilization as carbon and energy source for subsequent fermentation processes. Only few microbial strains are naturally endowed with the ability to both hydrolyse inulin and convert fructose into value-added chemicals. Consolidated bioprocesses which make use of biomass derived inulin exploiting wild-type strains have been reported for lactic acid (Choi et al., 2012), ethanol (Khatun et al., 2017) and poly-( $\gamma$ -glutamic acid) (Qiu et al., 2019b) but not for PHA production. *C. necator*, one of the most widely known PHA producer, is able to accumulate Polyhydroxybutyrate (PHB) with high productivity from fructose but lacks the ability to utilize inulin as C-source (Bhatia et al., 2018).

An enzymatic approach for inulin hydrolysis represents an environmentally friendly alternative to acid hydrolysis, preventing the formation of pigments and fermentation inhibitors, opening the way to combined hydrolysis and fermentation steps, with advantages in terms of overall time, cost and productivity of the process (Qiu et al., 2018). The key-enzymes involved in inulin hydrolysis are microbial inulinases, glycosylhydrolases, belonging to the GH32 family, that catalyse the hydrolysis of fructans. Based on their specific hydrolytic activity on glycosidic bonds, they can be classified into exo-inulinases

(E.C. 3.8.1.80), acting by removing fructose moieties from the non-reducing end of inulin, or endoinulinases (E.C. 3.2.1.7), that randomly break any  $\beta$ -2,1 glycosidic bond in inulin molecule, releasing inulotrioses (F3), inulotetraoses (F4), and other IOSs oligosaccharides (Hughes et al., 2017). While exo-inulinases have been shown to display a significant amount of activity toward sucrose, endoinulinases lack invertase activity (Z. Chi et al., 2009).

In **Paragraph 1.1** a collection of fungi was screened for the selection of new inulinases producer. The inulinase mixture obtained from the better performing fungus was characterized and used to optimize a protocol for inulin hydrolysis through an approach of statistical design of experiment. The fructose containing hydrolysate was used as carbon source to produce PHAs from *C. necator*, comparing different process configurations: Separated Hydrolysis and Fermentation (SHF) and Simultaneous Saccharification and Fermentation (SSF). **Paragraph 1.2** reports a novel approach for PHB production without any pre-treatment of inulin by using a co-culture of PHA-accumulating *C. necator* DSM 428 and inulin hydrolysing *Bacillus* strain.

- Bhatia, S. K., Bhatia, R. K., Choi, Y. K., Kan, E., Kim, Y. G., & Yang, Y. H. (2018). Biotechnological potential of microbial consortia and future perspectives. *Critical Reviews in Biotechnology*, 38(8), 1209–1229. <https://doi.org/10.1080/07388551.2018.1471445>
- Chi, Z., Chi, Z., Zhang, T., Liu, G., & Yue, L. (2009). Inulinase-expressing microorganisms and applications of inulinases. *Applied Microbiology and Biotechnology*, 82(2), 211–220. <https://doi.org/10.1007/s00253-008-1827-1>
- Chi, Z. M., Zhang, T., Cao, T. S., Liu, X. Y., Cui, W., & Zhao, C. H. (2011). Biotechnological potential of inulin for bioprocesses. *Bioresource Technology*, 102(6), 4295–4303. <https://doi.org/10.1016/j.biortech.2010.12.086>
- Hughes, S. R., Qureshi, N., López-Núñez, J. C., Jones, M. A., Jarodsky, J. M., Galindo-Leva, L. Á., & Lindquist, M. R. (2017). Utilization of inulin-containing waste in industrial fermentations to produce biofuels and bio-based chemicals. *World Journal of Microbiology and Biotechnology*, 33(4), 1–15. <https://doi.org/10.1007/s11274-017-2241-6>
- Khatun, M. M., Liu, C. G., Zhao, X. Q., Yuan, W. J., & Bai, F. W. (2017). Consolidated ethanol production from Jerusalem artichoke tubers at elevated temperature by *Saccharomyces cerevisiae* engineered with inulinase expression through cell surface display. *Journal of Industrial Microbiology and Biotechnology*, 44(2), 295–301. <https://doi.org/10.1007/s10295-016-1881-0>
- Kumar, P., Maharjan, A., Jun, H. B., & Kim, B. S. (2019). Bioconversion of lignin and its derivatives into polyhydroxyalkanoates: Challenges and opportunities.

- Biotechnology and Applied Biochemistry*, 66(2), 153–162. <https://doi.org/10.1002/bab.1720>
- Li, L., Li, L., Wang, Y., Du, Y., & Qin, S. (2013). Biorefinery products from the inulin-containing crop Jerusalem artichoke. *Biotechnology Letters*, 35(4), 471–477. <https://doi.org/10.1007/s10529-012-1104-3>
- Qiu, Y., Lei, P., Zhang, Y., Sha, Y., Zhan, Y., Xu, Z., Li, S., Xu, H., & Ouyang, P. (2018). Recent advances in bio-based multi-products of agricultural Jerusalem artichoke resources. *Biotechnology for Biofuels*, 11(1), 1–15. <https://doi.org/10.1186/s13068-018-1152-6>
- Qiu, Y., Zhang, Y., Zhu, Y., Sha, Y., Xu, Z., Feng, X., Li, S., & Xu, H. (2019a). Improving poly-( $\gamma$ -glutamic acid) production from a glutamic acid-independent strain from inulin substrate by consolidated bioprocessing. *Bioprocess and Biosystems Engineering*, 42(10), 1711–1720. <https://doi.org/10.1007/s00449-019-02167-w>
- Qiu, Y., Zhu, Y., Zhan, Y., Zhang, Y., Sha, Y., Xu, Z., Li, S., Feng, X., & Xu, H. (2019b). Systematic unravelling of the inulin hydrolase from *Bacillus amyloliquefaciens* for efficient conversion of inulin to poly-( $\gamma$ -glutamic acid). *Biotechnology for Biofuels*, 12(1), 1–14. <https://doi.org/10.1186/s13068-019-1485-9>
- Tsang, Y. F., Kumar, V., Samadar, P., Yang, Y., Lee, J., Ok, Y. S., Song, H., Kim, K. H., Kwon, E. E., & Jeon, Y. J. (2019). Production of bioplastic through food waste valorization. *Environment International*, 127(April), 625–644. <https://doi.org/10.1016/j.envint.2019.03.076>
- Vastano, M., Corrado, I., Sannia, G., Solaiman, D. K. Y., & Pezzella, C. (2019). Conversion of no/low value waste frying oils into biodiesel and polyhydroxyalkanoates. *Scientific Reports*, 9(1), 1–8. <https://doi.org/10.1038/s41598-019-50278-x>
- Zou, H., Zhang, T., Li, L., Huang, J., Zhang, N., Shi, M., Hao, H., & Xian, M. (2018). Systematic engineering for improved carbon economy in the biosynthesis of polyhydroxyalkanoates and isoprenoids. *Materials*, 11(8). <https://doi.org/10.3390/ma11081271>

## 1.1 Optimization of inulin Hydrolysis by *Penicillium Lanosocoeruleum* inulinases and efficient conversion into Polyhydroxyalkanoates



# Optimization of Inulin Hydrolysis by *Penicillium lanosocoeruleum* Inulinases and Efficient Conversion Into Polyhydroxyalkanoates

Iolanda Corrado<sup>1</sup>, Nicoletta Cascelli<sup>1</sup>, Georgia Ntasi<sup>1</sup>, Leila Birolo<sup>1</sup>, Giovanni Sannia<sup>1</sup> and Cinzia Pezzella<sup>2\*</sup>

<sup>1</sup> Department of Chemical Sciences, University of Naples Federico II, Complesso Universitario di Monte Sant'Angelo, Naples, Italy, <sup>2</sup> Department of Agricultural Sciences, University of Naples Federico II, Naples, Italy

### OPEN ACCESS

**Edited by:**  
Manuel Benedetti,  
University of L'Aquila, Italy

**Reviewed by:**  
Helen Treichel,  
Universidade Federal da Fronteira Sul,  
Brazil  
Naveen Kango,  
Dr. Hari Singh Gour University, India

**\*Correspondence:**  
Cinzia Pezzella  
cpezzella@unina.it

**Specialty section:**  
This article was submitted to  
Industrial Biotechnology,  
a section of the journal  
Frontiers in Bioengineering and  
Biotechnology

**Received:** 13 October 2020

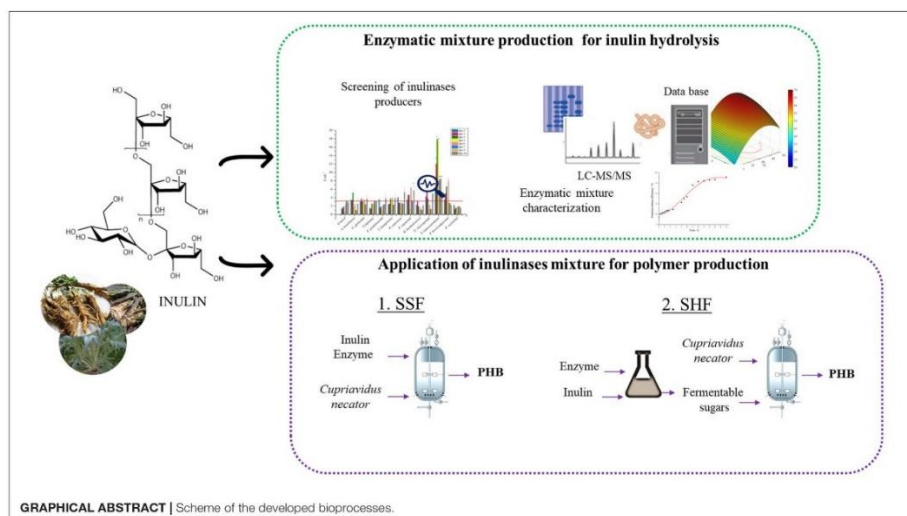
**Accepted:** 29 January 2021

**Published:** 01 March 2021

**Citation:**  
Corrado I, Cascelli N, Ntasi G,  
Birolo L, Sannia G and Pezzella C  
(2021) Optimization of Inulin  
Hydrolysis by *Penicillium*  
*lanosocoeruleum* Inulinases  
and Efficient Conversion Into  
Polyhydroxyalkanoates.  
*Front. Bioeng. Biotechnol.* 9:616908.  
doi: 10.3389/fbioe.2021.616908

Inulin, a polydisperse fructan found as a common storage polysaccharide in the roots of several plants, represents a renewable non-food biomass resource for the synthesis of bio-based products. Exploitation of inulin-containing feedstocks requires the integration of different processes, including inulinase production, saccharification of inulin, and microbial fermentation for the conversion of released sugars into added-value products. In this work paper, a new microbial source of inulinase, *Penicillium lanosocoeruleum*, was identified through the screening of a fungal library. Inulinase production using inulin as C-source was optimized, reaching up to 28 U mL<sup>-1</sup> at the 4th day of growth. The fungal inulinase mixture (*Plal*) was characterized for pH and temperature stability and activity profile, and its isoenzymes composition was investigated by proteomic strategies. Statistical optimization of inulin hydrolysis was performed using a central composite rotatable design (CCRD), by analyzing the effect of four factors. In the optimized conditions (T, 45.5°C; pH, 5.1; substrate concentration, 60 g L<sup>-1</sup>; enzyme loading, 50 U g<sub>substrate</sub><sup>-1</sup>), up to 96% inulin is converted in fructose within 20 h. The integration of *Plal* in a process for polyhydroxyalkanoate (PHA) production by *Cupriavidus necator* from inulin was tested in both separated hydrolysis and fermentation (SHF) and simultaneous saccharification and fermentation (SSF). A maximum of 3.2 g L<sup>-1</sup> of PHB accumulation, corresponding to 82% polymer content, was achieved in the SSF. The proved efficiency in inulin hydrolysis and its effective integration into a SSF process pave the way to a profitable exploitation of the *Plal* enzymatic mixture in inulin-based biorefineries.

**Keywords:** response surface methodology, simultaneous saccharification and fermentation, inulin hydrolysis, polyhydroxybutyrate, inulin, biorefinery



## INTRODUCTION

The biorefinery concept focuses on the sustainable conversion of renewable biomasses into a broad range of industrial products, materials, and energy. Inulin-rich biomasses represent inexpensive, renewable, and abundant feedstock to build up a biorefinery strategy (Li et al., 2013; Hughes et al., 2017; Bedzo et al., 2020). Inulin is a linear polysaccharide ( $\beta$ -2,1-linked d-fructose residues terminated by a glucose residue) accumulated as a storage carbohydrate in plants such as chicory and dahlia and, more interestingly, in low-requirement crops, such as *Jerusalem artichoke* and *Cynara cardunculus* (Hughes et al., 2017). Growing well in non-fertile and harsh lands, these inulin-containing biomasses do not compete with grain crops for arable land and have received attention as renewable resource for the production of several bio-based products through microbial bioprocesses (Chi et al., 2011; Qiu et al., 2018; Singh et al., 2019, 2020a).

Among the emerging bio-based products, bioplastics derived from microbial processes, polyhydroxyalkanoates (PHA), represent promising “green” alternatives to conventional plastics. Synthesized by a wide range of bacteria from renewable sources, PHA are fully biodegradable polyesters, exhibiting a wide spectrum of properties, very close to those of fossil-derived polyolefins (Samui and Kanai, 2019; Medeiros Garcia Alcántara et al., 2020). PHA properties are dependent on their monomer chain length (ranging from the most common C4 monomer, butyrate, to  $C \geq 6$  monomers) with a composition strictly influenced by the supplied carbon source and the specific metabolic pathway activated in the cell. This variability translates into a wide range of material properties allowing this polymer

to find applications in different sectors (Raza et al., 2018; Zhong et al., 2020). The use of low-cost substrates as starting feedstock for microbial fermentation therefore represents the keystone to promote a cost-effective and sustainable exploitation of this class of biopolymers (Kumar et al., 2019; Tsang et al., 2019; Vastano et al., 2019; Guzik et al., 2020; Surendran et al., 2020).

Hydrolysis into fermentable monosaccharides is a prerequisite for inulin utilization as carbon and energy source in the subsequent fermentation processes. Acid hydrolysis is a common method to achieve fast and cheap inulin conversion into fermentable sugars; however, it results in the formation of colored by-products as well as in the production of inhibitors of microbial growth. Enzymatic processes, conversely, besides representing an environmentally friendly alternative to acid hydrolysis, prevent the formation of pigments and inhibitors, paving the way to combined hydrolysis and fermentation steps, with an advantage in terms of overall time, costs, and productivity of the process (Qiu et al., 2018). The key enzymes involved in inulin hydrolysis are inulinases, which are glycosyl hydrolases, belonging to the GH32 family, that catalyze the hydrolysis of fructans. Based on their differential hydrolytic activity, they can be classified into exo-inulinases (E.C. 3.8.1.80), acting by removing fructose moieties from the non-reducing end of inulin, or endoinulinases (E.C. 3.2.1.7), which randomly break any  $\beta$ -2,1 glycosidic bond in the inulin molecule, thus releasing inulotrioses (F3), inulotetraoses (F4), and other IOSs oligosaccharides (Hughes et al., 2017). While exoinulinases have been shown to display a significant amount of activity toward sucrose, endoinulinases lack invertase activity (Chi et al., 2009; Singh et al., 2019, 2020b).

Inulinases have been reported to be present in plants, animals, and various microorganisms. The latter are the most preferred source of inulinases due to their easier manipulation, higher production levels, and variety of their properties (Singh and Chauhan, 2016, 2017). Numerous fungal, yeast, and bacterial strains have been isolated for their ability to produce inulinases (Rawat et al., 2017b; Singh et al., 2019); fungal inulinases are the most attractive for their production levels, low substrate requirement, and tolerance to low pH and high temperature (Singh and Singh, 2017). As a matter of fact, microbial inulinases have been widely exploited: exo-inulinases, in high-fructose syrup preparation (Rawat et al., 2017a; Singh et al., 2017) and endo-inulinases in the production of inulo-oligosaccharides (IOS) as functional probiotics (Singh and Singh, 2010; Chikkerur et al., 2020; Singh et al., 2020b, 2021).

Despite the high potential, the high price of commercial inulinases and the lack of efficient inulinase catalyzed processes still represent the main limitations to their effective exploitation (Qiu et al., 2019b). The cost-competitiveness of inulinase production can be achieved by using a cheap inulin-rich feedstock for their production, and several examples have been reported in this field (Singh et al., 2019). On the other hand, search for new, better-performing enzymes by exploring the potential of new inulinase producers represents a viable strategy to promote the exploitation of these enzymes in industrial processes as well as in the valorization of inulin-rich biomasses.

The production of different microbial products, including ethanol, butanol, citric and succinic acids, and single-cell proteins (Singh et al., 2020a), has been achieved while exploiting microbial inulinases in separate hydrolysis and fermentation (SHF) and simultaneous saccharification and fermentation (SSF) processes. Only few microbial strains are naturally endowed with the ability of both hydrolyzing inulin and converting fructose into value-added chemicals. Consolidated bioprocesses (CBP) based on biomass-derived inulin have been reported for the microbial production of lactic acid (Choi et al., 2012), ethanol (Khatun et al., 2017), poly- $\gamma$ -glutamic acid (Qiu et al., 2019a), xopolysaccharide (Meng et al., 2021), and single-cell oils (Zhao et al., 2010). On the other hand, PHA production from inulin has been less explored. *Cupriavidus necator*, one of the most widely known PHA producers, is able to accumulate polyhydroxybutyrate (PHB) with high productivity from fructose but lacks the ability to utilize inulin as C-source (Bhatia et al., 2018). As a fact, only examples of SHF processes for PHA production from inulin extracts have been reported for this strain (Koutinas et al., 2013; Haas et al., 2015).

In the perspective of designing processes for saccharification of inulin substrate, the optimization of inulinase reaction conditions is essential for their utilization in the SHF process, while expanding the pool of available inulinases will help to address the specific process conditions imposed by the SSF process (Zheng et al., 2018b).

In this work, a collection of fungi was screened as inulinase producers. The inulinase mixture obtained from the best-performing fungus was characterized and used to optimize a protocol for inulin hydrolysis through an approach of statistical

design of experiments. The fructose-containing hydrolyzate was used as starting feedstock for the production of PHAs from *C. necator* in an SHF process. Furthermore, the exploitation of the inulinase mixture in an SSF strategy for PHA production was also tested and the performances of the two processes were compared.

## MATERIALS AND METHODS

### Microbial Strains and Culture Conditions

Fungal strains were obtained from the *Mycotheca Universitatis Taurinensis* (MUT) culture collection. *C. necator* DSM 428 production was used for PHB production.

All fungi were grown and maintained on Malt Extract Agar medium (MEA) (for 1 L): 20.0 g malt extract, 2.0 g peptone, 20.0 g agar, and 20.0 g glucose through periodic transfer at 28°C (40°C for *Thermomyces lanuginosus*) for 7–9 days. A minimal medium (MM) (Vries et al., 2017) supplemented with inulin at 10 g L<sup>-1</sup> was used for the screening in liquid medium and for inulinase production. Inulin from chicory root, used in the culture media, was provided by Lineavi, Germany.

*Cupriavidus necator* DSM 428 strain was grown aerobically at 30°C in both rich (Tryptic Soy Broth, TSB) and minimal media (MM<sub>CN</sub>) according to Budde et al. (2011a,b).

### Screening of the Fungal Library

For screening in liquid medium, all fungi were grown on an MEA plate for 7–9 days. A mycelium plug (1 cm diameter) was transferred on the MM + Inulin 1% w/v agar plate for an additional 7–10 days before the inoculum in liquid medium. Shake flasks, smooth conventional or baffled (250 mL), containing 50 mL of MM were inoculated with four mycelium plugs (0.5 cm diameter) and incubated at 28°C (40°C for *Thermomyces lanuginosus*) in an orbital shaker at 200 rpm.

### Inulinase Production From *Penicillium lanosocoeruleum*

*Penicillium lanosocoeruleum* cultures were made on an agar MM medium with 1% glucose and then transferred to a liquid medium. 1% w/v of inulin, glucose, or fructose was tested as different carbon sources for the preinoculum phase. After 3 days of growth (28°C, 200 rpm), the preinoculum was milled, tenfold diluted into 1-L baffled flasks containing the MM medium plus 10 g L<sup>-1</sup> inulin, and grown for 10 days in the same conditions. Different medium/flask volume ratios were tested in the inoculum phase (1:2; 1:3; 1:5). Samples of fungal cultures were daily withdrawn and assayed for inulinase activity in the culture broth.

Different methods were tested to concentrate secreted inulinases in the crude extract: (i) precipitation by the addition of 80% (NH<sub>4</sub>)<sub>2</sub>SO<sub>4</sub> at 4°C; (ii) precipitation in cold acetone at fourfold volume with respect to the sample; and (iii) ultrafiltration in Amicon® Stirred Cell Millipore with a 10-kDa cutoff cellulose membrane.

Total protein content was determined according to the method of Bradford (1976) using bovine serum albumin (BSA)

as standard. The concentrated *P. lanosocoeruleum* enzymatic mixture recovered after the ultrafiltration step was herein defined *Plal*.

### Inulinase Activity Assay

Enzymatic activity on inulin and sucrose substrates was measured using the 3,5-dinitrosalicylic acid (DNS) reagent method in conformity with (Miller, 1959). A 0.2 mL of sample was added to 1.8 mL of 0.2 mol L<sup>-1</sup> sodium acetate buffer, pH 5.0, containing 0.5% w/v of high purity grade inulin (provided by Sigma) or 1% of sucrose. The mixture was incubated at 37°C for 15 min. Total reducing sugars were measured by adding 3 mL DNS reagent and boiling in a water bath for 5 min. Samples were allowed to cool, and their absorbance was read at 540 nm. A calibration curve was obtained using fructose as standard. One enzymatic unit (inulinase or invertase activity) was defined as the amount of the enzyme which produces 1 μmol of reducing sugars per minute. All the assays were carried out in duplicate.

The effect of pH on inulinase activity was measured at 37°C in a pH range of 3–10.5 using 0.1 mol L<sup>-1</sup> of citric acid–sodium citrate (pH 3–4), sodium acetate (pH 4.5–5.5), phosphate (pH 6–8), and sodium carbonate (pH 9.2–10.5) buffers. The effect of temperature was determined in 0.2 mol L<sup>-1</sup> M sodium acetate buffer at pH 5, incubating the mixture for 15 min in the temperature range 30–80°C. Thermal stability of the *Plal* mixture was determined by measuring the residual inulinase activity after incubation at 40, 60, and 80°C.

### Experimental Design

Inulin hydrolysis was optimized using response surface methodology (RSM) with central composite design (CCD). Four factors were selected to evaluate the response pattern and to determine the optimal combination of temperature, pH, substrate concentration, and enzyme loading. The coded values for each parameter were as follows [−1 0 1]: temperature in °C [28, 40, 50], pH [5, 6, 7], substrate concentration in g L<sup>-1</sup> [40, 50, 60], and enzyme loading in enzyme units for gram of inulin [20, 40, 60]. The experimental design was developed using JMP® 14.1.0 (SAS Institute Inc., 1989–2019, Cary, NC)<sup>1</sup> and resulted in 26 conditions; all conditions were tested in triplicate.

### Enzymatic Hydrolysis of Inulin

Enzymatic hydrolysis was performed in 10-mL glass vials with 5 mL working volume. Different amounts of *Plal* were added to Na-acetate (0.1 mol L<sup>-1</sup>, pH 5) or Na-phosphate buffer (0.1 mol L<sup>-1</sup>, pH 6, and 7) supplemented with inulin (high-grade purity) at the desired concentration. The vials were hermetically covered and incubated for 24 h while shaking at 250 rpm.

Kinetic of inulin hydrolysis was assessed in the optimal condition defined by DOE. Samples were withdrawn at different times and incubated at 100°C to inactivate the enzymatic mixture. For each reaction, a corresponding control was carried out in the absence of enzyme, to consider possible inulin spontaneous hydrolysis. The presence of free sugars into inulin powder without any incubation was taken at time 0 h. Conversion

<sup>1</sup>[https://www.jmp.com/it\\_it/home.html](https://www.jmp.com/it_it/home.html)

efficiency was calculated on the basis of maximum fructose released per gram of inulin. The complete inulin hydrolysis was carried out by incubating the *Aspergillus niger* endo-exo-inulinase enzyme mixture (SIGMA CAS: 9025-67-6) for 4 h at 50°C (5 U<sub>substrate</sub><sup>-1</sup>). Afterward, the mixture was kept in 100°C boiling water for 1 h to assure that the complete hydrolysis and fructose released was assayed. Concentrations of fructose and glucose were determined by D-fructose and D-glucose assay kits (K-FRUGL Megazyme).

### Gel Electrophoresis and Activity Staining on Polyacrylamide Gel

SDS-PAGE was performed according to Laemmli (1970). Native electrophoresis was carried out on 7% gel according to a method proposed by Chen et al. (1996). After that, PAGE gel was subjected to activity staining (Pessoni and Braga, 2007).

### In situ Digestion

The two gel bands that demonstrated inulinase activity were cut, destained, and *in situ* digested. Briefly, the gel pieces were washed with three cycles of 0.1 mol L<sup>-1</sup> NH<sub>4</sub>HCO<sub>3</sub> of pH 8.0 and acetonitrile, followed by reduction (10 mmol L<sup>-1</sup> DTT in 100 mmol L<sup>-1</sup> NH<sub>4</sub>HCO<sub>3</sub>, 45 min, and 37°C) and alkylation (55 mmol L<sup>-1</sup> IAM in 100 mmol L<sup>-1</sup> NH<sub>4</sub>HCO<sub>3</sub>, 30 min, and RT). The gel pieces were washed with three further cycles of 100 mmol L<sup>-1</sup> NH<sub>4</sub>HCO<sub>3</sub> of pH 8.0 and acetonitrile. Finally, the gel plugs were rehydrated in 40 mL sequencing grade modified trypsin (10 ng mL<sup>-1</sup> trypsin; 10 mmol L<sup>-1</sup> NH<sub>4</sub>HCO<sub>3</sub>) and incubated overnight at 37°C (Lettera et al., 2010). Peptide mixtures were eluted, vacuum-dried, and resuspended in 0.1% v/v formic acid for LC-MS/MS analysis.

### LC-MS/MS

LC-MS/MS analyses were carried out on a 6520 Accurate-Mass Q-TOF LC/MS System (Agilent Technologies, Palo Alto, CA, United States) equipped with a 1200 HPLC system and a chip cube (Agilent Technologies) and on an LTQ Orbitrap-XL (Thermo Scientific, Bremen, Germany) as reported in Linn et al. (2018), and raw data were analyzed as reported in Vinciguerra et al. (2015). Each LC-MS/MS analysis was preceded and followed by blank runs to avoid carryover contamination. MS/MS spectra were transformed in Mascot Generic files (.mgf) format, and the FASTA file of all the proteins from the gene expression profiling of *P. lanosocoeruleum* were used as database for protein identification. <sup>2</sup>(10698 sequences; 5093396 residues). A licensed version of MASCOT software<sup>3</sup> version 2.4.0 was used. Standard parameters in the searches were as follows: trypsin as the enzyme; 3 as the allowed number of missed cleavages; 10 ppm MS tolerance and 0.6 Da MS/MS tolerance; and peptide charge from 2+ to 4+. In all the database searches, carbamidomethylation of cysteine was inserted as fixed chemical modification, but possible oxidation of methionine and the transformation of N-terminal glutamate or glutamine

<sup>2</sup>[https://genomc.jgi.doe.gov/portal/PenlanEProfiling\\_FD/PenlanEProfiling\\_FD.info.html](https://genomc.jgi.doe.gov/portal/PenlanEProfiling_FD/PenlanEProfiling_FD.info.html)

<sup>3</sup>[www.matrixscience.com](http://www.matrixscience.com)

to pyroglutamate were considered as variable modifications. Only proteins presenting two or more peptides were considered as positively identified. Protein scores were derived from ion scores as a non-probabilistic basis for ranking protein hits.<sup>4</sup> The ion score is  $-10^8 \log(P)$ , where  $P$  is the probability that the observed peptide match is a random event. The individual ion score threshold provided by MASCOT software to evaluate the quality of matches in MS/MS data was used for the confidence threshold in protein identification. Basic Local Alignment Search Tool (BLAST) was used to calculate the sequence similarity among the amino acid sequences of the *P. lanosocoeruleum*-identified proteins with fungal proteins in the NCBI database.

### PHA Production and Extraction

*Cupriavidus necator* was grown on a rich medium (TSB) for 24 h and precultured in MM<sub>CN</sub> for an additional 48 h before the inoculum in fermentation media. PHA production was carried out in 250-mL Erlenmeyer flasks. For the SSF process, 20 g L<sup>-1</sup> inulin was supplemented to the minimal medium together with both 40 and 80 *Plal* inulinase U g<sub>substrate</sub><sup>-1</sup>. For the SHF process, inulin hydrolyzed in the best conditions defined by DOE was used as a carbon source. The pH was adjusted to 6.8 using 1 mol L<sup>-1</sup> NaOH, filtered, and added to MM<sub>CN</sub> (final concentration of fructose 20 g L<sup>-1</sup>). The flasks were inoculated at 0.1 OD mL<sup>-1</sup> and incubated at 30°C on shaker running at 200 rpm for 5 days. Single flasks were taken every 24 h, and the cells were recovered by centrifugation at 5,500 g for 15 min and lyophilized for determination of the cell dry weight (cdw). Analysis of fructose concentration was carried out on culture supernatants, while the PHA polymer was extracted from the lyophilized cell according to Sayyed et al. (2009).

### <sup>1</sup>H-NMR Spectroscopy

Polyhydroxyalkanoates extracts were analyzed by <sup>1</sup>H-NMR spectroscopy: samples (0.5–1.5 mg) were resuspended in deuterated chloroform (500 μL). <sup>1</sup>H-NMR spectra were recorded on Bruker DRX-400 (<sup>1</sup>H-NMR: 400 MHz) in CDCl<sub>3</sub> (internal standard, for <sup>1</sup>H: CHCl<sub>3</sub> at δ 7.26 ppm) (Mostafa et al., 2020).

### Statistical Analysis

The results were statistically analyzed using the JMP 14.1.0 (SAS Institute Inc., 1989–2019, Cary, NC)<sup>1</sup>. Arithmetic means and mean square errors (SD) were calculated in all cases. Significant differences in average values of inulinase activity measured in the liquid screening were tested using the Tukey-Kramer HSD test (significance level:  $P < 0.05$ ). ANOVA test has been applied to the experimental results of CCRD and to model validation experiments. The interaction and quadratic effect of parameters were determined based on an alpha 0.05 using the  $F$  test. The fitted models were evaluated by normal probability plots, R<sup>2</sup>, and adjusted R<sup>2</sup>.

<sup>4</sup>[http://www.matrixscience.com/help/interpretation\\_help.html](http://www.matrixscience.com/help/interpretation_help.html)

**TABLE 1** | Library of fungal strains constructed in this work.

Fungal strain	Note
<i>Penicillium brevicompactum</i> MUT 793	Inulinase activity detected (Abd et al., 2014) Annotated enzyme models: <b>4</b>
<i>Thermomyces lanuginosus</i> MUT 2896	Inulinase activity detected (Nguyen et al., 2013) Annotated enzyme models: nd
<i>Penicillium chrysogenum</i> MUT 618	Inulinase activity detected (Gujar et al., 2018) Annotated enzyme models: <b>6</b>
<i>Penicillium canescens</i> MUT 1158	Annotated enzyme models: <b>13</b>
<i>Penicillium lanosocoeruleum</i> MUT 3921	Annotated enzyme models: <b>9</b>
<i>Penicillium expansum</i> MUT 1164	Inulinase activity detected (Fernandes et al., 2012) Annotated enzyme models: <b>4</b>
<i>Penicillium raistrickii</i> MUT 1525	Annotated enzyme models: <b>5</b>
<i>Nectria haematococca</i> MUT 5670	Growth on inulin substrate (Battaglia et al., 2011) Annotated enzyme models: <b>6</b>
<i>Fusarium graminearum</i> MUT 209	Inulinase activity detected (Gonçalves et al., 2016) Annotated enzyme models: <b>5</b>
<i>Chaetomium globosum</i> MUT 337	Growth on inulin substrate (Battaglia et al., 2011) Annotated enzyme models: <b>6</b>
<i>Talaromyces stipitatus</i> MUT 237	Annotated enzyme models: <b>7</b> (Vries et al., 2017)
<i>Aspergillus brasiliensis</i> MUT 4853	Annotated enzyme models: <b>7</b> (Vries et al., 2017)

Information reported in the table is from scientific literature available on strains belonging to the same genus and species and/or whose genome sequence was deposited on the JGI genome portal (<https://genome.jgi.doe.gov/portal/>). The number of annotated enzyme models derives from CAZY database; nd, not detected.

## RESULTS AND DISCUSSION

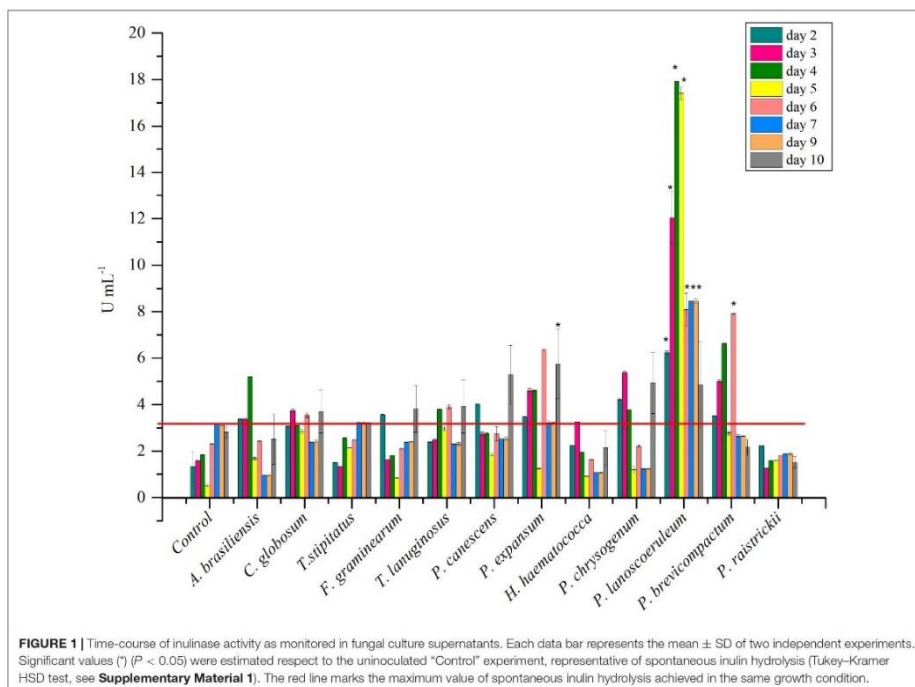
### Screening of a Library of Fungal Strains for Inulinase Production

#### Library Screening

A library of twelve fungi was assembled by choosing among strains with reported evidence in literature of inulinase production and/or for which the presence of genes belonging to the GH32 inulinase family was deduced from querying the CAZY database<sup>5</sup> (Table 1). All the strains were purchased from MUT collection, choosing, when available, those isolated from the rhizosphere or soil environment.

The strain collection was screened for inulinase production in liquid medium. *P. brevicompactum* and *P. lanosocoeruleum* exhibited the best performances. As a fact, the highest level of inulinase activity was detected in the extracellular media of the two abovementioned strains: about 18 U mL<sup>-1</sup> at the 4th day and 9 U mL<sup>-1</sup> at the 6th day, with an I/S ratio equal to 1 and 2, respectively, with these values being indicative of the prevalence of inulinase activity over the invertase one (Singh and Singh, 2010; Figure 1). For all the other tested strains, inulinase production does not go beyond ~5 U mL<sup>-1</sup>. Based on these results, *P. lanosocoeruleum* was selected for further exploitation.

<sup>5</sup><http://www.cazy.org/>



#### Inulinase Production From *P. lanosocoeruleum*

Inulinase production was carried out in liquid cultures (250 mL volume, smooth flasks) using inulin as C-source. When different medium/shake flask volume ratios were tested (1:5; 1:3; 1:2), comparable results were obtained at 1:5 and 1:3 ratios ( $\sim 15$  U mL<sup>-1</sup>), while a significant decrease in inulinase production levels was observed at the 1:2 ratio ( $\sim 5$  U mL<sup>-1</sup>). When the flask geometry was changed from smooth to baffled flasks, no relevant differences in terms of inulinase production levels were observed, whatever was the medium/flask volume ratio used. However, the use of baffled flasks assured more reproducible results, possibly because of a reduced formation of fungal pellets. Interestingly, when the culture was scaled up to 1 L, the use of baffled flasks yielded an almost three-fold higher inulinase production with respect to not-baffled ones ( $\sim 15$  U mL<sup>-1</sup> vs. 5 U mL<sup>-1</sup>), confirming the levels obtained on the small scale.

The type of C-source used for preinoculum growth was found to strongly affect enzyme production in the following inoculum. When the preinoculum was carried out using glucose as C-source, a notable increase in inulinase production was achieved in the following culture step with respect to inulin and fructose.

Inulinase production has been reported to be induced by the presence of inulin itself (Singh and Singh, 2017) and to be sensible to catabolite repression by free sugars (Mahmoud et al., 2011; Singh and Chauhan, 2017; Garuba and Onilude, 2020). Consistently, no inulinase production was observed when the fungus was grown in the presence of fructose or glucose as unique C-sources in the inoculum phase. Moreover, the high fructose concentration in the preinoculum (released by inulin hydrolysis, or directly available in the medium) was found to inhibit further inulinase production in the inoculum phase, while the presence of glucose (the minority monomer in inulin polymer) did not interfere with the following inulinase production (data not shown).

In the optimized condition, *P. lanosocoeruleum* inulinase activity production reached a maximum of 28 U mL<sup>-1</sup> at the 4th day of growth. Inulinase production seems to be growth-associated: as a fact, a decline in enzyme activity was observed after the 4th day, possibly ascribable to the secretion of proteolytic enzymes. A similar profile was already reported for inulinase production in shake-flask fermentations of many fungal species, i.e., *Penicillium* sp. (Rawat et al., 2015b), *Aspergillus fumigatus* (Chikkerur et al., 2018),

*Aspergillus niger* (Mahmoud et al., 2011), and *Aspergillus tritici* (Singh et al., 2020b).

Inulinase activity levels achieved in this work are among the highest ever obtained from submerged fermentation of *Penicillium* strains. A novel strain of *Penicillium subrubescens* (FBCC 1632<sup>1</sup>) isolated from soil has been found to produce up to 7.7 U/mL<sup>-1</sup> when tested on pure inulin (Mansouri et al., 2013), while a production level of 1 U/mL<sup>-1</sup> has been reported for *Penicillium* sp. NFCC 2768, and this strain is much more effective as inulinase producer (up to 3.9 U/mL<sup>-1</sup>) when grown on inulin-rich vegetable infusions with respect to pure inulin (Rawat et al., 2015b). Similarly, four *Penicillium* strains, selected from a fungal library of inulinase producers on inulin-rich plant extract, displayed a production level ranging from 0.5 to 2.7 U/mL<sup>-1</sup> (Rawat et al., 2015a). A higher production level (up to 20 U mL<sup>-1</sup>) has been achieved by Abdal-Aziz and coauthors (Abd Allah AbdAl-Aziz et al., 2012) with *Penicillium citrinum* grown on pure inulin, by increasing the incubation temperature to 35°C. A maximum of 46 U mL<sup>-1</sup> of inulinase production has been reported for *Penicillium* sp. XL10 in an inulin-containing medium after optimization of the supplied nitrogen source (Zheng et al., 2018b), while about 38 U/mL<sup>-1</sup> was obtained with *Penicillium oxalicum* BGPUP-4 in a growth media containing both inulin and lactose (Singh and Chauhan, 2017).

### Characterization of the Inulinase Enzymatic Mixture

Several methods to concentrate proteins from the growth medium were tested to recover an extracellular enzymatic mixture endowed with high inulinase activity, i.e., acetone precipitation, ammonium sulfate precipitation, and ultrafiltration. The latter method provided the highest recovery of enzymatic activity (~90%), as well as an almost doubling of the specific activity of the extract (from 453 to 905 U mg<sup>-1</sup>). Conversely, acetone and ammonium sulfate precipitation resulted in a dramatic drop of the recovered activity (~10% yield of recovered activity), probably due to the high glycosylation level typical of secreted fungal proteins. The notable specific activity of the *P. lanosoceruleum* crude extract (*Plal*) denotes a high inulinase production ability of the strain. As a fact, the specific activity so far reported for enzymatic extracts from *Penicillium* strains ranges from 80 to 740 U mg<sup>-1</sup> and has been achieved after at least two purification steps (Pandey et al., 2016).

The ultrafiltered broth enriched in inulinase activity, herein defined as *Plal*, was further characterized. The effect of temperature on the activity of the inulinase mixture was determined in the range 30–80°C. *Plal* displays a maximum at 50°C and retains >70% of its activity in the range 30–60°C (Figure 2A). The pH activity profile displays a maximum at pH 5, along with a retention of more than 50% of the enzymatic activity in the pH range 4.5–7 (Figure 2B). The heterogeneity of the enzymatic mixture may explain the deviation from a bell-shaped behavior between pH 6 and 7 (Figure 2B). The biochemical properties exhibited by *Plal* are in agreement with the characteristics reported for most of the purified fungal

inulinases, i.e., a pH optimum in a range 4–7 and a temperature optimum in the range 30–60°C (Rawat et al., 2017b).

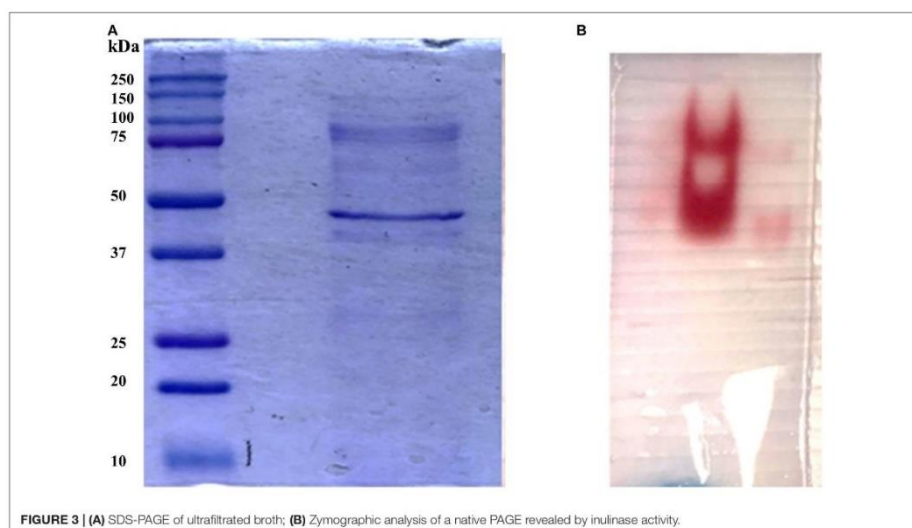
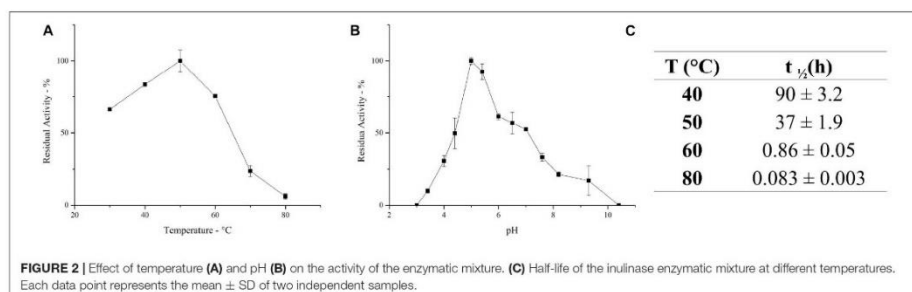
*Plal* thermostability was evaluated at selected temperatures, and  $t_{1/2}$  was calculated at each value (Figure 2C). The mixture shows a very good stability at 40°C, retaining its full activity up to 3 days of incubation. A reduction in thermal stability was observed at 50°C, although the enzymatic mixture still retains 50% of its activity after 37 h. The high activity of *Plal* at 50°C, combined with the observed stability at this temperature, represents an extremely advantageous feature for inulin processing on an industrial scale, allowing the solubilization of inulin at high concentrations (Flores-Gallegos et al., 2015; Qiu et al., 2018). However, a drastic drop in enzyme stability was recorded at higher temperatures: at 60°C, the half-life of the enzymatic mixture is lower than 1 h, while at 80°C it sharply reduces to a few minutes.

### Protein Characterization of the Inulinase Mixture

In order to identify the proteins endowed with inulinase activity, the *Plal* enzymatic mixture was analyzed by zymography, by staining for inulinase activity (Figure 3). The two active protein bands were detected, excised, and analyzed by an *in situ* proteomic approach, and the proteins were identified by searching raw LC-MSMS data against the set of putative proteins encoded in the annotated *P. lanosoceruleum* genome (see text footnote 2).

Table 2 reports the proteins identified in the two active bands (see Supplementary Material 2 for details of identified peptides). Several putative glycosyl hydrolase (GH) proteins of different families were identified in both bands. In the upper band in the gel, 10 proteins were identified; 9 proteins in the lower gel band. Three proteins (Protein ID: 323309; 417764; 371227) were found to be annotated as members of the GH32 family, with two of them present in both gel bands. When submitted to BlastP analysis, Penla1\_323309 displays 74.8 and 72.7% identity with *Aspergillus fumigatus* InuD exoinulinase (Q4WDS4) and *Aspergillus lentulus* exoinulinase InuE (A0A0S7DXQ8), respectively, and is closely related to several other fungal exoinulinases. Penla1\_417764 shows the highest identity (90.9%) with a putative GH32 hydrolase from *Penicillium rubens* as well as 63.4 and 62.5% identity with the exoinulinases InuE from *A. niger* (A2R0E0) and *A. awamori* (Q96TU3), respectively. From the multiple alignment with representative members of fungal exoinulinases, both Penla1\_323309 and Penla1\_417764 exhibit all the conserved motifs and residues characterizing this class of enzymes (Figure 4). Interestingly, the two putative *P. lanosoceruleum* exoinulinases differ for the length of an internal sequence reported to function as an additional non-catalytic inulin-affinity region in *Penicillium* sp. TN-88 InuD, responsible for a higher affinity for the substrate (Moriyama and Ohta, 2007).

Penla1\_371227, instead, resulted to be related to fungal endoinulinases, displaying 74.7 and 69.6% identities with *Penicillium subrubescens* endoinulinase Inu2 and *A. niger* InuA, respectively. Consistently, the Penla1\_371227 sequence reveals the presence of all the conserved motifs and the unique aminoacidic residues described for fungal endoinulinases (Chikkerur et al., 2018; Singh et al., 2020a; Figure 4).



### Inulin Hydrolysis by *Plal* Mixture Using Response Surface Methodology

An experimental design approach was applied to investigate the effect of different parameters on the *Plal*-catalyzed hydrolysis of inulin. In all the tested experimental conditions, inulin was efficiently converted into monomeric sugars (Table 3). ANOVA was used to determine the influence of independent variables on the dependent response. The  $F$  value, which substantiates the significance of the model, is 73.42, which is very high if compared to the critical value, thus indicating its significance (Supplementary Material 3). On the basis of a regression analysis, a second-order polynomial equation in terms of the coded value was generated:

$$\begin{aligned} \text{Fructose} = & -152.7 + 45.32 * A + 6.911 * B - 3.79 * C \\ & - 0.256 * D - 0.211 * A * B - 0.140 * A * C + 0.047 * \\ & A * D + 0.031 * B * C - 0.006 * B * D + 0.007 * C * \\ & D - 2.885 * A^2 - 0.081 * B^2 + 0.038 * C^2 + 0.004 * D^2 \end{aligned}$$

where A is the pH; B, the temperature ( $^{\circ}\text{C}$ ); C, the substrate concentration ( $\text{g L}^{-1}$ ); and D, the enzyme loading ( $\text{U g}^{-1}$ ).

The significance of each parameter's coefficient was assessed by  $\text{Prob} > F$  value: values less than 0.05 indicate the significance of the model terms, and values greater than 0.1 depicts insignificance model terms. In the selected model, all the tested factors (A, B, C, D) have an effect on the hydrolysis process. The interaction effects between pH and temperature ( $A * B$ )

**TABLE 2** | Protein identification in the active gel lanes by LC-MS/MS.

Band gel lane	Protein ID	Score	Number of identified peptides	Protein sequence coverage (%)	Genome annotation	
Lower gel band lane	<b>323309</b>	295	10	19	<b>GH32 family/GH116 family</b>	
	<b>371227</b>	204	8	16	<b>GH32 family</b>	
	376719	166	5	9	Multicopper oxidase	
	327740	165	6	16	GH43 family	
	383312	149	7	14	Glucosylglycosyltransferase	
	387674	122	6	10	GH64 family	
	383083	120	5	16	GH17 family	
	<b>417764</b>	111	4	7	<b>GH32 family</b>	
	381496	62	5	11	Putative oxidoreductase	
	Upper gel band lane	384244	423	20	54	GMC oxidoreductase family
		315441	274	12	42	GH2 family
400960		253	11	32	Uncharacterized protein	
<b>371227</b>		185	10	34	<b>GH32 family</b>	
385992		181	10	32	Amidase	
<b>323309</b>		177	12	33	<b>GH32 family/GH116 family</b>	
401322		99	7	18	GH20 family	
373946		147	11	28	GH3 family	
383654		145	11	31	Uncharacterized protein	
401322		99	7	18	GH20 family	

Protein bands were *in situ* digested and analyzed by LC-MS/MS, and raw data was searched on the protein database as described in details in the "Materials and Methods" section. Search details and extensive description of the identified peptides are reported in **Supplementary Material 2**. The proteins belonging to the Gh32 family are highlighted in bold.

Description of the glycosyl hydrolase (GH) families according to CAZypedia (<http://www.cazypedia.org/>): **GH2**: includes the following activities,  $\beta$ -galactosidases,  $\beta$ -glucuronidases,  $\beta$ -mannosidases, *exo*- $\beta$ -glucosaminidases, and a mannosylglycoprotein *endo*- $\beta$ -mannosidase; **GH3**: groups together *exo*-acting  $\beta$ -D-glucosidases,  $\alpha$ -L-arabinofuranosidases,  $\beta$ -D-xylopyranosidases, *N*-acetyl- $\beta$ -D-glucosaminidases, and *N*-acetyl- $\beta$ -D-glucosaminide phosphorylases; **GH17**: includes two major groups of enzymes with related but distinct substrate specificities, namely, 1,3- $\beta$ -D-glucan *endo*hydrolases and 1,3,1,4- $\beta$ -D-glucan *endo*hydrolases; **GH20**: includes *exo*-acting  $\beta$ -N-acetylglucosaminidases,  $\beta$ -N-acetylgalactosaminidase  $\beta$ -D-SO<sub>3</sub>-N-acetylglucosaminidases, and *exo*-acting lacto-N-biosidases; **GH32**: includes: enzymes able to hydrolyze fructose containing polysaccharides, i.e., inulinases, invertases, levanases, and other; **GH43**: includes the following major activities,  $\alpha$ -L-arabinofuranosidases, *endo*- $\alpha$ -L-arabinanases (or *endo*-processive arabinanases) and  $\beta$ -D-xylosidases; **GH64**: laminaripentaose-producing  $\beta$ (1,3)-glucanases; **GH116**: Includes enzymes with diverse specificities, including  $\beta$ -xylosidase,  $\beta$ -glucosidase, and *N*-acetylglucosaminidase; **GMC oxidoreductase**: glucose dehydrogenase/choline dehydrogenase/mandelonitrile lyase.

and substrate concentration and temperature (B°C) were also significant (**Supplementary Material 3**).

The quadratic terms of pH, temperature, and substrate concentration show significant contribution to the model. *P*-value < 0.0001 suggests that pH and temperature are the experimental variables with the greatest influence on inulin hydrolysis, and therefore a small variation in their value will strongly affect the product formation rate. Moreover, the negative sign of the coded coefficients A and B suggests that the curve is concave.

The *P*-value 0.008 for the quadratic substrate concentration term indicates an effect of this variable on the hydrolysis process, although less significant than that of the pH and T. The positive sign of the relative coefficient indicates that the curve is convex; thus, the uppermost is the substrate concentration, the higher is the amount of released fructose. On the contrary, the probability value of the coefficient of the quadratic effect of enzyme loading is very high (0.337), indicating that the quadratic model does not fit with the observed data. As a fact, the contribution of this parameter is better described by a linear model. The *Lack of Fit F*-value of a model is useful to describe the co-relation between response variable and independent factors. The fitness of our experimental model is proved by a non-significant *Lack of Fit F*-value (0.543). The goodness of the models is also confirmed by the determination ( $R^2 = 0.98$ ) and adjusted determination

coefficients (Adj. $R^2 = 0.97$ ). Moreover, a difference < 0.2 between adjusted  $R^2$  and predicted  $R^2$  (0.95) values further substantiated the robustness of the model.

On the basis of this model, the optimal conditions to maximize inulin conversion (69.4 g L<sup>-1</sup> of fructose) are as follows: T, 45.4°C; pH, 5.1; substrate concentration, 60 g L<sup>-1</sup>; enzyme loading, 50 U g<sub>substrate</sub><sup>-1</sup>.

The three-dimensional surface plots display the interaction between two independent variables on the dependent variables (fructose), while keeping the other two independent variables at their respective optimal values (45.4°C, pH 5.1, inulin 60 g L<sup>-1</sup>, and 50 U g<sub>substrate</sub><sup>-1</sup>) (**Figure 5**). The 3D graph plots of the combined effect of temperature with three variables, i.e., pH, enzyme loading, and substrate concentration, suggest that there is an optimal temperature range between about 35 and 55°C in which the highest fructose concentration can be achieved (**Figures 5A,C,E**). Specifically, in this temperature range, the highest fructose release can be reached if pH is lower than 6. Consequently, a decrease in the response yield is observed out of this temperature range at pH > 6 (**Figure 5A**).

It is worth noting that, in the same optimal temperature range, the substrate concentration has a remarkable effect on the release of fructose, with the highest value was obtained at an increasing inulin amount (**Figure 5B**). Conversely, the combined effect of

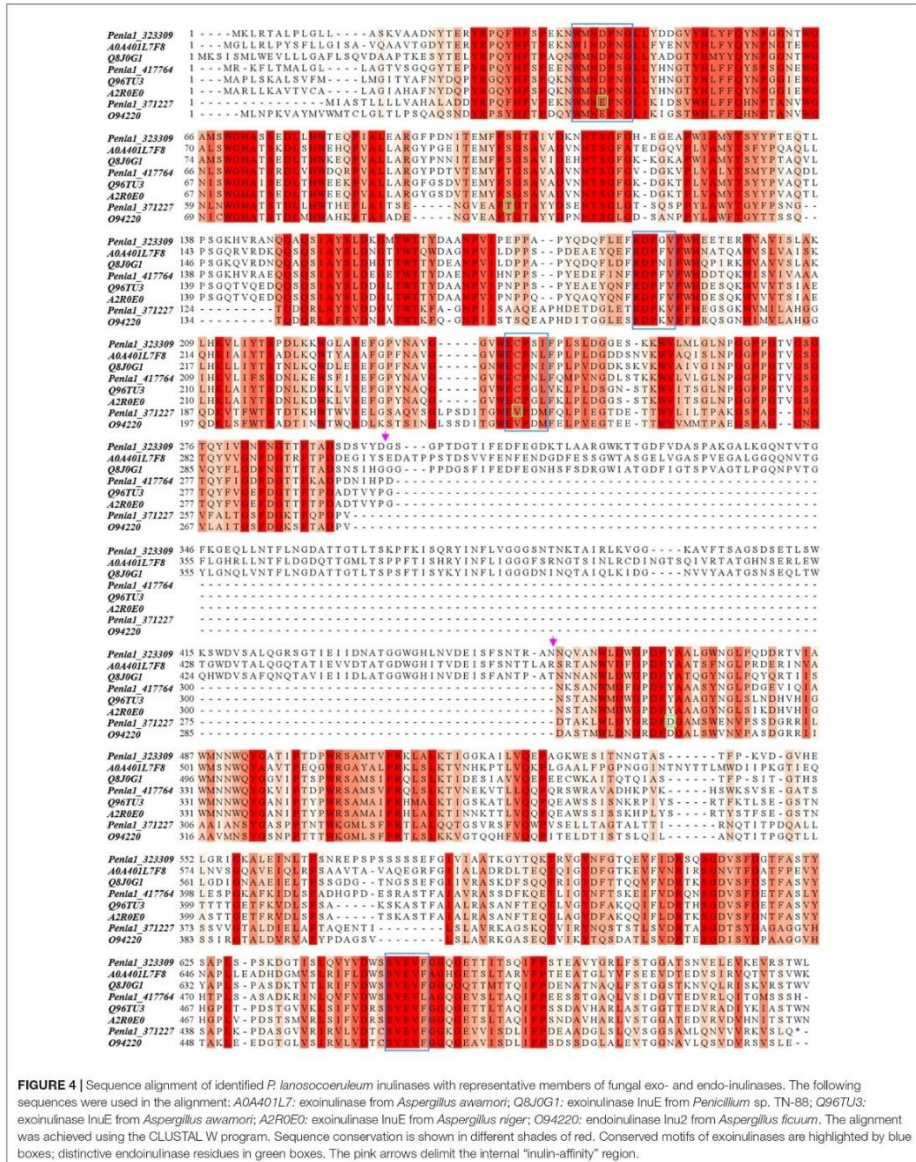


**TABLE 3** | Enzymatic inulin conversion under the experimental conditions (pH, T, substrate concentration, and enzyme loading) explored in the CCRD.

	pH	°C	Substrate concentration (g L <sup>-1</sup> )	U g <sub>substrate</sub> <sup>-1</sup>	Fructose (g L <sup>-1</sup> )	St. dev.	Conversion efficiency %
1	5	37.5	45	27.5	39.66	0.79	73.4
2	5	37.5	45	42.5	44.06	0.64	81.6
3	5	37.5	55	27.5	45.05	1.01	68.3
4	5	37.5	55	42.5	53.23	1.07	80.7
5	5	52.5	45	27.5	38.03	0.98	66.7
6	5	52.5	45	42.5	41.24	0.50	76.4
7	5	52.5	55	27.5	47.26	0.51	71.6
8	5	52.5	55	42.5	52.81	0.24	80.0
9	7	37.5	45	27.5	35.61	0.25	65.9
10	7	37.5	45	42.5	41.95	0.62	77.7
11	7	37.5	55	27.5	37.87	0.21	57.4
12	7	37.5	55	42.5	47.70	0.23	72.3
13	7	52.5	45	27.5	24.72	0.61	45.8
14	7	52.5	45	42.5	32.77	0.08	60.7
15	7	52.5	55	27.5	35.44	1.08	53.7
16	7	52.5	55	42.5	40.17	0.77	60.9
17	4	45	50	35	45.05	0.36	75.1
18	8	45	50	35	26.36	1.07	43.9
19	6	30	50	35	35.01	1.38	58.3
20	6	60	50	35	22.99	0.01	38.3
21	6	45	40	35	42.14	1.26	87.8
22	6	45	60	35	60.00	1.08	83.3
23	6	45	50	20	43.26	0.21	72.1
24	6	45	50	50	53.01	0.59	88.3
25	6	45	50	35	47.07	1.02	78.4
26	6	45	50	35	46.03	0.42	76.7

Fructose concentration has been determined after 24 h incubation. Conversion efficiency has been calculated as reported in the section "Enzymatic Hydrolysis of Inulin".

enzyme loading and temperature is not significant: at the optimal temperature, 45.4°C, more than 60 g L<sup>-1</sup> of fructose can be obtained even when lowering the enzyme amount from 50 to 30 U g<sub>substrate</sub><sup>-1</sup>. Within the optimal temperature range, about 50–60 g L<sup>-1</sup> of fructose is released whatever is the amount of enzyme used (20–50 U g<sub>substrate</sub><sup>-1</sup>) (Figure 5C).

The combined effect of pH and enzyme loading indicates that at the optimal pH (5.1) more than 60 g L<sup>-1</sup> of fructose is obtained using from 30 to 50 U g<sub>substrate</sub><sup>-1</sup>. However, when moving far from the optimum, a comparable response is assured by increasing the enzyme loading (Figure 5D). Similarly to what was observed for temperature, a pH optimal range (4–6.5) can also be identified, within which an increasing amount of fructose can be obtained by increasing the substrate concentration (Figure 5E). Taking together all the observed effects, it can be assumed that within the optimal range of pH and T, fructose release can be adjusted by acting on enzyme and substrate concentrations (Figure 5F). Interestingly, in the investigated range of substrate concentration, from 40 to more than 60 g L<sup>-1</sup> of released fructose can be achieved by using an intermediate enzyme loading (30 U g<sub>substrate</sub><sup>-1</sup>).

In order to validate the RSM model, experiments were carried out in the proximity of the estimated optimal conditions (Table 4). The predicted results were compared to the

experimentally obtained values, and the *T*-test at 95% confidence showed no significant differences between predicted and experimental values.

The ANOVA (*F*-test) applied to the experimental data resulted in an *F*-value of 21.64 and *R*<sup>2</sup> = 0.88. Thus, the proposed RSM model can be a useful tool to predict maximum inulin conversion.

The kinetics of inulin conversion in the optimized hydrolysis condition is reported in Figure 6. The release of fructose increases progressively to reach about 60% in the first 8 h. The 90% is achieved in 16 h, settling in a plateau level of 97% of conversion after 20 h. Experimental data were fitted with a third-order polynomial model. The goodness of the predictive models is confirmed by the determination coefficient (*R*<sup>2</sup> = 0.99).

Although the available literature data on inulin hydrolysis are not easily comparable because of the several variables affecting the process (source and amount of inulin, reaction conditions, determination of inulin conversion) (Sirisansaneeyakul et al., 2007; Mutanda et al., 2009; Saber and El-Nagg, 2009; Wang et al., 2013; Zheng et al., 2018a), the results obtained with *Plal* mixture are worth of notice, since an almost complete hydrolysis at high substrate concentration (60 g L<sup>-1</sup>) was achieved in the optimized conditions. In a similar RSM-based approach, up to 95% fructose yield has been obtained by hydrolysis of 60 g L<sup>-1</sup> Jerusalem artichoke-derived inulin,

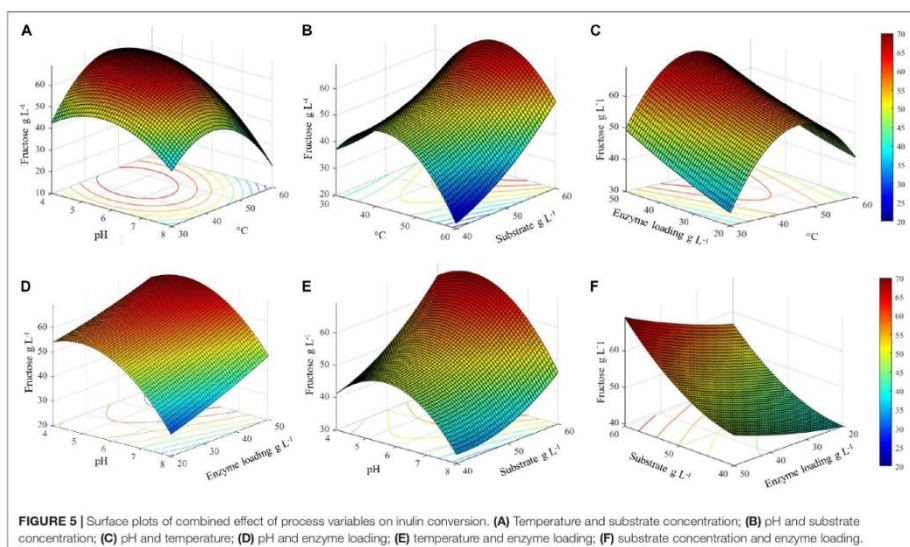


**TABLE 4** | Model validation: predicted and experimental enzymatic inulin conversion around the estimated optimal conditions.

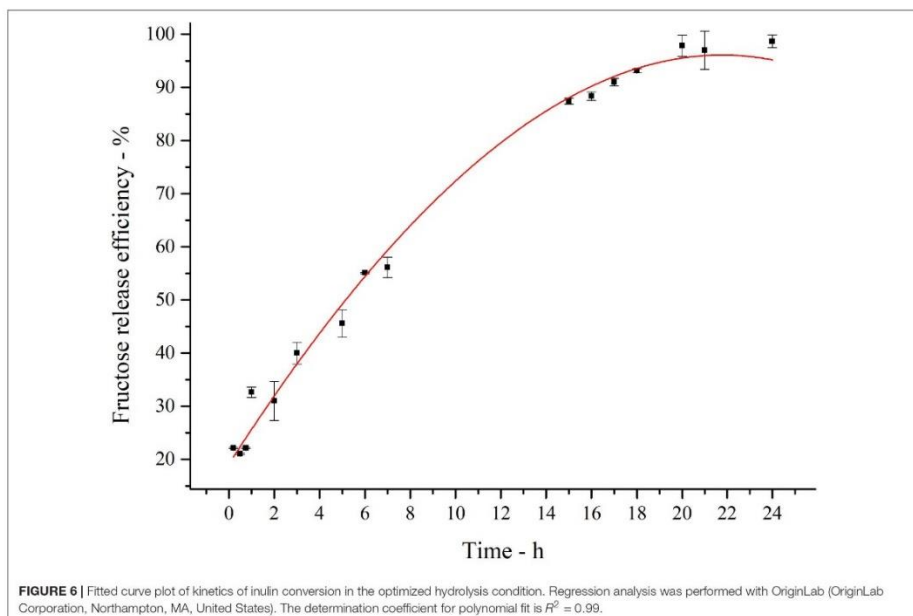
pH	Temperature °C	Substrate concentration $\text{g L}^{-1}$	Enzyme loading $\text{U g}_{\text{substrate}}^{-1}$	Fructose $\text{g L}^{-1}$	
				Predicted	Experimental
5.1	45.5	60	50	69.4	69.8 ± 1.5
5.6	38.2	60	50	65.1	64.2 ± 0.8
4.3	46.6	60	50	67.1	66.4 ± 0.6

with a commercial *A. niger* inulinase ( $10 \text{ U g}^{-1}$ ,  $48^\circ\text{C}$ , pH 4.8) (Sarchami and Rehmann, 2014). The definition of optimal T and pH for inulin hydrolysis by commercial Fructozyme (Novozyme) with an RSM approach has led to a fructose yield of 82.5% after 12 h at  $35^\circ\text{C}$  and pH 5.2, with  $30 \text{ U g}^{-1}$  of Jerusalem artichoke powder (Wang et al., 2013). Statistical optimization of inulin hydrolysis has been applied to immobilized inulinase from *A. tubingensis*, resulting, in the best conditions ( $60^\circ\text{C}$ ,  $10 \text{ U g}^{-1}$ , 12 h), in a hydrolysis yield higher than 70 and 85% from chicory and asparagus inulin, respectively, both supplied at 17.5% (Trivedi et al., 2015). High conversion efficiency (up to 88%) in a short time (5 h) using *P. citrinum* inulinases has been also reported, by using a lower amount of inulin ( $10 \text{ g L}^{-1}$ ) and a very high enzyme loading ( $2,500 \text{ U g}_{\text{substrate}}^{-1}$ ) (El-Hersh et al., 2011). Similarly, a variable degree of hydrolysis, in the range 50–70%, has been shown by using a high amount of *A. tamaritii* AR-IN9 inulinase ( $1,000\text{--}3,000 \text{ U g}$ ) at  $45^\circ\text{C}$ , pH 5.2, after 2 h, depending on the agro-waste used as inulin source (Saber and El-Nagg, 2009).

### Exploitation of *Plal* Mixture in a Process for PHA Production From Inulin

The applicability of the *Plal* mixture was tested in a combined process of inulin hydrolysis and PHA production by *C. necator* DSM428. Previous reports have shown that high PHB accumulation in *C. necator* has been achieved starting from an initial fructose concentration of  $20 \text{ g L}^{-1}$  (Budde et al., 2011a; Koutinas et al., 2013). For the design of an SSF process, *Plal* hydrolytic performances were preliminarily tested in conditions reproducing the *C. necator* culture media ( $\text{MM}_{\text{Cn}}$ , pH 6.8,  $30^\circ\text{C}$ ) containing  $20 \text{ g L}^{-1}$  inulin, corresponding to a maximum yield of  $24 \text{ g L}^{-1}$  releasable fructose.

When different *Plal* amounts ( $10, 20, 40$ , and  $80 \text{ U g}_{\text{substrate}}^{-1}$ ) were tested, the amount of released fructose after 24 h of incubation increases linearly ( $2.4, 3.8, 7.4$ , and  $10.3 \text{ g L}^{-1}$ , respectively). However, all the obtained values were largely below the theoretical ones expected from a complete substrate hydrolysis. Inulinase activity measured in culture resulted to be reduced up to 42% of the initial one, indicating that both the pH

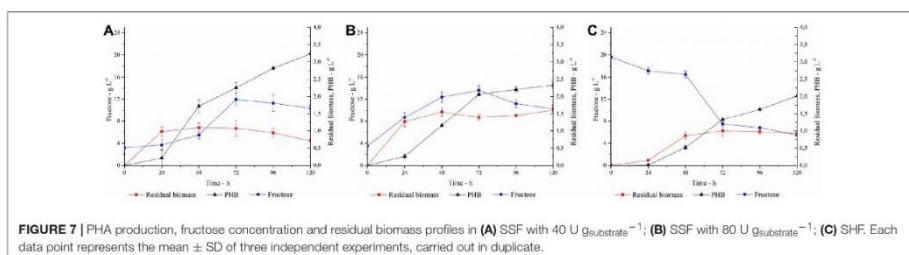


and salt concentration of the growth medium affected the *Plal* enzymatic activity.

In order to ensure an adequate amount of C-source for the microbial growth, the SSF process was carried out adding 40  $\text{U}_{\text{gsubstrate}}^{-1}$  (trial A) or 80  $\text{U}_{\text{gsubstrate}}^{-1}$  (trial B) of *Plal* to the culture medium containing 20  $\text{g L}^{-1}$  inulin, and the process triggered with the simultaneous inoculation of *C. necator* (Figures 7A,B). About 3  $\text{g L}^{-1}$  of fructose was measured at the zero time, the inoculum time, corresponding to the amount of free sugars present in the inulin substrate used in these trials.

In trial A, with a *Plal* concentration of 40  $\text{U}_{\text{gsubstrate}}^{-1}$ , a slow increase in fructose concentration coupled to cellular growth was observed in the first 24 h, after which the cells entered the stationary phase. PHA accumulation started at 24 h and constantly increased during the stationary phase, reaching up to 3.2  $\text{g L}^{-1}$  at 120 h, corresponding to 82% of polymer content. The fructose profile was monitored during the growth and reflects the simultaneity of the two processes, i.e., fructose release due to inulin hydrolysis and its consumption due to microbial growth. The rate of fructose release was higher than its consumption up to 72 h, determining an increase in fructose concentration. Conversely, after 72 h, fructose concentration slightly decreased, probably for a slowdown in the inulin hydrolysis, due to enzyme inactivation and/or inulin consumption. It is worth noting that the *Plal* mixture ensures a high level of fructose during the whole

process, supporting PHA accumulation, despite the unfavorable starting conditions of the growth media for its activity. Most likely, acidification of the culture media and salt consumption occurring during the microbial growth could help in restoring the conditions for optimal *Plal* activity. When the same process was carried out in the presence of 80  $\text{U}_{\text{gsubstrate}}^{-1}$  of *Plal* (Trial B), no increase in polymer accumulation was observed. As a fact, a maximum of 2.3  $\text{g L}^{-1}$  PHA was achieved after 120 h, corresponding to a 60% polymer content. Thus, comparing the two SSF processes, a higher biomass accumulation was obtained in Trial B. The kinetic of polymer accumulation also followed a different trend in the presence of a higher *Plal* loading, displaying a rapid increase up to 72 h, reaching an almost stationary level at 120 h. Hence, a slower and more gradual release of fructose in Trial A seems to be more favorable for PHA accumulation. In both processes, the released glucose was not utilized as C-source, in agreement with data already reported for the same *C. necator* strain (Azubuike et al., 2019). In both trials, a residual fructose settled to about 10  $\text{g L}^{-1}$  at the end of the process, probably due to the exhaustion of other medium components, such as N-source or oxygen, as already reported by Koutinas in 2013 (Koutinas et al., 2013). Further trials carried out using a higher inulin concentration in the growth medium (30  $\text{g L}^{-1}$ ) resulted in an overall inhibition of cellular growth, with about 0.8  $\text{g L}^{-1}$  cdw at 120 h (data not shown). On the other hand, negligible



PHA production ( $0.032 \text{ g L}^{-1}$ ) and biomass levels ( $0.4 \text{ g L}^{-1}$ ) were obtained at 120 h, in a control experiment performed in the absence of *Plal*.

The SSF processes were compared to the SHF one (Trial C) where the best conditions for inulin hydrolysis, as determined by DOE, were applied and the resulting hydrolyzate was used as C-source for the PHA production process (Figure 7C). The pH of the hydrolyzate was adjusted to 6.8, and the fermentation was carried out with a C-source content of  $2 \text{ g L}^{-1}$  and  $20 \text{ g L}^{-1}$  for glucose and fructose, respectively. In this condition, the growth is characterized by a long lag phase, with fructose concentration decreasing slowly in the first 48 h. Polymer accumulation occurred in the stationary growth phase, reaching up to  $2 \text{ g L}^{-1}$  after 120 h, corresponding to about 62% polymer content. As observed in Trial B, the availability of high fructose level in the first growth phase promotes a lower PHA accumulation with respect to the conditions that ensure a more gradual release of fructose (Trial A).

Only few examples have been reported so far on the use of inulin-rich biomasses as renewable feedstocks for PHA production (Koutinas et al., 2013; Haas et al., 2015). Koutinas et al. used ground Jerusalem artichoke tubers as substrate in solid-state fermentation of *Aspergillus awamori*, producing a crude enzymatic mixture that was later employed in the hydrolysis of the inulin extracted from the tubers. The crude hydrolyzate was tested as fermentation medium for PHB production from *C. necator*, achieving up to 52% of intracellular PHB content and a concentration of  $4 \text{ g L}^{-1}$  of polymer (Koutinas et al., 2013). Similarly, Haas et al. described a process for the production of PHB from chicory root hydrolyzate using a commercially available inulinase mix of endo/exo-inulinases, comparing the performances of three different *C. necator* strains. Up to 78% PHB accumulation has been reported for the best-performing strain (Haas et al., 2015).

To our knowledge, this is the first example of SSF finalized to PHA production from inulin. Although it is well reported that the SSF strategy usually leads to superior productivity of the target product with respect to SHF, since it circumvents the inhibitory effect of high sugar concentration on cell growth (Ge et al., 2010; Li et al., 2014); it is worth noting that this process is effective only if fermentation conditions are also optimal for enzyme activity (Wang et al., 2013). The encouraging results obtained in shaken flasks represents a proof of concept of the exploitability of the

*Plal* mixture in the PHA production process by *C. necator*. It is expected that the implementation of the proposed SSF process in bioreactors, with fine controls of oxygen levels, will further improve its performance.

In all the conditions tested (Trials A, B, C), the polymer was extracted and analyzed by H-NMR. The spectra display the presence of three groups of characteristic signals of the homopolymer polyhydroxybutyrate (PHB) (Mostafa et al., 2020): the resonance peak at 1.2 ppm is attributed to the methyl group coupled to one proton; a doublet of quadruplet at 2.4 ppm is attributed to a methylene group adjacent to an asymmetric carbon atom bearing a single proton; and a multiplet at 5.2 ppm is characteristic of the methine group (Supplementary Material 4).

## CONCLUSION

In this work, a new microbial source of inulinase, *P. lanosoceruleum*, was identified by screening a fungal library. Three potentially active inulinases, two related to the exoinulinase and one to the endoinulinase families, were identified in the *Plal* enzymatic mixture.

The application of a statistical experimental design allowed to define the optimal conditions for inulin hydrolysis by *Plal*, leading to envisage its exploitation as effective biocatalyst mixture for inulin processing.

The optimal conditions defined for the hydrolysis could be exported and incorporated into a process for industrial fructose syrup production, since in these conditions the formation of undesired color as well as the production of unwanted by products such as fructose dianhydrides are prevented (Mutanda et al., 2009). Additionally, information on the isoenzymes composition of the *Plal* mixture represents the starting point for further characterization of the single isoenzymes, to be carried out through their purification from the culture broth or their recombinant expression in suitable hosts. The availability of each single isoenzyme will allow the formulation of inulinase mixtures with different composition in terms of endo- and exo- inulinase activities, addressing specific applications, such as the generation of fructose as well as of inulo-oligosaccharides (IOS) for applications as probiotics in food and pharmaceutical industries.

The integration of *Plal*-catalyzed hydrolysis within a fermentation process finalized to the production of added-value

bio-based products was tested, using PHA production as a case study. Two different process configurations, such as SHF and SSF, were explored, with the latter displaying the best performances in terms of biopolymer yields.

In conclusion, the results herein described let to foresee a profitable and versatile utilization of the *Plal* mixture in inulin-based biorefineries.

## DATA AVAILABILITY STATEMENT

The original contributions presented in the study are included in the article/**Supplementary Material**, further inquiries can be directed to the corresponding author.

## AUTHOR CONTRIBUTIONS

IC: investigation, DOE experiments, PHA production, and formal analysis. NC: investigation, screening of fungal library, and inulinase characterization. GN: proteomic analysis. CP: conceptualization and writing of original draft. LB: supervision.

## REFERENCES

- Abd, A. A., Aty, E., Wehaidy, H. R., and Mostafa, F. A. (2014). Optimization of inulinase production from low cost substrates using Plackett - Burman and Taguchi methods. *Carbohydr. Polym.* 102, 261–268.
- Abd Allah AbdAl-Aziz, S., El-Metwally, M. M., and Ismail Ali Saber, W. E. (2012). Molecular identification of a novel inulinolytic fungus isolated from and grown on tubers of *Helianthus tuberosus* and statistical screening of medium components. *World J. Microbiol. Biotechnol.* 28, 3245–3254. doi: 10.1007/s11274-012-1134-y
- Azubuikwe, C., Edwards, M., Gatehouse, A., and Howard, T. P. (2019). Data driven modelling of a chemically defined growth medium for *Cupriavidus necator* H16. *bioRxiv* [Preprint]. doi: 10.1101/548891
- Battaglia, E., Benoit, I., Brink, J., Van Den Wiebenga, A., Coutinho, P. M., Henriksat, B., et al. (2011). Carbohydrate-active enzymes from the zygomycete fungus *Rhizopus oryzae*: a highly specialized approach to carbohydrate degradation depicted at genome level. *BMC Genom.* 12:38. doi: 10.1186/1471-2164-12-38
- Bedzo, O. K. K., Mandegari, M., and Görgens, J. F. (2020). Techno-economic analysis of inuloigosaccharides, protein, and biofuel co-production from *Jerusalem artichoke* tubers: a biorefinery approach. *Biofuels Bioprod. Bioref.* 14, 776–793. doi: 10.1002/bbb.2105
- Bhatia, S. K., Yoon, J. J., Kim, H. J., Hong, J. W., Gi Hong, Y., Song, H. S., et al. (2018). Engineering of artificial microbial consortia of *Ralstonia eutropha* and *Bacillus subtilis* for poly(3-hydroxybutyrate-co-3-hydroxyvalerate) copolymer production from sugarcane sugar without precursor feeding. *Bioresour. Technol.* 257, 92–101. doi: 10.1016/j.biortech.2018.02.056
- Bradford, M. M. (1976). A rapid and sensitive method for the quantitation of microgram quantities of protein utilizing the principle of protein-dye binding. *Anal. Biochem.* 72, 248–254.
- Budde, C. F., Riedel, S. L., Hübner, F., Risch, S., Popovix, M. K., Rha, C., et al. (2011a). Growth and polyhydroxybutyrate production by *Ralstonia eutropha* in emulsified plant oil medium. *Appl. Microbiol. Biotechnol.* 89, 1611–1619. doi: 10.1007/s00253-011-3102-0
- Budde, C. F., Riedel, S. L., Willis, L. B., Rha, C., and Sinskey, A. J. (2011b). Production of poly(3-hydroxybutyrate-co-3-hydroxyhexanoate) from plant oil by engineered *Ralstonia eutropha* strains. *Appl. Environ. Microbiol.* 77, 2847–2854. doi: 10.1128/AEM.02429-10
- Chen, J. S., Saxton, J., Hemming, F. W., and Peberdy, J. F. (1996). Purification and partial characterization of the high and low molecular weight form

GS: supervision and funding acquisition. All authors contributed to the article and approved the submitted version.

## FUNDING

This work was supported by grants from PRIN: Progetti di ricerca di Rilevante Interesse Nazionale – Bando 2017. “CARDoon valorisation by InteGrAted biorefiNery (CARDIGAN).” IC acknowledges Università degli Studi di Napoli Federico II for doctoral fellowships. GN received funding from the Marie Skłodowska-Curie Grant Agreement No. 722606, TEMPERA (Teaching Emerging Methods in Palaeoproteomics for the European Research Area).

## SUPPLEMENTARY MATERIAL

The Supplementary Material for this article can be found online at: <https://www.frontiersin.org/articles/10.3389/fbioe.2021.616908/full#supplementary-material>

- (S- and F-form) of invertase secreted by *Aspergillus nidulans*. *Biochim. Biophys. Acta Protein Struct. Mol. Enzymol.* 1296, 207–218. doi: 10.1016/0167-4838(96)00073-8
- Chi, Z., Chi, Z., Zhang, T., Liu, G., and Yue, L. (2009). Inulinase-expressing microorganisms and applications of inulinases. *Appl. Microbiol. Biotechnol.* 82, 211–220. doi: 10.1007/s00253-008-1827-1
- Chi, Z. M., Zhang, T., Cao, T. S., Liu, X. Y., Cui, W., and Zhao, C. H. (2011). Biotechnological potential of inulin for bioprocesses. *Bioresour. Technol.* 102, 4295–4303. doi: 10.1016/j.biortech.2010.12.086
- Chikkerur, J., Samanta, A. K., Dhali, A., Kolte, A. P., Roy, S., and Maria, P. (2018). In Silico evaluation and identification of fungi capable of producing endoinulinase enzyme. *PLoS One* 13:e0200607. doi: 10.1371/journal.pone.0200607
- Chikkerur, J., Samanta, A. K., Kolte, A. P., Dhali, A., and Roy, S. (2020). Production of short chain fructo-oligosaccharides from inulin of chicory root using fungal Endoinulinase. *Appl. Biochem. Biotechnol.* 191, 695–715. doi: 10.1007/s12010-019-03215-7
- Choi, H. Y., Ryu, H. K., Park, K. M., Lee, E. G., Lee, H., Kim, S. W., et al. (2012). Direct lactic acid fermentation of *Jerusalem artichoke* tuber extract using *Lactobacillus paracasei* without acidic or enzymatic inulin hydrolysis. *Bioresour. Technol.* 114, 745–747. doi: 10.1016/j.biortech.2012.03.075
- El-Hersh, M. S., Saber, W. I. A., and Ali El-Nag, N. E.-A. (2011). Production strategy of inulinase by *Penicillium citrinum* AR-IN2 on some agricultural by-products. *Microbiol. J.* 1, 79–88. doi: 10.3923/mj.2011.79.88
- Fernandes, M. R. V. S., Nsabimana, C., and Jiang, B. (2012). *Penicillium expansum* SK 16 as a novel inulinase-producing strain isolated from decomposed dahlia tubers. *Res. J. Biotechnol.* 7, 102–106.
- Flores-Gallegos, A. C., Contreras-Esquivel, J. C., Morlett-Chávez, J. A., Aguilar, C. N., and Rodríguez-Herrera, R. (2015). Comparative study of fungal strains for thermostable inulinase production. *J. Biosci. Bioeng.* 119, 421–426. doi: 10.1016/j.jbiosc.2014.09.020
- Garuba, E. O., and Onilude, A. A. (2020). Exo-Inulinase Production by a catabolite repression-resistant mutant *Thermophilic Aspergillus tamaris* -U4 in solid state fermentation. *Biotechnol. J. Inter.* 24, 21–31. doi: 10.9734/BJI/2020/v24i43 0110
- Ge, X. Y., Qian, H., and Zhang, W. G. (2010). Enhancement of L-lactic acid production in *Lactobacillus casei* from *Jerusalem artichoke* tubers by kinetic optimization and citrate metabolism. *J. Microbiol. Biotechnol.* 20, 101–109. doi: 10.4014/jmb.0905.05032
- Gonçalves, H. B., Jorge, J. A., and Guimarães, L. H. S. (2016). Production and characterization of an extracellular  $\beta$ -D-Fructofuranosidase from *Fusarium*

- Graminearum* during solid-state fermentation using wheat bran as a carbon source. *J. Food Biochem.* 40, 655–663. doi: 10.1111/jfbc.12253
- Gujar, V. V., Fuke, P., Khardanavis, A. A., and Purohit, H. J. (2018). Draft genome sequence of *Penicillium chrysogenum* strain HKF2, a fungus with potential for production of prebiotic synthesizing enzymes. *3 Biotech.* 5, 5–9.
- Guzik, M., Witko, T., Steinbüchel, A., Wojnarowska, M., Sołtysik, M., and Wawak, S. (2020). What has been trending in the research of Polyhydroxyalkanoates? A systematic review. *Front. Bioeng. Biotechnol.* 8:959. doi: 10.3389/fbioe.2020.00959
- Haas, C., Steinwandter, V., De Apodaca, E. D., Madurga, B. M., Smerilli, M., Dietrich, T., et al. (2015). Production of PHB from chicory roots - comparison of three *Cupriavidus necator* STRAINS. *Chem. Biochem. Eng. Q.* 29, 99–112. doi: 10.15255/CABEQ.2014.2250
- Hughes, S. R., Qureshi, N., López-Núñez, J. C., Jones, M. A., Jarodsky, J. M., Galindo-Leva, L. Á, et al. (2017). Utilization of inulin-containing waste in industrial fermentations to produce biofuels and bio-based chemicals. *World J. Microbiol. Biotechnol.* 33, 1–15. doi: 10.1007/s11274-017-2241-6
- Khatun, M. M., Liu, C. G., Zhao, X. Q., Yuan, W. J., and Bai, F. W. (2017). Consolidated ethanol production from *Jerusalem artichoke* tubers at elevated temperature by *Saccharomyces cerevisiae* engineered with inulinase expression through cell surface display. *J. Ind. Microbiol. Biotechnol.* 44, 295–301. doi: 10.1007/s10295-016-1881-0
- Koutinas, A. A., Garcia, I. L., Kopsahelis, N., Papanikolaou, S., Webb, C., Villar, M. A., et al. (2013). Production of fermentation feedstock from *jerusalem artichoke* tubers and its potential for polyhydroxybutyrate synthesis. *Waste Biomass Valoriz.* 4, 359–370. doi: 10.1007/s12649-012-9154-2
- Kumar, P., Maharjan, A., Jun, H. B., and Kim, B. S. (2019). Bioconversion of lignin and its derivatives into polyhydroxyalkanoates: challenges and opportunities. *Biotechnol. Appl. Biochem.* 66, 153–162. doi: 10.1002/bab.1720
- Laemmli, U. K. (1970). Cleavage of structural proteins during the assembly of the head of bacteriophage T4. *Nature* 227, 680–685.
- Lettera, V., Piscitelli, A., Leo, G., Birolo, L., Pezzella, C., and Sannia, G. (2010). Identification of a new member of *Pleurotus ostreatus* lactase family from mature fruiting body. *Fungal Biol.* 114, 724–730. doi: 10.1016/j.funbio.2010.06.004
- Li, L., Chen, C., Li, K., Wang, Y., Gao, C., Ma, C., et al. (2014). Efficient simultaneous saccharification and fermentation of inulin to 2,3-butanediol by thermophilic *Bacillus licheniformis* ATCC 14580. *Appl. Environ. Microbiol.* 80, 6458–6464. doi: 10.1128/AEM.01802-14
- Li, L., Li, L., Wang, Y., Du, Y., and Qin, S. (2013). Biorefinery products from the inulin-containing crop *Jerusalem artichoke*. *Biotechnol. Lett.* 35, 471–477. doi: 10.1007/s10529-012-1104-3
- Linn, R., Bonaduce, I., Ntasi, G., Birolo, L., Yasur-Landau, A., Cline, E. H., et al. (2018). Evolved gas analysis-mass spectrometry to identify the earliest organic binder in aegean style wall paintings. *Angew. Chem. Int. Edn.* 57, 13257–13260. doi: 10.1002/anie.201806520
- Mahmoud, D. A. R., Mahdy, E. S. M. F., Shousha, W. G., Refaat, H. W., and Abdel-Fattah, A. F. (2011). Raw garlic as a new substrate for inulinase production in comparison to dry garlic. *Aust. J. Basic Appl. Sci.* 5, 453–462.
- Mansouri, S., Houbraken, J., Samson, R. A., Frisvad, J. C., Christensen, M., Tuthill, D. E., et al. (2013). *Penicillium subrubescens*, a new species efficiently producing inulinase. *Antonie Leeuwenh. Int. J. Gen. Mol. Microbiol.* 103, 1343–1357. doi: 10.1007/s10482-013-9915-3
- Medeiros Garcia Alcántara, J., Distante, F., Storti, G., Moscatelli, D., Morbidelli, M., and Sponchioni, M. (2020). Current trends in the production of biodegradable bioplastics: the case of polyhydroxyalkanoates. *Biotechnol. Adv.* 42:107582. doi: 10.1016/j.biotechadv.2020.107582
- Meng, Q., Lu, C., Gao, H., Chen, G., Wu, L., Wu, J., et al. (2021). Efficient biosynthesis of exopolysaccharide from *Jerusalem artichoke* using a novel strain of *Bacillus velezensis* LT-2. *Bioresour. Technol.* 320:124346. doi: 10.1016/j.biortech.2020.124346
- Miller, G. L. (1959). Use of dinitrosalicylic acid reagent for determination of reducing sugar. *Anal. Chem.* 31, 426–428. doi: 10.1021/ac60147a030
- Moriyama, S., and Ohta, K. (2007). Functional characterization and evolutionary implication of the internal 157-amino-acid sequence of an exoinulinase from *Penicillium* sp. strain TN-88. *J. Biosci. Bioeng.* 103, 293–297. doi: 10.1263/jbb.103.293
- Mostafa, Y. S., Alrumman, S. A., Alamri, S. A., Otaif, K. A., Mostafa, M. S., and Alfaify, A. M. (2020). Bioplastic (poly-3-hydroxybutyrate) production by the marine bacterium *Pseudodonghicola xiamenensis* through date syrup valorization and structural assessment of the biopolymer. *Sci. Rep.* 10, 1–13. doi: 10.1038/s41598-020-65858-5
- Mutanda, T., Wilhelm, B., and Whiteley, C. G. (2009). Controlled production of fructose by an exoinulinase from *Aspergillus ficuum*. *Appl. Biochem. Biotechnol.* 159, 65–77. doi: 10.1007/s12010-008-8479-6
- Nguyen, Q. D., Sujtő, N. M., Bujna, E., Hoschke, Á, and Rezessy-szabó, J. M. (2013). Effects of medium composition and process parameters on the production of extracellular inulinase by *Thermomyces lanuginosus*. *Food Technol. Biotechnol.* 51, 36–44.
- Pandey, A., Negi, S., and Soccol, C. R. (2016). *Current Developments in Biotechnology and Bioengineering: Production, Isolation and Purification of Industrial Products*. Amsterdam: Elsevier. doi: 10.1016/j.jclepro.2017.05.040
- Pessoni, R. A. B., and Braga, M. R. (2007). Purification and properties of exoinulinases from *Penicillium janczewskii* growing on distinct carbon sources purification and properties of exo-inulinases from *Penicillium janczewskii* growing on distinct carbon sources. *Mycologia* 99, 493–503. doi: 10.3852/mycologia.99.4.493
- Qiu, Y., Lei, P., Zhang, Y., Sha, Y., Zhan, Y., Xu, Z., et al. (2018). Recent advances in bio-based multi-products of agricultural *Jerusalem artichoke* resources. *Biotechnol. Biofuels* 11, 1–15. doi: 10.1186/s13068-018-1152-6
- Qiu, Y., Zhang, Y., Zhu, Y., Sha, Y., Xu, Z., Feng, X., et al. (2019a). Improving poly-(γ-glutamic acid) production from a glutamic acid-independent strain from inulin substrate by consolidated bioprocessing. *Bioproc. Biosyst. Eng.* 42, 1711–1720. doi: 10.1007/s00449-019-02167-w
- Qiu, Y., Zhu, Y., Zhan, Y., Zhang, Y., Sha, Y., Xu, Z., et al. (2019b). Systematic unravelling of the inulin hydrolase from *Bacillus amyloliquefaciens* for efficient conversion of inulin to poly-(γ-glutamic acid). *Biotechnol. Biofuels* 12, 1–14. doi: 10.1186/s13068-019-1485-9
- Rawat, H. K., Ganaie, M. A., and Kango, N. (2015a). Production of inulinase, fructosyltransferase and sucrose from fungi on low-value inulin-rich substrates and their use in generation of fructose and fructo-oligosaccharides. *Antonie Leeuwenh. Int. J. Gen. Mol. Microbiol.* 107, 799–811. doi: 10.1007/s10482-014-0373-3
- Rawat, H. K., Jain, S. C., and Kango, N. (2015b). Production and properties of inulinase from *Penicillium* sp. NFCC 2768 grown on inulin-rich vegetal infusions. *Biocatal. Biotransform.* 33, 61–68. doi: 10.3109/10242422.2015.1018188
- Rawat, H. K., Soni, H., Kango, N., and Kumar, C. G. (2017a). Continuous generation of fructose from *Taraxacum officinale* tap root extract and inulin by immobilized inulinase in a packed-bed reactor. *Biocatal. Agric. Biotechnol.* 9, 134–140. doi: 10.1016/j.cbab.2016.11.007
- Rawat, H. K., Soni, H., Treichel, H., and Kango, N. (2017b). Biotechnological potential of microbial inulinases: recent perspective. *Crit. Rev. Food Sci. Nutr.* 57, 3818–3829. doi: 10.1080/10408398.2016.1147419
- Raza, Z. A., Abid, S., and Banat, I. M. (2018). Polyhydroxyalkanoates: characteristics, production, recent developments and applications. *Int. Biodeterior. Biodegrad.* 126, 45–56. doi: 10.1016/j.ibiod.2017.10.001
- Saber, W. I. A., and El-Nagg, N. E. (2009). Optimization of fermentation conditions for the biosynthesis of inulinase by the new source: *Aspergillus tamarii* and hydrolysis of some inulin containing agro-wastes. *Biotechnology* 8, 425–433. doi: 10.3923/biotech.2009.425.433
- Samui, A. B., and Kanai, T. (2019). Polyhydroxyalkanoates based copolymers. *Int. J. Biol. Macromol.* 140, 522–537. doi: 10.1016/j.ijbiomac.2019.08.147
- Sarchami, T., and Rehmann, L. (2014). Optimizing enzymatic hydrolysis of inulin from *Jerusalem artichoke* tubers for fermentative butanol production. *Biomass Bioenergy* 69, 175–182. doi: 10.1016/j.biombioe.2014.07.018
- Sayyed, R. Z., Gangurde, N. S., and Chincholkar, S. B. (2009). Hypochlorite digestion method for efficient recovery of PHB from *Alcaligenes faecalis*. *Indian J. Microbiol.* 49, 230–232. doi: 10.1007/s12088-009-0036-7
- Singh, N., Yadav, M., Khanna, S., and Sabu, O. (2017). Sustainable fragrance cum antimicrobial finishing on cotton: indigenous essential oil. *Sustain. Chem. Pharm.* 5, 22–29. doi: 10.1016/j.scp.2017.01.003

- Singh, R., and Chauhan, K. (2016). Production, purification, characterization and applications of fungal inulinases. *Curr. Biotechnol.* 7:19. doi: 10.2174/2211550105666160512142330
- Singh, R. S., and Chauhan, K. (2017). Inulinase production from a new inulinase producer, *Penicillium oxalicum* BGPUP-4. *Biocatal. Agric. Biotechnol.* 9, 1–10. doi: 10.1016/j.bcab.2016.10.012
- Singh, R. S., and Singh, R. P. (2010). Production of fructooligosaccharides from inulin by endoinulinases and their prebiotic potential. *Food Technol. Biotechnol.* 48, 435–450.
- Singh, R. S., and Singh, R. P. (2017). "18 - Inulinases," in *Current Developments in Biotechnology and Bioengineering*, eds A. Pandey, S. Negi, and C. R. Soccol (Amsterdam: Elsevier), 423–446.
- Singh, R. S., Singh, T., Hassan, M., and Kennedy, J. F. (2020a). Updates on inulinases: structural aspects and biotechnological applications. *Int. J. Biol. Macromol.* 164, 193–210. doi: 10.1016/j.ijbiomac.2020.07.078
- Singh, R. S., Singh, T., and Pandey, A. (2020b). Fungal endoinulinase production from raw *Asparagus inulin* for the production of fructooligosaccharides. *Bioresour. Technol. Rep.* 10:100417. doi: 10.1016/j.biteb.2020.100417
- Singh, R. S., Singh, T., and Kennedy, J. F. (2021). Understanding the interactive influence of hydrolytic conditions on biocatalytic production of fructooligosaccharides from inulin. *Int. J. Biol. Macromol.* 166, 9–17. doi: 10.1016/j.ijbiomac.2020.11.171
- Singh, R. S., Singh, T., and Larroche, C. (2019). Biotechnological applications of inulin-rich feedstocks. *Bioresour. Technol.* 273, 641–653. doi: 10.1016/j.biortech.2018.11.031
- Sirisansaneeyakul, S., Worawuthiyayan, N., Vanichsriratanana, W., Srinophakun, P., and Chisti, Y. (2007). Production of fructose from inulin using mixed inulinases from *Aspergillus niger* and *Candida guilliermondii*. *World J. Microbiol. Biotechnol.* 23, 543–552. doi: 10.1007/s11274-006-9258-6
- Surendran, A., Lakshmanan, M., Chee, J. Y., Sulaiman, A. M., Thuoc, D., and Van Suresh, K. (2020). Can polyhydroxyalkanoates be produced efficiently from waste plant and animal oils? *Front. Bioeng. Biotechnol.* 8:169. doi: 10.3389/fbioe.2020.00169
- Trivedi, S., Divecha, J., Shah, T., and Shah, A. (2015). Rapid and efficient bioconversion of chicory inulin to fructose by immobilized thermostable inulinase from *Aspergillus tubingensis* CR16. *Bioresour. Bioprocess.* 2:32. doi: 10.1186/s40643-015-0060-x
- Tsang, Y. F., Kumar, V., Samadar, P., Yang, Y., Lee, J., Ok, Y. S., et al. (2019). Production of bioplastic through food waste valorization. *Environ. Int.* 127, 625–644. doi: 10.1016/j.envint.2019.03.076
- Vastano, M., Corrado, I., Sannia, G., Solaiman, D. K. Y., and Pezzella, C. (2019). Conversion of no/low value waste frying oils into biodiesel and polyhydroxyalkanoates. *Sci. Rep.* 9, 1–8. doi: 10.1038/s41598-019-50278-x
- Vinciguerra, R., Galano, E., Vallone, F., Greco, G., Vergara, A., Bonaduce, I., et al. (2015). Deglycosylation step to improve the identification of egg proteins in art samples. *Anal. Chem.* 87, 10178–10182. doi: 10.1021/acs.analchem.5b02423
- Vries, R. P., De Riley, R., Wiebenga, A., Aguilar-osorio, G., Amillis, S., Uchima, C. A., et al. (2017). Comparative genomics reveals high biological diversity and specific adaptations in the industrially and medically important fungal genus *Aspergillus*. *Genome Biol.* 18:28. doi: 10.1186/s13059-017-1151-0
- Wang, L., Xue, Z., Zhao, B., Yu, B., Xu, P., and Ma, Y. (2013). Jerusalem artichoke powder: a useful material in producing high-optical-purity l-lactate using an efficient sugar-utilizing thermophilic *Bacillus coagulans* strain. *Bioresour. Technol.* 130, 174–180. doi: 10.1016/j.biortech.2012.11.144
- Zhao, C. H., Cui, W., Liu, X. Y., Chi, Z. M., and Madzak, C. (2010). Expression of inulinase gene in the oleaginous yeast *Yarrowia lipolytica* and single cell oil production from inulin-containing materials. *Metab. Eng.* 12, 510–517. doi: 10.1016/j.ymben.2010.09.001
- Zheng, Z., Xu, Q., and Liu, P. (2018a). Enhanced inulin Saccharification by self-produced inulinase from a newly isolated *Penicillium* sp. and its application in D -Lactic acid production. *Appl. Biochem. Biotechnol.* 186, 122–131.
- Zheng, Z., Xu, Q., Liu, P., Zhou, F., and Ouyang, J. (2018b). Enhanced inulin saccharification by self-produced inulinase from a newly isolated *Penicillium* sp. and its application in d-Lactic acid production. *Appl. Biochem. Biotechnol.* 186, 122–131. doi: 10.1007/s12010-018-2730-6
- Zhong, Y., Godwin, P., Jin, Y., and Xiao, H. (2020). Biodegradable polymers and green-based antimicrobial packaging materials: a mini-review. *Adv. Ind. Eng. Polym. Res.* 3, 27–35. doi: 10.1016/j.aiepr.2019.11.002

**Conflict of Interest:** The authors declare that the research was conducted in the absence of any commercial or financial relationships that could be construed as a potential conflict of interest.

Copyright © 2021 Corrado, Cascelli, Ntasi, Birolo, Sannia and Pezzella. This is an open-access article distributed under the terms of the Creative Commons Attribution License (CC BY). The use, distribution or reproduction in other forums is permitted, provided the original author(s) and the copyright owner(s) are credited and that the original publication in this journal is cited, in accordance with accepted academic practice. No use, distribution or reproduction is permitted which does not comply with these terms.



## Optimization of inulin Hydrolysis by *Penicillium lanoscoeruleum* inulinases and efficient conversion into Polyhydroxyalkanoates

### Supplementary materials

**S1.** Significance values were estimated through Tukey-Kramer HSD test ( $p < 0.05$ ), comparing each mean to a control experiment that represents spontaneous inulin hydrolysis. Means that non share a letter are significantly different.

	Day								
	2	3	4	5	6	7	9	10	
Control	3.1 <sup>a</sup>	3.1 <sup>a</sup>	3.1 <sup>a</sup>	3.1 <sup>a</sup>					
<i>A. brasiliensis</i>	3.4 <sup>b</sup>	3.4 <sup>a</sup>	5.2 <sup>d</sup>	1.7	2.4	1.0	1.0	2.5	
<i>C. globosum</i>	3.1 <sup>ab</sup>	3.7 <sup>ab</sup>	3.1 <sup>a</sup>	2.9	3.5 <sup>ab</sup>	2.4	2.4	3.7 <sup>a</sup>	
<i>T. stipitatus</i>	1.5	1.3	2.6	2.1	2.5	3.2 <sup>ab</sup>	3.2 <sup>a</sup>	3.2 <sup>a</sup>	
<i>F. graminearum</i>	3.6 <sup>d</sup>	1.6	1.8	0.8	2.1	2.4	2.4	3.8 <sup>a</sup>	
<i>T. lanuginosus</i>	2.4	2.5	3.8 <sup>b</sup>	3.0	3.9 <sup>b</sup>	2.3	2.3	3.9 <sup>a</sup>	
<i>P. canescens</i>	4.0 <sup>e</sup>	2.7	2.7	1.9	2.7	2.5	2.5	5.3 <sup>b</sup>	
<i>P. expansum</i>	3.5 <sup>bc</sup>	4.6 <sup>bc</sup>	4.6 <sup>c</sup>	1.3	7.3 <sup>c</sup>	3.2 <sup>ab</sup>	3.2 <sup>a</sup>	5.8 <sup>c</sup>	
<i>H. haematococca</i>	2.2	3.3	2.0	0.9	1.6	1.1	1.1	2.1	
<i>P. chrysogenum</i>	4.2 <sup>f</sup>	5.4 <sup>c</sup>	3.8 <sup>b</sup>	1.2	2.2	1.2	1.2	4.9 <sup>ab</sup>	
<i>P. lanoscoeruleum</i>	6.2 <sup>g</sup>	12.0 <sup>d</sup>	17.9 <sup>f</sup>	17.4 <sup>b</sup>	8.1 <sup>d</sup>	8.5 <sup>c</sup>	8.5 <sup>b</sup>	4.8 <sup>ab</sup>	
<i>P. brevicompactum</i>	3.5 <sup>cd</sup>	5.0 <sup>c</sup>	6.6 <sup>e</sup>	2.8	7.9 <sup>c</sup>	2.6	2.6	2.2	
<i>P. raistrickii</i>	2.2	1.3	1.6	1.6	1.8	1.9	1.9	1.5	

**S2. Identification of all *P. lanosocoeruleum* proteins in two active gel band lanes by LC-MS/MS analysis.**

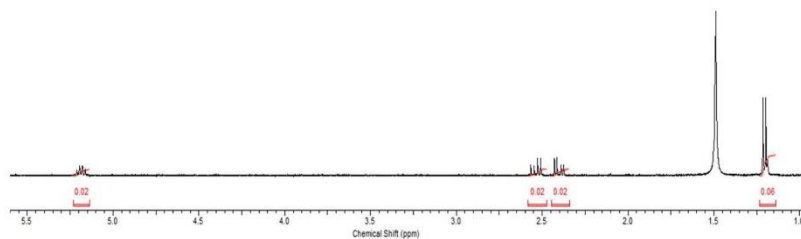
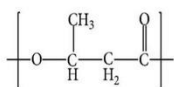
Protein code	m/z	Ion Score	Charge	Lower gel band lane	
					Peptide
323309	381.2071	17	2		R.SAMTVPR.K
	491.2646	47	2		K.VDGVHELGR.I
	493.8103	21	2		R.WVAVISLAK.L
	513.3074	45	2		K.AILVQEPAGK.W
	574.8382	38	3		K.VLIYTSPLDK.K
	639.3499	15	2		K.ALEINLTFSNR.E
	479.2473	26	3		R.YRPQFHFSPEK.N
	501.2348	28	3		R.DPGVFWHEETER.W
	826.4368	12	2		R.LFSTGGATSNVELEVK.E
	1051.546	23	3		K.ALEINLTFSNREPSPPSSSSSEFGVIAATK.G
371227	404.2174	24	2		K.GMLSFPRT
	461.7475	28	2		K.LWLDYGR.D
	504.2562	34	2		K.VFFHEGSGK.W
	587.3369	56	2		R.TLALQQTGSVR.S
	593.3001	15	2		K.VTFWTSTDTK.H
	609.8106	18	2		K.TFQDPVDLAK.L
	685.8377	13	2		R.YNQSTLSVDR.T
	675.9683	17	3		R.DFDGAMSWENVPSSDGRR.I
417764	468.2746	32	2		R.ASTFAIAVR.A
	492.2741	24	2		K.VIPTDPWR.S
	541.8222	45	2		K.VTLQLQPQR.S
	520.2441	19	3		K.IDLSFADHGPDES.R.A
376719	428.718	2	34		K.SSPGSFF.K
	451.2537	2	13		K.APSLDSAL.K
	498.7664	2	28		K.AFVIGSAMG.K
	555.2903	2	38		K.FTWGSAIEA.K
	426.8992	3	46		K.LDKEPGSYTI.R
327740	433.7392	2	20		K.SITGPYT.K
	474.7482	2	28		R.GGSIDPAGF.K
	554.2916	2	49		R.VQVAVSDDF.K
	402.4562	4	31		R.GGSIDPAGFKDKDGS.R
	599.3307	3	5		K.VGADGVTPIGDAVQILD.R
	421.8962	3	32		K.RVQVAVSDDF.K
383312	427.2345	2	31		K.EADIHL.R
	465.753	2	19		K.EIPISTD.R
	579.3351	2	21		K.GAVNIDLSQL.K
	582.282	2	16		K.EEQGVYPW.R
	602.8451	2	6		K.AIFSPVLSSGA.R
	424.2209	3	45		K.VWYGEHNL.P.R
387674	512.2699	3	11		R.GAGHNFIVTSATF.R
	300.712	2	16		K.LVIQ.K
	336.6978	2	14		K.NGVNL.R
	381.7208	2	16		R.LAAAFN.R
	525.2803	2	36		R.LWVQDN.K
	405.5417	3	33		R.ICHSVNIDT.R
	462.9207	3	16		K.DNAGWDLVIQ.K
	480.2723	2	19		K.KDWAAIQ.K
	527.3052	2	37		K.TPENILPAA.K
	538.79	2	27		K.NLLEEPSF.K
383083	630.8381	2	22		K.GVLVGTAESWN.K
	510.9559	3	2		K.VVLGMVWGKPTDT.K
	539.2985	2	24		R.YGLAADQVLK
	491.5819	3	17		K.AKYDPNDIFYAR

381496	492.925	3	15	K.KVFGTNYDCLR
	507.6094	3	11	K.VSGDVHNAVLPAWR
	521.6253	3	16	R.STGAGALAIWTHHLK
<b>Upper gel band lane</b>				
371227	404.2158	19	2	K.GMLSFPRT
	587.3391	15	2	R.TLALQQTGSVR.S
	609.8107	14	2	K.TFQDPDPTAK.L
	658.334	13	2	K.NWMNEPNGLIK.I
	685.8384	10	2	R.YNQSTSTLSVDR.T
	727.8692	12	2	R.LAYSVDDGVTWK.F
	935.4006	13	2	R.DFDGAMSWENVPSSDGR.R
	988.027	18	2	R.ILAAIANSYGGSPPTNTWK.G
	764.0957	28	3	R.SFVQWPVSELLTAGTALTTR.N
	847.0821	37	3	K.FAGNPIISAAGEAPHDETDGLETR.D
384244	584.3059	11	2	K.AVNFNVYAN.R
	609.8239	16	2	R.EWLLPNYQ.R
	626.3339	13	2	R.IAESILEDYA.K
	659.3335	19	2	K.LDQWAEETVA.R
	782.4213	15	2	R.ALMNTVSAFGAPIQ.K + Oxidation(M)
	824.9556	11	2	K.INFDIWNLPFT.R
	574.6376	21	3	R.GVSMIPNNLHENQL.R
	892.9588	33	2	K.FFMNELDLLGQAAAT.K + Oxidation(M)
	935.5109	20	2	K.TYDYVIAGGGLTGLTVAA.K
	729.7245	31	3	K.GIELLDT.KLDQWAEETVA.R
	760.3507	15	3	K.VFGMEGWNWDMVFOYMQ.K
	1145.576	20	2	R.GSVHILSSDPYLWQYANDP.K
	777.4545	27	3	R.EVLLAAGSSISPLILEYSGIGI.K
	787.0504	27	3	R.NWLLDEDVAFALFFDTEG.K
	871.8002	51	3	K.AGVEQLLELPVGLNMQDQTTTTV.R
	677.1094	11	4	R.VIDGSIPPTQVSSHVMVTFYGMAL.R
315441	779.9056	21	4	K.SGLGLGGSTLINGDSWT.RPD.KVQIDSWE.K
	1052.57	44	3	K.SVLDKAGVEQLLELPVGLNMQDQTTTTV.R
	830.1417	15	4	R.S.RPPTDAQIEAGHFYDPACHGTDGTVHAGP.R
	404.2388	13	2	R.FVVDVT.K
	415.7339	19	2	K.NLNGVWK
	618.3332	13	2	R.QLDLMVNOF.K
	670.8417	11	2	K.EAMVYDLQML.K + Oxidation(M)
	743.853	16	2	K.LGDDQVESYTF.R
	641.6876	20	3	K.VGTNPWPEYP.RPLLQ.R
	667.6922	14	3	R.SPGYALKEPPLTTPWTD.K
	782.0635	26	3	R.DANGNSVTILPNEQQIEFA.R
	834.0953	29	3	R..RDANGNSVTILPNEQQIEFA.R
	978.49	26	3	K.FDQSNELLVFVHDPTDDGGYVIPIG.K
400960	1008.137	12	3	R.LYACSGGVWQTDDVEGEVNGLMTYD.R
	1158.919	41	3	K.SFPSIVTWIYNEGWGQITAYNPEFALTD.R
	880.9503	40	4	K.IETDLFYQACDELGLLVIQDMPSL.RPLQS.R
	1176.264	30	4	R.LVDSTSGWVDHGAGDFSDNHYANPQCGSPFYSTPSSPYDSS.R
	742.9103	19	2	R.NIDVDPITINGVS.K
	975.9612	20	2	R.AQDMNNIASWTDEINT.K
	722.0839	17	3	K.FTSNGIIPPAITGLHNGDAL.R
	805.4335	12	3	R.LAEWPITLTHQEMASASFLA.R
	852.7726	17	3	K.IAAFAPTTGFTTESVAGVINNFDG.R
	903.7664	15	3	K.ENAMWPLFTTAAANNFDGMQINP.R
	1458.703	35	2	R.VNLNTQIDDMFLETEIYSPAGENF.R
3717485	1024.839	21	3	R.RVNLNTQIDDMFLETEIYSPAGENF.R
	1127.202	41	3	K.FGTSIAGGCCDNGVEQLVSFTDISDFPTSGL.K
	1217.258	60	3	R.IYYNCDTPACTVAEWIATSAGAGTFQDLLAIE.K
	371.7485	14	2	K.AGALLL.G.K
	355.1764	15	3	R.DSYVWHGM.R
	631.3589	16	2	R.GYLERPLPVAF
	484.9088	11	3	R.DYLSEVENTNI.R

385992	509.9729	18	3	R.NSVVGIKPTVGLTS.R
	601.3202	14	3	R.METTAGSWALLGNVVP.R
	691.6985	25	3	K.DRMETTAGSWALLGNVVP.R
	856.4602	20	3	R.VHQTOPYLNAILQVNPDAFSIA.K
	1020.547	24	3	K.GAVFGIPWESFWALGDADQIAQLDLV.K
	1383.357	46	3	R.SVEDLVQYNIDNYGSEGLPGIHPAFGSGQDGLLASLET.K
323309	381.2074	11	2	R.SAMTVP.R
	327.8467	14	3	K.VDGVHEL.G.R
	604.8002	14	2	K.TTGDVFDASPA.K
	426.2597	14	3	K.VLIYTPDL.K.K
	768.8942	12	2	R.ANQQAQSIAYS.LD.K
	822.9132	15	2	R.VGYNFGTQEVFID.R
	826.4343	10	2	R.LFSTGGATSNVELEV.K
	1260.625	12	2	R.TVIAWMNNWQYGATIPDTPW.R
	1001.834	32	3	R.SGTIEIDNATGGWGHNLNVEISFSNT.R
	1101.858	33	3	R.ANNQVANWLDWGPDFYAALGWNGLPQDD.R
	1118.878	12	3	K.GMTWTTIDAANPVIPPEPPAPYQDFLEF.R
	1154.906	19	3	K.WGLASEFGPVNAVGGVWECPSIFPLSLDGGES.K
	373946	357.7337	12	2
672.3169		11	2	K.ANVASVMCSYN.K
480.9267		14	3	K.ATVDVTADHASV.V.R
524.3142		15	3	K.GLGVHVQLGPAAGPLG.K
607.3166		18	3	R.ATHEL.YLWPFMNAV.K
698.0213		17	3	R.YANPVTAFPAGINAGATWD.R
757.0534		25	3	K.SLAIIGQDAINPDGANACVD.R
842.5154		31	3	K.NVIWVHVSVPPILELTAQPSV.K
967.8222		7	3	R.ILAAWYLLGQDQGYPEVTFSSWDGG.K
994.7978		29	3	K.QSSDYGAGWDSALVDNFVEDLFIDY.R
1005.164		8	3	R.GCNTGTLAMGWGSGTSEFFYLVAPLDAI.K
460.7505		14	2	K.YGVPLDT.R
383654		682.8629	11	2
	779.3626	11	2	K.DYTESSNLASSLD.R
	551.6083	18	3	K.SGDSGFLNDHYSLL.K
	886.9118	10	2	K.GDWEFTAAVSSVST.R
	670.9875	17	3	R.NAIAWEYEGSTDGVAYH.K
	1040.523	21	2	R.AMFISDLATWINETPTN.R
	785.3874	15	3	R.QAFGATQLCGT.KD.KMYMFL.K
	633.8404	23	4	R.RVEHDSIATAGQEYLTV.TLSLV.R
	873.4398	18	3	R.AISSSWPVFGFSYNLGSVDSSPVS.K
	1133.925	21	3	K.EISSNGNMNTVDVIFPAYPIFLYTNPELL.K
	527.3255	10	2	K.GGLIEQPV.K
	404.2158	13	3	K.IEDAPLYPH.R
	401322	672.3646	16	2
562.0702		18	4	K.GGLIEQPVKIEDAPLYPH.R
918.5099		33	3	R.INAQTVWVGLHAFTTLQOIIISDG.K
975.5015		22	3	K.HIVGAEAPLWSEQVDDVTVSSVFWP.R
782.8748		17	4	K.LNLVHWHLDDSQSWPVQMSSYPEMT.K
551.2947		19	2	R.AVEQSLDAI.R
378182	575.7995	13	2	K.AFDSEFPLP.K
	688.8705	16	2	K.FGQAIAGSDAQL.K
	702.3894	18	2	K.NVGFVLSVTEN.K
	819.9089	18	2	R.AGMIADSGALAASGYQ.R
	546.9513	17	3	R.ERDFPIPDLOFF.K
	758.4009	13	3	R.TGDVRPEEDQTLFPVMLGL.R
	902.4756	14	3	R.FLRTGDVRPEEDQTLFPVMLGL.R
327740	898.4892	19	2	K.VGADGVTPIGDAVQILD.R
	947.9703	16	2	K.GAWLGLNTNFPDPSFM.K
	704.3441	19	4	R.HHCVGTAIADHPAGPYVPSNTPLSC.R
	1171.246	25	3	K.SWTLLEDVALPTLSTWETENDHWAPDVVM.R

## S3. Analysis of variance of fitted model

Source	Sum of squares	Degrees of freedom	Mean square	F Value	p Value Prof>F
<b>Model</b>	2017.1	14	144.1	73.42	<.0001*
<b>pH (A)</b>	420.9	1	420.9	214.5	<.0001*
<b>°C (B)</b>	143.7	1	143.7	73.2	<.0001*
<b>Enzyme concentration (C)</b>	214.7	1	214.7	109.4	<.0001*
<b>Substrate Concentration (D)</b>	410.1	1	410.1	208.98	<.0001*
<b>AB</b>	40.2	1	40.2	20.47	0.0007*
<b>AC</b>	1.96	1	1.96	1.00	0.3374
<b>BC</b>	1.7	1	1.7	0.87	0.3704
<b>AD</b>	7.89	1	7.89	4.02	0.0681
<b>BD</b>	21.1	1	21.1	10.75	0.0066*
<b>CD</b>	1.15	1	1.15	0.59	0.4583
<b>A<sup>2</sup></b>	177.5	1	177.5	90.46	<.0001*
<b>B<sup>2</sup></b>	443.8	1	443.8	226.16	<.0001*
<b>C<sup>2</sup></b>	1.06	1	1.06	0.54	0.4766
<b>D<sup>2</sup></b>	19.6	1	19.6	9.98	0.0082*
<b>R-squared</b>					0.98
<b>Adj squared</b>					0.97
<b>R-squared (pred)</b>					0.93

S4. <sup>1</sup>H NMR spectra of PHA extract



SUBMITTED

## 1.2 The power of two: an artificial microbial consortium for the conversion of inulin into Polyhydroxyalkanoates

Iolanda Corrado<sup>1\*</sup>, Claudia Petrillo<sup>2\*</sup>, Rachele Isticato<sup>2</sup>, Angela Casillo<sup>1</sup>, Maria Michela Corsaro<sup>1</sup>, Giovanni Sanna, Cinzia Pezzella<sup>3\*\*</sup>

<sup>1</sup>Department of Chemical Sciences, University of Naples Federico II, Via Cinthia, 4 - 80126 Napoli, Italy

<sup>2</sup>Department of Biology, University of Naples Federico II, Via Cinthia, 4 - 80126 Napoli, Italy

<sup>3</sup>Department of Agricultural Sciences, University of Naples Federico II, Via Università, 80126 Naples, Italy

\*Equally contributing authors

\*\*Corresponding author: [cpezzella@unina.it](mailto:cpezzella@unina.it)

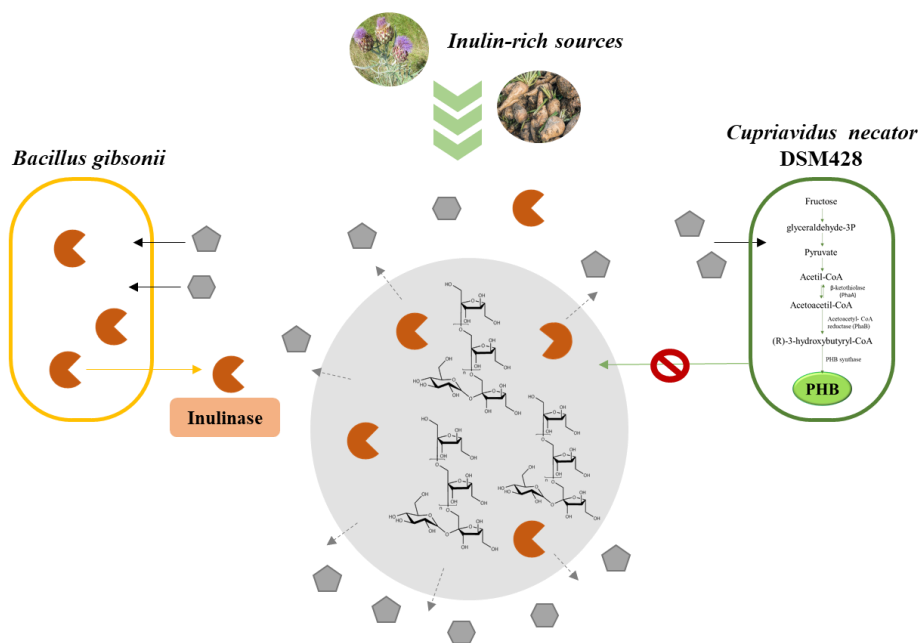
### Abstract

One of the major issues for the microbial production of polyhydroxyalkanoates (PHA) is to secure renewable, non-food biomass feedstocks to feed the fermentation process. Inulin, a polydisperse fructan that accumulates as reserve polysaccharide in the roots of several low-requirement crops, has the potential to face this challenge.

In this work, a “substrate facilitator” microbial consortium was designed to address PHA production using inulin as feedstock. A microbial collection of *Bacillus* species was screened for efficient inulinase producer and the genome of the selected strain, RHF15, identified as *Bacillus gibsonii*, was analysed unravelling its wide catabolic potential. RHF15 was co-cultured with *Cupriavidus necator*, an established PHA producer, lacking the ability to metabolize inulin. A Central Composite Rotary Design (CCRD) was applied to optimise PHA synthesis from inulin by the designed artificial microbial consortium, assessing the impact of species inoculum ratio and inulin

and N-source concentrations. In the optimized conditions, a maximum of  $1.9 \text{ g L}^{-1}$  of Polyhydroxybutyrate (PHB), corresponding to  $\sim 80\%$  ( $\text{g}_{\text{polymer}}/\text{g}_{\text{CDW}}$ ) polymer content was achieved. The investigated approach represents an effective process optimization method, potentially applicable to the production of PHA from other complex C-sources.

### Graphical Abstract



**Keywords:** artificial microbial consortium; inulin; Central Composite Rotary Design

### Highlights

- *C. necator* is an established PHA producer lacking the ability to metabolize inulin
- *Bacillus gibsonii* RHF15 was discovered as a new inulinase producer
- Co-culturing the two bacterial strains on inulin lead to effective PHB accumulation
- Central Composite Rotary Design allowed optimization of consortium performances

## Introduction

The extensive worldwide use of plastic and the impact of its production chain have seriously harmed the environment, increasing, at the same time, the demand for fossil resources, therefore, plastic pollution of soil and water is urgently asking for biodegradable plastics.

Polyhydroxyalkanoates (PHAs) are a family of biodegradable polyesters produced by various microbial species for energy storage. Being produced from renewable sources, they have been proposed as green alternative to traditional chemical plastics, including polyethylene (PE), polypropylene (PP), and polyethylene terephthalate (PET) (Tan et al., 2021). Besides Polyhydroxybutyrate (PHB), the best characterized member of PHA family, several hydroxyalkanoic acid monomers, differing in their chain length, have been identified so far, giving rise to different PHA copolymers with tunable properties (Turco et al., 2021).

The main limit for exploitation of PHA is related to their production cost, with the starting feedstocks accounting for more than 50% of the total. As a fact, the use of biomass and waste feedstocks has emerged as the main breakthrough for cost-effective PHA production, and, to this purpose, different lignocellulosic materials and food wastes have been tested (El-malek et al., 2020; Sirohi et al., 2020). To be considered as appropriate feedstocks for microbial synthesis of PHAs, the complex C-sources contained in raw materials require a preliminary catabolic step to be converted into suitable substrates for microbial fermentation. The isolation of strains for direct high yield PHA synthesis from low-cost waste streams has been reported in few cases (Bustamante et al., 2019; Tan et al., 2021). On the other hand, *in vivo* engineering approaches have been applied, focusing on the introduction of specific catabolic genes into native PHA producers or, vice versa, on the implementation of PHA-synthetic genes into non-native producers endowed with the ability to metabolize complex C-sources. Although effective on different waste materials, both the above-mentioned strategies are time-consuming and challenging (Favaro et al., 2019).

The design and construction of artificial microbial consortia has opened a new perspective in this field. The production of several

microbial products by co-culture has been successfully reported, highlighting their advantages in terms of productivity and process economic over pure cultures (Bhatia, Bhatia, et al., 2018). Microbial consortia represent a valuable strategy to deal with the need to use complex C-sources that would be not metabolized by an individual species, and/or to relieve the negative effect of side products inhibiting one of the species of the consortium (Ai et al., 2021; Diender et al., 2021).

Co-culture based approaches have been applied to PHA synthesis (Ai et al., 2021). Bhatia et al., (2018b) have co-cultured *Ralstonia eutropha* and *Bacillus subtilis*, respectively as PHA and invertase producers, to address PHA production from sucrose as substrate. These bacteria form a mutually beneficial symbiotic relationship, since glucose, fructose and propionic acid produced by *B. subtilis* are efficiently converted into P(3HB-co-3HV) copolymer by *R. eutropha*. Simultaneous production of PHA and xanthan gum has been reported by a mixed culture of *Cupriavidus necator* and *Xanthomonas campestris* from palm oil (Rodrigues et al., 2019). Sawant et al., (2017) have ascribed the increased efficiency in PHA production from lignocellulosic substrates by *Saccharophagus degradans* and *Bacillus cereus* co-culture, to the occurrence of mutual communication and cooperative growth between the two bacteria. Finally, a mutually beneficial symbiotic relationship based on nutrient supply and detoxification, has been achieved by properly engineering *Escherichia coli* and *Pseudomonas malodorous* strains, during fermentation of mixed glucose and xylose substrates (Liu et al., 2020).

Inulin is a linear polysaccharide composed of  $\beta$ -2,1-linked D-fructose residues terminated by a glucose residue, accumulated as a reserve carbohydrate in the roots and tubers of various crops, such as chicory and dahlia and, more interestingly, in low-requirement crops, such as Jerusalem artichoke and *Cynara cardunculus* (Bedzo et al., 2020; Hughes et al., 2017). These inulin sources have a high potential for applications in biorefineries, being able to cope with drought, pests and diseases and growing well in marginal lands with little fertilizer applications (Bedzo et al., 2020). Inulin hydrolysis into fermentable sugars, catalysed by microbial inulinases, is mandatory for its utilization as carbon and energy source in microbial processes. The

synthesis of several microbial products has been reported from these inulin-rich biomasses (H. Y. Choi et al., 2012; Khatun et al., 2017; Qiu et al., 2019), although PHA production is still less explored. In the reported examples, PHA production has been achieved by exploiting microbial inulinases in separate hydrolysis and fermentation (SHF) (Haas et al., 2015; Koutinas et al., 2013) and simultaneous saccharification and fermentation (SSF) processes (Corrado et al., 2021), since no PHA-producing strain naturally endowed with the ability of hydrolyse inulin has been isolated so far.

*Cupriavidus necator* is an established PHA producer, able to accumulate polymer with high productivity from fructose, however it lacks the hydrolytic enzymes necessary to convert inulin into fermentable sugars (Corrado et al., 2021). In this work, an artificial microbial consortium was designed to address PHA production from inulin, by complementing this *C. necator* enzymatic deficiency with a properly isolated inulin-hydrolysing microorganism. To this aim, a microbial collection of halophilic *Bacillus* species was screened for efficient inulinase producers. Halophilic bacteria are a useful source of enzymes suitable for industrial processes. To adapt to saline conditions, this group of microorganisms has developed different strategies, as the production of a large variety of extracellular hydrolytic enzymes. Moreover, these enzymes exhibit optimal activities at various ranges of salt concentration, pH and temperature, making them suitable to be used in many industrial processes (Moreno et al., 2013).

A Central Composite Rotary Design (CCRD) was applied to optimise PHA synthesis from inulin by the designed artificial microbial consortium, assessing the impact of species inoculum ratio and inulin and N-source concentrations. The investigated approach represents an effective process optimization method, potentially applicable to the production of PHA from other complex C- sources.

## **Materials and Methods**

### *Microbial strains and culture conditions*

Halophilic *Bacillus* sp. strains used in this work are listed in Table S1. Tryptone Yeast extract (TY) medium was used for *Bacillus* strains maintenance and pre-inoculum growth. Minimal medium (MM) supplemented with inulin 1 % (w/v) was used for inulinase producers

screening in liquid cultures (Budde et al., 2011). *Bacillus* strains were grown at 37°C with shaking (150 rpm).

*C. necator* DSM 428 strain was grown aerobically at 30 °C both in rich (Tryptic Soy Broth, TSB) and minimal medium (MM<sub>Cn</sub>) according to Budde, 2011 (Budde et al., 2011).

Powder inulin used in this study were a commercial mixture of chicory roots inulin provided by Sigma chemical as high purity grade substrate for *in vitro* assays (inulin from chicory, 9005-80-5, Sigma-aldrich) and a low purity grade inulin from chicory as carbon source for microbial growth (provided by Lineavi, Inulinpulver, Jeder Tag Ein Wohlfühltag).

#### *Screening for inulinase producers*

Iodine agar plate assay was used for screening on solid medium. Microorganisms were grown on MM supplemented with inulin 1 % w/v agar plates and after for 24 hours they were incubated in a close jar sutured of iodine vapors for 6 minutes at room temperature.

For screening in liquid medium, bacterial strains were grown in TY medium for 16 h and inoculated in MM+ Inulin 1% (w/v) at 0.4 OD<sub>600</sub>/ml (250 mL Flasks with 25 mL of medium) for 30 h.

#### *Inulinase enzymatic assay*

The culture medium was centrifuged at 5000 g for 15 min and the supernatant was used as the inulinases source. Enzymatic activity was measured by determination of reducing sugars released from substrate inulin by DNS-method (Muller 1996) according to Corrado et al. (2021). One unit of the enzyme (inulinases or invertase activity) was defined as the amount of the enzyme which produces 1 µmol of reducing sugars per minute. All the assays were carried out in duplicate.

#### *Whole genomic annotation*

The Rapid Annotation using Subsystems Technology (RAST) was applied to RHF15 genome, already available (Petrillo et al., 2021) for gene prediction and annotation (Aziz et al., 2008; Overbeek et al., 2014). CG View (Circular Genome Viewer) server 1.0 was used to construct a circular genome map of strain RHF15 (Stothard & Wishart, 2004).

#### *Response surface methodology*

A 2<sup>3</sup> full factorial central composite rotary design (CCRD) was employed to find out the interactive effects of inulin, NH<sub>4</sub>Cl concentration, bacteria strains inoculum concentration on both cell biomass production and PHA accumulation. CCRD was designed using Minitab 19 and resulted in 31 conditions with eight axial points and seven replicates at the center point (Table 1). The combination of predictor setting that optimized the fitted response was used to verify the model.

Experiments were performed at 20 mL scale in MM<sub>Cn</sub> at 30 °C for 96h. The four components (Inulin, NH<sub>4</sub>Cl, RHF15 and *C. necator*) were added to the media according to the designed values (Table 1). After 96h cells were recovered by centrifugation (5500 g 15 min) and lyophilized for CDW determination and PHA extraction. Regression analysis using ANOVA was performed, and model fitting methods applied for data analysis. Contour and surface plots were created to visualize the interactive effects of all components on PHA accumulation.

*Verification of the model for PHA production using inulin as carbon source.*

To validate the model a numerical optimization method via Minitab 19 was applied to predict the variables value. The high and low variables values were determined according to overlaid plots for all responses. Optimized conditions turn out to be 0.3 OD mL<sup>-1</sup> for bacteria inoculum, 2 g L<sup>-1</sup> of NH<sub>4</sub>Cl and 30 g L<sup>-1</sup> of inulin. *Bacillus* strain and *C. necator* were co-cultured in MM<sub>Cn</sub> media at 20 mL scale up to 96 h. Samples were collected at 24 h intervals and analysed for biomass production (Cell Dry Weight, CDW) and PHA accumulation (% g<sub>polymer</sub>/g<sub>CDW</sub>). Concentration of glucose, fructose and residual inulin in the culture broth were assayed by D-fructose and D-glucose, and fructan assay kits (Megazyme).

*PHA extraction and analysis*

Polymer extraction was performed on lyophilized cells (Corrado et al., 2021). Gas chromatography mass spectrometry method (GC-MS) was used to analyse PHA production and composition as previously described by Vastano et al. (2015).

*NMR*

<sup>1</sup>H NMR spectrum of the extracted polymer was performed in CDCl<sub>3</sub>:CD<sub>3</sub>OD (1:1), at 298K using a 600 MHz Bruker (Bruker Italia, Italy) instrument equipped with a cryogenic probe.

## Results and Discussion

### Screening of halophilic bacteria for inulinase production

A halophilic bacteria collection was screened for the ability to produce inulinases (Table S1). All microorganisms belong to a larger collection isolated from samples of sand and rhizosphere of *Juniperus sabina* collected from saltpans (Castaldi et al., 2021; Petrillo et al., 2021)). The selected strains are facultative anaerobic belonging to the *Bacillus* genus, all classified as moderate halophilic bacteria, being able to grow between 0.5 and 2.5 M of salt (Kushner, 1978). The 8 strains were chosen for their exoenzymatic activity profile, being able

to hydrolyse substrates like cellulose, starch or xylan (Petrillo et al. 2021).

After the primary screening on agar, four strains were selected, based on the diameter of the hydrolytic zone. Once cultured in liquid medium, the strain RHF15, displayed the highest level of inulinase production, reaching up to  $14 \text{ U mL}^{-1}$  (Figure 1) after 15 h, in line with the values reported for other inulinase producers (Ram Sarup Singh et al., 2017). The enzymatic activity was detected in the culture broth in the early stage of growth, probably as a result of inulin induction (Ram Sarup Singh et al., 2017). The inulinase/saccharase activity ratio, I/S, was equal to 2, indicating the prevalence of inulinase over invertase activity (Ram S. Singh & Singh, 2010). As a fact, the release of both glucose (the minority component of inulin) and fructose was recorded from the beginning of the process. Then, whilst glucose level remains almost neglectable, fructose concentration rises steeply up to 12 h, when it approaches a constant level in correspondence with the entry into the stationary growth phase. It is noteworthy that high inulinase activity levels were preserved in the culture broth even after prolonged stationary phase, representing an advantage for the exploitation of this strain as inulinase-producer in a properly designed artificial microbial consortium. Based on these results, the strain RHF15, identified as *B. gibsonii*, was selected for further analysis.

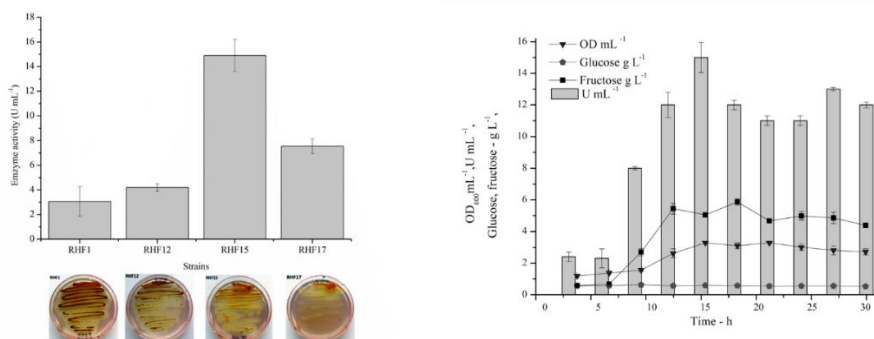


**Figure 1. a)** Screening for inulinase producers. Maximum of Inulinase activity ( $\text{U mL}^{-1}$ ) registered in liquid medium for the strains selected based on the hydrolytic zone shown on plate (pictures below). **b)** Kinetic profiles of OD

mL<sup>-1</sup>; inulinase U mL<sup>-1</sup>; fructose, g L<sup>-1</sup>; glucose g L<sup>-1</sup> in liquid medium for RHF15.

### **Whole genome investigation of putative inulinase coding genes of the strain RHF15**

The genome of strain RHF15 (Figure S2) was analysed by the RAST annotation server (Aziz et al., 2008; Overbeek et al., 2014), revealing 100 RNAs and a total number of 4282 predicted protein-coding sequences (CDSs), where “Amino Acids and Derivatives” (17.4 %) and “Carbohydrates” (14.4 %) were the most represented subsystem features (Table S3). In order to identify proteins responsible for inulin hydrolysis, predicted amino acid sequences from Carbohydrates subsystem were analysed scanning for Carbohydrate-Active enZymes (CAZymes). CAZymes are a group of enzymes involved in carbohydrate metabolism, divided into classes according to their catalytic activity. The analysis revealed the presence of 129 CAZymes, including 16 Carbohydrate Esterases, 40 Glycoside Hydrolases (GH), 34 Glycosyl Transferases, 5 Polysaccharide Lyases and, 34 enzymes involved in Auxiliary Activities (Figure 2A). The abundance of hydrolytic enzymes belonging to different CAZY families, highlighted by this analysis, is in accordance with the wide hydrolytic abilities towards different substrates (xylan, cellulose, amylose, chitin) recently reported for this strain (Petrillo et al., 2021). Among GH, the Glycoside Hydrolase Family 32 includes members of the  $\beta$ -fructosidase superfamily, able to hydrolyse non-reducing  $\beta$ -D fructosidic bonds releasing fructose (Barrangou et al., 2003) and for this reason, more attention was dedicated to this group of enzymes. Interestingly, 3 genes putatively coding for enzymes related to this family (Figure 2B) have been identified. A multiple alignment of the deduced aminoacidic sequences with those of well-known GH32 hydrolases able to cleave inulin (Table S4) was performed using SeaView software (Gouy et al., 2009) (Figure S5), highlighting the typical highly conserved motifs of the GH32 family (Lammens et al., 2009; Pons et al., 2004; Reddy & Maley, 1990) in the selected RHF15 enzymes.

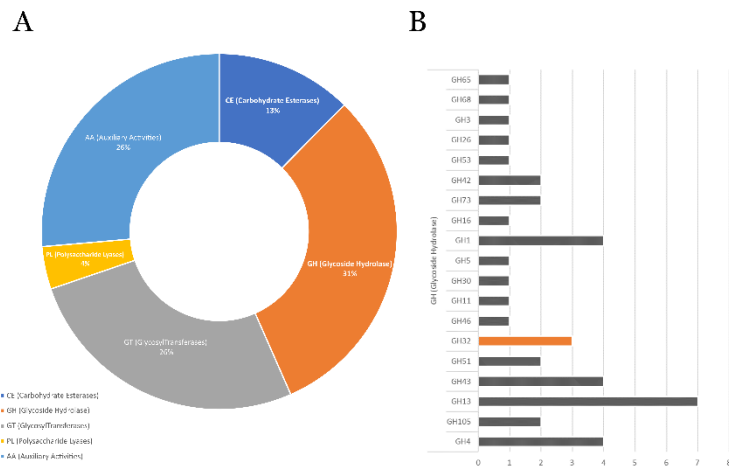


**Figure 2. Annotation of CAZymes in *B. gibsonii* RHF15 genome** **A)** Distribution of CAZyme classes in strain RHF15. **B)** Distribution of CAZyme families in the GH class, and number of proteins belonging to each family.

A blastP analysis of the aminoacidic sequences of the three putative inulinase coding genes was run against the NCBI database. The best hits were obtained with the levanase SacC, the sucrose-6-phosphate hydrolase ScrB and the levanbiose-producing levanase LevB of *B. subtilis* with a sequence similarity score ranging between 99 and 100 % (Table 2). *B. subtilis* levanase SacC has been depicted as an exofructosidase, capable of hydrolyzing both levan and inulin, leading to the production of free fructose (Martin et al., 1989). Regarding ScrB, no data are available on the ability of this enzyme to hydrolyze inulin, while, from previous studies, it is known that *B. subtilis* LevB is an endolevanase that selectively cleaves the ( $\beta$ -2,6) fructosyl bonds and does not hydrolyze inulin (Jensen et al., 2016). Since the hydrolytic activity has been detected in the supernatant fraction, a predicted signal peptide in the primary structure of the SacC and ScrB homologous proteins has been searched using SignalP 3.0 Server (Bendtsen et al., 2004). The performed analysis allowed to identify the presence of a signal peptide (position 1-23) and a probable cleavage site (position 24 -25) in SacC (Tjalsma et al., 2000), while no significant result was obtained with ScrB, suggesting a cytoplasmic role of this enzyme. According to the collected information, the inulin

hydrolytic activity associated with strain RHF15 is most likely due to the levanase SacC homologue.

**Table 2** Summary of the blastP analysis run between the three selected enzymes of strain RHF15 (Query ID) and the NCBI database. Only the best hits are shown.

Query ID	Subject ID	Source	Type	Similarity (%)	Expect value	Bit score
33193_RHF15_00488	WP_153940225.1	<i>B. subtilis</i>	Levanase SacC	100.00	0.0	1399
33193_RHF15_02998	WP_106073378.1	<i>B. subtilis</i>	Levanbiose-producing levanase LevB	99.80	0.0	1062
33193_RHF15_02621	WP_072692791.1	<i>B. subtilis</i>	Sucrose-6-phosphate hydrolase ScrB	99.79	0.0	1005

### Response surface design for optimization of PHA production from microbial co-culture

An artificial microbial co-culture able to utilize inulin as a carbon source for PHA production was designed exploiting the RHF15 strain and *C. necator* as inulinase and PHA producers, respectively. No genes coding for essential proteins in the PHA biosynthesis (PhbA,  $\beta$ -ketothiolase; PhbB, acetoacetyl coenzyme A reductase; and PhbC, Polyhydroxyalkanoate-synthase) were identified in the genome of the RHF15.

A central composite rotary design (CCRD) was used to explore the effectiveness in PHA production of the co-culture as a function of inulin and  $\text{NH}_4\text{Cl}$  concentrations as well as of the inoculum amount of each strain. The design resulted into 31 experiments (Table 1). Cell dry weight (CDW  $\text{g L}^{-1}$ ) and PHA content (PHA %) were assumed as the parameters influenced by the four independent variables. Biomass production and PHA accumulation were determined after 96 h. Inulinase activity was also assayed in culture supernatants at the end of the process (Table 1). The experimental results were fitted with a second order polynomial equations:

$$\text{PHA}\% = -10.59 + 53.1*A + 116.7*B - 1.03*C + 0.79*D + 207*A^2 - 383.2*B^2 + 2.12*C^2 - 0.02*D^2 + 866*A*B - 60.3A*C + 3.04*A*D - 28.9*B*C - 0.35*B*D - 0.03*C*D$$

$$\text{CDW g L}^{-1} = -1.234 + 0.69*A + 11.22*B - 1.05*C + 0.09*D + 3.57*A^2 - 39.72*B^2 - 0.38*C^2 - 0.002*D^2 + 4.89*A*B - 1.14A*C + 0.086*A*D + 0.99*B*C + 0.06*B*D - 0.002*C*D$$

being A) *C. necator* inoculum concentration (OD mL<sup>-1</sup>); B) RHF15 inoculum concentration (OD mL<sup>-1</sup>); C) NH<sub>4</sub>Cl, concentration (g L<sup>-1</sup>); D) inulin concentration (g L<sup>-1</sup>).

The significance of the model is depicted by F-value of 30.15 and 60.08 for both CDW and PHA, respectively. Analysis of variance (ANOVA) was used to determine the influence and the significance of the independent variables on the dependent responses (Table 3). The significance of model terms is defined by their P values, where only the terms with a Prob > F lower than 0.05 are considered significant.

In this work, the P value for model terms A, B, D, B<sup>2</sup>, C<sup>2</sup>, D<sup>2</sup> and A, B, C, D, AB, AC, AD, BC, B<sup>2</sup>, C<sup>2</sup> was found to be lower than 0.05, therefore they are significant terms for both CDW production and PHA accumulation, respectively (Table 3). Conversely the model terms C, AB, AC, AD, BC, BD, CD, A<sup>2</sup> and BD, CD, C<sup>2</sup> with a P value higher than 0.05 are not significant for both CDW and PHA, respectively.

The goodness of fit is confirmed by R<sup>2</sup>, that reflects a good co-relation between actual and predicted value. The value of R<sup>2</sup>, adjusted R<sup>2</sup> and predicted R<sup>2</sup> are 0.96, 0.93, 0.76 for CDW production and 0.98, 0.96, 0.89 for PHA accumulation. The difference, smaller than 0.2, between adjusted R<sup>2</sup> and predicted R<sup>2</sup> further validates the model.

*Lack of fit*-F value of the quadratic model proves the co-relation between response variables and independent factors. The *Lack of fit*-F value for both CDW production and PHA production are 3.59 and 3.51, respectively. The non-significant value justifies the fitness of model.

The significance of interactive model terms for PHA production is depicted by contour plot and relative three-dimensional surface plots presented in Figure 3. 3D graphs display the effect of the interaction between RHF15:*C. necator*, NH<sub>4</sub>Cl:*C. necator*, NH<sub>4</sub>Cl:RHF15 and Inulin:*C. necator* on the dependent variable "PHA accumulation". The combined effect of the variables was studied keeping the following mid-values: 0.15 OD mL<sup>-1</sup> inoculum concentration for both bacterial strains, 20 g L<sup>-1</sup> inulin and 1.7 g L<sup>-1</sup> NH<sub>4</sub>Cl. It is evident from the plot that PHA production reaches a maximum with the increase of the concentration of both bacterial species (Figure 3, Panel A). Furthermore, for a *C. necator* inoculum in the range 0.2-0.3 OD mL<sup>-1</sup>, PHA production holds at ~70 % with NH<sub>4</sub>Cl concentration below 1 g L<sup>-1</sup>.

<sup>1</sup> (Figure 3, Panel B). From the interactive plot NH<sub>4</sub>Cl:RHF15, it is evident that a positive effect on polymer production is linked to an increase of RHF15 inoculum together with a decrease of NH<sub>4</sub>Cl (Figure 3, Panel C). This phenomenon can be due to the negative effect of NH<sub>4</sub>Cl on inulinase production. As a fact, in the co-culture system, high concentration of NH<sub>4</sub>Cl seems to negatively affects production of inulinases (compare runs 14 and 16). Conversely, in the absence of *C. necator*, a higher NH<sub>4</sub>Cl amount seems to promote inulinase production (runs 6 and 8) (Table 2). Thus, a major contribution of RHF15 to the co-culture seems to be a prerequisite to promote PHA accumulation.

As for the interactive effect inulin:*C. necator*, their concomitant increase positively affects polymer production, assuring up to 70 % PHA content at more than 20 g L<sup>-1</sup> inulin together with more than 0.25 OD mL<sup>-1</sup> *C. necator* (Figure 3, Panel D).

**Table 1.** Optimization of growth variables for CDW production and PHA accumulation from co-cultures, using central composite rotatable design (CCRD)

Run	<i>C. necator</i> OD mL <sup>-1</sup>	RHF15 OD mL <sup>-1</sup>	NH <sub>4</sub> Cl g L <sup>-1</sup>	Inulin g L <sup>-1</sup>	CDW g L <sup>-1</sup>	PHB %	U mL <sup>-1</sup>
1	0	0	0.5	10	0.0	0.0	0
2	0	0	0.5	30	0.0	0.0	0
3	0	0	2	10	0.0	0.0	0
4	0	0	2	30	0.0	0.0	0
5	0	0.2	0.5	10	0.8	0.0	6.8
6	0	0.2	0.5	30	0.9	0.0	13.4
7	0	0.2	2	10	1.3	0.0	2.0
8	0	0.2	2	30	1.5	0.0	22.7
9	0.2	0	0.5	10	0.3	12.4	0
10	0.2	0	0.5	30	0.6	28.2	0
11	0.2	0	2	10	0.2	5.2	0
12	0.2	0	2	30	0.4	16.5	0
13	0.2	0.2	0.5	10	1.4	58.4	3.2
14	0.2	0.2	0.5	30	2.1	68.7	13.3
15	0.2	0.2	2	10	1.5	31.2	2.1
16	0.2	0.2	2	30	1.9	42.5	1.9
17	0	0.1	1.25	20	1.3	0.0	5.3
18	0.1	0	1.25	20	0.4	7.9	0
19	0.1	0.1	1.25	20	1.5	14.7	3.5
20	0.1	0.1	1.25	20	1.7	19.0	3.3
21	0.1	0.1	1.25	20	1.5	21.2	3.3
22	0.1	0.1	1.25	20	1.4	19.9	2.7
23	0.1	0.1	1.25	20	1.6	17.8	4.1
24	0.1	0.1	1.25	20	1.7	20.3	3.3
25	0.1	0.1	1.25	20	1.6	17.9	3.3
26	0.3	0.1	1.25	20	2.0	59.7	2.3
27	0.1	0.3	1.25	20	1.1	18.2	5.1
28	0.1	0.1	0	20	0.9	34.4	3.2
29	0.1	0.1	2.75	20	0.6	16.7	8.32
30	0.1	0.1	1.25	40	1.3	23.0	13.3
31	0.1	0.1	1.25	0	0.0	5.7	1.2

**Table 1.** Analysis of variance (ANOVA) and regression analysis of quadratic model for *CDW and polymer production* (<sup>a</sup>SS, sum of squares; <sup>b</sup>DF, Degree of freedom; <sup>c</sup>MS, mean square).

Source	ANOVA						Regression analysis			
	CDW g L <sup>-1</sup>			PHA %			CDW g L <sup>-1</sup>		PHA %	
	SS <sup>a</sup>	DF <sup>b</sup>	p Value Prob>F	SS <sup>a</sup>	DF <sup>b</sup>	p Value Prob>F	MS <sup>c</sup>	F Value	MS <sup>c</sup>	F Value
<b>Model</b>	12.8991	14	<.0001*	10264.5	14	<.0001*	0.9214	30.15	733.18	60.08
<b>C. necator (A)</b>	0.7506	1	<.0001*	5274.3	1	<.0001*	0.7506	24.56	5274.3	432.20
<b>RHF15(B)</b>	0.6856	1	<.0001*	765.4	1	<.0001*	0.6856	22.44	765.4	62.72
<b>NH<sub>4</sub>Cl(C)</b>	0.0204	1	0.425	618.3	1	<.0001*	0.0204	0.67	618.3	50.66
<b>Inulin(D)</b>	0.8447	1	<.0001*	396.6	1	<.0001*	0.8447	27.65	396.6	30.29
<b>AB</b>	0.0383	1	0.279	1200.0	1	<.0001*	0.0383	1.25	1200.0	98.33
<b>AC</b>	0.1161	1	0.069	327.6	1	<.0001*	0.1161	3.80	327.6	26.84
<b>AD</b>	0.1195	1	0.065	148.1	1	0.003	0.1195	3.91	148.1	12.14
<b>BC</b>	0.0889	1	0.107	75.3	1	0.024	0.0889	2.91	75.3	6.17
<b>BD</b>	0.0514	1	0.213	1.9	1	0.697	0.0514	1.68	1.9	0.16
<b>CD</b>	0.0052	1	0.687	0.8	1	0.803	0.0052	0.17	0.8	0.06
<b>A<sup>2</sup></b>	0.0211	1	0.418	70.9	1	0.028	0.0211	0.69	70.9	5.81
<b>B<sup>2</sup></b>	2.6100	1	<.0001*	242.9	1	<.0001*	2.6100	85.42	242.9	19.9
<b>C<sup>2</sup></b>	1.0093	1	<.0001*	31.6	1	0.127	1.0093	33.03	31.6	2.59
<b>D<sup>2</sup></b>	1.2465	1	<.0001*	72.1	1	0.027	1.2465	40.80	72.1	2.55

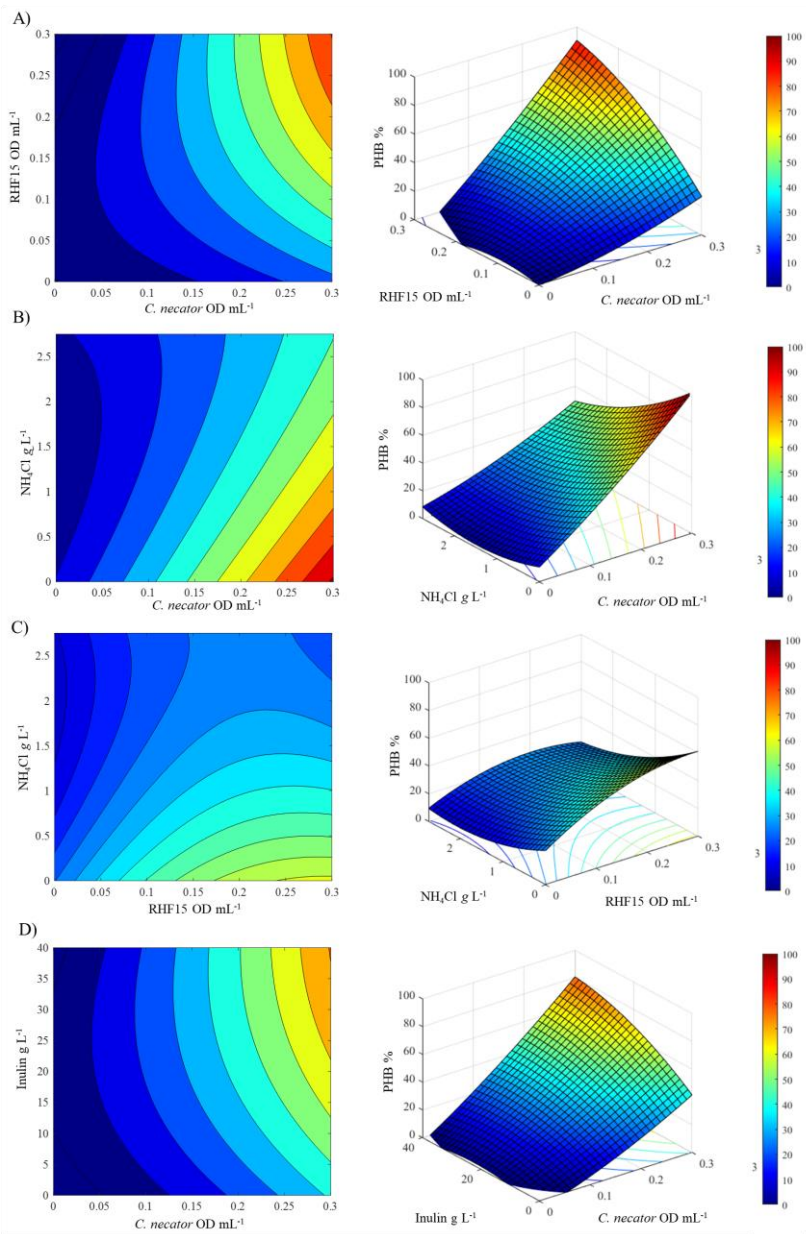


**Figure 3.** Contour and 3D surface plots for the significant interactive model terms for PHA production

To validate the models and define the variable values that allow obtaining up to  $2 \text{ g L}^{-1}$  of CDW and up to 80 % of PHA accumulation, overlaid contour plots were constructed (Figure 4). In the plot each set of contours defines the boundaries of acceptable response values. The solid contour line and the dotted one correspond to the lower and the upper bounds respectively, whilst the white portion in the plot represents the acceptable range wherein the possible combination of parameter settings can be obtained. In the case study, two overlaid contour plots were taken into account: *C. necator*:  $\text{NH}_4\text{Cl}$  and *C. necator*: RHF15.

From the first plot (Figure 4A) the optimal solutions are defined by  $0.1\text{-}0.3 \text{ OD mL}^{-1}$  for *C. necator* and a wide range of  $\text{NH}_4\text{Cl}$  concentration, being RHF15 and inulin at the mid value ( $0.15 \text{ OD mL}^{-1}$  and  $20 \text{ g L}^{-1}$  respectively). In particular, at low concentrations of  $\text{NH}_4\text{Cl}$ , a PHA content higher than 20 % can be obtained at low inoculum concentration, while when the N-source is increased, it is necessary to increase the inoculum. From the overlaid plot RHF15:*C. necator* (Figure 4B) it is evident that at low RHF15 inoculum it is necessary to increase the *C. necator* concentration at least to  $0.25 \text{ OD mL}^{-1}$  to obtain more than  $1 \text{ g L}^{-1}$  CDW together with a minimum of 20 % PHA. On the other hand, the increase in RHF15 inoculum allows to reduce the contribution of *C. necator* to be in the acceptable range.

The possible combination settings were used as starting values for the numerical optimization of the models. The inoculum concentration of bacterial strains was set to  $0.3 \text{ OD mL}^{-1}$ ,  $\text{NH}_4\text{Cl}$  was set in the range  $1.5\text{-}2 \text{ g L}^{-1}$ , and a concentration of inulin higher than  $20 \text{ g L}^{-1}$  was chosen.

The optimum variable values were  $0.3 \text{ OD mL}^{-1}$  for inoculum,  $2 \text{ g L}^{-1}$  of  $\text{NH}_4\text{Cl}$  and  $30 \text{ g L}^{-1}$  of inulin. The result obtained using predicted response verified the model with a degree of accuracy higher than 95 %. In the optimum conditions, up to  $2.4 \text{ g L}^{-1}$  of CDW and 75 % of PHA production were achieved.

The composition of the polymers produced in all the conditions explored in the CCRD design was determined by GC-MS analysis, and revealed the presence of 3-hydroxybutyrate (3HB) as the only component.

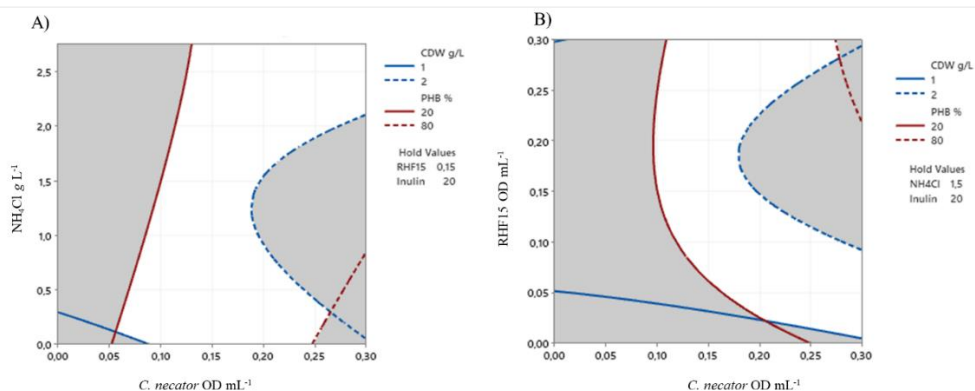


**Figure 4.** Overlaid contour plot: A) *C. necator*: NH<sub>4</sub>Cl; B) *C. necator*: RHF15. The solid contour line and the dotted one correspond the lower and the upper bounds respectively; the white portion represents the acceptable range (1-2 g L<sup>-1</sup> for CDW, 20-80% PHB) wherein the possible combination of parameter settings can be obtained.

### Kinetics of Polymer production

Figure 5 displays the kinetics of PHB production in the optimized conditions defined for the artificial microbial consortium. An increase in cell biomass was observed in the earlier phase, whilst polymer synthesis started only after 48 h. From this point onward, the cellular growth slowed down and PHA production sharply increased reaching up to 1.9 g L<sup>-1</sup> at 96 h, corresponding to a polymer accumulation ( $Y_{P/X}$ ) of 78.8 % and a productivity of 0.02 g L<sup>-1</sup> h<sup>-1</sup>. The efficiency of the mutual species interaction is visible from the profiles of C-sources consumption. Inulin concentration dropped rapidly in the first 24 h and, concomitantly fructose concentration increased, indicating an efficient polysaccharide conversion into fermentable sugars, in accordance with inulinases production in the early growth phase, observed for RHF15 strain. After 48 h, almost all the inulin was consumed, whilst fructose was available at high level (~ 10 g L<sup>-1</sup>), thus assuring the carbon source excess necessary for polymer accumulation. At the end of the process, 93 % of inulin was converted, with yield coefficients  $Y_{P/S} = 0.07$  and  $Y_{X/S} = 0.09$ . No residual glucose was detected in the culture broth, indicating its consumption by the co-culture. Although glucose is the minority monomer in inulin (about 3 g L<sup>-1</sup> estimated from the total hydrolysis of 30 g L<sup>-1</sup> inulin), its release promote the growth of

RHF15, being *C. necator* DSM 428 not able to metabolize glucose (Azubuike et al., 2019), thus leaving a higher amount of fructose available for PHB production.

Finally, the purity of the extracted polymer was checked by  $^1\text{H}$  NMR. The spectrum confirmed the presence of the characteristic signals attributable to the homopolymer polyhydroxybutyrate (Sabarinathan et al., 2018) (Figure S6).

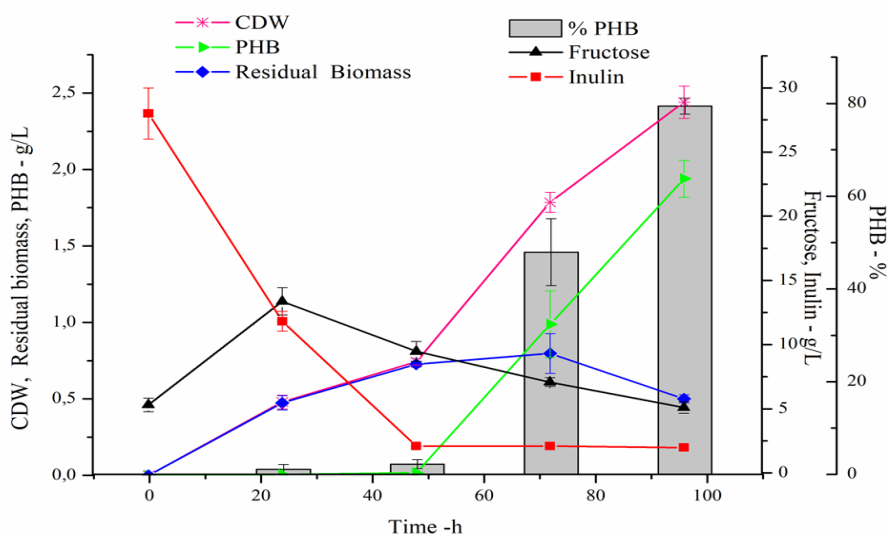


**Figure 5.** Kinetic profiles of CDW, g/L; PHB, g/L; Residual Biomass, g/L 1; Fructose, g/L; Inulin, g/L in the optimized conditions for the co-culture

The use of inulin-rich biomass for PHA production has been reported in Separated Hydrolysis and Fermentation (SHF) processes using various fungal inulinase mixtures and different *C. necator* strains (Table 4). In these examples, the PHB volumetric productivities refer only to the fermentation process and do not take into account the overall process time, including also the production of the enzyme and the inulin hydrolysis steps. Recently, the efficiency of a Simultaneous Saccharification and Fermentation (SSF) process for one-step inulin hydrolysis by a *Penicillium lanosocoeruleum* inulinase mixture and PHA production by *C. necator* H16 has been demonstrated, with a PHB productivity of  $0.03 \text{ g L}^{-1} \text{ h}^{-1}$  (Corrado et al., 2021). Although leading to a slightly reduced productivity if compared to the SSF

reported by Corrado et al (2021), the process with the co-culture is carried out in “one-pot”, allowing to reduce the overall production time by skipping the enzyme production step.

To our knowledge, this is the first example of the use of a “substrate-facilitator” (Bhatia, Bhatia, et al., 2018) microbial consortium for PHA production from inulin. A similar strategy has been applied by Bathia et al. (2018b) to a different substrate, saccharose, co-culturing *R. eutropha* 5119 strain with the sucrose hydrolysing *B. subtilis*. Interestingly, in this example, the synthesis of a P(3HB-co-3HV) copolymer has been reported, thanks to the supplying of the required precursor (propionate) from *B. subtilis* (Bhatia, Yoon, et al., 2018). Despite the similarity of the microbial species involved as well as of the supplied carbon sources, it is worth to note that differences in metabolic profiles of each strain of the consortium, their mutual interactions, together with the applied experimental conditions (concentration of the C and N sources, ratio between the two strains) might translate into substantial variation in polymer composition.

Noteworthy, besides the PHB-containing cells, about 12 U ml<sup>-1</sup> of inulinase activity were detected in the supernatant of the co-culture system developed in this work, leading to envisage the possibility to recover these enzymes as extracellular co-products of the process, enhancing its overall cost-competitiveness (de Jesus Assis et al., 2019; Kumar & Kim, 2018; Turco et al., 2021).

In conclusion, several engineering strategies have been applied for the designing of consolidated bioprocesses involving strains able to convert complex substrates into different microbial products (Favaro et al., 2019; Sirohi et al., 2020). The use of artificial consortia, although still less explored, allows to overcome the need for strain engineering, providing that the compatibility of the consortium members has been verified. The results of this work add a piece of knowledge in this field, providing an optimized process based on an artificial microbial consortium for inulin conversion into PHA.

**Table 4.** Comparison of processes for PHA production from inulin-based substrates. SHF (Separated Hydrolysis and Fermentation), SSF (Simultaneous Saccharification and Fermentation)

Process	Substrate	Strain	CDW gL <sup>-1</sup>	PHB gL <sup>-1</sup>	Y <sub>P/X</sub> (%)	Productivity, g L <sup>-1</sup> h <sup>-1</sup>	Ref.
Microbial co-culture (Shake flasks)	Inulin from chicory roots	<i>C. necator</i> 428 and <i>B. gibsonii</i> RHF15	2.4	1.9	79	0.02	This work
SHF (Shake flasks)	Inulin from Jerusalem artichoke tubers	<i>C. necator</i> 4058	7.7	4	52	0.07	Koutinas, 2013
SHF (Bioreactor)	Inulin from chicory roots	<i>C. necator</i> 428	11.0	7.3	66	0.062	Haas, 2015
		<i>C. necator</i> 531	3.5	1.6	45	0.016	
		<i>C. necator</i> 545	14.0	11.0	78	0.15	
SHF SSF (Shake flasks)	Inulin from chicory roots	<i>C. necator</i> 428	3.2	2.0	62	0.02	Corrado, 2021
		<i>C. necator</i> 428	3.9	3.2	82	0.03	

## Conclusions

A “substrate facilitator” microbial consortium, composed of the inulin-hydrolysing *B. gibsonii* strain RHF15 and the PHA-producer *C. necator*, was designed to address polymer production from inulin. The RHF15 strain was isolated from the screening of a halophilic microbial collection for its ability to produce inulinase, and its genome investigated, highlighting its hydrolytic potential.

The co-culture performances were optimized through response surface methodology, achieving a maximum of 1.9 g L<sup>-1</sup> of PHB, corresponding to ~ 80 % (g<sub>polymer</sub>/g<sub>CDW</sub>) polymer content.

The applied methodology can be extended to other complex carbon sources, exploiting the reservoir of hydrolytic activities discovered in RHF15 genome combined with other PHA producing strains with different substrate preferences.

## Acknowledgments

This work was supported by grants from PRIN: PROGETTI DI RICERCA DI RILEVANTE INTERESSE NAZIONALE – Bando 2017. “CARDoon valorisation by InteGrAted biorefiNery (CARDIGAN)”. Iolanda Corrado acknowledges Università degli Studi di Napoli Federico II for doctoral fellowships

## Bibliography

- Ai, M., Zhu, Y., & Jia, X. (2021). Recent advances in constructing artificial microbial consortia for the production of medium-chain-length polyhydroxyalkanoates. *World Journal of Microbiology and Biotechnology*, 37(1), 1–14. <https://doi.org/10.1007/s11274-020-02986-0>
- Aramvash, A., Moazzeni Zavareh, F., & Gholami Banadkuki, N. (2018). Comparison of different solvents for extraction of polyhydroxybutyrate from *Cupriavidus necator*. *Engineering in Life Sciences*, 18(1), 20–28. <https://doi.org/10.1002/elsc.201700102>

- Aziz, R. K., Bartels, D., Best, A. A., DeJongh, M., Disz, T., Edwards, R. A., Formsma, K., Gerdes, S., Glass, E. M., Kubal, M., Meyer, F., Olsen, G. J., Olson, R., Osterman, A. L., Overbeek, R. A., McNeil, L. K., Paarmann, D., Paczian, T., Parrello, B., ... Zagnitko, O. (2008). The RAST Server: rapid annotations using subsystems technology. *BMC Genomics*, *9*, 75. <https://doi.org/10.1186/1471-2164-9-75>
- Azubiike, C., Edwards, M., Gatehouse, A., & Howard, T. P. (2019). Data Driven Modelling of a Chemically Defined Growth Medium for *Cupriavidus necator* H16. *BioRxiv*, *15*, 548891. <https://doi.org/10.1101/548891>
- Barrangou, R., Altermann, E., Hutkins, R., Cano, R., & Klaenhammer, T. R. (2003). Functional and comparative genomic analyses of an operon involved in fructooligosaccharide utilization by *Lactobacillus acidophilus*. *Proceedings of the National Academy of Sciences*, *100*(15), 8957–8962. <https://doi.org/10.1073/pnas.1332765100>
- Bedzo, O. K. K., Mandegari, M., & Görgens, J. F. (2020). Techno-economic analysis of inulooligosaccharides, protein, and biofuel co-production from Jerusalem artichoke tubers: A biorefinery approach. *Biofuels, Bioproducts and Biorefining*, *14*(4), 776–793. <https://doi.org/10.1002/bbb.2105>
- Bendtsen, J. D., Nielsen, H., von Heijne, G., & Brunak, S. (2004). Improved prediction of signal peptides: SignalP 3.0. *Journal of Molecular Biology*, *340*(4), 783–795. <https://doi.org/10.1016/j.jmb.2004.05.028>
- Bhatia, S. K., Bhatia, R. K., Choi, Y. K., Kan, E., Kim, Y. G., & Yang, Y. H. (2018). Biotechnological potential of microbial consortia and future perspectives. *Critical Reviews in Biotechnology*, *38*(8), 1209–1229. <https://doi.org/10.1080/07388551.2018.1471445>
- Bhatia, S. K., Yoon, J. J., Kim, H. J., Hong, J. W., Gi Hong, Y., Song, H. S., Moon, Y. M., Jeon, J. M., Kim, Y. G., & Yang, Y. H. (2018). Engineering of artificial microbial consortia of *Ralstonia eutropha* and *Bacillus subtilis* for poly(3-hydroxybutyrate-co-3-hydroxyvalerate) copolymer production from sugarcane sugar without precursor feeding. *Bioresource Technology*, *257*(December 2017), 92–101. <https://doi.org/10.1016/j.biortech.2018.02.056>
- Bioplastics, E. (n.d.). *European bioplastics*. <https://www.european-bioplastics.org/>
- Budde, C. F., Riedel, S. L., Hübner, F., Risch, S., Popović, M. K., Rha, C., & Sinskey, A. J. (2011). Growth and polyhydroxybutyrate production by *Ralstonia eutropha* in emulsified plant oil medium. *Applied Microbiology and Biotechnology*, *89*(5), 1611–1619. <https://doi.org/10.1007/s00253-011-3102-0>
- Bugnicourt, E., Cinelli, P., Lazzeri, A., & Alvarez, V. (2014). Polyhydroxyalkanoate (PHA): Review of synthesis, characteristics, processing and potential applications in packaging. *Express Polymer Letters*, *8*(11), 791–808. <https://doi.org/10.3144/expresspolymlett.2014.82>
- Bustamante, D., Segarra, S., Tortajada, M., Ramón, D., del Cerro, C., Auxiliadora Prieto, M., Iglesias, J. R., & Rojas, A. (2019). In silico prospection of microorganisms to produce polyhydroxyalkanoate from whey: *Caulobacter segnis* DSM 29236 as a suitable industrial strain. *Microbial Biotechnology*, *12*(3), 487–501. <https://doi.org/10.1111/1751-7915.13371>

- Castaldi, S., Petrillo, C., Donadio, G., Piazz, F., Cimmino, A., Masi, M., Evidente, A., Istatico, R., Federico, N., Universitario, C., & Angelo, S. (2021). *Growth promotion function of Bacillus sp. strains isolated from salt-pan rhizosphere and their biocontrol potential against Macrophomina phaseolina*. February.
- Castilho, L. R., Mitchell, D. A., & Freire, D. M. G. (2009). Production of polyhydroxyalkanoates (PHAs) from waste materials and by-products by submerged and solid-state fermentation. *Bioresource Technology*, *100*(23), 5996–6009. <https://doi.org/10.1016/j.biortech.2009.03.088>
- Chen, G. Q., & Jiang, X. R. (2017). Engineering bacteria for enhanced polyhydroxyalkanoates (PHA) biosynthesis. *Synthetic and Systems Biotechnology*, *2*(3), 192–197. <https://doi.org/10.1016/j.synbio.2017.09.001>
- Choi, H. Y., Ryu, H. K., Park, K. M., Lee, E. G., Lee, H., Kim, S. W., & Choi, E. S. (2012). Direct lactic acid fermentation of Jerusalem artichoke tuber extract using *Lactobacillus paracasei* without acidic or enzymatic inulin hydrolysis. *Bioresource Technology*, *114*, 745–747. <https://doi.org/10.1016/j.biortech.2012.03.075>
- Choi, S. Y., Rhie, M. N., Kim, H. T., Joo, J. C., Cho, I. J., Son, J., Jo, S. Y., Sohn, Y. J., Baritugo, K. A., Pyo, J., Lee, Y., Lee, S. Y., & Park, S. J. (2020). Metabolic engineering for the synthesis of polyesters: A 100-year journey from polyhydroxyalkanoates to non-natural microbial polyesters. *Metabolic Engineering*, *58*(February), 47–81. <https://doi.org/10.1016/j.ymben.2019.05.009>
- Corrado, I., Cascelli, N., Ntasi, G., Birolo, L., Sannia, G., & Pezzella, C. (2021). Optimization of Inulin Hydrolysis by *Penicillium lanosocoeruleum* Inulinases and Efficient Conversion Into Polyhydroxyalkanoates. *Frontiers in Bioengineering and Biotechnology*, *9*(March), 1–17. <https://doi.org/10.3389/fbioe.2021.616908>
- de Jesus Assis, D., Santos, J., de Jesus, C. S., de Souza, C. O., Costa, S. S., Miranda, A. L., da Silva, J. R., Oliveira, M. B. P. P., & Druzian, J. I. (2019). Valorization of crude glycerol based on biological processes for accumulation of lipophilic compounds. *International Journal of Biological Macromolecules*, *129*, 728–736. <https://doi.org/10.1016/j.ijbiomac.2019.02.077>
- Diender, M., Parera Olm, I., & Sousa, D. Z. (2021). Synthetic co-cultures: novel avenues for bio-based processes. *Current Opinion in Biotechnology*, *67*, 72–79. <https://doi.org/10.1016/j.copbio.2021.01.006>
- El-malek, F. A., Khairy, H., Farag, A., & Omar, S. (2020). The sustainability of microbial bioplastics, production and applications. *International Journal of Biological Macromolecules*, *157*, 319–328. <https://doi.org/10.1016/j.ijbiomac.2020.04.076>
- Eriksen, M., Lebreton, L. C. M., Carson, H. S., Thiel, M., Moore, C. J., Borrorro, J. C., Galgani, F., Ryan, P. G., & Reisser, J. (2014). Plastic Pollution in the World's Oceans: More than 5 Trillion Plastic Pieces Weighing over 250,000 Tons Afloat at Sea. *PLoS ONE*, *9*(12), 1–15. <https://doi.org/10.1371/journal.pone.0111913>
- Favaro, L., Basaglia, M., & Casella, S. (2019). Improving polyhydroxyalkanoate production from inexpensive carbon sources by genetic approaches: a review.

- Biofuels, Bioproducts and Biorefining*, 13(1), 208–227. <https://doi.org/10.1002/bbb.1944>
- Gao, X., Chen, J. C., Wu, Q., & Chen, G. Q. (2011). Polyhydroxyalkanoates as a source of chemicals, polymers, and biofuels. *Current Opinion in Biotechnology*, 22(6), 768–774. <https://doi.org/10.1016/j.copbio.2011.06.005>
- Gouy, M., Guindon, S., & Gascuel, O. (2009). SeaView Version 4: A Multiplatform Graphical User Interface for Sequence Alignment and Phylogenetic Tree Building. *Molecular Biology and Evolution*, 27(2), 221–224. <https://doi.org/10.1093/molbev/msp259>
- Haas, C., Steinwandter, V., De Apodaca, E. D., Madurga, B. M., Smerilli, M., Dietrich, T., & Neureiter, M. (2015). Production of PHB from chicory roots - Comparison of three *Cupriavidus necator* strains. *Chemical and Biochemical Engineering Quarterly*, 29(2), 99–112. <https://doi.org/10.15255/CABEQ.2014.2250>
- Hannah Ritchie and Max Roser. (2018). *Plastic Pollution*. Our World in Data. <https://ourworldindata.org/plastic-pollution>
- Hughes, S. R., Qureshi, N., López-Núñez, J. C., Jones, M. A., Jarodsky, J. M., Galindo-Leva, L. Á., & Lindquist, M. R. (2017). Utilization of inulin-containing waste in industrial fermentations to produce biofuels and bio-based chemicals. *World Journal of Microbiology and Biotechnology*, 33(4), 1–15. <https://doi.org/10.1007/s11274-017-2241-6>
- Jensen, S. L., Diemer, M. B., Lundmark, M., Larsen, F. H., Blennow, A., Mogensen, H. K., & Nielsen, T. H. (2016). Levanase from *Bacillus subtilis* hydrolyses  $\beta$ -2,6 fructosyl bonds in bacterial levans and in grass fructans. *International Journal of Biological Macromolecules*, 85, 514–521. <https://doi.org/10.1016/j.ijbiomac.2016.01.008>
- Kargbo, D. M. (2010). Biodiesel production from municipal sewage sludges. *Energy and Fuels*, 24(5), 2791–2794. <https://doi.org/10.1021/ef1001106>
- Khatun, M. M., Liu, C. G., Zhao, X. Q., Yuan, W. J., & Bai, F. W. (2017). Consolidated ethanol production from Jerusalem artichoke tubers at elevated temperature by *Saccharomyces cerevisiae* engineered with inulinase expression through cell surface display. *Journal of Industrial Microbiology and Biotechnology*, 44(2), 295–301. <https://doi.org/10.1007/s10295-016-1881-0>
- Koller, M., Maršálek, L., de Sousa Dias, M. M., & Braunnegg, G. (2017). Producing microbial polyhydroxyalkanoate (PHA) biopolyesters in a sustainable manner. *New Biotechnology*, 37, 24–38. <https://doi.org/10.1016/j.nbt.2016.05.001>
- Kourmentza, C., Plácido, J., Venetsaneas, N., Burniol-Figols, A., Varrone, C., Gavala, H. N., & Reis, M. A. M. (2017). Recent advances and challenges towards sustainable polyhydroxyalkanoate (PHA) production. *Bioengineering*, 4(2), 1–43. <https://doi.org/10.3390/bioengineering4020055>
- Koutinas, A. A., Garcia, I. L., Kopsahelis, N., Papanikolaou, S., Webb, C., Villar, M. A., & López, J. A. (2013). Production of fermentation feedstock from jerusalem artichoke tubers and its potential for polyhydroxybutyrate synthesis. *Waste and Biomass Valorization*, 4(2), 359–370. <https://doi.org/10.1007/s12649-012-9154-2>

- Kumar, P., & Kim, B. S. (2018). Valorization of polyhydroxyalkanoates production process by co-synthesis of value-added products. *Bioresource Technology*, 269(July), 544–556. <https://doi.org/10.1016/j.biortech.2018.08.120>
- Kushner, D. J. (1978). *Microbial life in extreme environments*. Academic Press.
- Lammens, W., Le Roy, K., Schroeven, L., Van Laere, A., Rabijns, A., & Van den Ende, W. (2009). Structural insights into glycoside hydrolase family 32 and 68 enzymes: functional implications. *Journal of Experimental Botany*, 60(3), 727–740. <https://doi.org/10.1093/jxb/ern333>
- Lee, Y., Cho, I. J., Choi, S. Y., & Lee, S. Y. (2019). Systems Metabolic Engineering Strategies for Non-Natural Microbial Polyester Production. *Biotechnology Journal*, 14(9), 1800426. <https://doi.org/10.1002/biot.201800426>
- Li, Z., Yang, J., & Loh, X. J. (2016). Polyhydroxyalkanoates: Opening doors for a sustainable future. *NPG Asia Materials*, 8(4), 1–20. <https://doi.org/10.1038/am.2016.48>
- Licciardello, G., Catara, A. F., & Catara, V. (2019). Production of polyhydroxyalkanoates and extracellular products using *Pseudomonas corrugata* and *P. mediterranea*: A review. *Bioengineering*, 6(4). <https://doi.org/10.3390/bioengineering6040105>
- Liu, Y., Yang, S., & Jia, X. (2020). Construction of a “nutrition supply–detoxification” coculture consortium for medium-chain-length polyhydroxyalkanoate production with a glucose–xylose mixture. *Journal of Industrial Microbiology and Biotechnology*, 47(3), 343–354. <https://doi.org/10.1007/s10295-020-02267-7>
- Martin, I., Debarbouille, M., Klier, A., & Rapoport, G. (1989). Induction and metabolite regulation of levanase synthesis in *Bacillus subtilis*. *Journal of Bacteriology*, 171(4), 1885–1892. <https://doi.org/10.1128/jb.171.4.1885-1892.1989>
- Moreno, M. de L., Pérez, D., García, M. T., & Mellado, E. (2013). Halophilic bacteria as a source of novel hydrolytic enzymes. *Life*, 3(1), 38–51. <https://doi.org/10.3390/life3010038>
- Mozejko, J., & Ciesielski, S. (2014). Pulsed feeding strategy is more favorable to medium-chain-length polyhydroxyalkanoates production from waste rapeseed oil. *Biotechnology Progress*, 30(5), 1243–1246. <https://doi.org/10.1002/btpr.1914>
- Muhammadi, Shabina, Afzal, M., & Hameed, S. (2015). *Green Chemistry Letters and Reviews Bacterial polyhydroxyalkanoates-eco-friendly next generation plastic : Production , biocompatibility , biodegradation , physical properties and applications*. 8253. <https://doi.org/10.1080/17518253.2015.1109715>
- Nikodinovic-Runic, J., Guzik, M., Kenny, S. T., Babu, R., Werker, A., & O'Connor, K. E. (2013). Carbon-rich wastes as feedstocks for biodegradable polymer (polyhydroxyalkanoate) production using bacteria. In *Advances in Applied Microbiology* (Vol. 84). <https://doi.org/10.1016/B978-0-12-407673-0.00004-7>
- Ojumu, T. V., Yu, J., & Solomon, B. O. (2004). Production of Polyhydroxyalkanoates, a bacterial biodegradable polymer. *African Journal of Biotechnology*, 3(1), 18–24. <https://doi.org/10.5897/AJB2004.000-2004>

- Overbeek, R., Olson, R., Pusch, G. D., Olsen, G. J., Davis, J. J., Disz, T., Edwards, R. A., Gerdes, S., Parrello, B., Shukla, M., Vonstein, V., Wattam, A. R., Xia, F., Stevens, R., Martin, I., Débarbouillé, M., Ferrari, E., Klier, A., & Rapoport, G. (2014). The SEED and the Rapid Annotation of microbial genomes using Subsystems Technology (RAST). *Nucleic Acids Research*, 42(Database issue), D206–D214. <https://doi.org/10.1093/nar/gkt1226>
- Petrillo, C., Castaldi, S., Selci, M., Giovannelli, D., Isticato, R. (2021). Genomic Mining of Halophilic Bacilli Exhibiting Promising Plant Growth-Promoting and Biocontrol Potentials. *Preprint*.
- Pons, T., Naumoff, D. G., Martínez-Fleites, C., & Hernández, L. (2004). Three acidic residues are at the active site of a beta-propeller architecture in glycoside hydrolase families 32, 43, 62, and 68. *Proteins*, 54(3), 424–432. <https://doi.org/10.1002/prot.10604>
- Qiu, Y., Zhang, Y., Zhu, Y., Sha, Y., Xu, Z., Feng, X., Li, S., & Xu, H. (2019). Improving poly-( $\gamma$ -glutamic acid) production from a glutamic acid-independent strain from inulin substrate by consolidated bioprocessing. *Bioprocess and Biosystems Engineering*, 42(10), 1711–1720. <https://doi.org/10.1007/s00449-019-02167-w>
- Rai, R., Keshavarz, T., Roether, J. A., Boccaccini, A. R., & Roy, I. (2011). Medium chain length polyhydroxyalkanoates, promising new biomedical materials for the future. *Materials Science and Engineering R: Reports*, 72(3), 29–47. <https://doi.org/10.1016/j.mser.2010.11.002>
- Raza, Z. A., Abid, S., & Banat, I. M. (2018). Polyhydroxyalkanoates: Characteristics, production, recent developments and applications. *International Biodeterioration and Biodegradation*, 126(September 2017), 45–56. <https://doi.org/10.1016/j.ibiod.2017.10.001>
- Raza, Z. A., Tariq, M. R., Majeed, M. I., & Banat, I. M. (2019). Recent developments in bioreactor scale production of bacterial polyhydroxyalkanoates. *Bioprocess and Biosystems Engineering*, 42(6), 901–919. <https://doi.org/10.1007/s00449-019-02093-x>
- Reddy, V. A., & Maley, F. (1990). Identification of an active-site residue in yeast invertase by affinity labeling and site-directed mutagenesis. *The Journal of Biological Chemistry*, 265(19), 10817–10820.
- Rehm, B. H. A. (2003). Polyester synthases: Natural catalysts for plastics. *Biochemical Journal*, 376(1), 15–33. <https://doi.org/10.1042/BJ20031254>
- Rodrigues, P. R., Assis, D. J., & Druzian, J. I. (2019). Simultaneous production of polyhydroxyalkanoate and xanthan gum: From axenic to mixed cultivation. *Bioresource Technology*, 283(March), 332–339. <https://doi.org/10.1016/j.biortech.2019.03.095>
- Rutkowska, M., Krasowska, K., Heimowska, A., Steinka, I., Janik, H., Haponiuk, J., & Karlsson, S. (2002). Biodegradation of Modified Poly( $\epsilon$ -caprolactone) in Different Environments. *Polish Journal of Environmental Studies*, 11(4), 413–420.
- Sabapathy, P. C., Devaraj, S., & Kathirvel, P. (2017). Parthenium hysterophorus: Low cost substrate for the production of polyhydroxyalkanoates. *Current*

- Science*, 112(10), 2106–2111. <https://doi.org/10.18520/cs/v112/i10/2106-2111>
- Sabapathy, P. C., Devaraj, S., Meixner, K., Anburajan, P., Kathirvel, P., Ravikumar, Y., & Zayed, H. M. (2020). Bioresource Technology Recent developments in Polyhydroxyalkanoates ( PHAs ) production – A review. *Bioresource Technology*, 306(January), 123132. <https://doi.org/10.1016/j.biortech.2020.123132>
- Sabarinathan, D., Chandrika, S. P., Venkatraman, P., Easwaran, M., Sureka, C. S., & Preethi, K. (2018). Production of polyhydroxybutyrate (PHB) from *Pseudomonas plecoglossicida* and its application towards cancer detection. *Informatics in Medicine Unlocked*, 11(April), 61–67. <https://doi.org/10.1016/j.imu.2018.04.009>
- Saratale, G. D., Rijuta, G. R., Varjani, S., Cho, S., Ghodake, G. S., Kadam, A., Mulla, S. I., Bharagava, R. N., Kim, D., & Shin, H. S. (2020). Industrial Crops & Products Development of ultrasound aided chemical pretreatment methods to enrich saccharification of wheat waste biomass for polyhydroxybutyrate production and its characterization. *Industrial Crops & Products*, 150(April), 112425. <https://doi.org/10.1016/j.indcrop.2020.112425>
- Saratale, R. G., Cho, S., Ghodake, G. S., Shin, H., Saratale, G. D., Park, Y., Lee, H., Bharagava, R. N., & Kim, D. (2020). Utilization of Noxious Weed Water Hyacinth Biomass as a Potential Feedstock for Biopolymers Production: *Polymers*, 12. <https://doi.org/10.3390/polym12081704>
- Sawant, S. S., Salunke, B. K., Taylor, L. E., & Kim, B. S. (2017). Enhanced agarose and xylan degradation for production of polyhydroxyalkanoates by co-culture of marine bacterium, *Saccharophagus degradans* and its contaminant, *Bacillus Cereus*. *Applied Sciences (Switzerland)*, 7(3). <https://doi.org/10.3390/app7030225>
- Singh, Ram S., & Singh, R. P. (2010). Production of fructooligosaccharides from inulin by endoinulinases and their prebiotic potential. *Food Technology and Biotechnology*, 48(4), 435–450.
- Singh, Ram Sarup, Chauhan, K., & Kennedy, J. F. (2017). A panorama of bacterial inulinases: Production, purification, characterization and industrial applications. *International Journal of Biological Macromolecules*, 96, 312–322. <https://doi.org/10.1016/j.ijbiomac.2016.12.004>
- Sirohi, R., Prakash Pandey, J., Kumar Gaur, V., Gnansounou, E., & Sindhu, R. (2020). Critical overview of biomass feedstocks as sustainable substrates for the production of polyhydroxybutyrate (PHB). *Bioresource Technology*, 311(May), 123536. <https://doi.org/10.1016/j.biortech.2020.123536>
- Sohn, Y. J., Kim, H. T., Baritugo, K., Jo, S. Y., Song, H. M., Park, S. Y., Park, S. K., Pyo, J., Cha, H. G., Kim, H., Na, J., Park, C., Choi, J., Joo, J. C., & Park, S. J. (2020). Recent Advances in Sustainable Plastic Upcycling and Biopolymers. *Biotechnology Journal*, 1900489, 1–16. <https://doi.org/10.1002/biot.201900489>
- Stothard, P., & Wishart, D. S. (2004). Circular genome visualization and exploration using CGView. *Bioinformatics*, 21(4), 537–539. <https://doi.org/10.1093/bioinformatics/bti054>
- Sudesh, K., Abe, H., & Doi, Y. (2000). Synthesis, structure and properties of

- polyhydroxyalkanoates: Biological polyesters. *Progress in Polymer Science (Oxford)*, 25(10), 1503–1555. [https://doi.org/10.1016/S0079-6700\(00\)00035-6](https://doi.org/10.1016/S0079-6700(00)00035-6)
- Tan, D., Wang, Y., Tong, Y., & Chen, G. Q. (2021). Grand Challenges for Industrializing Polyhydroxyalkanoates (PHAs). *Trends in Biotechnology*, 1–11. <https://doi.org/10.1016/j.tibtech.2020.11.010>
- Tjalsma, H., Bolhuis, A., Jongbloed, J. D., Bron, S., & van Dijl, J. M. (2000). Signal peptide-dependent protein transport in *Bacillus subtilis*: a genome-based survey of the secretome. *Microbiology and Molecular Biology Reviews: MMBR*, 64(3), 515–547. <https://doi.org/10.1128/mmbr.64.3.515-547.2000>
- Tsuge, T. (2016). Fundamental factors determining the molecular weight of polyhydroxyalkanoate during biosynthesis. *Polymer Journal*, 48(11), 1051–1057. <https://doi.org/10.1038/pj.2016.78>
- Turco, R., Santagata, G., Corrado, I., Pezzella, C., & Di Serio, M. (2021). In vivo and Post-synthesis Strategies to Enhance the Properties of PHB-Based Materials: A Review. *Frontiers in Bioengineering and Biotechnology*, 8. <https://doi.org/10.3389/fbioe.2020.619266>
- Vastano, M., Casillo, A., Corsaro, M. M., Sannia, G., & Pezzella, C. (2015). Production of medium chain length polyhydroxyalkanoates from waste oils by recombinant *Escherichia coli*. *Engineering in Life Sciences*, 15(7). <https://doi.org/10.1002/elsc.201500022>
- Verlinden, R. A. J., Hill, D. J., Kenward, M. A., Williams, C. D., & Radecka, I. (2007). Bacterial synthesis of biodegradable polyhydroxyalkanoates. *Journal of Applied Microbiology*, 102(6), 1437–1449. <https://doi.org/10.1111/j.1365-2672.2007.03335.x>
- Zhang, L., Shi, Z. Y., Wu, Q., & Chen, G. Q. (2009). Microbial production of 4-hydroxybutyrate, poly-4-hydroxybutyrate, and poly(3-hydroxybutyrate-co-4-hydroxybutyrate) by recombinant microorganisms. *Applied Microbiology and Biotechnology*, 84(5), 909–916. <https://doi.org/10.1007/s00253-009-2023-7>

**SUBMITTED****The power of two: an artificial microbial consortium for the conversion of inulin into Polyhydroxyalkanoates****Supplementary materials****Table S1.** List of the halophilic bacteria screened for inulinase production (Petrillo et al. 2021).

Strain	Species
RHF1	<i>Bacillus licheniformis</i>
RHF2	<i>Bacillus subtilis</i> 168
RHF4	<i>Bacillus cereus</i>
RHF6	<i>Bacillus amyloliquefaciens</i>
RHF12	<i>Bacillus halotolerans</i>
RHF13	<i>Bacillus subtilis</i>
RHF15	<i>Bacillus gibsonii</i>
RHF17	<i>Bacillus licheniformis</i>

**Table S2.** Circular genome map of strain RHF15's genome obtained with CG View (Stothard and Wishart, 2004). The contents of the feature rings (starting with the outermost ring) are as follows: Ring 1 depicts the identified CDSs. Ring 2 shows GC content and Ring 3 shows GC skew.

- GC Content
- GC Skew+
- GC Skew-
- tRNA
- CDS
- tmRNA

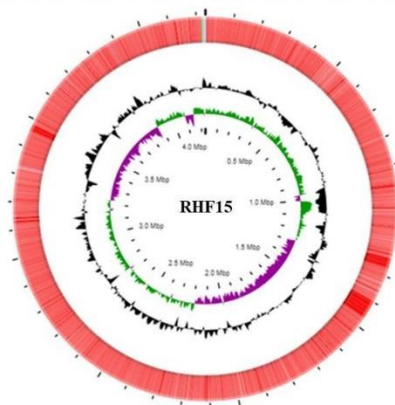


**Table S3.** Functional classification of RHF15's genome CDSs performed with RASTA server. The detected categories are reported.

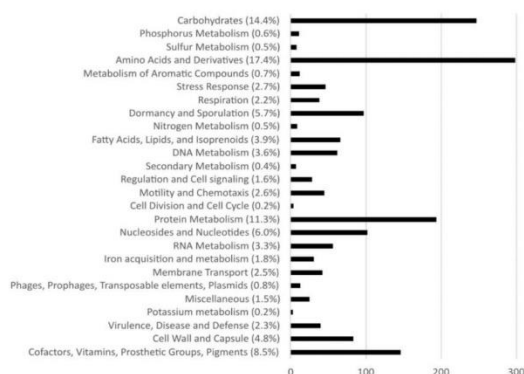


**Table S4.** List of well-known bacterial and fungal inulin hydrolases used for the multiple alignment analysis (Figure S5). Accession number from NCBI database, source and enzyme type are specified for each entry.

Acc. No	Source	Type	Size	Refere
CAC44220.1	<i>Aspergillus awamori</i> subsp. <i>awamori</i>	Exo-	573 aa	<a href="https://">https://</a>
CAK41278.1	<i>Aspergillus niger</i>	Exo-	537 aa	<a href="https://">https://</a>
AMX81520.1	<i>Kluyveromyces marxianus</i>	Exo-	555 aa	<a href="https://">https://</a>
BAB19132.1	<i>Penicillium</i> sp. <i>TN-88</i>	Endo-	515 aa	<a href="https://">https://</a>
AHN08014.1	<i>Paenibacillus polymyxa</i>	Exo-	485 aa	<a href="https://">https://</a>
BAC45010.1	<i>Geobacillus stearothermophilus</i>	Exo-	493 aa	<a href="https://">https://</a>
AAL34524.1	<i>Aspergillus niger</i>	Endo-	516 aa	<a href="https://">https://</a>
OLG11497.1	<i>B. paralicheniformis</i>	Levanase	515 aa	<a href="https://">https://</a>
WP_153940225.1	<i>B. subtilis</i>	Levanase	677 aa	<a href="https://">https://</a>
WP_106073378.1	<i>B. subtilis</i>	2,6-beta-fructan 6-levanbiohydrolase	516 aa	<a href="https://">https://</a>
B7HW11	<i>B. cereus</i>	Sucrose-6-phosphate hydrolase	491 aa	<a href="https://">https://</a>
NP_391683.2	<i>B. subtilis</i>	Sucrose-6-phosphate hydrolase	479 aa	<a href="https://">https://</a>

**Figure S5.** Multiple sequence alignment between well-known GH32 hydrolases and the selected enzymes of strain RHF15 obtained using SeaView software. The red boxes highlight the highly conserved catalytic motifs.

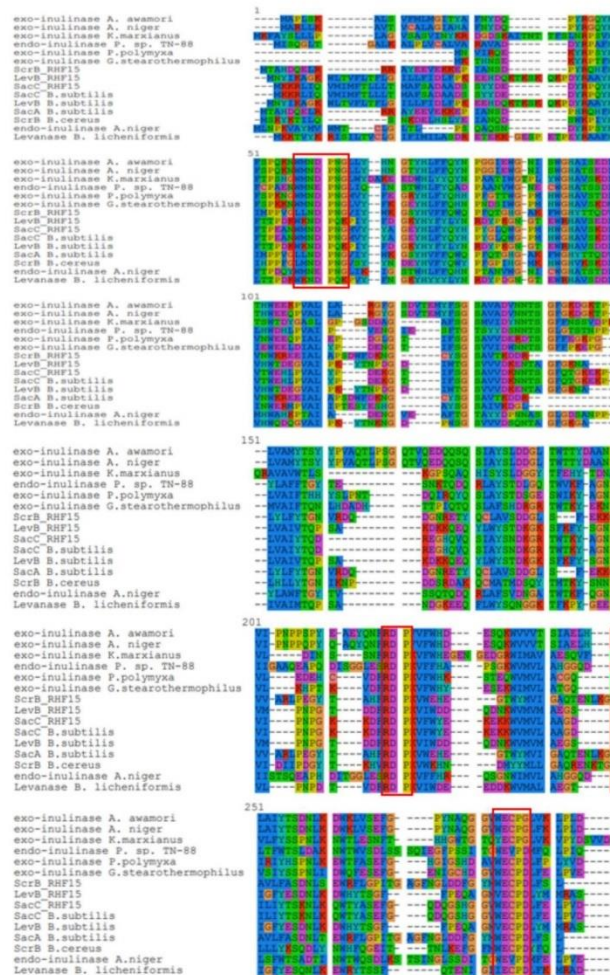
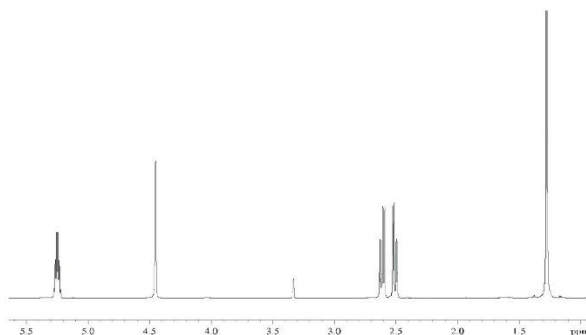


**Figure S6.**  $^1\text{H}$  NMR spectrum recorded in  $\text{CDCl}_3:\text{CD}_3\text{OD}$  (1:1) of PHB produced in the optimized co-culture condition



### Bibliography

- Petrillo, C., Castaldi, S., Selci, M., Giovannelli, D., Isticato, R., 2021. Genomic Mining of Halophilic Bacilli Exhibiting Promising Plant Growth-Promoting and Biocontrol Potentials. Preprint.
- Stothard, P., Wishart, D.S., 2004. Circular genome visualization and exploration using CGView. *Bioinformatics* 21, 537–539. <https://doi.org/10.1093/bioinformatics/bti054>

## Chapter 2 Polymer application

The concept of nanotechnology was introduced in 1959 by Richard Feynman and the term “nanotechnology” was later coined again by Norio Taniguchi in 1974. The application of nanotechnology to polymers involves the design, manufacturing, processing and application of polymer materials filled with nano- particles and/or devices of nano range dimensions. In the **Paragraph 2.1** blending of PHA-based nanoparticles (PHA-NPs) and Whey Protein (WP) -based materials is reported as strategy for obtaining new polymeric materials with improved properties. WP-based films, like all the hydrocolloid films, suffer from limitations in barrier and mechanical features, often requiring additives to improve resistance to moisture transfer as well as to enhance their flexibility (Ramos et al., 2012). The addition of PHA-NPs to WP-based materials resulted in a plasticizing effect producing a resistant and more extensible biomaterial. Moreover, the presence of NPs inside the matrix enhances the film barrier property towards O<sub>2</sub>, letting to envisage a possible application of this novel material in food packaging, especially for those products requiring preservation from oxidative reactions.

In the field of nanobiotechnology, drug delivery systems (DDSs) aim to deliver drugs in an ideal, controlled time and space-related process, defining the right drug concentration, minimizing side effects, and reducing drugs degradation. All these advantages, together with the possibility of a wide range of drugs delivery, expand the DDSs applicability in different fields, from pharmaceutical to food industries. Among the carriers, biopolymeric nanoparticles gain a widespread interest due to low toxicity, good encapsulation, and the additional targeted biodegradability (Rodríguez-Contreras et al., 2013).

Polyhydroxyalkanoates (PHAs) as biodegradable and biocompatible polyesters are good candidates in developing of biodegradable nano-vehicles for active molecules delivery (Giufreda et al., 2016; Perveen et al., 2020; Rodríguez-Contreras et al., 2013). Interestingly PHAs differ from other polyesters for the nontoxic degradation products thus allowing this promising material to be applied *in vivo* in biomedical field. Many examples of NPs PHA-based production are reported in literature together with different applications.

Among active molecules, scientists shifted their attention toward herbal medicine e.g plant products, such as Essential Oils (EOs). EOs are a mixture of volatile compounds largely employed for their

antibacterial, antifungal, and insecticidal activities (Burt, 2004; Stefanakis et al., 2013). Because of the great number of constituents, essential oils seem to have no specific cellular targets. As typical lipophiles, they pass through the cell wall and cytoplasmic membrane, disrupting the structure of the layers of polysaccharides, fatty acids, and phospholipids and permeabilizing them. In bacteria, permeabilization of the membranes is associated with loss of ions and reduction of membrane potential (Turina et al., 2006). Despite their high potential the volatile compounds found in EOs can be easily oxidized, so a process such as microencapsulation can suppress or retard oxidation, improving solubility and stability, while masking their strong odour (Chouhan et al., 2017; Lammari et al., 2020). Recently, the possibility to encapsulate EOs into polymeric NPs has been investigated, shielding their stability, controlling their delivery, and enhancing their bioavailability (Bilia et al., 2014). The possibility of using nanoparticles PHA-based as carriers for bioactive compounds was investigated encapsulating oregano essential oils (**Paragraph 2.2**).

## References

- Bilia, A. R., Guccione, C., Isacchi, B., Righeschi, C., Firenzuoli, F., & Bergonzi, M. C. (2014). Essential oils loaded in nanosystems: A developing strategy for a successful therapeutic approach. *Evidence-Based Complementary and Alternative Medicine*, 2014(May). <https://doi.org/10.1155/2014/651593>
- Burt, S. (2004). Essential oils: Their antibacterial properties and potential applications in foods - A review. *International Journal of Food Microbiology*, 94(3), 223–253. <https://doi.org/10.1016/j.ijfoodmicro.2004.03.022>
- Chouhan, S., Sharma, K., & Sanjay, G. (2017). Antimicrobial Activity of Some Essential Oils—Present Status and Future Perspectives. *Medicines*, 4(3), 58. <https://doi.org/10.3390/medicines4030058>
- Giufreda, W. M., Cabral, V. F., Cardoso-Filho, L., dos Santos Conti, D., de Campos, V. E. B., & da Rocha, S. R. P. (2016). Medroxyprogesterone-encapsulated poly(3-hydroxybutyrate-co-3-hydroxyvalerate) nanoparticles using supercritical fluid extraction of emulsions. *Journal of Supercritical Fluids*, 118, 79–88. <https://doi.org/10.1016/j.supflu.2016.07.026>
- Lammari, N., Louaer, O., Meniai, A. H., & Elaissari, A. (2020). Encapsulation of essential oils via nanoprecipitation process: Overview, progress, challenges and prospects. *Pharmaceutics*, 12(5), 1–21. <https://doi.org/10.3390/pharmaceutics12050431>
- Perveen, K., Masood, F., & Hameed, A. (2020). Preparation, characterization and evaluation of antibacterial properties of epirubicin loaded PHB and PHBV nanoparticles. *International Journal of Biological Macromolecules*, 144, 259–

266. <https://doi.org/10.1016/j.ijbiomac.2019.12.049>
- Ramos, Ó. L., Pereira, J. O., Silva, S. I., Fernandes, J. C., Franco, M. I., Lopes-da-Silva, J. A., Pintado, M. E., & Malcata, F. X. (2012). Evaluation of antimicrobial edible coatings from a whey protein isolate base to improve the shelf life of cheese. *Journal of Dairy Science*, *95*(11), 6282–6292. <https://doi.org/10.3168/jds.2012-5478>
- Rodríguez-Contreras, A., Canal, C., Calafell-Monfort, M., Ginebra, M. P., Julio-Moran, G., & Marqués-Calvo, M. S. (2013). Methods for the preparation of doxycycline-loaded phb micro- and nano-spheres. *European Polymer Journal*, *49*(11), 3501–3511. <https://doi.org/10.1016/j.eurpolymj.2013.08.010>
- Stefanakis, M. K., Touloupakis, E., Anastasopoulos, E., Ghanotakis, D., Katerinopoulos, H. E., & Makridis, P. (2013). Antibacterial activity of essential oils from plants of the genus *Origanum*. *Food Control*, *34*(2), 539–546. <https://doi.org/10.1016/j.foodcont.2013.05.024>
- Turina, A. del V., Nolan, M. V., Zygadlo, J. A., & Perillo, M. A. (2006). Natural terpenes: Self-assembly and membrane partitioning. *Biophysical Chemistry*, *122*(2), 101–113. <https://doi.org/10.1016/j.bpc.2006.02.007>

## 2.1 Design and characterization of poly (3-hydroxybutyrate-co-hydroxyhexanoate) nanoparticles and their grafting in whey protein-based nanocomposites

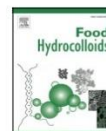
Food Hydrocolloids 110 (2021) 106167



Contents lists available at ScienceDirect

Food Hydrocolloids

journal homepage: <http://www.elsevier.com/locate/foodhyd>



### Design and characterization of poly (3-hydroxybutyrate-co-hydroxyhexanoate) nanoparticles and their grafting in whey protein-based nanocomposites

Iolanda Corrado<sup>a,1</sup>, Manar Abdalrazeq<sup>a,1</sup>, Cinzia Pezzella<sup>b,\*</sup>, Rocco Di Girolamo<sup>a</sup>, Raffaele Porta<sup>a</sup>, Giovanni Sannia<sup>a</sup>, C. Valeria L. Giosafatto<sup>a</sup>

<sup>a</sup> Department of Chemical Sciences, University Federico II, Via Cinthia 4, 80126, Naples, Italy

<sup>b</sup> Department of Agricultural Sciences, University Federico II, Via Università 100, 8055, Portici, Italy

#### ARTICLE INFO

##### Keywords:

Poly-3-hydroxybutyrate-co-hydroxyhexanoate  
Whey proteins films  
Nanoparticles

#### ABSTRACT

This work succeeded in the preparation of a nano-biocomposite material based on the use of poly-3-hydroxybutyrate-co-hydroxyhexanoate nanoparticles (PHBHx-NPs) within a scaffold of whey protein (WP) based films. The experimental conditions for PHBHx-NPs preparation by solvent-evaporation technique were set up, and the obtained NPs characterized. Dynamic light scattering analyses showed that PHBHx-NPs are stable, exhibiting a zeta-potential value close to  $-40$  mV and a Z-average size of 80 nm. Morphological characterization by transmission and scanning electron microscopy confirmed nanoparticle average dimensions. The addition of PHBHx-NPs to WP-based films improved the mechanical properties of the derived bioplastics, producing more extensible materials preserving their mechanical resistance. The grafting of PHBHx-NPs as material fillers also enhanced the film barrier properties towards O<sub>2</sub>, the permeability to both water vapor and CO<sub>2</sub> remaining unaffected.

#### 1. Introduction

The redesigning of plastic materials under a “green perspective” is, nowadays, necessary to address the issue of plastic pollution as well as of shortening of fossil resources. In the bioplastics scenario, materials derived from natural bio-based polymers (i.e. polysaccharides, proteins) or produced by bacteria from renewable resources (i.e. poly-hydroxyalkanoates, PHA) play a key role, due to their renewable origin and biodegradability features. In particular, the formulation of new biobased composites based on the combination of different classes of biopolymers represents an area of increasing interest for numerous application fields (Li, Yang, & Loh, 2016; Raza, Abid, & Banat, 2018; Zhang, Shishatskaya, Volova, da Silva, & Chen, 2018).

PHAs are a family of polyesters accumulated by various bacteria as carbon and energy storage under stressful conditions. Due to their intrinsic biodegradability and demonstrated biocompatibility (Elmowafy et al., 2019; Koller, 2018), PHA found a range of applications, from food packaging to biomedical sectors. The spectrum of properties displayed by PHA-derived materials is very close to

that of conventional petro-plastics, and is dependent on their monomer structure and relative content, which influence the physicochemical parameters of the biopolymers as well as their kinetics of biodegradation (Chanprateep, Buasri, Muangwong, & Utiswanakul, 2010). In the last decade, different PHAs (poly-hydroxybutyrate, PHB; poly-3-hydroxybutyrate-co-hydroxyvalerate, PHBV; poly-3-hydroxybutyrate-co-hydroxyhexanoate, PHBHx) have been exploited for the preparation of nanoparticles (NPs), able to encapsulate and release various drugs (Kalia, 2019; Kiliay et al., 2011; Murueva, Shishatskaya, Kuzmina, Volova, & Sinskey, 2013; Naureen et al., 2015; Sandoval, Rivera, Barrera-Rivera, & Martínez-Richa, 2010; Shrivastav, Kim, & Kim, 2013). Among the different polymers, PHBHx displays peculiar elastic properties, thus emerging as promising biopolymeric source for the designing of nanocomposites with improved flexibility (Raza et al., 2018; M.; Vastano et al., 2017; Vastano, Corrado, Sannia, Solaiman, & Pezzella, 2019).

However, despite their potential, the effective exploitation of PHA-based materials is still hindered by their high production costs.

\* Corresponding author.

E-mail address: [cpezzella@umina.it](mailto:cpezzella@umina.it) (C. Pezzella).

<sup>1</sup> Equally contributing authors.

<https://doi.org/10.1016/j.foodhyd.2020.106167>

Received 23 April 2020; Received in revised form 9 July 2020; Accepted 10 July 2020

Available online 15 July 2020

0268-005X/© 2020 Elsevier Ltd. All rights reserved.

Consequently, sustainable strategies for PHA production are based on the use of waste materials as starting feedstock for microbial fermentation and are considered even more effective if integrated in a bio-refinery concept (Kumar & Kim, 2018; Nugroho Prasetyo et al., 2010; Vastano et al., 2019). In this regard, an engineered *Escherichia coli* strain able to produce PHBHHx (40:60 M ratio) was developed (Vastano et al., 2017) and its ability to accumulate the biopolymer through the valorisation of waste materials was recently demonstrated (Vastano et al., 2019).

Another class of renewable biomacromolecules that deserves a special attention is represented by proteins derived from agro-food by-products as they are quite abundant and their recovery might contribute to waste reduction. In particular, it is important to mention proteins present in the whey, a by-product of dairy industries produced in huge amounts following milk casein coagulation. The total worldwide whey production is estimated to be more than 180 million tons/year, the major amount (approximately 70%) coming from the EU and USA (Yadav et al., 2015). Only 50% of whey is recycled and converted into high added value products (Mollea, Marmo, & Bosco, 2013). For both the large volume and the high organic content the direct disposal of whey is not environmental friendly and it is virtually forbidden all over the world. The great majority of whey proteins (WPs) is represented by  $\beta$ -lactoglobulin and  $\alpha$ -lactalbumin, endowed with different features such as solubility, foaming, and gelling ability (Norwood, Croguennec, Le Floch-Fouéré, Schuck, & Jeantet, 2018) suitable for several biotechnological applications. In particular, it was recently found out that under alkaline conditions these proteins have the ability to give rise to promising edible bioplastic materials (Abdalrazeq et al., 2019). However, WP-based films, like all the hydrocolloid films, suffer from limitations in barrier and mechanical features, often requiring additives to improve resistance to moisture transfer as well as to enhance their flexibility (Ramos et al., 2012). Many authors investigated the possibility to improve the features of WP-based films by blending them with polysaccharides. Addition of polysaccharides has a significant effect on the physical properties of protein-based edible films (Ciesla, Salmieri, & Lacroix, 2006). In this respect, Di Piero et al. (2013) (Di Piero et al., 2013) examined the behaviour of pectin and thermally denatured WPs at various protein/polysaccharide ratios and at various pH values. The same authors also investigated the effect of the addition of chitosan to WP-formulations, in order not only to enhance the film technological properties but also to confer antimicrobial activity to the derived bioplastics thus extending fresh dairy product shelf-life (Di Piero, Sorrentino, Mariniello, Giosafatto, & Porta, 2011). Moreover, further investigations have been focused on the use of different NPs, such as the ones prepared by nanocellulose, usually used to improve the properties of diverse biomaterials (Sharif Hossain, Uddin, Veetil, & Fawzi, 2018). As matter of fact, cellulose nanostructures have been most usually applied as reinforcing phases, but they may also be used as matrices for a variety of materials including films for food packaging applications (Azeredo, Rosa, & Mattoso, 2017). As far as WP-based films reinforcement some efforts have been made by using porous silica (SiO<sub>2</sub>) coated titania (TiO<sub>2</sub>) NPs (TiO<sub>2</sub>@SiO<sub>2</sub>) (Kadam et al., 2013), and it was demonstrated that the incorporation of TiO<sub>2</sub>@SiO<sub>2</sub> NPs helps to improve WP-based film mechanical properties. However, the optical properties of the WP films were dramatically modified following incorporation of these NPs, changing from a transparent appearance to an opaque one, even though the embedded NPs contributed effectively to increase the thickness of films and to alter the contact angle of their surface. Therefore, the development of high strength, flexible nano-biocomposites controlling nanoparticle properties, their volume fraction and their topographic distribution within the scaffold still remains a significant challenge.

With the aim to decrease the hydrophilicity of WP-based materials and, consequently, to improve their performance, the possibility to prepare nano-biocomposites by blending WP-proteins with NPs obtained from PHBHHx has been studied. In this paper, the optimal

formulation of PHBHHx-NPs into the whey protein film matrix was explored and the technological properties of the derived films investigated.

## 2. Material and methods

### 2.1. Materials

Commercial WP isolate (~90% dry basis protein) was obtained from BioLine (New Zealand), Glycerol (GLY) and all other reagents were of analytical grade and they were purchased from Sigma (Steinheim, Germany).

### 2.2. Recombinant production of PHBHHx

For PHBHHx production, recombinant *Escherichia coli* strain, LipōB, was cultured in an Eppendorf NewBrunswick, BioFlo/CelliGen®115 according to (Vastano et al., 2017). LipōB strain was grown in Luria-Bertani (LB) broth at 37 °C, supplemented with ampicillin (100 µg mL<sup>-1</sup>). After 12 h, the pre-inoculum was transferred in M9 medium at OD<sub>600nm</sub> of 0.1. The composition of M9 medium is as follows (for 1 L): 100 mL M9 salt [10x]; 0.1 mL of CaCl<sub>2</sub> [1 mol L<sup>-1</sup>]; 5 mL of Glucose [40%]; 2 mL of MgSO<sub>4</sub> [1 mol L<sup>-1</sup>]. Composition of M9 salt [10x] for 1 L [pH 7.4] is as follows: 60 g Na<sub>2</sub>HPO<sub>4</sub>; 30 g KH<sub>2</sub>PO<sub>4</sub>; 5 g NaCl; 10 g NH<sub>4</sub>Cl. The media were completed after sterilization with the carbon source and other components were prepared in a concentrated solution. A stock solution [20 g L<sup>-1</sup>] of yeast extract was autoclaved and then added to complete medium at 2 g L<sup>-1</sup>. M9 was supplemented with 0.01 mM of FeSO<sub>4</sub>. Sodium octanoate was prepared in a stock solution of 40 [g L<sup>-1</sup>] and sterilized by filtering. This additional carbon source was added to the cultures (0.1 w/v) as extra-volume. Induction of protein expression was performed after 5 h from the inoculum with 0.5 mM IPTG (isopropyl- $\beta$ -D-thiogalactopyranoside). Cultures were carried out for additional 48 h. At the end of the batch fermentation, cells were recovered by centrifugation and solvent extracted with chloroform by using Soxhlet apparatus (100 mL for gram of lyophilized cells). The dissolved biopolymer was then precipitated by the dropwise addition of cold methanol (10 vol). The polymer was collected by centrifugation (5500 g, 30 min at 4 °C), recovered using fresh chloroform and dried under a N<sub>2</sub> flux at 21 °C. The purified polymer was stored at 4 °C until further use.

### 2.3. Synthesis of PHBHHx-NPs

Synthesis of PHBHHx-NPs was carried out using solvent evaporation protocol. Briefly, polymer was dissolved in chloroform at different concentrations and was then added to 5 mL of aqueous solution of sodium dodecyl sulphate (SDS) (4.44 mg/mL). The mixture was stirred at room temperature for an hour on a magnetic stirring plate, resulting in monodisperse chloroform droplets containing the dissolved polymer, separated from water by the SDS. Sonication (Sonopuls HD 2070; with standard horn) was then used (40% amplitude, 5 s pulse, 8 min) to emulsify the droplets and form the PHBHHx-NPs. Chloroform was removed by evaporation leaving the emulsion at room temperature under stirring for 24 h. Residual chloroform was removed in a rotary evaporator under partial vacuum at RT. NPs were recovered by centrifugation (5500 g, 10', 4 °C), resuspended in 10 mL of distilled water and filtrated using sterile filter paper disk (0.45 µm). Different organic: aqueous phase ratios, and SDS to PHBHHx mass ratios were assessed (see Results and discussion). The yield of recovered NPs was calculated as:  $Y = M_p \cdot 100 / M_{NP}$ , where  $M_p$  is the mass of recovered NPs, and  $M_p$  the amount of polymer used for their preparation.

### 2.4. Film preparation

Film forming solutions (FFSs) were prepared by dissolving WP

isolate (500 mg) in 25 mL distilled water and adjusting the pH to 12 by 0.1 N NaOH addition. The derived solutions were stirred for 1 h and, then, aqueous dispersion of PHBHHx-NPs (1, 2, 4 or 8%, w/w of WPs) was added under continued stirring at 700 rpm for 15 min. GLY (40%, w/w of WPs), used as a plasticizer, was finally added, under continued stirring for 15 min, just before casting. Each FFS (25 mL) was poured into 8 cm diameter polyester Petri dishes and the films were then obtained by drying all the FFSs at 25 °C and 45% RH for 24 h.

### 2.5. Zeta potential and particle size measurements

PHBHHx-NPs dispersion (0.1 mg/mL) in water and 1.0 mL of each WP-based FFSs were analysed for zeta potential and particle size by using a Zetasizer Nano-ZSP (Malvern®, Worcestershire, UK). The device was equipped with a helium-neon laser of 4 mW output power with a fixed wavelength of 633 nm (wavelength of laser red emission). The instrument software programmer calculated the zeta potential through the electrophoretic mobility by applying a voltage of 200 mV and using the Henry equation.

### 2.6. Film mechanical properties

All dried films were cut into 1 cm × 8 cm strips by using a sharp scissor, conditioned at 25 °C and 50% RH for 24 h by placing them into a glass chamber over a saturated solution of Mg(NO<sub>3</sub>)<sub>2</sub> before being tested. Film thickness was measured in six different points with a micrometer (Electronic digital micrometer, DC-516, sensitivity 0.001 mm) and film tensile strength (TS), elongation at break (EB) and Young's modulus (YM) were determined on five specimens of each sample (5 cm gage length, 1 kN load and 5 mm/min speed) by using an Instron universal testing instrument model no. 5543 A (Instron Engineering Corp., Norwood, MA, USA).

### 2.7. Film permeability

Gas (CO<sub>2</sub> and O<sub>2</sub>) and water vapor permeability (WWP) was determined using a modification of ASTM Standard Method D 3985-8126 with MultiPerm apparatus (ExtraSolutions s.r.l., Pisa, Italy). The samples, duplicates of each film, were conditioned for 2 day at 50% RH before measurement. Aluminum masks were used to reduce film test area to 5 cm<sup>2</sup>. The testing was performed at 25 °C under 50% RH.

### 2.8. Film transparency

The opacity of each sample was investigated as described by Shevkani et al. (2015) (Shevkani & Singh, 2015). This method is based on the measurement of absorbance at 600 nm (spectrophotometer UV/Vis SmartSpec 3000 Bio-Rad, Segrate, Milan, Italy) divided by the thickness (mm). All the samples were cut into pieces of 1 cm × 3 cm and they were let adhere perfectly to the wall of the cuvette. For studying the transmittance, film strips (1 cm × 4 cm) were placed in a quartz cuvette and their whole light transmittance was obtained by using an Agilent UV-vis spectrophotometer (Santa Clara, CA, USA) in the range of 200–800 nm with a scan rate of 250 nm/min.

### 2.9. Scanning electron microscopy (SEM)

A field emission scanning electron microscope (FE-SEM, FEI Nova NanoSEM450) was used to study the morphology of both films (cross-section and surface) and PHBHHx-NPs. For cross section imaging, the films were previously frozen using liquid nitrogen and then cryo-fractured. To investigate the PHBHHx samples, a droplet of NPs (suspension in water) was deposited on carbon stickers on aluminum stubs and then dried at room temperature. The images were acquired using an incident electron beam energy between 2 and 5 kV and by collecting secondary electrons (SE) with an ETD or TLD detector.

### 2.10. Transmission electron microscopy (TEM)

Samples for TEM analysis were prepared by placing a drop of a water dispersion of the PHBHHx-NPs on a carbon-coated copper TEM grid and allowing the solvent to evaporate. TEM images were collected using a FEI TECNAI G2 S-twin apparatus operating at 120 kV (LaB<sub>6</sub> source).

### 2.11. Statistical analysis

The results were analysed statistically using the JMP software 5.0 (SAS Institute, Cary, NC, USA). Arithmetic means and mean square errors were calculated in all cases. Data are referred to experiments carried out in triplicate, both for NPs preparation and film characterization. Significant differences in average values were tested using the Tukey-Kramer HSD test (significance level:  $P < 0.05$ ).

## 3. Results and discussion

### 3.1. Characterization of PHBHHx-NPs

PHBHHx-NPs were prepared using the solvent evaporation technique, by dispersing a polymer solution in the aqueous phase containing SDS as surfactant. The effect of different parameters on the Z-average size, polydispersity index (Pdl) and zeta potential of PHBHHx-NPs was assessed (Table 1). Taking the SDS concentration invariable, the polymer amount was reduced from 50 to 5 mg mL<sup>-1</sup>, keeping constant the volume of the organic phase (0.25 mL). This allowed to explore a SDS: PHBHHx mass ratio, ranging from 1.8 to 17.6 mg of surfactant for mg of polymer (Table 1, trials A-D). The highest polymer concentration resulted into the greatest particle size (trial A). The increase of the SDS: PHBHHx mass ratio corresponds to a decrease into particle size down to 82 nm (Trial D), while the Pdl is almost comparable (Trials B-D) and indicative of very monodisperse NPs. In all the tested conditions, PHBHHx-NPs revealed a good stability, with zeta potential values < -30 mV. An increase in the NPs recovery efficiency was also observed increasing the SDS: PHBHHx ratio. Another variable explored in PHBHHx-NPs preparation, was the organic: aqueous phase ratio. The effect of this parameter was tested, keeping constant the volume of the aqueous phase and increasing the organic one from 0.5 to 2.5 mL (Table 1, Trials E-G). In these conditions, the same amount of PHBHHx (12.5 mg) was used, leaving constant the SDS: PHBHHx mass ratio. However, particle size was almost unaffected by decreasing the solvent ratios, achieving a diameter of about 110 nm, whilst the Pdl slightly increased from trials E to G (remaining always < 0.2), thus indicating a homogeneous particle dispersion. All these conditions produced stable NPs, as revealed by their zeta potential values.

In the preparation of NPs via solvent evaporation, the surfactant plays a crucial role in term of size distribution of the formed NPs. The ionic surfactant forms a repulsive barrier around the droplet in the form of an electrical double layer, thus avoiding coalescence phenomena. Usually, an increase in surfactant concentration makes the particles size to decrease down to a minimum value over which the particles start to increase again (Komaiko & McClements, 2015), probably because of the large increase in viscosity that makes emulsification difficult (Jaouani, Tabka, & Penninckx, 2006; Saberi, Fang, & McClements, 2013; Tebaldi, Maia, Poletto, de Andrade, & Soares, 2019). In trials A to D, a decrease in particle size was observed with increasing SDS: PHBHHx ratio. This result derives from the combination of two effects: *i*) a higher amount of surfactant is available to surround polymer particles; *ii*) a lower polymer concentration reduces the viscosity of the organic phase, thus increasing the stirring efficiency. Similarly, Radu et al. (Radu et al., 2019) have shown that an increase in polyvinyl alcohol to PHBHV ratio causes a progressive reduction into particle size up to an equilibrium, under which smaller particles could not be obtained. The increase in organic/aqueous phase volume ratio was reported to cause a decrease in poly(lactic-co-glycolic acid) NP size prepared by emulsification-solvent

**Table 1**

Effect of SDS/PHBHHx mass ratio and aqueous/organic (A/O) phase volume ratio on Z-average size, polydispersity index (PDI) and zeta potential during PHBHHx-NPs production.

Values are mean  $\pm$  SD; the different letters indicate significant differences from the values reported in the same column (Tukey-Kramer test,  $p < 0.05$ ).

Trial	PHBHHx (mg)	Organic solution (mL)	Polymer concentration (mg mL <sup>-1</sup> )	SDS/PHBHHx mass ratio	A/O phase (mL)	Z-average size (d.nm)	PDI	Zeta potential (mV)	Method efficiency (%)
A	12.5	0.25	50	1.8	20	127 <sup>a</sup>	0.153	-30 <sup>a</sup>	59.8%
B	6.5	0.25	25	3.5	20	99 <sup>b,c</sup>	0.185	-53 <sup>b</sup>	71.3%
C	2.5	0.25	10	8.9	20	90 <sup>c</sup>	0.191	-40 <sup>c</sup>	79.4%
D	1.25	0.25	5	17.6	20	82 <sup>c</sup>	0.195	-44 <sup>c,d</sup>	80.5%
E	1.25	0.5	25	1.8	10	123 <sup>a,b</sup>	0.128	-38 <sup>b,c</sup>	57.6%
F	1.25	1	12.5	1.8	5	117 <sup>a</sup>	0.148	-62 <sup>a</sup>	55.8%
G	1.25	2.5	5	1.8	2	133 <sup>a</sup>	0.184	-50 <sup>b,d</sup>	67.8%

evaporation technique (Mainardes & Evangelista, 2005; Poletto et al., 2008). In this case, the coalescence of droplets is prevented by a greater amount of organic phase available for diffusion in the forming emulsion. The conditions explored in our study (trials E-D) did not lead to the same effect. On the other hand, another study demonstrated that the diameter of poly (lactic-co-glycolic acid) nanoparticles prepared with the same method was not influenced by increasing volumes of organic phase (Budhian, Siegel, & Winey, 2007), indicating that the solvent effect is finely dependent on the applied experimental conditions.

Taken together, the results in Table 1 indicate that condition D assures the smallest particle size (in the nano-range) together with a good stability and high recovery efficiency. In addition, these NPs formed a stable colloidal suspension in water which could be stored at RT for at least 7 days without aggregation. The NPs derived from condition D were further characterized by SEM and TEM analyses. Images in Fig. 1 indicate that PHBHHx-NPs derived from condition D were regular and spherical in shape (Fig. 1). Furthermore, their dimensions measured from SEM and TEM images are in accordance with those obtained by Z-average size measurements. In particular, SEM images (Fig. 1A and B) show the presence of aggregated polymeric nanoparticles whereas TEM image, reported in Fig. 1C, highlights the presence of isolated NPs with an average diameter of 60–90 nm.

### 3.2. Characterization of WP/PHB-NPs composites

PHBHHx-NPs were tested as nanofillers in the preparation of WP-based films. To this aim, PHBHHx-NPs were added to WP containing FFSs, plasticized with 40% (w/w) glycerol at different concentrations (from 1 to 8%, w/w of WPs), and then mechanically stirred for 15 min. The FFSs prepared either in the absence or presence of different amounts of NPs, were analysed for their zeta potential and particle size, resulting into the formation of stable solutions with zeta potential values between -30.1 and 33.7 mV (Table 2). The addition of PHBHHx-NPs led to a significant reduction in the particle size (Fernandez-Bats, Di Piero,

Villalonga-Santana, Garcia-Almendarez, & Porta, 2018), with a more pronounced effect observed at the highest concentration of NPs tested (Table 2). Then, the FFSs were cast and the derived films characterized. It is worthy to point out that all the films analysed in this study were prepared under alkaline conditions (pH 12.0) without any preliminary WP heat treatment, an experimental condition that allowed to obtain handleable, transparent as well as flexible films (Abdalrazeq et al., 2019).

#### 3.2.1. Film mechanical properties

Mechanical properties of both WP films and WP/PHBHHx-NPs composite films were determined by calculating the stress-strain curves. The data reported in Table 3 show that PHBHHx-NPs have a significant plasticizing effect on the WP-based films, as indicated by the marked decrease of YM and concurrent increase of EB observed by increasing the NP amount into the film matrix. On the other hand, a significant TS reduction was detected only at the highest concentration of NPs tested, thus indicating that PHBHHx-NPs concentrations up to 4% made the films grafted with NPs more extensible without loss of their original resistance. Similar results were obtained by using zinc oxide NPs incorporated into pectin/alginate edible films (Ngo, Dang, Tran, & Rachtanapun, 2018).

**Table 2**

Effect of different concentrations of PHBHHx-NPs on WP FFS zeta potential and Z-average size.

Values are mean  $\pm$  SD; the different letters indicate significant differences from the values reported in the same column (Tukey-Kramer test,  $p < 0.05$ ).

PHBHHx addition	Z-average size (d.nm)	Zeta potential (mV)
none	844.8 $\pm$ 43.3 <sup>a</sup>	-32.0 $\pm$ 5.9 <sup>a</sup>
+ 1%	1241.0 $\pm$ 46.4 <sup>b</sup>	-32.6 $\pm$ 3.0 <sup>a</sup>
+ 2%	505.9 $\pm$ 9.6 <sup>c</sup>	-30.1 $\pm$ 4.7 <sup>a</sup>
+ 4%	494.7 $\pm$ 27.6 <sup>c</sup>	-30.1 $\pm$ 2.4 <sup>a</sup>
+ 8%	382.7 $\pm$ 21.1 <sup>c</sup>	-33.7 $\pm$ 4.6 <sup>a</sup>

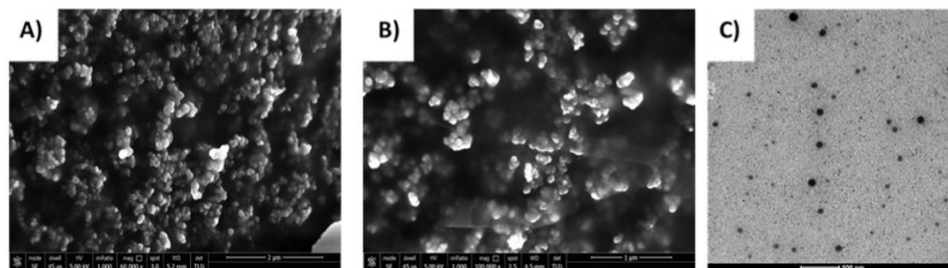


Fig. 1. SEM (A and B) and TEM (C) images of PHBHHx-NPs ( $2.10^{-1}$  and  $2.10^{-5}$  mg/mL, respectively).

PHBHHx-NPs were prepared under the experimental condition D described in Table 1; SEM images were obtained at two different magnifications.

**Table 3**

Effect of different concentrations of PHBHHx-NPs on the thickness and mechanical properties of WP-based films. (TS, tensile strength; EB, elongation at break; YM, Young's modulus). Values are mean  $\pm$  SD; the different letters indicate significant differences from the values reported in the same column (Tukey-Kramer test,  $p < 0.05$ ).

Film	TS (MPa)	EB (%)	YM (MPa)	Thickness ( $\mu$ m)
WP	3.1 $\pm$ 0.8 <sub>a</sub>	8.8 $\pm$ 1.1 <sup>a</sup>	104.1 $\pm$ 12.9 <sub>ab</sub>	85 $\pm$ 4 <sup>a</sup>
WP+1% PHBHHx-NPs	3.3 $\pm$ 0.5 <sub>a</sub>	7.3 $\pm$ 2.5 <sup>a</sup>	130.4 $\pm$ 13.2 <sub>c</sub>	83 $\pm$ 3 <sup>a</sup>
WP+2% PHBHHx-NPs	3.0 $\pm$ 0.2 <sub>a</sub>	10.1 $\pm$ 2.2 <sub>a</sub>	109.1 $\pm$ 6.2 <sup>a</sup>	71 $\pm$ 3 <sup>b</sup>
WP+4% PHBHHx-NPs	3.2 $\pm$ 0.2 <sub>a</sub>	16.6 $\pm$ 0.8 <sup>b</sup>	78.3 $\pm$ 3.4 <sup>b</sup>	72 $\pm$ 1 <sup>b</sup>
WP+8% PHBHHx-NPs	2.0 $\pm$ 0.2 <sub>b</sub>	24.0 $\pm$ 3.4 <sup>c</sup>	28.5 $\pm$ 6.8 <sup>d</sup>	67 $\pm$ 5 <sup>b</sup>

Finally, also the film thickness was observed to decrease significantly in parallel with the increasing amount of NPs inside the matrix, and also this result is in strict agreement with previous data obtained by analysing a different nanocomposite film constituted by a starch-based matrix containing TiO<sub>2</sub> NPs (Goudarzi, Shahabi-Ghahfarokhi, & Babaei-Ghazvini, 2017).

### 3.2.2. Film permeability

Water vapor (WV) and O<sub>2</sub> and CO<sub>2</sub> permeabilities are important biomaterial features for their use in various industrial sectors, especially in food packaging. The data reported in Table 4 demonstrate that the presence of PHBHHx-NPs inside the film matrix significantly increased only the O<sub>2</sub> barrier property of the WP-based films. It is well known that the addition of iso-dimensional or elongated nanoparticles in a matrix generally induces a variation of gas (O<sub>2</sub>, CO<sub>2</sub>) permeability that usually, but not always, decreases with the addition of fillers with high-aspect ratio. However, the final barrier properties are not easy to predict since they are the result of the combination of many variables such as filler/matrix affinity, filler aspect-ratio and the related tortuosity effect, filler orientation and agglomeration (Wolf, Angellier-Coussy, Gontard, Doghieri, & Guillard, 2018). It is worth to highlight that O<sub>2</sub> permeability is one of the most important properties of a packaging material as it is the main factor of organoleptic and nutritional quality degradation of food during storage throughout the oxidation of lipids, proteins, vitamins, pigments and various aroma compounds.

### 3.2.3. Film transparency

Film transparency is also a crucial parameter specifically influencing the appearance of a product and its acceptance by consumers. Films with low transparency are not generally suitable for food packaging applications especially when they are prepared as a see-through packaging material and used to enhance product visibility. Therefore, analyses of the opacity of the prepared nanocomposite films was carried out by measuring light transmission at a wavelength of 600 nm (Galus & Kadzińska, 2016). As shown in Fig. 2 the obtained WP-based films are quite transparent ( $A_{600 \text{ nm/mm}} = 1.8 \pm 0.1$ ), and they did not significantly change this property when they were grafted with PHBHHx-NPs

**Table 4**

Barrier properties of WP-based films prepared in the absence or presence of 4% (w/w protein) PHBHHx-NPs. Values are mean  $\pm$  SD; the different letters indicate significant differences from the values reported in the same column (Tukey-Kramer test,  $p < 0.05$ ).

Film	Permeability ( $\text{cm}^3 \text{ mm m}^{-2} \text{ day}^{-1} \text{ kPa}^{-1}$ )		
	CO <sub>2</sub>	O <sub>2</sub>	WV
WP	0.45 $\pm$ 0.01 <sup>a</sup>	0.89 $\pm$ 0.02 <sup>a</sup>	0.36 $\pm$ 0.02 <sup>a</sup>
WP+4% PHBHHx-NPs	0.37 $\pm$ 0.03 <sup>a</sup>	0.55 $\pm$ 0.01 <sup>b</sup>	0.34 $\pm$ 0.01 <sup>a</sup>

( $A_{600 \text{ nm/mm}} = 2.1 \pm 0.3$ ). Fig. 2 also shows that the presence of NPs inside the WP biopolymer matrix conferred to the film a higher visible and UV barrier property as indicated by the lower light transmission in the range between 200 and 280 nm and 350 and 800 nm, respectively (Leceta, Guerrero, & De La Caba, 2013). It is worthy to highlight that the prevention of lipid oxidation induced by UV is a further requirement in food packaging (Leceta et al., 2013).

### 3.2.4. Film morphology

SEM micrographs of both surface and cross-section of film samples prepared in the absence and presence of PHBHHx-NPs are shown in Fig. 3. The images show a smooth surface without any fracture in the WP film prepared without NPs (panel A of Fig. 3). In addition, also the film cross-section appears quite smooth (Fig. 3, panel A') despite the presence of some holes, probably due to non-protein colloidal particles, such as fat globule membranes, deriving from the whey (Brooker, 1985). Conversely, as expected, PHBHHx-NPs created rougher structures (white spots) on the surface of the WP film (panel B of Fig. 3), which tend to migrate through the film with a reasonable dispersion (panel B' of Fig. 3).

## 4. Conclusions

PHBHH-NPs were produced, characterized and used as nanofillers to obtain WP bio-nanocomposite films under different experimental conditions. The addition of PHBHHx-NPs to WP-based FFSs resulted in a plasticizing effect on the biobased material, producing a resistant but more extensible biomaterial. Moreover, the presence of PHBHHx-NPs inside the matrix enhanced the film barrier property towards O<sub>2</sub>, letting to envisage a possible application of this novel material in food packaging, especially suitable for the products requiring preservation from oxidative reactions. This is the first report in which PHA-NPs are successfully used to improve the properties of the protein-based films by achieving the dispersion of a hydrophobic biopolymer into an aqueous FFS. Although this process might open the way to design further smart biomaterials through the incorporation of bio-active molecules into the NPs used, further studies are needed to assess the potential risks of the films grafted with PHBHHx-NPs for both consumers and environment safety.

### Declaration of competing interest

The authors declare that they have no known competing financial interests or personal relationships that could have appeared to influence the work reported in this paper.

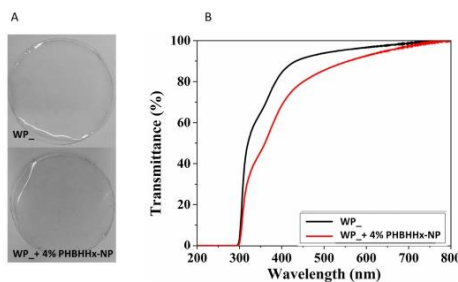


Fig. 2. Images of WP-based films prepared in the absence or presence of 4% PHBHHx-NPs (A) and their whole transmittance spectra (B).

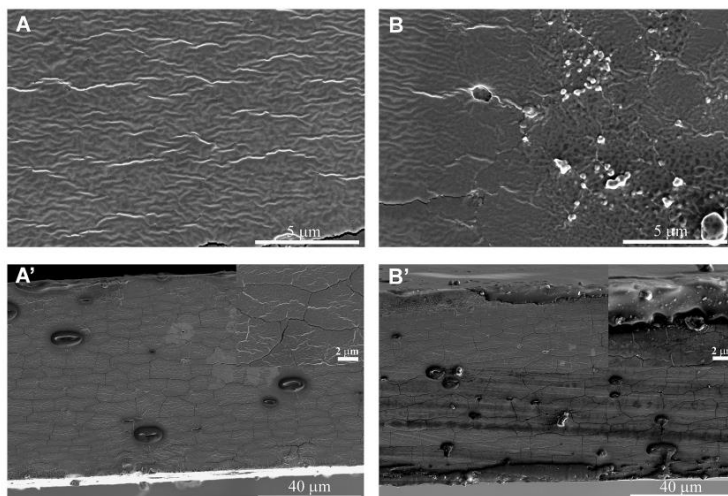


Fig. 3. SEM images of the surface of WP-based films prepared in the absence (A) and presence (B) of 4% PHBHHx-NPs and of the respective cryo-fractured cross-sections (A' and B'). Insets in A' and B' show details at higher magnification.

#### CRedit authorship contribution statement

**Iolanda Corrado:** Investigation, Formal analysis. **Manar Abdalrazeq:** Investigation, Formal analysis. **Cinzia Pezzella:** Conceptualization, Writing - original draft. **Rocco Di Girolamo:** Investigation. **Raffaele Porta:** Supervision, Funding acquisition. **Giovanni Sannia:** Supervision, Funding acquisition. **C. Valeria L. Giosafatto:** Conceptualization, Writing - original draft.

#### Acknowledgments

This work was supported by grants from PRIN: PROGETTI DI RICERCA DI RILEVANTE INTERESSE NAZIONALE – Bando 2017. “CARDONO valorisation by InteGrated bioefiNery (CARDIGAN)”. Iolanda Corrado and Manar Abdalrazeq acknowledge Università degli Studi di Napoli Federico II for doctoral fellowships.

#### References

- Abdalrazeq, M., Giosafatto, C. V. L., Esposito, M., Fenderico, M., Di Piero, P., & Porta, R. (2019). Glycerol-plasticized films obtained from whey proteins denatured at alkaline pH. *Coatings*, 9(5). <https://doi.org/10.3390/coatings9050322>.
- Azeredo, H. M. C., Rosa, M. F., & Mattoso, L. H. C. (2017). Nanocellulose in bio-based food packaging applications. *Industrial Crops and Products*, 97, 664–671. <https://doi.org/10.1016/j.indcrop.2016.03.013>.
- Brooker, B. (1985). Observations on the air-serum interface of milk foams. *Food Structure*, 4(2), 12.
- Budhian, A., Siegel, S. J., & Winey, K. I. (2007). Haloperidol-loaded PLGA nanoparticles: Systematic study of particle size and drug content. *International Journal of Pharmaceutics*, 336(2), 367–375. <https://doi.org/10.1016/j.ijpharm.2006.11.061>.
- Chanprateep, S., Buaeri, K., Muangwong, A., & Utiswankul, P. (2010). Biosynthesis and biocompatibility of biodegradable poly(3-hydroxybutyrate-co-4-hydroxybutyrate). *Polymer Degradation and Stability*, 95(10), 2003–2012. <https://doi.org/10.1016/j.polydegradstab.2010.07.014>.
- Ciesla, K., Salmieri, S., & Lacroix, M. (2006). Modification of the properties of milk protein films by gamma radiation and polysaccharide addition. *Journal of the Science of Food and Agriculture*, 86(6), 908–914. <https://doi.org/10.1002/jfda.2436>.
- Di Piero, P., Rossi Marquez, G., Mariniello, L., Sorrentino, A., Villalonga, R., & Porta, R. (2013). Effect of transglutaminase on the mechanical and barrier properties of whey protein/pectin films prepared at complexation pH. *Journal of Agricultural and Food Chemistry*, 61(19), 4593–4598. <https://doi.org/10.1021/jf401119q>.

- Di Piero, P., Sorrentino, A., Mariniello, L., Giosafatto, C. V. L., & Porta, R. (2011). Chitosan/whey protein film as active coating to extend Ricotta cheese shelf-life. *Lebensmittel-Wissenschaft und -Technologie: Food Science and Technology*, 44(10), 2324–2327. <https://doi.org/10.1016/j.lwt.2010.11.031>.
- Elmowafy, E., Abdal-Hay, A., Skouras, A., Tiboni, M., Casertari, L., & Guarino, V. (2019). Polyhydroxyalkanoate (PHA): Applications in drug delivery and tissue engineering. *Expert Review of Medical Devices*, 16(6), 467–482. <https://doi.org/10.1080/17434440.2019.1615439>.
- Fernandez-Bats, I., Di Piero, P., Villalonga-Santana, R., Garcia-Almendarez, B., & Porta, R. (2018). Bioactive mesoporous silica nanocomposite films obtained from native and transglutaminase-crosslinked bitter vetch proteins. *Food Hydrocolloids*, 82, 106–115. <https://doi.org/10.1016/j.foodhyd.2018.03.041>.
- Galus, S., & Kadzińska, J. (2016). Moisture sensitivity, optical, mechanical and structural properties of whey protein-based edible films incorporated with rapeseed oil. *Food Technology and Biotechnology*, 54(1), 78–89. <https://doi.org/10.17113/ftb.54.01.16.3889>.
- Goudarzi, V., Shahabi-Ghahfarokhi, I., & Babaei-Ghazvini, A. (2017). Preparation of ecofriendly UV-protective food packaging material by starch/TiO<sub>2</sub> bio-nanocomposite: Characterization. *International Journal of Biological Macromolecules*, 95, 306–313. <https://doi.org/10.1016/j.ijbiomac.2016.11.065>.
- Jaoouani, A., Tabba, M. G., & Penninckx, M. J. (2006). Lignin modifying enzymes of Coriopsis polyzona and their role in olive oil mill wastewaters decolorisation. *Chemosphere*, 62(9), 1421–1430. <https://doi.org/10.1016/j.chemosphere.2005.05.040>.
- Kadam, D. M., Thunga, M., Wang, S., Kessler, M. R., Grewell, D., Lamsal, B., et al. (2013). Preparation and characterization of whey protein isolate films reinforced with porous silica coated titania nanoparticles. *Journal of Food Engineering*, 117(1), 133–140. <https://doi.org/10.1016/j.jfoodeng.2013.01.046>.
- Kalia, V. C. (2019). Biotechnological applications of polyhydroxyalkanoates. *Biotechnological Applications of Polyhydroxyalkanoates*. <https://doi.org/10.1007/978-981-13-3759-8>.
- Kilicay, E., Demireliler, M., Türk, M., Güven, E., Hazar, B., & Denizli, E. B. (2011). Preparation and characterization of poly(3-hydroxybutyrate-co-3-hydroxyhexanoate) (PHBHHx) based nanoparticles for targeted cancer therapy. *European Journal of Pharmaceutical Sciences*, 44(3), 310–320. <https://doi.org/10.1016/j.ejps.2011.08.013>.
- Koller, M. (2018). Biodegradable and biocompatible polyhydroxy-alkanoates (PHA): Auspicious microbial macromolecules for pharmaceutical and therapeutic applications. *Molecules*, 23(2). <https://doi.org/10.3390/molecules23020362>.
- Komaiko, J., & McClements, D. J. (2015). Low-energy formation of edible nanoemulsions by spontaneous emulsification: Factors influencing particle size. *Journal of Food Engineering*, 146, 122–128. <https://doi.org/10.1016/j.jfoodeng.2014.09.003>.
- Kumar, P., & Kim, B. S. (2019). Valorization of polyhydroxyalkanoates production process by co-synthesis of value-added products. *Bioresour. Technology*, 269(July), 544–556. <https://doi.org/10.1016/j.biortech.2018.08.120>.

- Leceta, I., Guerrero, P., & De La Caba, K. (2013). Functional properties of chitosan-based films. *Carbohydrate Polymers*, 93(1), 339–346. <https://doi.org/10.1016/j.carbpol.2012.04.031>.
- Li, Z., Yang, J., & Loh, X. J. (2016). Polyhydroxyalkanoates: Opening doors for a sustainable future. *NPG Asia Materials*, 8(4). <https://doi.org/10.1038/am.2016.48.e265-20>.
- Mainardes, R. M., & Evangelista, R. C. (2005). PLGA nanoparticles containing praziquantel: Effect of formulation variables on size distribution. *International Journal of Pharmaceutics*, 290(1–2), 137–144. <https://doi.org/10.1016/j.ijpharm.2004.11.027>.
- Mollea, C., Marmo, L., & Bosco, F. (2013). Valorization of cheese whey, a by-product from the dairy industry. *Food Industry*. <https://doi.org/10.5772/53159>.
- Murueva, A. V., Shishatskaya, E. I., Kuzmina, A. M., Volova, T. G., & Sinskey, A. J. (2013). Microparticles prepared from biodegradable polyhydroxyalkanoates as matrix for encapsulation of cytostatic drug. *Journal of Materials Science: Materials in Medicine*, 24(8), 1905–1915. <https://doi.org/10.1007/s10856-013-4941-2>.
- Naureen, R., Tariq, M., Yusoff, I., Jalal, A., Chowdhury, K., & Ashraf, M. A. (2015). Synthesis, spectroscopic and chromatographic studies of sunflower oil biodiesel using optimized base catalyzed methanolysis. *Saudi Journal of Biological Sciences*, 22(3), 332–339. <https://doi.org/10.1016/j.sjbs.2014.11.017>.
- Ngo, T. M. P., Dang, T. M. Q., Tran, T. X., & Rachtanapun, P. (2016). Effects of zinc oxide nanoparticles on the properties of pectin/alginate edible films. *International Journal of Polymer Science*. <https://doi.org/10.1155/2016/5645797>, 2016.
- Norwood, E. A., Croguennec, T., Le Floch-Fouéré, C., Schuck, P., & Jeantet, R. (2018). Changes in whey protein powders during storage. *Whey Proteins: From Milk to Medicine*. <https://doi.org/10.1016/B978-0-12-812124-5.00004-7>.
- Nugroho Prasetyo, E., Kudanga, T., Østergaard, L., Rencoret, J., Gutiérrez, A., del Río, J. C., et al. (2010). Polymerization of lignosulfonates by the laccase-HBT (1-hydroxybenzotriazole) system improves dispersibility. *Bioresource Technology*, 101(14), 5054–5062. <https://doi.org/10.1016/j.biortech.2010.01.048>.
- Poletto, F. S., Fiel, L. A., Donida, B., Ré, M. I., Gutierrez, S. S., & Pohlmann, A. R. (2008). Controlling the size of poly(hydroxybutyrate-co-hydroxyvalerate) nanoparticles prepared by emulsification-diffusion technique using ethanol as surface agent. *Colloids and Surfaces A: Physicochemical and Engineering Aspects*, 324(1–3), 105–112. <https://doi.org/10.1016/j.colsurfa.2008.04.003>.
- Radu, I. C., Hudita, A., Zaharia, C., Galateanu, B., Iovu, H., Tanasa, E., Vasile, ... Costache, M. (2019). Poly(3-hydroxybutyrate-co-3-hydroxyvalerate) PHBV biocompatible nanocarriers for 5-FU delivery targeting colorectal cancer. *Drug Delivery*, 26(1), 318–327. <https://doi.org/10.1080/10717544.2019.1582729>.
- Ramos, O. L., Pereira, J. O., Silva, S. I., Fernandes, J. C., Franco, M. I., Lopes-da-Silva, J. A., et al. (2012). Evaluation of antimicrobial edible coatings from a whey protein isolate base to improve the shelf life of cheese. *Journal of Dairy Science*, 95(11), 6282–6292. <https://doi.org/10.3168/jds.2012-5478>.
- Raza, Z. A., Abid, S., & Banat, I. M. (2018). Polyhydroxyalkanoates: Characteristics, production, recent developments and applications. *International Biodeterioration & Biodegradation*, 126(September 2017), 45–56. <https://doi.org/10.1016/j.ibiod.2017.10.001>.
- Saberi, A. H., Fang, Y., & McClements, D. J. (2013). Fabrication of vitamin E-enriched nanoemulsions: Factors affecting particle size using spontaneous emulsification. *Journal of Colloid and Interface Science*, 391(1), 95–102. <https://doi.org/10.1016/j.jcis.2012.08.069>.
- Sandoval, G., Rivera, I., Barrera-Rivera, K.A., & Martínez-Richa, A. (2010). Biopolymer synthesis catalyzed by tailored lipases. *Macromolecular Symposia*, 289(1), 135–139. <https://doi.org/10.1002/masy.200900016>.
- Sharif Hossain, A. B. M., Uddin, M. M., Veetil, V. N., & Fawzi, M. (2018). Nano-cellulose based nano-coating biomaterial dataset using corn leaf biomass: An innovative biodegradable plant biomaterial. *Data in Brief*, 17, 162–168. <https://doi.org/10.1016/j.dib.2017.12.046>.
- Shevkani, K., & Singh, N. (2015). Relationship between protein characteristics and film-forming properties of kidney bean, field pea and amaranth protein isolates. *International Journal of Food Science and Technology*, 50(4), 1033–1043. <https://doi.org/10.1111/ijfs.12733>.
- Shrivastav, A., Kim, H. Y., & Kim, Y. R. (2013). Advances in the applications of polyhydroxyalkanoate nanoparticles for novel drug delivery system. *BioMed Research International*. <https://doi.org/10.1155/2013/581664>, 2013(Med).
- Tebaldi, M. L., Maia, A. L. C., Poletto, F., de Andrade, F. V., & Soares, D. C. F. (2019). Poly(3-hydroxybutyrate-co-3-hydroxyvalerate) (PHBV): Current advances in synthesis methodologies, antitumor applications and biocompatibility. *Journal of Drug Delivery Science and Technology*, 51(February), 115–126. <https://doi.org/10.1016/j.jddst.2019.02.007>.
- Vastano, M., Corrado, I., Sannia, G., Solaiman, D. K. Y., & Pezzella, C. (2019). Conversion of no/low value waste frying oils into biodiesel and polyhydroxyalkanoates. *Scientific Reports*, 9(1), 1–8. <https://doi.org/10.1038/s41598-019-50278-x>.
- Vastano, M., Pellis, A., Immirzi, B., Dal Poggetto, G., Malinconico, M., Sannia, G., et al. (2017). Enzymatic production of clickable and PEGylated recombinant polyhydroxyalkanoates. *Green Chemistry*, 19(22), 5494–5504. <https://doi.org/10.1039/c7gc01872j>.
- Wolf, C., Angellier-Cousy, H., Gontard, N., Doghieri, F., & Guillard, V. (2018). How the shape of fillers affects the barrier properties of polymer/non-porous particles nanocomposites: A review. *Journal of Membrane Science*, 556(January), 393–418. <https://doi.org/10.1016/j.memsci.2018.03.085>.
- Yadav, J. S. S., Yan, S., Pilli, S., Kumar, L., Tyagi, R. D., & Surampalli, R. Y. (2015). Cheese whey: A potential resource to transform into bioprotein, functional/nutritional proteins and bioactive peptides. *Biotechnology Advances*, 33(6), 756–774. <https://doi.org/10.1016/j.biotechadv.2015.07.002>.
- Zhang, J., Shishatskaya, E. I., Volova, T. G., da Silva, L. F., & Chen, G. Q. (2018). Polyhydroxyalkanoates (PHA) for therapeutic applications. *Materials Science and Engineering: C*, 86(December 2017), 144–150. <https://doi.org/10.1016/j.msec.2017.12.035>.

## 2.2 Polyhydroxyalkanoates-based nanoparticles as essential oil delivery carriers

The activities reported in this paragraph are in the frame of a Scientific and technology Cooperation program that allowed me to collaborate with Prof. Carlos Regalado and Prof. Blanca García Almendares at the Universidad Autónoma de Querétaro (UAQ), Mexico. The main objective during the visit to Universidad Autónoma de Querétaro was the encapsulation of antimicrobial compound, such as essential oils of Mexican oregano (*Lippia graveolens* Kunth), in nanoparticles of PHAs that can be blend with whey protein, obtaining activated film.

### Results

#### *Encapsulation of EOs into PHA-based nanoparticles*

PHA-based nanoparticles were prepared by the solvent evaporation method, by dispersing a polymer solution in the aqueous phase containing a proper surfactant. Two different PHA polymers were tested: i) the homopolymer P3HB, derived from bioprocesses described in Paragraph 1.1, and ii) the copolymer poly-(3 hydroxybutyrate)-co- (3-Hydroxyhexanoate) (P(3HB-co-3HHx), produced by recombinant *E. coli* as described in Paragraph 2.1.

Oregano essential oils (EOs) were extracted from *Lippia graveolens*, Mexico oregano (MXO) at the University of Querétaro, Santiago de Querétaro, México. Hydro-distillation allowed to obtain a yield of 4 % (w/w dry mass). This result is in line with already extraction yields reported for MXO oregano. EOs, already characterized by GCMS, are mainly composed of thymol (>50%) and at low concentration of Carvacrol (<0.1%) (Hernández-Hernández et al., 2014).

Encapsulation of EOs into PHA-nanoparticles was carried out by exploring the effect of different parameters, such as concentration of surfactant, Aqueous/Organic phase volume ratio (A/O phase) and  $\text{mg}_{\text{EOs}}/\text{mg}_{\text{Polymer}}$ , on particles size and morphology, and encapsulation efficiency.

Preliminary experiments were carried on PHB. Figure 1 (Panels A, B) shows the mean particle size, polydispersity index (PDI) and Z-potential of NPs obtained by using two different concentrations of Sodium Dodecyl sulphate (SDS), (2.2 and 4.4  $\text{mg ml}^{-1}$ ), different  $\text{mg}_{\text{EOs}}/\text{mg}_{\text{Polymer}}$  ratios (1:1; 0.5:1), at a constant A/O phase (20),

corresponding to 1.25 mg of polymer. In general, the higher concentration of surfactant the smaller the size of the nanoparticles but its excess can increase particle size (Komaiko & McClements, 2015).

In the absence of EOs, SDS at 4.4 mg ml<sup>-1</sup> provided the formation of smaller particles (below 150 nm) with a Z-potential below -60 mV and a PDI of 0.2, while a decrease of SDS concentration at 2.2 led to higher particle size (below 200 nm), a PDI index higher than 0.2 and a better Z-potential value (-40mV). The addition of EOs caused a marked increase in NPs size in all the tested conditions. However, an increase in PDI was also observed, indicating a higher heterogeneity in the particle size distribution. It is worth to note that, the formation of EOs micelles with a size of 500 nm was observed when EOs were subjected to the same experimental protocol in the absence of polymer. Thus, the formation of SDS-stabilized EOs emulsions could explain the observed heterogeneity of particle size, especially in the conditions with higher SDS amount. In line with this, at a lower mg<sub>EOs</sub>/mg<sub>Polymer</sub> (0.5), the PDI decreases to about 0.4, since a greater amount of polymer is available for the interaction with the EOs, thus preventing the formation of stable EOs micelles.

In order to promote polymer/EOs interaction and thus improving oil encapsulation into the polymeric matrix, a lower A/O phase ratio (2), corresponding to a ten-fold increase of polymer amount (12.5 mg) was tested, setting the SDS at 2.2 mg ml<sup>-1</sup> (panel C). In these conditions, monodisperse NPs with a particle size below 200 nm and a Z-potential below -30 mV were obtained in the absence of EOs. Interestingly, the addition of EOs slightly affected the size of the obtained NPs when compared to the unloaded ones and did not impair the PDI that remains about 0.2. A further increase of polymer amount (25 mg, keeping the A/O phase ratio to 2 caused an increase in the size of unloaded NPs, that remained almost constant after EOs addition at the highest mg<sub>EOs</sub>/mg<sub>Polymer</sub> ratio (1) (Panel D). Furthermore, the PDI was almost unaffected by the addition of the EOs. In particular, high monodisperse NPs were obtained at the lowest mg<sub>EOs</sub>/mg<sub>Polymer</sub> ratio (0.5), indicating that in these conditions, the formation of loaded NPs is favoured with respect to the formation of EOs micelles.

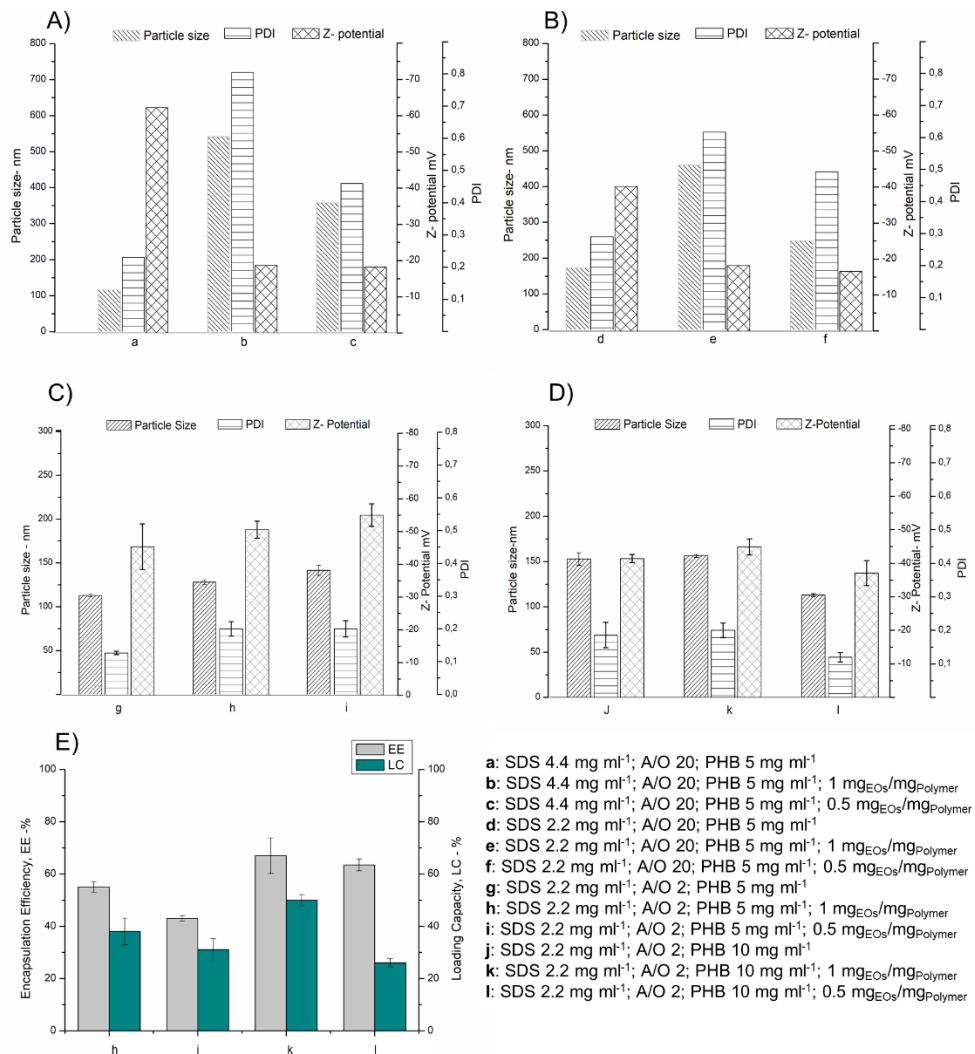


**Figure 1.** Effect of parameter settings on particle size, PDI and Z-potential. A) SDS at 2.2 mg ml<sup>-1</sup>, A/O 20 and PHB 5 mg ml<sup>-1</sup>; B) SDS at 4.4 mg ml<sup>-1</sup>, A/O 20 and PHB 5 mg ml<sup>-1</sup>; C) SDS at 2.2 mg ml<sup>-1</sup>, A/O 2 and PHB 5 mg ml<sup>-1</sup>; D) SDS at 2.2 mg ml<sup>-1</sup>, A/O 2 and PHB 10 mg ml<sup>-1</sup>; E) Effect of polymer concentration on Encapsulation efficiency and loading capacity.

Conditions reported in Panels C and D were further investigated, taking into account the EOs encapsulation efficiency (EE) and the loading capacity (LC). The highest percentage of EE together with the

highest percentage of LC were obtained at the highest amount of polymer ( $10 \text{ mg mL}^{-1}$ ) (Panel E), reaching up to 68% and 50% respectively at the highest  $\text{mg}_{\text{EOs}}/\text{mg}_{\text{Polymer}}$  ratio (trial **k** figure 3).

In this condition NPs resulted to be stable for more than one week without separation, precipitation, or agglomeration.

The same experimental conditions used for PHB were applied for the synthesis of P(3HB-3HHx) based NPs. However, despite the obtained NPs showed a particle size of 180 nm with a PDI of 0.176 and an acceptable Z- potential, they resulted to be unstable, with a precipitation and phase separation after 48 h. To obtain monodisperse and stable NPs, a higher concentration of surfactant ( $4.4 \text{ mg mL}^{-1}$ ) was needed; moreover, to promote polymer/EOs interaction and thus improving oil encapsulation into the polymeric matrix a higher concentration of polymer solution ( $20 \text{ mg mL}^{-1}$ ) was used (Figure 2). In these conditions, the NPs produced showed a particle size of 210 nm, PDI of 0.125 and Z-potential value of  $-47.4 \text{ mV}$  with an EE of 62 % and a loading capacity of 45%. Moreover, as for the loaded PHB-NPs the encapsulation of EOs slightly affected the particle size with respect to the unloaded ones (Figure 2). In general, at higher concentration of polymer, the collision frequency of polymer droplets and possible coalescence can increase. In this case this phenomenon is avoided by using higher concentration of surfactant that helps the formation of droplets and reduces coalescence (Tadros, 2009).

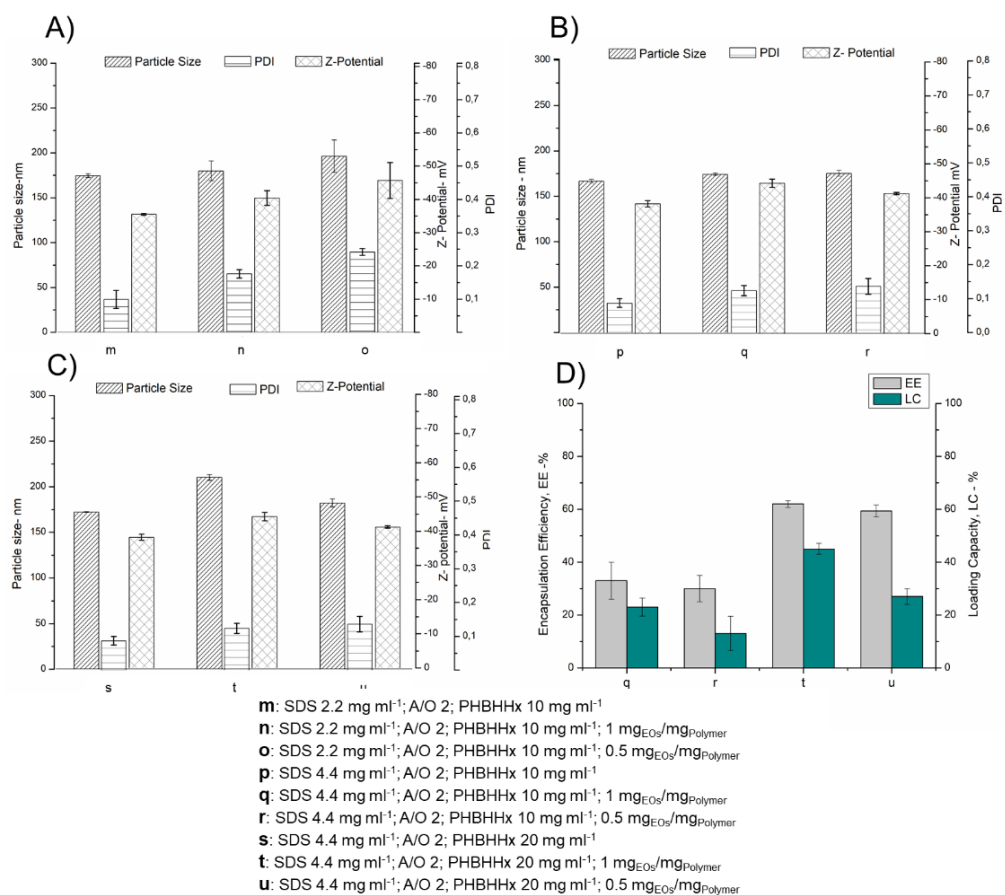


**Figure 2.** Effect of parameter settings on particle size, PDI and Z-potential. A) SDS at 2.2 mg ml<sup>-1</sup>, A/O 2 and PHBHHX 10 mg ml<sup>-1</sup>; B) SDS at 4.4 mg ml<sup>-1</sup>, A/O 2 and PHB HHx 10 mg ml<sup>-1</sup>; C) SDS at 4.4 mg ml<sup>-1</sup>, A/O 2 and PHBHHx 20 mg ml<sup>-1</sup> D) Effect of polymer concentration on Encapsulation efficiency and loading capacity.

Figure 3 shows a representative SEM image of PHB and PHBHHx nanoparticles prepared by solvent evaporation. The PHB loaded nanoparticles were found to be spherical in shape even if with an irregular surface. The size of the particles is quite homogeneous. The situation is different for PHBHHx loaded NPs, as a fact upon drying sample NPs lost their morphology, this can be due to the more flexible polymer matrix (Figure 3 panel C).

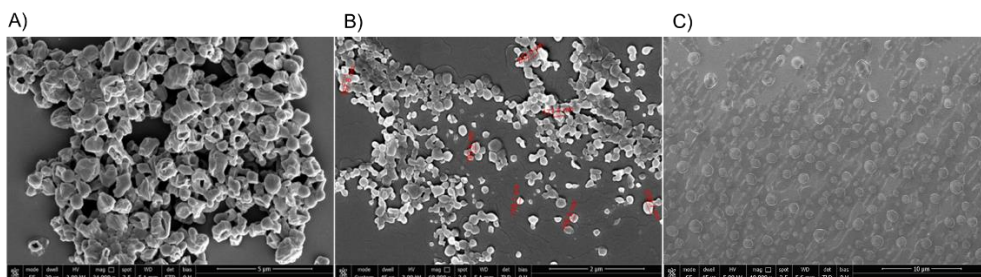


**Figure 3.** Scanning electron microscope image from EOs loaded PHB based NPs (panel A and B) and PHBHHx loaded NPs (panel C).

### *In vitro* EOs release

The release profile was studied for EOs loaded PHB and PHBHHx nanoparticles produced under conditions “k” (PHB) and “t” (PHBHHx), characterized by 68% and 62% of EE and 51% and 45% of LC, respectively. The release was studied by dialysis method at pH 4 and 6. The release profile is biphasic for both NPs, showing an initial burst followed by a constant release during the time (figure 4). Approximately 20% and 17% of the total EOs was released from PHB-NPs and P3HBHHx-NPs respectively within the first 3h, whilst further release was very slow. The burst release can be explained by the fast release of EOs close-to or attached-to the surface of the nanoparticles. The release from both PHB based NPs seems to be not affected by the pH. On the other hand, at pH 4 copolymer-based nanoparticles showed a higher release than at pH 6, reaching up to 30% after 72h.

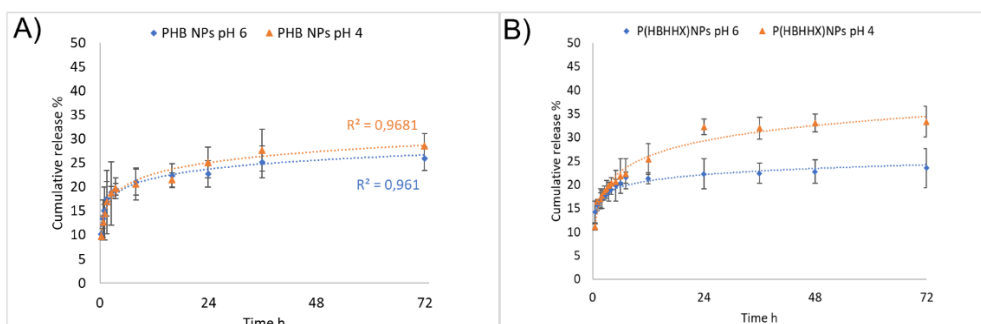


**Figure 5.** In vitro release profile from A) PHB and B) PHBHHx loaded NPs

### *Assessment of antimicrobial activity of EOs loaded nanoparticles*

*Micrococcus luteus* NCIB 8166 was chosen as positive control because of its high sensitivity to the tested EOs (Hernández-Hernández et al., 2017) Main targets of EOs components, such as thymol and carvacrol, are the cytoplasmic membrane of microorganisms and the outer membrane of Gram-negative bacteria. In addition, these compounds can interact with membrane proteins and enzymes, as well as with other intracellular targets (Burt, 2004; Hyldgaard et al., 2012).

The Minimum inhibitory concentration (MIC) and the minimum bactericidal concentration (MBC) against *Micrococcus luteus* of EOs-loaded NPs were determined in comparison with free EOs using broth dilution method (Table 1). Both loaded nanoparticles were found to be effective against *M. luteus*. In particular, for PHB based nanoparticles no turbidity occurred when 0.5 mg mL<sup>-1</sup> of NPs was added. On the other hand, for the copolymer-based nanoparticles a lower MIC was determined, corresponding to 0.25 mg mL<sup>-1</sup>. Unloaded nanoparticles did not affect microbial growth up to 2 mg mL<sup>-1</sup>. The measured MIC for the loaded NPs resulted lower or comparable to that of free EOs (0.2 mg mL<sup>-1</sup>). As a fact, the direct application of EOs may present rapid volatilization of their components, stability issues and poor water solubility decreasing their antimicrobial activity. On the other hand, their encapsulation prevents their volatilization and protects active compounds from environmental factors such as water, light, oxygen, pH thus enhancing their bioavailability (Arana-Sánchez et al., 2010; Liolios et al., 2009). In addition, Minimum Bactericidal Concentration (MBC) of loaded PHB and PHBHHx was determined using concentration above MIC value. MBC was 1 mg mL<sup>-1</sup> and 0.4 for PHB and PHBHHx NPs, respectively.

**Table 1.** MIC and MBC of free and encapsulated EOs against *M. luteus*

	<b>MIC (mg mL<sup>-1</sup>)</b>	<b>MBC (mg mL<sup>-1</sup>)</b>
<b>EOs</b>	0.2	0.3
<b>EOs loaded PHB-NPs</b>	0.5 (EOs 0.25)	1 (EOs 0.51)
<b>EOs loaded PHBHHx-NPs</b>	0.25 (EOs 0.11)	0.4 (EOs 0.18)

## Conclusions

In this work EOs from oregano Mexico were encapsulated into PHA based nanoparticles. Two formulations of nanoparticles by using PHB and PHBHHx polymers were prepared. Both formulations presented a good size below 200 nm with a low polydispersity index and high encapsulation efficiency > 60%. The polymeric nanoparticles showed better or comparable results in inactivating the tested microorganism respect to free EOs, thus improving their bioavailability. Furthermore, the developed carriers may reduce the quantity needed to inhibit or inactivate bacteria. The results obtained demonstrate the efficiency of polymeric NPs as drug delivery system. Further studies will be carried out to develop new activated materials blending PHA-based nanoparticles (PHA-NPs) and Whey Protein-based films (WP).

## Materials and methods

### *Materials*

The homopolymer P3HB derived from bioprocesses described in Paragraph 1.1. The copolymer poly-(3 hydroxybutyrate)-co- (3-Hydroxyhexanoate) (P(3HB-co-3HHx)), produced by recombinant *E. coli* as described in Paragraph 2.1. All reagent employed were purchased from Sigma Aldrich. Deionized water from WliX system was used in all experiment. *Micrococcus luteus* was used for antimicrobial activity testing. In this study EOs was extracted by hydro distillation from *Lippia graveolens*, Mexico oregano (MXO). MXO leaves and flowers were harvested and sun-dried in Toliman (Queretaro, Mexico). Dry material was stored in black polyethylene bags at 25°C until use. The EOs were recovered by hydro-distillation of 400 g of material plants with 5 L of distilled water using a Clevenger-type apparatus (Cristalab, DF, Mexico) according to Hernández-Hernández et al., 2014. After 3h the oily layer on top of the aqueous distillate was removed and dried with anhydrous sodium sulphate obtaining ~15 mL of EOs. The EO's were stored in sealed vials protected from light at 4°C until further analysis.

### *Nanoparticles preparation via microemulsification method*

Nanoparticles were prepared according to M&M paragraph 1.1. Two miscible phases were prepared: an aqueous phase and an organic one. The organic phase was prepared dissolving PHB and PHBHHx in  $\text{CHCl}_3$  at different concentrations (5, 10 mg  $\text{mL}^{-1}$ ). The aqueous phase consisted of 5 mL of sodium dodecyl sulphate (SDS) tested at different concentration. To obtain EOs-loaded nanoparticles, different amounts of essential oil (0.5-1 mg

for mg of polymer) was solubilized in the organic phase before being added to the aqueous one. Nanoparticles were recovered by centrifugation at 5000 g for 15 minutes. The supernatant was used for encapsulation efficiency and loading capacity determination.

#### *Nanoparticles Characterization*

NPs-PHA based were characterized in terms of hydrodynamic size, zeta potential, morphology, for EOs encapsulation efficiency.

##### *Particle size and Z-potential*

NPs dispersion (0.1 mg/mL) in water was analysed for zeta potential and particle size by using a Zetasizer Nano-ZSP (Malvern®, Worcestershire, UK). The device was equipped with a helium-neon laser of 4 mW output power with a fixed wavelength of 633 nm (wavelength of laser red emission). The instrument software programmer calculated the zeta potential through the electrophoretic mobility by applying a voltage of 200 mV and using the Henry equation.

##### *Encapsulation efficiency and Loading capacity*

The encapsulation efficiency percentage (EE%) was determined considering the total phenolic contents of EOs. The total phenolic content was estimated using the Folin Ciocalteu reagent as described by Singleton et al., 1965. The calibration curve was plotted by mixing 0.100 ml aliquots of 50, 100, 150, 200, 250, 300 mg ml<sup>-1</sup> Gallic acid solutions with 0.5 ml of Folin Ciocalteu reagent (diluted tenfold) and 0.4 ml of sodium carbonate solution (75 g/l). The absorbance was measured after 30 min at 765 nm. Both EOs, and supernatant (containing non-encapsulated EOs) upon centrifugation of nanoparticles suspension were subjected to the same assay as described for calibration curve.

The phenolic content of EOs was established to be 568 µg per mg of EO.

To determine the encapsulation efficiency the following equation was employed (Ayres Cacciatore et al., 2020; Chen et al., 2014):

$$EE \% = \frac{(\text{phenol of EOs used})\text{mg} - (\text{phenol in the supernatant})\text{mg}}{(\text{phenol of EOs used})\text{mg}} \times 100$$

To determine the loading capacity the following equation was employed:

$$LC \% = \frac{(\text{phenol of EOs used})\text{mg} - (\text{phenol in the supernatant})\text{mg}}{(\text{NPs})\text{mg}} \times 100$$

#### *In vitro release of EOs from PHA based nanoparticles*

In vitro release studies of EOs from EOs loaded P(3HB) NPs were carried out using a dialysis membrane according to Chen et al., 2014. Briefly, four mg of NPs were put into a cellulose dialysis tube containing 2 mL total volume. The dialysis bag was placed in 20.0 mL phosphate (pH 7) and acetate (pH 4) buffer solutions, and stirred at 150 rpm and 28°C. At regular

time intervals 0.2 mL of supernatant was sucked out and was replaced with an equivalent volume of fresh buffer solution. A control experiment to determine the release behaviour of the free drug across the dialysis membrane was also performed placing the same amount of EOs as it was in loaded NPs.

To determine the cumulative release % the following equation was employed:

$$\text{Cumulative release\% (t)} = \frac{C_t \times V_{\text{Buffer}} + V \sum_{i=0}^{t-1} C_i}{EO_s} \times 100$$

where  $C_t$  is the concentration of sample measured at time  $t$ ,  $V_{\text{buffer}}$  is the volume of dialysis buffer (20 mL),  $V$  is the Volume of sample withdrawn,  $C_i$  is the concentration of each sample previous to 't',  $EO_s$  is the total amount of the drug encapsulated in the NPs.

#### *Study of antimicrobial activity of PHA loaded nanoparticles*

Minimum inhibitory concentration (MIC) of NPs was determined by a broth dilution method, as recommended by the NCCLS 2000. *Micrococcus luteus* was used as test microorganisms. The bacterium was inoculated in NB medium at 37°C for 24h. The culture suspension was adjusted to  $10^5$  CFU mL<sup>-1</sup>. Bacterial suspension (1mL was) inoculated in the sample series. After 24h samples (10 µl) from all tubes without turbidity were transferred to NB agar plate and incubated at 37°C for 24h. The Minimum bactericidal concentration (MBC) was determined as the concentration of the sample which corresponding no bacterial growth. Tests were performed in triplicate for each sample.

#### *Scanning electron microscopy (SEM)*

A field emission scanning electron microscope (FE-SEM, FEI Nova NanoSEM450) was used to study the morphology of both NPs formulations. A droplet of nanoparticles (suspension in water) was deposited on carbon stickers on aluminium stubs and then dried at room temperature. The images were acquired using an incident electron beam energy between 2 and 5 kV and by collecting secondary electrons (SE) with an ETD or TLD detector.

## References

- Arana-Sánchez, A., Estarrón-Espinosa, M., Obledo-Vázquez, E. N., Padilla-Camberos, E., Silva-Vázquez, R., & Lugo-Cervantes, E. (2010). Antimicrobial and antioxidant activities of Mexican oregano essential oils (*Lippia graveolens* H. B. K.) with different composition when microencapsulated in  $\beta$ -cyclodextrin. *Letters in Applied Microbiology*, 50(6), 585–590. <https://doi.org/10.1111/j.1472-765X.2010.02837.x>
- Ayres Cacciatore, F., Dalmás, M., Maders, C., Ataíde Isaía, H., Brandelli, A., & da

- Silva Malheiros, P. (2020). Carvacrol encapsulation into nanostructures: Characterization and antimicrobial activity against foodborne pathogens adhered to stainless steel. *Food Research International*, 133(December 2019), 109143. <https://doi.org/10.1016/j.foodres.2020.109143>
- Burt, S. (2004). Essential oils: Their antibacterial properties and potential applications in foods - A review. *International Journal of Food Microbiology*, 94(3), 223–253. <https://doi.org/10.1016/j.ijfoodmicro.2004.03.022>
- Chen, J., Huang, L., Lai, H., Lu, C., Fang, M., Zhang, Q., & Luo, X. (2014). Methotrexate-loaded PEGylated chitosan nanoparticles: Synthesis, characterization, and in vitro and in vivo antitumoral activity. *Molecular Pharmaceutics*, 11(7), 2213–2223. <https://doi.org/10.1021/mp400269z>
- Hernández-Hernández, E., Lira-Moreno, C. Y., Guerrero-Legarreta, I., Wild-Padua, G., Di Pierro, P., García-Almendárez, B. E., & Regalado-González, C. (2017). Effect of Nanoemulsified and Microencapsulated Mexican Oregano (*Lippia graveolens* Kunth) Essential Oil Coatings on Quality of Fresh Pork Meat. *Journal of Food Science*, 82(6), 1423–1432. <https://doi.org/10.1111/1750-3841.13728>
- Hernández-Hernández, E., Regalado-González, C., Vázquez-Landaverde, P., Guerrero-Legarreta, I., & García-Almendárez, B. E. (2014). Microencapsulation, chemical characterization, and antimicrobial activity of Mexican (*Lippia graveolens* H.B.K.) and European (*Origanum vulgare* L.) oregano essential oils. *Scientific World Journal*, 2014. <https://doi.org/10.1155/2014/641814>
- Hyldgaard, M., Mygind, T., & Meyer, R. L. (2012). Essential oils in food preservation: Mode of action, synergies, and interactions with food matrix components. *Frontiers in Microbiology*, 3(JAN), 1–24. <https://doi.org/10.3389/fmicb.2012.00012>
- Komaiko, J., & McClements, D. J. (2015). Low-energy formation of edible nanoemulsions by spontaneous emulsification: Factors influencing particle size. *Journal of Food Engineering*, 146, 122–128. <https://doi.org/10.1016/j.jfoodeng.2014.09.003>
- Liolios, C. C., Gortzi, O., Lalas, S., Tsaknis, J., & Chinou, I. (2009). Liposomal incorporation of carvacrol and thymol isolated from the essential oil of *Origanum dictamnus* L. and in vitro antimicrobial activity. *Food Chemistry*, 112(1), 77–83. <https://doi.org/10.1016/j.foodchem.2008.05.060>
- Singleton, V. L., Rossi, J. A., & Jr, J. (1965). Colorimetry of Total Phenolics With Phosphomolybdic-Phosphotungstic Acid Reagents. *American Journal of Enology and Viticulture*, 16(3), 144–158.
- Tadros, T. F. (2009). Emulsion Science and Technology. In *Emulsion Science and Technology*. <https://doi.org/10.1002/9783527626564>

## **Concluding remarks**

The PhD project, developed and described in this thesis, was focused on the development of consolidated bioprocesses for PHA production, valorising renewable inulin rich biomasses, and on the application of the produced polymers. The achieved results can be summarized as reported below:

- Identification of *Penicillium lanosocoeruleum* as good inulinases producer; characterization of the mixture of secreted hydrolytic enzymes and inulin hydrolysis optimization through a statistical approach.
- Design of two consolidate bioprocesses for the conversion of inulin into PHB: i) separate hydrolysis and fermentation process **SHF**; ii) simultaneous saccharification and fermentation process **SSF**.
- Construction of a “**facilitator microbial consortium**” for the conversion of inulin into PHB using a statistical approach for optimization of the coculture growth conditions.
- Use of PHA-based nanoparticles for the enhancement of mechanical and barrier properties of protein-based films.
- Development of PHA-based nanoparticles as carriers of active molecules: determination of the efficiency of the antimicrobial activity of encapsulated essential oils from Mexican oregano.

---

The interest in biobased and biodegradable materials is widespread at national and international level, as reflected by the increasing number of calls for projects focused on the development of innovative, sustainable, biobased and biodegradable plastics. The Horizon Europe (HORIZON) program, which will run from 2021 until 2027, gives many examples of this. Some of the upcoming calls are focused on the development of processes aimed to combine environmental sustainability, the circularity and functionality of the obtained products; others emphasize the need to develop materials with new properties, i.e. antimicrobial activity. PHAs as bio-based, biodegradable, and biocompatible polymers represent good candidates in these fields. Among the main representatives calls, the ones connected with the topic of this thesis, are focused on the use of renewable feedstock for the development of biobased and biodegradable plastics with enhanced functionalities (“Sustainable biodegradable novel bio-based plastics: innovation for sustainability and end-of-life options of plastics”; topic ID HORIZON-CL6-2022-CIRCBIO-02-03-two-stage) as well as the sustainable synthesis of nanocoatings (including bio-based materials) especially with effectiveness against a range of pathogens (“Antimicrobial, Antiviral, and Antifungal Nanocoatings (RIA)”; topic ID: HORIZON-CL4-2021-RESILIENCE-01-20).

The results achieved in this thesis lay the basis for a future exploitation of the developed technologies, and for the establishment of a contact networking with other national and international research groups bringing complementary competences.

## **Appendix**

Research visit to the Autonomous University of Querétaro (11sept 2018 -10 oct 2018). **PROGRAMA EJECUTIVO DE COOPERACIÓN CIENTÍFICA Y TECNOLÓGICA MÉXICO-ITALIA.** Laboratory of Dr. Carlos Regalado González Professor of Food Biotechnology of Universidad Autónoma De Querétaro Facultad De Química División De Estudios De Posgrado

## Posters

- **Iolanda Corrado**, Mario Malinconico, Cinzia Pezzella, Giovanni Sanna, Gabriella Santagata, Rosa Turco, Martino Di Serio. **“A holistic zero waste biorefinery approach for Cardoon biomass exploitation: bioplastics design”** 3rd International Conference for Bioresource Technology for Bioenergy, Bioproducts & Environmental Sustainability 2021.  
**ORAL PRESENTATION**
- **Iolanda Corrado**, Nicoletta Cascelli, Giovanni Sanna, Cinzia Pezzella. **“Inulin-based biorefinery: inulinases for microbial Polyhydroxyalkanoates production”**. XVII PhD-Chem Day-Webinar, Consorzio interuniversitario Reattività chimica e catalisi, April 29, 2021.  
**ORAL PRESENTATION**
- **Iolanda Corrado**, Nicoletta Cascelli, Giovanni Sanna, Carlos RegaladoGonzález, Blanca GarciaAlmendárez, Cinzia Pezzella. **“BIOACTIVE NANOPARTICLES BASED ON POLYHYDROXYALKANOATES BIOPOLYMERS”** IFIB2019 – International Forum On Industrial Biotechnology And Bioeconomy, Naples, 3-4 October 2019. **POSTER BEST POSTER AWARD**
- **Iolanda Corrado**, Giovanni Sanna, Cinzia Pezzella, Rocco Di Girolamo, C. Valeria L. Giosafatto, Carlos RegaladoGonzález, Raffaele Porta and ManarAbdalrazeq. **“WHEY PROTEIN/POLYHYDROXYALKANOATE BIONANOCOMPOSITES”** 60th Congress of the Italian Society of Biochemistry and Molecular Biology, Lecce, 18-20 September 2019. **POSTER**
- Claudia Petrillo, **Iolanda Corrado**, Stefany Castaldi, Cinzia Pezzella, RacheleIsticato **IDENTIFICATION OF NATURAL INULINASE PRODUCING BACILLI, FOR INDUSTRIAL APPLICATIONS** 14th International Symposium on the Genetic of industrial microorganisms (GIM) 8-11 September 2019 Pisa (Italy).

---

**POSTER****Publications**

- **Corrado I**, Abdalrazeq M, Pezzella C, Di Girolamo R, Porta R, Sannia G, Giosafatto CVL. Design and characterization of poly (3-hydroxybutyrate-co-hydroxyhexanoate) nanoparticles and their grafting in whey protein-based nanocomposites. 2021, Food Hydrocoll, Vol. 110: 106167. <https://doi.org/10.1016/j.foodhyd.2020.106167>. (**\$2.1**)
- Turco R, Santagata G, **Corrado I**, Pezzella C, Di Serio M. *In vivo* and Post-synthesis Strategies to Enhance the Properties of PHB-Based Materials: A Review. 2021, Front Bioeng Biotechnol, Vol. 8: 619266. <https://doi.org/10.3389/fbioe.2020.619266>
- **Corrado I**, Cascelli N, Ntasi G, Birolo L, Sannia G, Pezzella C. Optimization of Inulin Hydrolysis by *Penicillium lanosocoeruleum* Inulinases and Efficient Conversion Into Polyhydroxyalkanoates. 2021, Front Bioeng Biotechnol, Vol. 9: 616908. <https://doi.org/10.3389/fbioe.2021.616908>. (**\$1.1**)
- **Corrado I**, Vastano M, Cascelli N, Sannia G, Pezzella C. Turning Wastes into Resources: Exploiting Microbial Potential for the Conversion of Food Wastes into Polyhydroxyalkanoates. 2021, Biovalorization of waste. Ed. Springer Singapore. pp. 133-168. [https://doi.org/10.1007/978-981-15-9696-4\\_6](https://doi.org/10.1007/978-981-15-9696-4_6)



# *In vivo* and *Post-synthesis* Strategies to Enhance the Properties of PHB-Based Materials: A Review

Rosa Turco<sup>1</sup>, Gabriella Santagata<sup>2</sup>, Iolanda Corrado<sup>1</sup>, Cinzia Pezzella<sup>3\*</sup> and Martino Di Serio<sup>1</sup>

<sup>1</sup> Department of Chemical Sciences, University of Naples Federico II, Complesso Universitario di Monte Sant'Angelo, Naples, Italy, <sup>2</sup> Institute for Polymers, Composites and Biomaterials, National Council of Research, Pozzuoli, Italy, <sup>3</sup> Department of Agricultural Sciences, University of Naples Federico II, Portici, Italy

## OPEN ACCESS

### Edited by:

Ligia R. Rodrigues,  
University of Minho, Portugal

### Reviewed by:

Anouk Duque,  
NOVA University of Lisbon, Portugal  
Mualla Oner,  
Yildiz Technical University, Turkey

### \*Correspondence:

Cinzia Pezzella  
cpezzella@unina.it

### Specialty section:

This article was submitted to  
Industrial Biotechnology,  
a section of the journal  
Frontiers in Bioengineering and  
Biotechnology

**Received:** 19 October 2020

**Accepted:** 30 November 2020

**Published:** 14 January 2021

### Citation:

Turco R, Santagata G, Corrado I, Pezzella C and Di Serio M (2021) *In vivo* and *Post-synthesis* Strategies to Enhance the Properties of PHB-Based Materials: A Review. *Front. Bioeng. Biotechnol.* 8:619266. doi: 10.3389/fbioe.2020.619266

The transition toward “green” alternatives to petroleum-based plastics is driven by the need for “drop-in” replacement materials able to combine characteristics of existing plastics with biodegradability and renewability features. Promising alternatives are the polyhydroxyalkanoates (PHAs), microbial biodegradable polyesters produced by a wide range of microorganisms as carbon, energy, and redox storage material, displaying properties very close to fossil-fuel-derived polyolefins. Among PHAs, polyhydroxybutyrate (PHB) is by far the most well-studied polymer. PHB is a thermoplastic polyester, with very narrow processability window, due to very low resistance to thermal degradation. Since the melting temperature of PHB is around 170–180°C, the processing temperature should be at least 180–190°C. The thermal degradation of PHB at these temperatures proceeds very quickly, causing a rapid decrease in its molecular weight. Moreover, due to its high crystallinity, PHB is stiff and brittle resulting in very poor mechanical properties with low extension at break, which limits its range of application. A further limit to the effective exploitation of these polymers is related to their production costs, which is mostly affected by the costs of the starting feedstocks. Since the first identification of PHB, researchers have faced these issues, and several strategies to improve the processability and reduce brittleness of this polymer have been developed. These approaches range from the *in vivo* synthesis of PHA copolymers, to the enhancement of *post-synthesis* PHB-based material performances, thus the addition of additives and plasticizers, acting on the crystallization process as well as on polymer glass transition temperature. In addition, reactive polymer blending with other bio-based polymers represents a versatile approach to modulate polymer properties while preserving its biodegradability. This review examines the state of the art of PHA processing, shedding light on the green and cost-effective tailored strategies aimed at modulating and optimizing polymer performances. Pioneering examples in this field will be examined, and prospects and challenges for their exploitation will be presented.

Furthermore, since the establishment of a PHA-based industry passes through the designing of cost-competitive production processes, this review will inspect reported examples assessing this economic aspect, examining the most recent progresses toward process sustainability.

**Keywords:** polyhydroxybutyrate, plasticizer, reactive processing, biopolymer, bio-based network

## INTRODUCTION

The exploitation of fossil resources to satisfy the current demand for plastic materials is a serious threat for the environment, with consequences in terms of global warming, human health risks, and ecosystem toxicity (Harding et al., 2007). The superior chemical and physical properties of petro-plastics, which are responsible for their wide applicability, turn out into very low degradation rate in the environment, determining their accumulation as serious pollutants. European policies in relation to waste management, emission reduction, and sustainable development strongly encourage the search for new green solutions to the plastic issue (Directive 2008/98/EC on waste).

Polyhydroxyalkanoates (PHAs) are biodegradable and naturally synthesized polyesters, accumulated by various microorganisms as carbon, energy, and redox storage material, in response to stressful/unbalanced growth conditions. The discovery of polyhydroxybutyrate (PHB) accumulation in *Bacillus megaterium* dates back to 1926 by Lemoigne. Since then, several steps ahead have been done in the field, from the identification of other hydroxyalkanoic acid monomers (1974), to the cloning and characterization of the genes involved in PHA biosynthesis (1988) (Choi et al., 2020). In 1995, the occurrence of more than 91 PHA monomers had been reported, with this number increasing to up to 150 (R)-hydroxyalkanoic acids at present (Muneer et al., 2020). Other important milestones in this field, including the characterization of the first copolymers and the description of the PHA biosynthetic pathways (1990s), up to the elucidation of the first crystal structure of the main PHA biosynthetic enzymes (2017) (Kim et al., 2017), have contributed to progresses in PHA production process as well as

in modulation of polymer composition (Sudesh et al., 2000; Choi et al., 2020).

According to their monomer chain length, PHAs have been classified into three main categories: short chain length (scl)-PHA (C4 and C5), medium chain length (mcl)-PHA (C ≥ 6), and long chain length (lcl)-PHA (C > 14). Since their discovery and characterization, PHAs and particularly PHB gained intensive attention from the scientific community, being the first example of bio-based and biodegradable polyesters synthesized *in vivo* by microorganisms for the intracellular storage. Hence, differently from the other bio-based polymers, PHAs are polymerized by several bacterial strains, and being natural polyesters, they are considered the most easily biodegradable polymers in aerobic (soil, compost, and marine) and anaerobic (sewage sludge, digesters, and landfills) environments, thanks to the biotic degradative action of several bacterial and fungal enzymes. Furthermore, PHA degradation products are easily assimilated into usable products for microbial growth. As a matter of fact, also PLA is a bio-based polymer produced through fermentation of lactic acid, but it is chemically polymerized and, most noteworthy, it is a compostable polymer, making it unsuitable to reduce the plastic waste pollution (Meereboer et al., 2020).

Among the PHAs, polyhydroxybutyrate (PHB), a scl-PHA, is by far the most well-studied PHA polymer, accumulated to up to 80% of cell dry weight by native as well as recombinant microorganisms (Aldor and Keasling, 2003). Being thermoplastic, it can develop bio-plastics by exploiting the common processing methodologies widely used for the oil-derived polymers and biodegradable polyesters, i.e., film casting and blowing, injection molding, extrusion, thermoforming, etc. (Raza et al., 2018). Due to its mechanical and barrier properties, which are similar to those of oil-based polymers such as polypropylene, this material can be proposed as an excellent candidate to substitute petroleum-derived plastics increasingly drawing the commercial attention. Indeed, PHB high melting temperature and high tensile strength are similar to that of polypropylene, whereas its gas barrier properties result in its being even better and more promising than those of polypropylene and polyethylene terephthalate; in light of the above, PHB deserves many attention for its great potential in several applications such as in food packaging. As an assessment, in **Table 1**, the main properties of PHB compared with that of PP are detailed (Masood, 2017; Markl, 2018). In particular, the molar mass of the polymers, representing the measure of the distribution of the individual molar masses around an average value, is reported. For the PHB, this value is measured to be very high and depends on the type of microorganism used and the conditions adopted for the fermentation process, the growth

**Abbreviations:** 3HD, 3-hydroxy-9-decanoate; 9DEO, 9-decenol; ATBC, acetyl tributyl citrate; AVE, aloe vera fibers; BDO, 1,4-butanediol; BIB, di-(2-tert-butylperoxyisopropyl)-benzene; CT, chain transfer; DBS, dibutyl sebacate; DCP, dicumyl peroxide; DDA, dodecanoic acid; DHBA, 2,3-dihydroxybutyrate; DOS, dioctyl sebacate; EB, elongation at break; FC, cellulose fibers; FDA, federation; G, geraniol; GA, geraniol acetate; HB, hydroxybutyrate; HD, hydroxydecanoate; HDD, hydroxydodecanoate; HHX, hydroxyhexanoate; HP, hydroxypropionate; HPhV, hydroxy-3-phenylvalerate; HTD, hydroxytetradecanoate; HV, hydroxyvalerate; IRR, internal rate of return; L, linalool; L503, Lapro1503; LA, levulinic acid; MA, maleic anhydride; NA, nucleating agents; NCS, neural stem cells; PCL, polycaprolactone; PCT, popionyl CoA transferase; PDLLA, poly(DL-lactide); PDO, 1,3-propanediol; PE, polyethylene; PEG, polyethylene glycol; PhaP, PHA binding protein; PLA, polylactic acid; PP, Polypropylene; PVA, 5-phenylvaleric acid; RBS, ribosome-binding site; RGD, arginyl-glycyl-aspartic acid peptide; TBC, tributyl citrate; Tc, crystallization temperature; TC, triethyl citrate; Tcc, cold crystallization temperature; Tg, glass transition temperature; Tm, melting temperature; YM, Young's modulus;  $\delta$ , solubility parameter.

**TABLE 1 |** Range of typical properties of PHB (Bucci et al., 2005; Bugnicourt et al., 2014; dos Santos et al., 2017; Keskin et al., 2017; Rajan et al., 2017).

Property	Value	PP
Density, $\rho$ (g/cm <sup>3</sup> )	1.23	0.095
Glass transition temperature, $T_g$ (°C)	4–7	–10
Melting temperature, $T_m$ (°C)	175–180	176
Crystallinity, Xcr (%)	50–90	50–70
Young's modulus, YM (GPa)	1–2	1.5–1.7
Tensile strength, TS (MPa)	15–40	38
Elongation at break, EB (%)	1–15	4
Water vapor transmission rate, WVTR (g-mm/m <sup>2</sup> -day MPa)	1–5	0.2–0.4
Oxygen transmission rate, OTR (cc-mm/m <sup>2</sup> -day)	2	67.7

rate of the polymer, and the final purification procedures. This parameter is very important, since it significantly influences molecular, processing, and final properties of the polymer, in particular its mechanical performance (dos Santos et al., 2018).

In addition, PHB is biocompatible, and its degradation inside the body occurs slowly. For this reason, PHB can be used both as a polymer drug carrier in case of gradual and controlled releasing kinetics and as scaffold in the field of tissue engineering (Degli Esposti et al., 2019; Babos et al., 2020). Anyway, despite the comparable features with synthetic polymers, PHB exploitation is strongly limited due to its high stiffness, brittleness, and narrow processability window.

Although this phenomenon is not clearly elucidated, it is assumed that the interlamellar amorphous chains are progressively tightened up resulting in an increase in the amorphous rigid fraction (Crétois et al., 2016). This outcome could be explained by two plausible hypothesis. The first one is related to a secondary crystallization slowly occurring during the storage at room temperature: small crystallites not only can bridge crystalline lamellae but also freeze the remaining amorphous PHB chains, leading to the embrittlement of the material (Di Lorenzo and Righetti, 2013). The second assumption is based on the physical aging of the amorphous phase strictly linked to the non-equilibrium character of the glassy state. Actually, based on this theory, two types of amorphous phase coexist: a mobile amorphous fraction (MAF) far from the crystalline lamellae and a rigid amorphous fraction (RAF), which, due to the interaction with the crystals, evidences restricted mobility; in this last case, the boundary  $T_g$  associated is disturbed by the presence of crystals, and the physical aging process occurs below this  $T_g$  (Esposito et al., 2016).

Actually, both phenomena have strong consequences on the physical properties of PHB such as crystallinity, impact strength, Young's modulus, toughness, and elongation at break that undergo continuous worsening even to several days above its processing (dos Santos et al., 2017).

From the structural point of view, crystallinity is strongly related to its regular structure, which in turn depends on the type of synthesis adopted to obtain it. The isotactic PHB is characterized by the only presence of a chiral carbon in absolute

configuration R (Michel and Billington, 2012) and is produced by bacterial fermentation (Vroman and Tighzert, 2009), while the syndiotactic PHB is synthesized starting from the monomers with R and S configuration (Barham et al., 1984). In this way, the fermentation route allows to obtain the highest crystallinity. Depending on the several approaches used to synthesize and process PHB, it is possible to affirm that they shoot in a high range between 40 and 80% (dos Santos et al., 2017).

In addition to its marked brittleness, with very low deformability, PHB has a very strong susceptibility to rapid thermal degradation, posing serious problems to processing using conventional technologies for thermoplastics (Erceg et al., 2005). Indeed, the polyester undergoes thermal degradation and depolymerization at temperatures close to its melting point at around 180°C, so that the acceptable residence time in the processing equipment is severely limited to only few minutes (Erceg et al., 2005).

The thermal degradation is believed to happen almost exclusively via a random chain cleavage mechanism. The degradative reaction, occurring with the elimination of cis  $\beta$ -CH and a six-membered ring transition (Gras et al., 1984; Doi et al., 1994), leads to a rapid decrease in molecular weight (Bugnicourt et al., 2014); however, some kinetically favorable cleavages occur near the ends of macromolecules (Erceg et al., 2005). Thus, several degraded products such as olefinic compounds, carboxylic acids, crotonic acid, and oligomers form (Figure 1).

Most of the bio-based polymers suffer from these shortcomings to such an extent that their diffusion as commodity materials has been confined to niche applications. As a result of the above flaws and to curb the previous drawbacks, several investigations reported in the literature have been performed aimed at producing PHB-based materials with improved properties.

In this review, the most promising strategies finalized to obtain PHB-based materials with suitable and performing properties have been outlined (Figure 2). In particular, green and cost-effective approaches aimed to modulate and optimize the polymer technological performances have been discussed, as well as pioneering examples, prospects, and challenges for their effective exploitation have been detailed, too.

Specifically, in this review, two different approaches have been followed. The first one concerned the modification of the monomeric composition of PHA polymers; different kinds of PHAs have been *in vivo* biosynthesized by incorporating additional units into the PHB backbone, thus providing the possibility to fine tune the polymer properties: a general decrease in the glass transition and melting temperatures are observed with a consequent decreasing material brittleness and broadening processing window. In addition, *in vivo* biosynthetic methodologies aimed to modulate polymer molecular weight and cost competitiveness of the overall process have been also reviewed.

The second overture concerned the fine tuning of the properties of *post-synthesis* PHB-based polymers. To this aim, several studies related to PHB processing with compatible organic or inorganic materials, in order to obtain polymer physical blends, chemical reactive modifications, and

bionanocomposites, have been recently reported, and a short account of them will be detailed in the following sections, together with the description of the main chemical-physical and mechanical properties. In particular, since the toughness and processability of PHB can be improved by incorporating natural additives, like plasticizers, a closer analysis on PHB, their main function, and of course, their most suitable plasticizers will be provided.

In this work, the literature data of the past 20 years, focusing specifically on the past decade, has been reviewed.

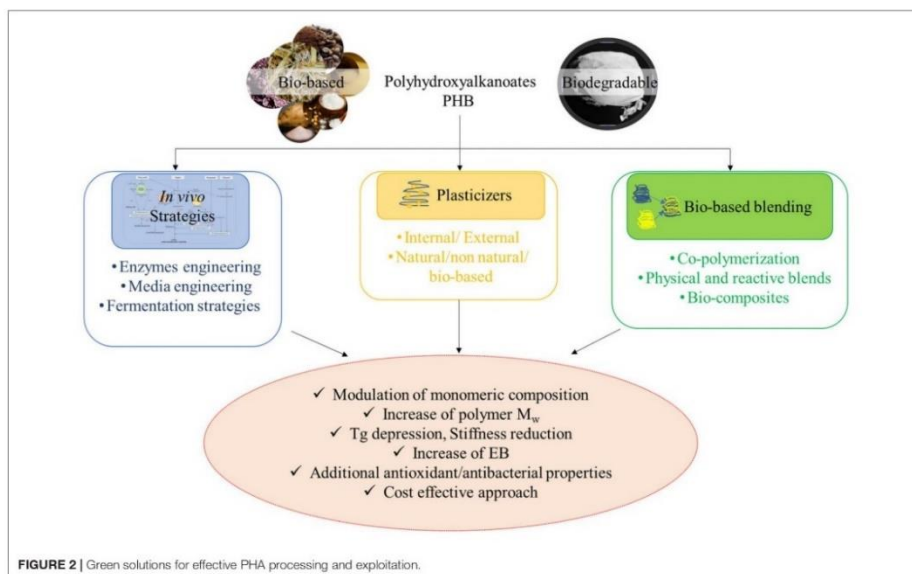
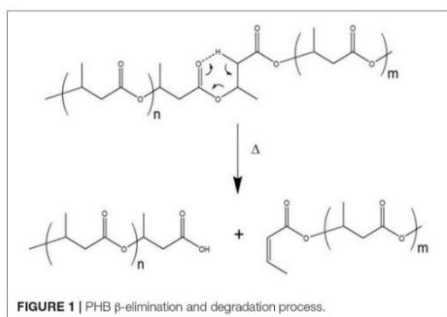
## IN VIVO STRATEGIES TO MODULATE PHB PROPERTIES: SYNTHESIS AND APPLICATIONS

### Copolymer Synthesis

The synthesis of copolymers of various molecular weights, compositions, and architectures has led to the ability to broaden the knowledge and the exploitation of new materials with unique properties. In addition to the control of the stereochemical microstructure, the copolymerization represents a way to opportunely modulate the physical properties of the polymeric materials. By varying the composition, monomer sequencing, and molecular weight, the polymer microstructure can be tailored for specific applications, mostly if a proper balance between the mechanical and thermal properties, together with degradation rate, is needed.

The introduction of other monomeric units in the PHB backbone has been reported to change polymer properties in favor of a reduced stiffness, higher elongation to break, and lower melting point.

Copolymerization is obtained by the activation of different pathways for PHA biosynthesis in the microbial cell. Depending on the available carbon source, three main pathways regulate PHA biosynthesis *in vivo* (Figure 3), although up to 13 different



routes allowing channeling specific precursors into PHA have been described (Tan et al., 2014b). If sugars are supplied, pathways I and III can be followed, yielding short chain length PHA (scl-PHA) and medium chain length PHA (mcl-PHA), respectively. These carbon sources are unrelated since their structure is different from that of PHA. If related carbon sources, such as fatty acids, are supplied, pathway II is followed, yielding mcl-PHA. Both pathways II and III can also produce PHA copolymers (Verlinden et al., 2007). It follows that the polymer composition is strictly related to the supplied C-source and to the activated pathway within the cell.

*In vivo* approaches for tailored copolymer synthesis are based on the use of both pure cultures and mixed microbial cultures (MMCs), in which the supplying of precursor compounds, structurally related to the monomer of interest, determines the activation of the metabolic pathway/s required for its synthesis. In the case of MMC, a raw complex organic substrate is first fermented to obtain volatile fatty acids (VFAs) by anaerobic acidogenic fermentation; then, the VFA-rich stream is used to select for PHA-producing microorganisms against the non-producing ones. Finally, the enriched microbial population is fed with the VFA under optimal conditions to maximize PHA production (Mannina et al., 2020). The type of starting feedstock, the operating conditions for VFA production, and their relative proportions, as well as the applied enrichment strategies directly affect the yield, productivity, and monomeric composition of the produced polymer (Kourmentza et al., 2017). Being based on natural principles of selection and competition among the microorganisms, MMC-based processes display an economic advantage since they are carried in unsterile conditions. Moreover, they allow to broaden the choice of possible feedstocks as the microbial consortium naturally adapts itself to the provided C-source (Mannina et al., 2020).

On the other hand, the use of pure cultures, although requiring sterile and thus costly conditions, is widely applied for PHA production (Anjum et al., 2016; Kourmentza et al., 2017). Both naturally occurring microorganisms as well as engineered strains have been used for copolymer synthesis, taking advantage of their heterogeneous metabolic pathways or finely manipulating them. Protein engineering, applied to the key enzymes of the biosynthetic pathway (Figure 3), also allowed to tailor their substrate specificity, favoring the incorporation of monomer of interests and, more recently, also of non-natural ones (Choi et al., 2020).

This section will cover the most significant examples in the field of copolymer synthesis. The mechanical and thermal properties of the most relevant examples of PHA copolymers have been collected in Table 2.

#### Poly (3-Hydroxybutyrate-co-Hydroxyvalerate)

Poly (3-hydroxybutyrate-co-hydroxyvalerate) is one of the most studied copolymers, has been developed on an industrial scale (Chang et al., 2014), and has recently attracted the attention of both industry and researchers as a promising material due to its biotechnological potentiality and its applicability in the medical, agricultural, and packaging fields (Rivera-Briso and Serrano-Aroca, 2018). PHBV has gained attention due to its better

flexibility, strength, reduced chain packaging, and toughness compared to PHB (Tebaldi et al., 2019). The higher is the amount of the HV fraction, the lower is the melting point of the resulting PHBV copolymer, which broadens the processing window of the material (Ishida et al., 2005; Wang et al., 2013b). In addition, due to the longer side chain of HV, the segmental mobility in the amorphous phase of this copolymer increases, thus reducing the Tg (Ishida et al., 2005). Ultimately, PHBV copolymers show improvement in flexibility and ductility in comparison to PHB (Wang et al., 2013b).

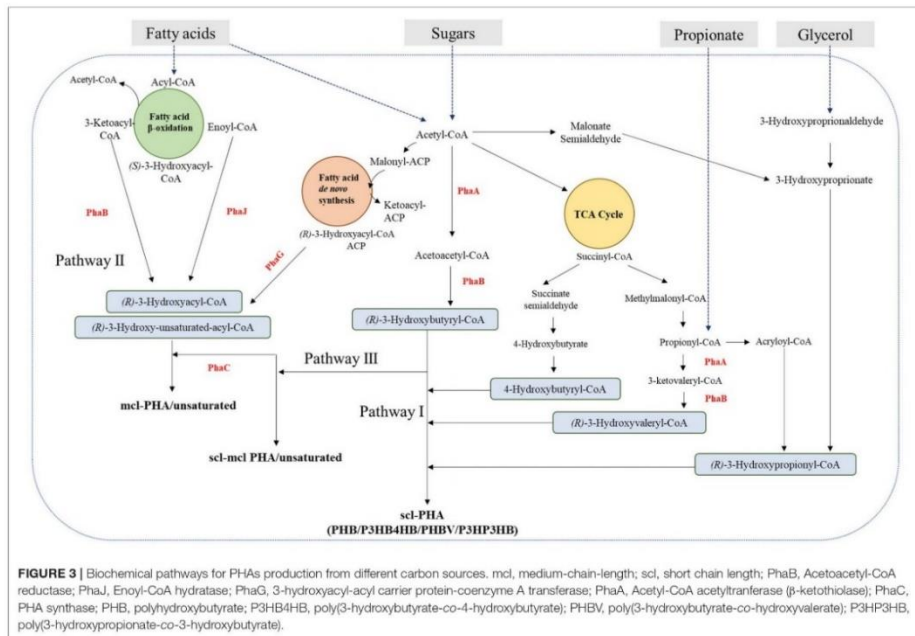
PHBV thermomechanical properties vary widely depending on the mol% of 3-hydroxyvalerate (3HV). Although the incorporation of 3HV moieties in the PHB polymer is expected to reduce its crystallinity, this reduction is limited by the occurrence of the isodimorphism phenomenon, by which 3HB and 3HV are able to co-crystallize (Yeo et al., 2018). As a fact, PHBV still exhibits a high degree of crystallinity throughout a wide range of compositions from 0 to 95 mol% HV (Cai and Qiu, 2009).

Different cultivation strategies have been designed for the incorporation of 3HV monomers in the forming polymeric chain, using organic acid precursors, such as propionic and valeric acid (Zinn et al., 2003; Masood et al., 2012; Follonier et al., 2014; Hilliou et al., 2016; Martla et al., 2018).

In one of the first examples Madden et al. (1998) applied an alternate feeding strategy of glucose and propionic acid to *Ralstonia eutropha* cultures, to produce mixtures of PHB and smaller amount of 3HV-rich (7–18 mol% HV) random copolymer, PHBV. The process of chain termination resulted in the synthesis of polymer mixtures rather than block copolymers.

The demand for cost-competitive PHA production processes has translated into an increasing number of examples reporting the production of PHBV from waste materials and/or less costly, renewable precursors of HV moieties. Gahlawat and Soni (2017) tested the feeding with different acids to *Cupriavidus necator* cultures growing on waste glycerol from jatropha oil as the main carbon source. A multiple-pulse feeding strategy was applied to prevent growth inhibition caused by high acid concentration. In the best conditions, up to 25% HV content was achieved in the copolymer, reaching around 5 g/L polymer accumulation. The polymers produced in these conditions display a low molecular weight, consistently with the role of glycerol as chain termination agents. Similar production levels, although with a lower HV content (2.8–8%) were obtained by García et al. (2013) using all crude by-products (waste glycerol and rapeseed hydrolysates) as C-sources. A different approach to improve PHBV productivity as well as HV content (up to 36.7%) was applied by de Paula et al. (2017), through the selection of a *Pandoraea* sp. MA03 mutant strain with the highest performances on crude glycerol supplemented with propionic and valeric acids. In all the cases, the copolymers composition was found to be affected by the specific precursor feed rate, resulting into PHBV with different 3HV mol%. Saturated fatty acids from the animal processing industry were used as main C-source for the synthesis of PHBV copolymer from *C. necator* (Koller et al., 2014).

In view of process sustainability, the use of levulinic acid (LA) as 3HV precursor has been suggested by several authors. LA



can be produced from a wide range of renewable biomaterials, such as cellulose-containing agricultural and forest wastes, in a cost-effective manner. Although *R. eutropha* could grow in the presence of LA as the sole carbon source, accumulation of PHBV occurred in significant amount only in the presence of glucose as cosubstrate and was strongly affected by the type of added nitrogen source (Wang et al., 2013b). More recently, the fine engineering of LA catabolic pathway in *Pseudomonas putida* EM42 allowed the production of various type of scl-PHA, containing 3HV and 4-hydroxyvalerate (4HV) with different monomer compositions and proportions, depending on the expression of different PHA reductases and synthases endowed with different substrate specificities (Cha et al., 2020). The incorporation of 4HV in place of 3HV into PHBV has been reported to further decrease the melting point of the final copolymer (Schmack et al., 1998) and improve toughness without affecting the degradation temperature (Sheu et al., 2018).

Hydrolysates of residual spent coffee ground after oil extraction are also interesting source of LA, promoting the accumulation of PHBV copolymer (up to 11.6 mol% HV) by *Burkholderia cepacia* (Obruca et al., 2014). Another original example of waste valorization has been described by Pramanik et al. (2014), who reported the production of PHBV (13.8 mol% 3HV) from an alkaliphilic microbe, *Alkaliphilus oremlandii*

OhILAs strain, through the biodegradation of linseed oil-based elastomeric film.

To overcome the need for acid cosubstrates, which cannot only inhibit cell growth but also increase production costs, PHBV copolymer synthesis has been also approached using glucose as C-source. To this aim, fine engineering strategies, focused on the pathways responsible for propionyl-CoA synthesis in *Haloflex mediterranei*, have been applied (Chen et al., 2011; Tan et al., 2014a; Yang et al., 2014). In one of the most recent examples, the CRISP/cas9 approach was used to simultaneously target different genes of the tricarboxylic acid cycle without compromising cell growth, resulting in up to 25 mol% 3HV in the synthesized polymer (Chen et al., 2019).

PHBV copolymers have also been produced in MMC-based processes, starting from a various range of complex organic substrates, such as food waste (Gouveia et al., 2017), municipal wastewater sludge (Wijeyekoon et al., 2018), the liquid fraction resulting from pyrolysis processes (Bio-oil) (Moita Fidalgo et al., 2014), and brewery wastewaters (Tamang et al., 2019). In an interesting example, the modulation of pH in the range of 4.5–7 during the acidogenic reactor operating conditions led to different monomer precursor profiles, which resulted in PHBV copolymers with different compositions starting from cheese whey as model feedstock (Gouveia et al., 2017). By increasing the

**TABLE 2 |** Main properties of PHA copolymers.

Copolymer	Strain, bioprocess	Properties		References
		Thermal	Mechanical	
P(3HB-co-10.2 mol% 3HV)	<i>Ralstonia eutropha</i> , alternate feeding with glucose or propionate	$M_w$ (g mol <sup>-1</sup> ) $6.7 \times 10^{-5}$ $T_m$ (°C) 169 $T_g$ (°C) -1 $T_c$ (°C) 75	TS (MPa) 29.0 EB (%) 17.4 YM (MPa) 472	Madden et al., 1998
P(3HB-co-18.1 mol% 3HV)		$M_w$ (g mol <sup>-1</sup> ) $5.6 \times 10^{-5}$ $T_m$ (°C) 161 $T_g$ (°C) -3 $T_c$ (°C) 80	TS (MPa) 28.7 EB (%) 121.1 YM (MPa) 286	
P(3HB-co-7.5 mol% 3HV)		$M_w$ (g mol <sup>-1</sup> ) $6.9 \times 10^{-5}$ $T_m$ (°C) 174 $T_g$ (°C) -3 $T_c$ (°C) 70	TS (MPa) 19.0 EB (%) 13.6 YM (MPa) 272	
P(3HB-co-7.3 mol% 3HV)		$M_w$ (g mol <sup>-1</sup> ) $7.1 \times 10^{-5}$ $T_m$ (°C) 172 $T_g$ (°C) n.d. $T_c$ (°C) 60	n.d.	
P(3HB-co-5 mol% 3HV)	<i>A. hydrophila</i> 4AK4, grown on lauric acid and/or valerate	$M_w$ (g mol <sup>-1</sup> ) n.d. $T_m$ (°C) 170 $T_g$ (°C) 2.2	TS (MPa) 18.1 EB (%) 2.3 YM (MPa) 1465	Zhang et al., 2009
P(3HB-co-6 mol% 3HV)	<i>Cupriavidus necator</i> , odd-numbered carboxylic acid mix (FAM) as carbon source for large scale production of copolymers	$M_w$ (g mol <sup>-1</sup> ) $4.4 \times 10^5$ $T_m$ (°C) 159 $T_g$ (°C) 2.2 $T_c$ (°C) 50.9	n.d.	Koller et al., 2014
P(3HB-co-9 mol% 3HV)		$M_w$ (g mol <sup>-1</sup> ) $4.5 \times 10^5$ $T_m$ (°C) 159 $T_g$ (°C) 3.3 $T_c$ (°C) 56	n.d.	
P(3HB-co-12 mol% 3HV)	<i>C. necator</i> , grown on waste glycerol and rapeseed hydrolysates	$T_m$ (°C) 155 $T_g$ (°C) -1.9 $T_c$ (°C) n.d.	n.d.	García et al., 2013
P(3HB-co-13.5 mol% 3HV)	<i>A. oremlandii</i> , biodegradation of linseed oil-based elastomeric film	$M_w$ (g mol <sup>-1</sup> ) $2.3 \times 10^5$ $T_m$ (°C) 152 $T_g$ (°C) -3.8 $T_c$ (°C) n.d.	n.d.	Pramanik et al., 2014
P(3HB-co-26 mol% 3HV)	<i>C. necator</i> DSM 545, multiple-pulse feeding with valeric acid	$M_w$ (g mol <sup>-1</sup> ) $1.1 \times 10^5$ $T_m^1$ (°C) 142 $T_m^2$ (°C) 156	n.d.	Gahlawat and Soni, 2017
P(3HB-co-59 mol% 3HV)	Recombinant <i>Escherichia coli</i> , functionalization of copolymer PHBV with ascorbic acid	$T_m$ (°C) 135	n.d.	Bhatia et al., 2019a
P(3HB-co-2.35 mol% 3HV)	<i>H. bluephagenesis</i> ; engineering of TCA cycle by CRISPR/cas9 approach for copolymer production from glucose	$T_m$ (°C) 166 $T_g$ (°C) -0.4	n.d.	Chen et al., 2019
P(3HB-co-4.01 mol% 3HV)		$T_m$ (°C) 163 $T_g$ (°C) -0.5	n.d.	
P(3HB-co-8.6 mol% 3HV)		$T_m$ (°C) 158 $T_g$ (°C) 3.1	n.d.	
P(3HB-co-11.7 mol% 3HV)		$T_m$ (°C) 156 $T_g$ (°C) 2.3	n.d.	
P(3HB-co-15.2 mol% 3HV)		$T_m$ (°C) 158 $T_g$ (°C) 2.8	n.d.	
P(3HB-co-19.6 mol% 3HV)		$T_m$ (°C) 137 $T_g$ (°C) 0.5	n.d.	
P(3HB-co-11 mol% 4HB)	Recombinant <i>E. coli</i> , unrelated carbon sources	$T_m$ (°C) 131 $T_g$ (°C) -4.4	TS (MPa) 20 EB (%) 698	Li et al., 2010
P(3HB-co-18 mol% 4HB)		$T_m$ (°C) 130 $T_g$ (°C) -9.2	TS(MPa) 9.9 EB (%) 729	

(Continued)

TABLE 2 | Continued

Copolymer	Strain, bioprocess	Properties		References
		Thermal	Mechanical	
P(3HB-co-38 mol% 4HB)	<i>C. necator</i> strain A-04, different ratios of fructose and 1,4-butanediol	$M_w$ (g mol <sup>-1</sup> ) $1.0 \times 10^5$ $T_m$ (°C) 152 $T_g$ (°C) -10 $T_c$ (°C) 55	TS (MPa) 2.9 EB (%) 48 YM (MPa) $0.6 \times 10^3$	Chanprateep et al., 2010
P(3HB-co-5 mol% 4HB)		$M_w$ (g mol <sup>-1</sup> ) $1.4 \times 10^5$ $T_m$ (°C) 161 $T_g$ (°C) -5 $T_c$ (°C) 83	TS (MPa) 0.9 EB (%) 22 YM (MPa) $0.8 \times 10^3$	
P(3HB-co-24 mol% 4HB)		$M_w$ (g mol <sup>-1</sup> ) $1.0 \times 10^5$ $T_m$ (°C) 168 $T_g$ (°C) -2 $T_c$ (°C) 104	TS (MPa) 1.4 EB (%) 11 YM (MPa) $1.4 \times 10^3$	
P(3HB-co-95 mol% 4HB)	<i>C. malaysiensis</i> , batch	$M_w$ (g mol <sup>-1</sup> ) $4.4 \times 10^5$	TS (MPa) 23 EB (%) 463 YM (MPa) 187	Norhafini et al., 2017
P(3HB-co-97 mol% 4HB)	<i>C. malaysiensis</i> ; pulse feed of C and N sources	$M_w$ (g mol <sup>-1</sup> ) $3.4 \times 10^5$	TS (MPa) 31 EB (%) 473 YM (MPa) 272	
P(3HB-co-95 mol% 4HB)	<i>C. malaysiensis</i> ; mixed feeding strategy	$M_w$ (g mol <sup>-1</sup> ) $1.7 \times 10^5$	TS (MPa) 24 EB (%) 471 YM (MPa) 214	
P(3HB-co-97 mol% 4HB)	<i>C. malaysiensis</i> ; constant feeding strategy	$M_w$ (g mol <sup>-1</sup> ) $3.2 \times 10^5$	TS (MPa) 31 EB (%) 515 YM (MPa) 256	
P(3HB-co-99 mol% 4HB)	<i>C. malaysiensis</i> ; twice pulse feed of C and N sources	$M_w$ (g mol <sup>-1</sup> ) $3.3 \times 10^5$	TS(MPa) 25 EB (%) 368 YM (MPa) 184	
P(3HB-co-20 mol% 4HB)	Recombinant, <i>Cupriavidus</i> sp. USMAA1020	$M_w$ (g mol <sup>-1</sup> ) $391 \times 10^3$ $T_m$ (°C) 129 $T_g$ (°C) -16	TS (MPa) 12 EB (%) 353 YM 72	Syafiq et al., 2017
P(3HB-co-85 mol% 4HB)		$M_w$ (g mol <sup>-1</sup> ) $87 \times 10^3$ $T_m$ (°C) 63 $T_g$ (°C) -41	TS (MPa) 11 EB (%) 390 YM(MPa) 103	
P(3HB-co-91 mol% 4HB)		$M_w$ (g mol <sup>-1</sup> ) $60 \times 10^3$ $T_m$ (°C) 53 $T_g$ (°C) -53	TS (MPa) 14 EB (%) 402 YM(MPa) 93	
P(3HB-co-10 mol% 4HB)	<i>C. necator</i> B10646, valeric acid, hexanoic acid, and $\gamma$ -butyrolactone as precursor for copolymer production	$M_w$ (g mol <sup>-1</sup> ) $5.7 \times 10^5$ $T_m$ (°C) 150 $T_g$ (°C) 3.4 $T_c$ (°C) 66	TS (MPa) 14.8 EB (%) 5.7 YM (MPa) 957	Zhila and Shishatskaya, 2018
P(3HB-co-29 mol% 4HB)		$M_w$ (g mol <sup>-1</sup> ) $8.3 \times 10^5$ $T_m$ (°C) 162 $T_g$ (°C) n.d. $T_c$ (°C) 96	TS (MPa) 7.8 EB (%) 31 YM (MPa) 243	
P(3HB-co-75 mol% 4HB)		$M_w$ (g mol <sup>-1</sup> ) $7.0 \times 10^5$ $T_m$ (°C) 158 $T_g$ (°C) n.d. $T_c$ (°C) 88	TS (MPa) 15.4 EB (%) 323 YM (MPa) 425	
P3HP	Recombinant <i>E. coli</i> , grown on mixtures of 1,3- propanediol (PDO) and 1,4-butanediol (BDO)	$M_w$ (g mol <sup>-1</sup> ) $1.6 \times 10^5$ $T_m$ (°C) 78 $T_g$ (°C) -18	TS (MPa) 22 EB (%) 498 YM (MPa) 2889	Meng et al., 2012
P(3HP-co-38 mol% 4HB)		$M_w$ (g mol <sup>-1</sup> ) $2.8 \times 10^5$ $T_m$ (°C) 63 $T_g$ (°C) -36	TS (MPa) 0.5 EB (%) 1611 YM (MPa) 4.4	
P(3HP-co-82 mol% 4HB)		$M_w$ (g mol <sup>-1</sup> ) $3.0 \times 10^5$ $T_m$ (°C) 36 $T_g$ (°C) -29	TS (MPa) 6.3 EB (%) 595 YM (MPa) 18.5	

(Continued)

TABLE 2 | Continued

Copolymer	Strain, bioprocess	Properties		References
		Thermal	Mechanical	
P3HP	Recombinant <i>E. coli</i> for the synthesis of a block copolymer consisting of highly elastic P4HB portion with a P3HP block, PDO-BDO alternate feeding	$M_w$ (g mol <sup>-1</sup> ) $1.6 \times 10^5$ $T_m$ (°C) 78 $T_g$ (°C) -18	TS (MPa) 21 EB (%) 498 YM (MPa) 2889	Tripathi et al., 2013b
P4HB		$M_w$ (g mol <sup>-1</sup> ) $3.9 \times 10^5$ $T_m$ (°C) 61 $T_g$ (°C) -47	TS (MPa) 35 EB (%) 697 YM (MPa) 181	
P(3HP-co-25 mol% 4HB)		$M_w$ (g mol <sup>-1</sup> ) $2.6 \times 10^5$ $T_m$ (°C) 63 $T_g$ (°C) -31	TS (MPa) 6.4 EB (%) 963 YM (MPa) 15.5	
P(3HP-co-38 mol% 4HB)		$M_w$ (g mol <sup>-1</sup> ) $2.8 \times 10^5$ $T_m$ (°C) 63 $T_g$ (°C) -36	TS (MPa) 0.6 EB (%) 1611 YM (MPa) 4.4	
P3HP-b-29 mol% P4HB		$M_w$ (g mol <sup>-1</sup> ) $5.5 \times 10^5$ $T_m$ (°C) 55,68 $T_g$ (°C) -20; -46	TS (MPa) 45 EB (%) 877 YM (MPa) 177	
P3HP-b-37 mol% P4HB		$M_w$ (g mol <sup>-1</sup> ) $5.5 \times 10^5$ $T_m$ (°C) 53,67 $T_g$ (°C) -22; -45	TS (MPa) 25.3 EB (%) 1031 YM (MPa) 113	
P(3HB-co-8 mol% 3HV)	Wild-type <i>A. hydrophila</i> , using lauric acid as carbon source	$T_m$ (°C) 170 $T_g$ (°C) 2	n.d.	Noda et al., 2005
P(3HB-co-12 mol% 3HHx)		$T_m$ (°C) 110 $T_g$ (°C) -2.5	n.d.	
P(3HB-co-8 mol% 3HHx)		$T_m$ (°C) 140 $T_g$ (°C) 0	n.d.	
P(3HB-co-2.7 mol% 3HHx)	<i>C. necator</i> , regulation of 3HHx mol% by expression of R-specific enoyl-CoA hydratases	$T_m$ (°C) 151 $T_g$ (°C) -2.3 $T_c$ (°C) 50	n.d.	Arikawa et al., 2016
P(3HB-co-5.9 mol% 3HHx)		$T_m$ (°C) 139 $T_g$ (°C) -2.4 $T_c$ (°C) -	n.d.	
P(3HB-co-7.9 mol% 3HHx)		$T_m$ (°C) 131 $T_g$ (°C) -2.2 $T_c$ (°C) -	n.d.	
P(3HB-co-10.8 mol% 3HHx)		$T_m$ (°C) 113 $T_g$ (°C) -4.7 $T_c$ (°C) -	n.d.	
P(3HB-co-7 mol% 3HHx)	Crystallization study on commercial PHBPHHx (Kaneka corporation) containing different mol% HHx monomer	$M_w$ (g mol <sup>-1</sup> ) $2.3 \times 10^5$ $T_m$ (°C) 122; 141 $T_g$ (°C) 2.3 $T_{cc}$ (°C) 62	n.d.	Cai and Qiu, 2009
P(3HB-co-10 mol% 3HHx)		$M_w$ (g mol <sup>-1</sup> ) $4.5 \times 10^5$ $T_m$ (°C) 121;139 $T_g$ (°C) 2.9 $T_{cc}$ (°C) 58	n.d.	
P(3HB-co-18 mol% 3HHx)		$M_w$ (g mol <sup>-1</sup> ) $2.6 \times 10^5$ $T_m$ (°C) n.d. $T_g$ (°C) 1.3 $T_{cc}$ (°C) n.d.	n.d.	
P(3HB-co-22 mol% 3HHx)	Recombinant <i>A. hydrophila</i>	$M_w$ (g mol <sup>-1</sup> ) $2.9 \times 10^5$	n.d.	Tian et al., 2005
P(3HB-co-3HO)	Enriched culture of <i>Pseudomonas</i> sp.; production of PHA from acidified oil mill wastewater	$M_w$ (g mol <sup>-1</sup> ) $49 \times 10^4$ $T_m$ (°C) 150; 163 $T_g$ (°C) 0.4	n.d.	Ntaikou et al., 2014

(Continued)

TABLE 2 | Continued

Copolymer	Strain, bioprocess	Properties		References
		Thermal	Mechanical	
mcl copolymer from heptadecanoic acid	<i>P. aeruginosa</i> ATCC 27853, odd-chain fatty acids from C17 to C21 under nitrogen starvation	$M_w$ (g mol <sup>-1</sup> ) $77 \times 10^{-3}$ $T_m$ (°C) 52 $T_g$ (°C) -45	n.d.	Impallomeni et al., 2018
mcl copolymer from non-adeanoic acid		$M_w$ (g mol <sup>-1</sup> ) $97 \times 10^{-3}$ $T_m$ (°C) 48 $T_g$ (°C) -43	n.d.	
mcl copolymer from heneicosanoic acid		$M_w$ (g mol <sup>-1</sup> ) $188 \times 10^{-3}$ $T_m$ (°C) 49 $T_g$ (°C) -39	n.d.	
P(16 mol%3HD-co-3HDD)	<i>P. putida</i> mutant, grown on dodecanoate	$M_w$ (g mol <sup>-1</sup> ) $15.5 \times 10^4$ $T_m$ (°C) 78 $T_g$ (°C) -32	TS (MPa) 5.2 EB (%) 88 YM (MPa) 103	Liu et al., 2011b
100% 3HD		$M_w$ (g mol <sup>-1</sup> ) $36.1 \times 10^4$ $T_m$ (°C) 72 $T_g$ (°C) -37	TS (MPa) 12 EB (%) 313 YM (MPa) 20	
P(15 mol% 3HHx-co-40 mol% 3HO-co-30 mol% 3HD-co-15 mol% 3HDD)	<i>P. putida</i> mutant, sequential supplementation of hexanoate and dodecanoic acid	$M_w$ (g mol <sup>-1</sup> ) $10 \times 10^4$ $T_m$ (°C) 53 $T_g$ (°C) -44	TS (MPa) 8.7 EB (%) 189 YM (MPa) 3.6	Tripathi et al., 2013a
P(15.86 mol% 3HD-co-35.25 mol% 3HDD)		$M_w$ (g mol <sup>-1</sup> ) $16 \times 10^4$ $T_m$ (°C) 33;66 $T_g$ (°C) -43	TS (MPa) 16 EB (%) 369 YM (MPa) 38	
P(3HDD-co-10 mol%3H9D)	<i>P. entomophila</i> with deficient $\beta$ -oxidation pathway	$M_w$ (g mol <sup>-1</sup> ) $9.5 \times 10^4$ $T_m$ (°C) 69 $T_g$ (°C) -48	TS (MPa) 4.0 EB (%) 221 YM (MPa) 51	Li et al., 2014
P(3HDD-co-40 mol%3H9D)		$M_w$ (g mol <sup>-1</sup> ) $8.8 \times 10^4$ $T_m$ (°C) 52 $T_g$ (°C) -54	TS (MPa) 3.5 EB (%) 206 YM (MPa) 20	
P(3HDD-co-52 mol%3H9D)		$M_w$ (g mol <sup>-1</sup> ) $1.0 \times 10^5$ $T_m$ (°C) 45 $T_g$ (°C) -55	TS (MPa) 2.2 EB (%) 124 YM (MPa) 3	
P(3HDD-co-77 mol%3H9D)		$M_w$ (g mol <sup>-1</sup> ) $9.9 \times 10^4$ $T_m$ (°C) 43 $T_g$ (°C) -55	TS (MPa) 3.6 EB (%) 173 YM (MPa) 3	
P(3HDD-co-81 mol%3H9D)		$M_w$ (g mol <sup>-1</sup> ) $9.4 \times 10^4$ $T_m$ (°C) 43 $T_g$ (°C) -56	TS (MPa) 3.7 EB (%) 105 YM (MPa) 4.7	
P3HDD-b-70 mol%P3H9D		$M_w$ (g mol <sup>-1</sup> ) $13 \times 10^4$ $T_m$ (°C) 46 $T_g$ (°C) -55	TS (MPa) 3 EB (%) 138 YM (MPa) 8	
P(3HDD-co-29 mol% 3HD-co-12 mol% 3HTD-co-10 mol%3HO-co-6 mol%3HHx)	<i>Ps. chlororaphis subsp. aurantiaca</i> , using crude glycerol from biodiesel production as the sole carbon source	$M_w$ (g mol <sup>-1</sup> ) $1.1 \times 10^6$ $T_m$ (°C) 43 $T_g$ (°C) -47	TS (MPa) 3.9 EB (%) 273 YM (MPa) 8	Pereira et al., 2019
mcl-PHA (75 mol% 3HD)	Mixed culture of <i>Pseudomonas aeruginosa</i> , <i>Pseudomonas</i> sp., and <i>Ralstonia</i> sp.	$T_m$ (°C) 50; 82 $T_g$ (°C) -38 $T_c$ (°C) 20	n.d.	Sangkharak et al., 2020
mcl-PHA (75 mol% 3HD)/TGCN		$T_m$ (°C) 50; 82 $T_g$ (°C) -37 $T_c$ (°C) 12	n.d.	
P(3HDD-co-12 mol% 3HTD-co-10 mol% 3HO-co-6 mol% 3HHx)	mcl-PHA by <i>Pseudomonas mendocina</i> CH50 from waste oils; plasticising effect of the oligomeric mcl-PHA on P(3HB)	$M_w$ (g mol <sup>-1</sup> ) $21 \times 10^4$	n.d.	Lukasiewicz et al., 2018

(Continued)

TABLE 2 | Continued

Copolymer	Strain, bioprocess	Properties		References
		Thermal	Mechanical	
OligoHA: hydrolyzed P(3HHx-3HO-3HD-3HDD) P3HB-OligoHA blend (95/5)		$M_w$ (g mol <sup>-1</sup> ) $10 \times 10^3$	n.d.	
P3HB-OligoHA blend (90/10)		$T_m$ (°C) 172	TS (MPa) 12.5 EB (%) 4 YM (MPa) 1000	
P3HB-OligoHA blend (80/20)		$T_m$ (°C) 175	TS (MPa) 15 EB (%) 6 YM (MPa) 1200	
P3HB		$T_m$ (°C) 173	TS (MPa) 6 EB (%) 16 YM (MPa) 480	
P3HB		$T_m$ (°C) 177	TS (MPa) 20 EB (%) 5 YM (MPa) 1440	
P(3HDD-co-3HPhV)	<i>P. entomophila</i> grown on 5-phenylvaleric acid (PVA) and dodecanoic acid for synthesis of controllable composition of 3HDD and phenyl group on the side chain	$M_w$ (g mol <sup>-1</sup> ) $10 \times 10^4$ $T_m$ (°C) 82 $T_g$ (°C) -49	TS (MPa) 5.5 EB (%) 60 YM (MPa) 61	Shen et al., 2014
P(3HDD-co-2.9 mol% 3HPhV)		$M_w$ (g mol <sup>-1</sup> ) $6.6 \times 10^4$ $T_m$ (°C) 81 $T_g$ (°C) -33	TS (MPa) 2.0 EB (%) 37 YM (MPa) 94	
P(3HDD-co-18.7 mol% 3HPhV)		$M_w$ (g mol <sup>-1</sup> ) $7.3 \times 10^4$ $T_m$ (°C) 80 $T_g$ (°C) -36	TS (MPa) 4.4 EB (%) 86 YM (MPa) 95	
P(3HDD-co-32 mol% 3HPhV)		$M_w$ (g mol <sup>-1</sup> ) $6.1 \times 10^4$ $T_m$ (°C) 76 $T_g$ (°C) -35	TS (MPa) 3.1 EB (%) 32 YM (MPa) 49	
P(3HPhV)		$M_w$ (g mol <sup>-1</sup> ) $4.41 \times 10^4$ $T_m$ (°C) 50 $T_g$ (°C) 6	TS (MPa) n.d. EB (%) n.d. YM (MPa) n.d.	
P(3HB-co-11 mol% 3HV-co-10 mol% 3HHx)	Recombinant <i>A. hydrophila</i> 4AK4, grown on lauric acid, and sodium valerate	n.d.	TS (MPa) 8.4 EB (%) 34 YM (MPa) 235	Zhang et al., 2009
P(3HB-co-17 mol% 3HV-co-10 mol% 3HHx)		n.d.	TS (MPa) 14 EB (%) 740 YM (MPa) 97	
P(3HB-co-13 mol% 3HV-co-15 mol% 3HHx)		n.d.	TS (MPa) 13 EB (%) 833 YM (MPa) 66	
P(3HB-co-10 mol% 3HV-co-38 mol% 4HB)	<i>Cupriavidus eutrophus</i> B10646, valeric acid, hexanoic acid, and $\gamma$ -butyrolactone as precursor for copolymer production	$M_w$ (g mol <sup>-1</sup> ) $4.9 \times 10^5$ $T_m$ (°C) 164 $T_g$ (°C) -5 $T_c$ (°C) 61	TS (MPa) 5.3 EB (%) 130 YM (MPa) 48	Zhila and Shishatskaya, 2018
P(3HB-co-17 mol% 3HV-co-55 mol% 4HB)		$M_w$ (g mol <sup>-1</sup> ) $5.4 \times 10^5$ $T_m$ (°C) 166 $T_g$ (°C) n.d. $T_c$ (°C) 25	TS (MPa) 8.8 EB (%) 365 YM (MPa) 34	
P(3HB-co-21 mol% 3HV-co-13 mol% 4HB-co-2 mol% 3HHx)		$M_w$ (g mol <sup>-1</sup> ) $7.9 \times 10^5$ $T_m$ (°C) 169 $T_g$ (°C) -0.7 $T_c$ (°C) 51	TS (MPa) 7.3 EB (%) 94 YM (MPa) 128	
P(3HB-co-6 mol% 3HV-co-9 mol% 4HB-co-1 mol% 3HHx)		$M_w$ (g mol <sup>-1</sup> ) $7.6 \times 10^5$ $T_m$ (°C) 161 $T_g$ (°C) -4.4 $T_c$ (°C) 63	TS (MPa) 12 EB (%) 49 YM (MPa) 419	

operating pH of the acidogenic reactor, up to 30 mol% HV could be achieved, while at low pH (<6), the HV content significantly reduced to 5 mol%. Similarly, Huang et al. investigated the effect of pH of  $\beta$ -cyclodextrin and glycerol on the profile of odd C-number VFA in the anaerobic digestion of waste-activated sludge. The glycerol amount was found to be the predominant factor in regulating the odd VFA proportion, being the latter positively correlated to the mol% HV of the synthesized copolymers (Huang et al., 2018).

In another recent report, a valerate-dominant sludge hydrolysate was fed to enrich a PHA culture under feast–famine conditions. The valerate uptake was shown to correlate with the production of 3HV and 3-hydroxy-2-methylvalerate (3H2MV) precursors, resulting in a P(3HB-co-23.7% 3HV-co-7.9% 3H2MV) mmol C % copolymer. Microbial analysis revealed that such valerate-rich feedstock caused *Delftia* to be the prevailing group over other PHA-producing bacteria (Hao et al., 2017).

Furthermore, the use of phototrophic mixed cultures (PMCs) for PHBV production has also been proposed to decrease operational costs, as these microorganisms are able to draw energy from sunlight and not require oxygen to produce ATP. Fradinho et al. (2019) applied an anaerobic permanent feast strategy to select for a PMC consortium able to regulate internal reducing power via PHA production. When the selected PMC was applied to fermented cheese whey, a PHBV copolymer with 12 mol% HV was obtained, using light intensities corresponding to those of direct sunlight illumination and without any aeration requirement.

The PHBV properties as a function of HV content (Table 2) indicate a gradual decrease in the  $T_m$  together with an improvement in EB, resulting in a range of polymers with enlarged processability, useful to make films and fibers with different elasticities (Anjum et al., 2016; Keskin et al., 2017). Biopol is the trade name of a PHBV copolymer, currently produced by MetaboliX, having a range of uses such as packaging, disposable cutlery, razors, cups, shampoo bottles, as well as surgical stitches, pins, and medical patches (Anjum et al., 2016). Evidencing good gas barrier properties, this polymer can be a good candidate for the production of biodegradable food packaging material, able to both extend the shelf life of food products and delay the foods' spoilage. The physical–chemical and structural stability of PHBV (3 mol% HV) films under food contact conditions was evaluated by Chea et al. (2016). It was concluded that mechanical properties and water vapor permeability of PHBV films were preserved after contact at 40°C for 10 days with different food simulating liquids tested (water, acetic acid 3% w/v, ethanol 20% w/v, iso-octane) except with ethanol 95% (v/v).

Processing of PHBV material via traditional melt spinning is hampered by the transition from viscoelasticity to brittleness that occurs with increase in storage time (Wang et al., 2016). The obtaining of PLA/PHBV fibers via conventional melt-spinning and hot-drawing processes represented a solution to overcome this problem (Li et al., 2015a). Mechanical properties of PHBV fibers were also improved through the application of drawing and heat setting processes after the formation of the fibers (Hufenus et al., 2015).

The use of PHBV electrospun fibers to develop active multilayer materials for food packaging application was also investigated (Castro-Mayorga et al., 2017a; Figueroa-Lopez et al., 2020). An active PHBV-based multilayer, loaded with silver nanoparticles, was found effective against *Salmonella enterica*. The mechanical performance of the PHBV was not altered by the incorporation of the electrospun PHBV coating, and the presence of AgNPs did not affect the properties of the coated system as well (Castro-Mayorga et al., 2017a). In a more recent example, a novel multilayer system based on PHBV (2–3 mol% HV) with antimicrobial properties was developed. Electrospun mats of PHBV fibers containing eugenol were used as an active interlayer between a food contact layer of PHBV and a cast-extruded PHB sheet. After the annealing at mild temperature, the novel multilayer active packaging material exhibited, besides antimicrobial activity, high hydrophobicity, strong mechanical resistance, and improved barrier properties against water vapor and limonene vapors (Figueroa-Lopez et al., 2020).

Additional updated examples of PHBV bioactive nanocomposites will be detailed in section *PHBV-Based Bionanocomposites*.

The uses of PHBV copolymers have been also investigated in biomedical sectors, where they have been shown to provide a positive effect on cellular growth and adhesion (Keen et al., 2007; Ahmed et al., 2010). Furthermore, the more amorphous structure displayed by PHBV copolymer has favored its exploitation in drug delivery applications due to easy diffusion of active molecules. Despite the improved polymer properties, copolymers often exhibit slow degradability and resorbability due to their intrinsic hydrophobicity, which limits cell colonization. Bhatia et al. (2019b) addressed this issue through the functionalization of PHBV copolymer (59% HV) with ascorbic acid, mediated by *Candida antarctica* lipase B. The modified polymer displayed antioxidant activity as well as a 1.6-fold increase in biodegradability as compared to the neat copolymer. In addition, the functionalization also resulted into a lower degree of crystallinity (due to imperfection of crystals) and higher thermal degradation temperature and hydrophilicity degree.

### Poly (3-Hydroxybutyrate-co-Hexanoate)

Poly (3-hydroxybutyrate-co-hexanoate) (PHBHHx) is a promising copolymer based on 3HB with minor contents of 3HHx comonomer. Differently from PHBV, the presence of short chain branches of three carbon atoms in PHBHHx has a marked effect on reducing the regularity of the polymer chain, thus lowering both crystallinity and  $T_m$  (Noda et al., 2010). Actually, although the crystallization mechanism and the crystal cell structure do not change, the overall isothermal crystallization rate of PHBHHx copolymers reduces with HHx content and occurs at lower crystallization temperature from the melt (Cai and Qiu, 2009). Indeed, due to their steric hindrance, the 3HHx does not co-crystallize with 3HB units; thus, PHBHHx displays slower crystallization rate than PHB homopolymers, which can be a challenge for its efficient processing (Vandewijngaarden et al., 2016). The fact is that due to reduced crystallinity, when PHBHHx copolymers with different mol% HHx are subjected to

anaerobic biodegradation, the higher is the HHx, the faster is the rate of weight loss (Morse et al., 2011).

The synthesis of PHBHHx copolymer has been mainly obtained through strain engineering approaches, focusing on the specificity of the key PHA biosynthetic enzymes toward HHx precursors. The mol% HHx in PHBHHx copolymer was finely regulated (from 2.7 to 10.8%) by acting on the expression level of the *phaJs* in a *C. necator* strain harboring the PHA synthase gene from *Aeromonas caviae*. The same gene target was also overexpressed in *R. eutropha* Re2133, together with a PhaC2 synthase from *Rhodococcus aetherivorans* endowed with a broad specificity for *mcl*-monomer, as well as with the deletion of *phaB* genes. This strategy was effective in promoting up to 22% HHx using coffee waste oil as the substrate (Bhatia et al., 2018).

*Escherichia coli* has been used as chassis for the production of PHBHHx by introducing synthase genes specific for *mcl*-precursors and/or acting on the pathways channeling specific precursors (Taguchi et al., 1999; Lu et al., 2003). A high mol% HHx (50 mol%) has been achieved in *E. coli* strain engineered with the PHA biosynthetic operon from *Bacillus cereus*, using fatty acids as well as complex C-sources such as waste frying oils as substrates (Vastano et al., 2017, 2019).

Most of the engineering approaches have been focused on *Aeromonas hydrophila*, this strain being naturally able to produce PHBHHx from dodecanoate. First attempts of strain engineering reveal the synergic effect of the overexpression of phasins—proteins associated to PHA granules in the cells—and *PhaI* coding genes in increasing 3HHx fraction (Han et al., 2004). An increase in 3HHx content is also obtained by deleting acetic acid pathway-related genes (Liu et al., 2011a). Interestingly, the overexpression of phasin coding genes in the engineered *A. hydrophila* strain not only determines an increase in 3HHx content but also causes a reduction in polymer molecular weight due to the formation of more PHA granules with reduced size (Tian et al., 2005).

To address PHBHHx production from glucose or gluconate instead of fatty acids, *A. hydrophila* and *P. putida* have been engineered with different combinations of target genes, with *tesA* thioesterase and *phaG* being the key targets in the two strains, respectively (Qiu et al., 2005).

In terms of thermomechanical properties, PHBHHx combines those of polyethylene (PE) (i.e., strength, flexibility, toughness, and elasticity), with printability and dyeability features (Anjum et al., 2016). Compared to conventional polymers used in packaging, PHBHHx films obtained by compression molding display relatively low oxygen permeability and a water vapor permeability slightly higher than those of PE, PP, and PS. CO<sub>2</sub> permeability is rather high if compared to known barrier materials (PET, PA, and EVOH) but also lower than those for packaging materials such as PP and PE (Vandewijngaarden et al., 2014). Despite its potential in food packaging application, the slow crystallization that characterizes this copolymer has represented an obstacle for its industrial processing. In fact, the addition of different additives acting as nucleating agents has been proposed. Ultrafine talc was reported to drastically improve PHBHHx crystallization, causing also an increase in the YM (Vandewijngaarden et al., 2016) without modification of the

material barrier properties, thus opening the way to its use as a protection layer for moisture-sensitive O<sub>2</sub> barrier layers. The use of zinc oxide as filler, on the other hand, also improved PHBHHx crystallization but strongly affected its opacity, although resulting in a successful UV-blocking property.

The exploitation of PHBHHx copolymers in combination with reinforcing materials (Dehouche et al., 2020) as well as in blending with other polyesters, mainly polylactic acid (PLA), can provide final materials with improved properties. Bio-composites based on PHBHHx and aloe vera fibers (AVFs) have been prepared by testing different surface treatment methods of AVF in order to improve the interfacial adhesion between the fiber and the polymer matrix (Dehouche et al., 2020). Blending of PHBHHx (11% HHx) with poly(DL-lactide) (PDLLA) from solvent casting, at ratios of 2:1 and 1:2, exhibit a lower YM and a higher EB compared to unblended PDLLA, whereas melt compounding of PLA and PHBHHx in different ratios inhibits PLA crystallization, resulting in enhanced elongation and toughness with respect to neat PLA (Lim et al., 2013).

Due to its biocompatibility and higher elasticity compared with PHB and PHBV, PHBHHx has been widely applied as scaffold matrix in tissue engineering and cell transplantation (Gao et al., 2006).

3HHx content affects *in vitro* growth and differentiation of smooth muscle cells (Qu et al., 2006a). When compared to PHB, PHBHHx reveals a higher degradation rate in subcutaneous implants in rabbits, and, most importantly, the copolymer elicits a very mild tissue response during implantation (Qu et al., 2006b). In one of the most recent examples, PHBHHx supports the residence, survival, and stemness of the transplanted neural stem cells (NSCs) cells in rat brain (Wang et al., 2019).

Surface modification of PHBHHx films under alkaline conditions has been found effective in promoting osteoblast cell response for application in bone-tissue engineering (Li et al., 2005). In a pioneering approach, Li et al. (2015b) have coated PHBHHx scaffolds with PHA binding protein (PhaP) fused with the arginyl-glycyl-aspartic acid peptide (PhaP-RGD) to promote proliferation and differentiation of mesenchymal stem cells seeded on them. Due to their reliable safety profile and strong hydrophobicity, PHBHHx is suitable for prolonged release delivery systems. Implantable sandwich PHBHHx films have been designed to address long time release of drugs, reducing the burst release effect (Peng et al., 2018). In addition, PHBHHx nanoparticles have been applied to this aim (Peng et al., 2013; Heathman et al., 2014). Interestingly, a hybrid copolymer, such as PEG200-end capped PHBHHx, has been synthesized by *A. hydrophila* in microbial fermentation and the derived nanoparticle tested as intracellular delivery nanocarriers for sustained drug release (Lu et al., 2004). Noteworthy, besides drug delivery, incorporation of PHBHHx nanoparticle in whey protein-based films, improves the mechanical properties of the derived bio-plastics producing more extensible materials preserving their mechanical resistance (Corrado et al., 2021).

### Poly (3-Hydroxybutyrate-co-4-Hydroxybutyrate)

Several studies have been focused on the synthesis of poly (3-hydroxybutyrate-co-4-hydroxybutyrate) (P3HB4HB)

copolymers, using wild-type strains under feeding of 4HB precursors such as 4-hydroxybutyric acid,  $\gamma$ -butyrolactone, 1,4-butanediol, etc. (Choi et al., 1999; Lee et al., 2004).

Copolymers with different mol% 4HB (from 5 to 64%) have been produced in *C. necator* strain A-04 by tuning the ratios of fructose to 1,4-butanediol. The characterization of the copolymers reveals an increase in both elongation at break and tensile strength, as well as a reduction in polymer toughness, with increasing 4HB content (Chanprateep et al., 2010).

Co-feeding of soybean oil and  $\gamma$ -butyrolactone produces high yield of copolymer accumulation, although higher supplementation of the precursor has been shown to increase the 4HB fraction while inhibiting cell growth (Park and Kim, 2011). High PHA density fed-batch cultivation strategies employing mixed precursors (5:1 ratios 1,4-butanediol and 1,6-hexanediol) have been developed to boost the 4HB content up to 99 mol% in *Cupriavidus malaysiensis* transformed with additional copies of PHA synthase gene (PhaC) (Norhafini et al., 2017, 2019; Syaifiq et al., 2017).

Waste materials such as saccharose from sugarcane industry (de Sousa Dias et al., 2017) and waste frying oils (Rao et al., 2010) have been also used in combination with 4HB precursors in processes employing *Burkholderia sacchari* and *C. necator*, respectively. Accumulation of P3HB4HB from slaughterhouse residues was achieved by using *Defftia acidovorans* DSM39 expressing and heterologous lipase (Romanelli et al., 2014).

The high cost of the 4HB precursors supplied to the growth media has encouraged the construction of engineered strains able to produce P3HB4HB copolymer from unrelated C-sources. An engineered *E. coli* strain has been designed to produce up to 65.5% P3HB4HB (11.1 mol% 4HB) accumulation using glucose as C-source. To enhance the carbon flux to 4HB biosynthesis, genes involved in succinate formation from succinate semi-aldehyde (succinate semi-aldehyde dehydrogenase) have been deleted (Li et al., 2010). A significant increase in copolymer accumulation has been achieved by the “enlarged cell strategy,” based on the alteration of the genes involved in cell division, in order to get filamentary *E. coli* with larger internal space. As an additional advantage, this filamentary recombinant *E. coli* also allows easier downstream separation from the fermentation broth (Wang et al., 2014). A P4HB homopolymer (PHA4400) is currently commercialized by Tephra Inc. (Cambridge, MA), which uses a proprietary transgenic fermentation process based on *E. coli*. The polymer is characterized by remarkable flexibility and good absorbability behavior *in vivo*, being well-suited for implantable medical applications. Noteworthy, the first products approved by the Food and Drug Administration (FDA) for clinical uses were P3HB4HB-based devices produced by Tephra (US) (Zhila and Shishatskaya, 2018).

A low-cost platform for non-sterile and continuous production of P3HB4HB from glucose has been designed using the halophilic *Halomonas bluephagenesis* as chassis. In this example, combinatorial deletions of multiple orthologs of succinate semi-aldehyde dehydrogenases has allowed to increase the 4HB molar fraction up to 24-fold (Ye et al., 2018).

Finally, a complex engineering strategy has been applied to *E. coli* to get co-polyesters of 3-hydroxypropionate (3HP)

and 4HB by redesigning the pathways for the synthesis of the corresponding monomers from 1,3-propanediol (PDO) and 1,4-butanediol (BDO). P(3HP-co-4HB) with adjustable monomer ratios have been produced and characterized (Meng et al., 2012). Interestingly, the same recombinant *E. coli* strain has been used for the synthesis of a block copolymer consisting of highly elastic P4HB portion together with a P3HP block endowed with enormous tensile strength, by applying an alternate PDO-BDO feeding. In comparison to the homopolymers P3HP and P4HB, the block microstructure displays reduced Tm as well as increased YM and TS (Tripathi et al., 2013b).

### Medium Chain Length PHA Copolymers

The incorporation of longer monomers ( $C \geq 6$ ) within the PHA polymeric chain determines the shift toward a more elastomeric behavior of the resulting polymer. These properties suit well with applications in tissue engineering and drug delivery, justifying the great interest in this research area.

Most of mcl-PHA are produced from *Pseudomonas* sp., which possess the specific metabolic pathways necessary for the synthesis of mcl-precursors from fatty acids. Mcl-copolymers with monomer composition ranging from C5 to C17 are synthesized by *P. aeruginosa* ATCC 27853 grown on odd-chain fatty acids from C17 to C21 under nitrogen starvation. The highest yield is obtained for heptadecanoic acid, probably because of limitation in the uptake of longer fatty acids. The characterized polymers are soft, sticky, rubber-like materials (Impallomeni et al., 2018). Previously, mcl-PHA production has been achieved by supplying even-chain n-alkanoic acids from C8 to C22 (Ballistreri et al., 2001). The use of complex oily sources, including waste frying oils, has been also explored for the synthesis of mcl-PHA from different *Pseudomonas* strains (Haba et al., 2007; Gamal et al., 2013; Follonier et al., 2014; Vastano et al., 2019).

The comonomer composition can be finely regulated by using  $\beta$ -oxidation weakened mutants of *P. putida* (Wang et al., 2011), so that the monomer composition is strictly related to the nature of the supplied fatty acid (Liu et al., 2011b). In an interesting example, a  $\beta$ -oxidation *P. putida* mutant has been exploited for the production of a novel diblock copolymer P3HHx-b-P(3HD-co-3HDD) by sequential supplementation of hexanoate and dodecanoic acid (Tripathi et al., 2013a). The incorporation of block microstructure determines an increase in TS, YM, and EB if compared to corresponding random copolymers. Thus, the blocky feature helps to capture the amorphous nature of the mcl-polymers, as well as to gain crystallinity, improving the overall polymer properties (Tripathi et al., 2013a). The incorporation of unsaturated PHA site chains represents a useful strategy to obtain functional and easily modifiable PHAs. By using a *Pseudomonas entomophila* strain with deficient  $\beta$ -oxidation pathway, the incorporation of 3-hydroxydodecanoate (3HDD) and 3-hydroxy-9-decenoate (3H9D) moieties in different ratios has been obtained from feeding with mixture of dodecanoic acid (DDA) and 9-decenol (9DEO). Due to the presence of unsaturated bonds, the copolymers can be cross-linked under UV radiation. Moreover, a diblock polymer P3HDD-b-P3H9D has been synthesized under specific feeding strategies. This polymer

displays a 2-fold increase in YM compared with the random copolymer with similar 3HDD/3H9D ratios (Li et al., 2014).

A rather unique copolymer composed of 3HB and 3HO units was obtained using an enriched culture of *Pseudomonas* sp. as initial inoculum for the production of PHA from acidified oil mill wastewater. The weight average molecular mass of polymer was characterized by a wide polydispersion index, as a consequence of the high complexity of the final microbial consortium (Ntaikou et al., 2014).

When the so-called glycogen-accumulating organisms (GAOs) from mixed culture anaerobic-aerobic wastewater treatment processes were used to produce PHAs from acetate, the applied operational conditions were found to affect polymer microstructure. As a fact, a mixture of true copolymers consisting of monomers HB, HV, 3H2MV, and 3-hydroxy-2-methylbutyrate (HMB) was produced under anaerobic conditions, while the aerobic process primarily produced the HB monomer, most likely forming separate homopolymer blocks (Dai et al., 2008).

Despite their potential, the widespread use of mcl-PHA is limited by the difficulty in their processing, which is due to low viscosity, poor melt strength, adhesive-sticky nature, and very slow crystallization. Gopi et al. (2018) have proposed a chemical modification strategy involving the reaction with dicumylperoxide and triallylotrimersate co-agent to introduce branching and thus enhancing the crystallization kinetics of poly(3-hydroxydecanoate) (P3HD). The authors pointed out a possible application of these improved polymers in 3D printing of biomedical products.

The adhesive properties of an mcl-PHA (43 mol% HDD, 12 mol% HTD, 10 mol% HO, 6 mol% HHx) produced by *Pseudomonas chlororaphis* subsp. *aurantiaca* when grown on crude glycerol were investigated by Pereira et al. (2019). The films displayed good adhesion properties toward porcine and human skins, together with high tension and shear bond strength, suggesting the potential use of this material as novel natural adhesive for wound dressing. A different applicative scenario for this class of polymers has been recently reported (Sangkharak et al., 2020). The authors designed a novel biocomposite of an mcl-PHA (75 mol% HD) incorporating torch ginger cellulose nanowhiskers (TGNs) as a filtering material for wastewater treatment.

Finally, an mcl-PHA (7.6 mol% HHx, 45.4 mol% HO, 41.8 mol% HD, 5.2 mol% HDD) produced by *Pseudomonas mendocina* CH50 from waste oils was transformed into an oligomeric derivative by acid hydrolysis and efficiently used as a plasticizer for PHB, resulting in softer and more flexible materials. The obtained materials, entirely based on PHA, were found applicable in soft tissue engineering, thanks to their improved properties as well as the demonstrated *in vitro* biocompatibility (Lukasiewicz et al., 2018).

### Other Copolymers

Manipulation of synthetic pathways for PHA production has allowed to design new engineered strains able to incorporate unnatural monomers within the polymer backbone (Choi et al., 2020). Whatever is the unnatural monomer to be introduced in the bio-polyester, the designing of new evolved PHA synthases

endowed with proper specificity in recognizing uncommon substrates is a *sine qua non*-condition for effective *in vivo* synthesis (Park et al., 2012). The introduction of a phenyl group on the side chain has been obtained in *P. entomophila*  $\beta$ -oxidation weaken mutant, in the presence of 5-phenylvaleric acid (PVA) as precursor (Shen et al., 2014). A microbial cell factory for the production of P(LA-co-3HB) copolymer has been designed through fine *E. coli* engineering (Taguchi et al., 2008). Besides the PhaA and PhaB from *R. eutropha*, the recombinant strain expresses a propionyl-CoA transferase (PCT) from *Megasphaera elsdenii*, able to catalyze coenzyme A addition to lactic acid, and a mutated PHA synthase from *Pseudomonas* sp. 61-3, endowed with the ability to polymerize lactoyl-CoA precursor. Interestingly, the same strain was exploited for the production of P(LA-co-3HB) from on a lignocellulosic feedstock, taking advantage of the *E. coli* abilities to metabolize both xylose and galactose derived from woody-extract hemicellulosic hydrolysate (Takisawa et al., 2017).

A similar approach allows to incorporate 2,3-dihydroxybutyrate (DHBA) in engineered *E. coli* using glycolate as the sole C-source (Insomphun et al., 2016).

Properly designed feeding strategies, combined with a set of PHA synthetic genes with suitable specificities, have been developed to obtain complex ter- or quarter-polymers. Terpolyesters composed of HB, HV, and HHx monomers have been produced by providing *Aeromonas hydrophila* 4AK4 strain with a set of PHA synthesis genes, allowing to supply the corresponding monomer precursors from lauric acid and/or valerate. Among the different synthesized polyesters, P(3HB-co-11% 3HV-co-10% 3HHx; PHBV11HHx10), and P(3HB-co-17% 3HV-co-10% 3HHx; PHBV17HHx10) have the suitable combination of YM, EB, and TS ranging from 97 to 235 MPa, 341 to 740%, and 8.4 to 14.3 MPa, respectively (Zhang et al., 2009).

In a similar approach, *R. eutropha* has been engineered with *A. hydrophila* PHA biosynthetic operon to produce PHBV7HHx11 and PHBV18HHx11 when fed with increasing amount of propionic acid. Compared with PHBHHx with 12 mol% HHx (PHBHHx12), the terpolymer has higher crystallization rate and degree of crystallinity. Crystallization studies have revealed that the simultaneous introduction of 3HHx and 3HV monomers in PHB improves the mobility of chain stems along the chain direction, leading to easier intralamellar slip during heating or drawing, finally resulting in improvement of mechanical properties (Ye et al., 2010). Furthermore, different P3HB4HB biopolymers, P3HBHV4HB terpolymers, and P3HBHV4HBHHx quarter-polymers with varying 4HB amount have been synthesized by *C. necator* strains under specific feeding strategies. The effect of 4H monomer unit into all the synthesized copolymers is in lowering the melting and the crystallization temperatures, thus improving processing-related properties of these materials. All the copolymers also display enhanced EB compared to PHB (Zhila and Shishatskaya, 2018).

### Tuning Polymer Molecular Weight

The average molecular weight of PHB synthesized by bacteria is usually in the range of  $0.1\text{--}2.0 \times 10^6$  g mol<sup>-1</sup> in *R. eutropha* (Tsuge, 2016). However, ultrahigh molecular weight

PHB (UHMW-PHB) with defined  $M_w$   $43.0 \times 10^6 \text{ g mol}^{-1}$  display high mechanical strength (TS, 1,320 MPa; EB, 35%; YM, 18.1 GPa) and are preferred in applications requiring high mechanical strength, such as in developing high-strength fibers and films (Iwata, 2005).

Several factors have been shown to increase molecular weight during *in vivo* synthesis of PHA polymers: the concentration and the activity of the PHA synthase, the occurrence of chain transfer (CT) reactions, and the simultaneous degradation of PHA during biosynthesis (Tsuge, 2016). The molecular weight has been shown to decrease with increasing PHA synthase concentration and to increase proportionally with its catalytic activity. A CRISPRi-based approach to modulate PhaC expression level in *E. coli* has come to the same correlation: the higher the PhaC activity, the more the PHA accumulation, yet the less the molecular weight and the wider the polydispersity (Li et al., 2017).

The CT reaction is caused by the presence of molecules (CT agent) that promote the transesterification reaction between their hydroxy group and the carboxy group of the growing polymer chain-PHA synthase complex. Commonly occurring CT agents include water, 3HB, and ethanol. Thus, high-molecular-weight PHA can be synthesized, for example, by ensuring sufficient culture aeration to facilitate cell growth while preventing ethanol production. Furthermore, deletion of PHA depolymerase genes promotes the production of high-molecular weight PHA by turning off the polymer degradation within the cell (Tsuge, 2016).

## CHEMICAL AND PHYSICAL STRATEGIES TO IMPROVE POST-SYNTHESIS PHB-BASED MATERIALS

### Use of Plasticizers

In general, in the field of polymers, it is possible to identify two types of plasticizers: internal and external (Viděki et al., 2007). The internal plasticizers are part of the polymer molecules, as they are chemically bound to the polymer chains, grafted or reacted with the original polymer, thus making the polymer chains more difficult to adapt and compact together closely. Their main role is to soften the polymers by lowering their glass transition temperature ( $T_g$ ) and reducing their elastic modulus (Vieira et al., 2011). External plasticizers, instead, are low volatility molecules added to interact with polymers, widening the polymer chains without chemical reaction. In this case, the internal molecular forces between plasticizer molecules and between a plasticizer and a polymer play a fundamental role, such as dispersion forces, induction forces, dipole-dipole interaction, and hydrogen bonds (Mekonnen et al., 2013). Several theories have been proposed to explain the mechanism and role of plasticizers in polymers. The most important are (a) the lubricity theory, (b) the gel theory, and (c) the free volume theory (Vieira et al., 2014).

Although these theories are widely accepted and used in plasticizer selection for polymers, Shtarkman and Razinskaya (1983) have emphasized the limitation of current theories on the mechanism of plasticization. Indeed, according to these authors, it is not possible to establish a plasticization mechanism because

of the huge versatility of the investigated polymer and plasticizer systems; hence, instead of trusting on the above theories, it would be much more useful to consider the direct correlation between compatibility–efficiency–property of each investigated polymer–plasticizer blend. As an example, since the behavior of a single polymer highly depends on its thermal history, different film processing can provide substantial diverse crystalline pattern, and the effect of the same plasticizer on these polymer substrate will, therefore, be quite different.

Therefore, the choice of a plasticizer involves several important criteria, including a high degree of compatibility with the polymer matrix, responsible of its easy solubility and inclusion in both crystalline (toughening) and amorphous (softening) regions. The compatibility should be consistent with the whole temperature range of applications; hence, plasticizer molecular mass and chemical structure, including polarity, shape, and size, must be considered to assure a suitable plasticizing effect. Generally, plasticizers are responsible for  $T_g$  lowering and elastic modulus decreasing, as reported above. Hence, the efficiency may be expressed in terms of  $T_g$  depression and stiffness reduction. With the lowering of  $T_g$ , elongation at break and flexibility of the polymer increases. In fact, elongation and impact resistance strongly depend on polymer  $T_g$  and molecular structural organization. In addition, the plasticizers should remain inside the polymer matrix. The larger the plasticizer, the lower its vapor pressure, and thus, the greater its permanence inside the polymer; on the other hand, bigger molecules are slowly diffused inside the macromolecular chains, since the highest diffusion rate is associated to small molecules that, on contrary, show higher vapor pressures (Vieira et al., 2011).

As noted above, the blending with the plasticizers is considered to be one of the simplest route to overcome the limitations of PHB, allowing for a broader application window. Generally, the use of natural or non-natural plasticizers would allow to lower the glass transition and melting temperature, through the enhanced macromolecular movement. In this way, it would be possible to process the polymer at lower temperatures without inducing its thermal degradation (Baltieri et al., 2003; Erceg et al., 2005). Furthermore, plasticizers could improve both the toughness and softness of the polymer by decreasing its crystallinity, weakening the intramacromolecular bond, and facilitating conformational changes.

For these reasons, many efforts have focused on the industrial formulation of PHB with external plasticizers able to improve their thermal and mechanical properties (Mangeon et al., 2018). The relevant literature is rich in number and type of plasticizers for PHB. They vary from those of natural origin to synthetic one from those with low to high molecular weight, from linear to branched structures. Table 3 summarizes some of the best known plasticizers in the literature, together with the main properties investigated, when used in mixing with PHB with a molecular weight in the range of 100,000–300,000  $\text{g mol}^{-1}$ .

From Table 3, it emerges that blending with plasticizers induce a general lowering of the glass transition temperature and an improvement in elongation at break for almost all the additives used, with few exceptions. The difference can be

**TABLE 3 |** Main plasticizers for PHB.

Plasticizers	Acronyms	M <sub>w</sub> (g mol <sup>-1</sup> )	% w/w	T <sub>g</sub> (°C)	T <sub>m</sub> (°C)	EB (%)	TS (MPa)	YM (MPa)	References
Glycerol	G	92	13		170	0.9	24.8	2835	Jost and Langowski, 2015
Triacetyl glycerol	TAG	218	20	-16.7	161	10.3	14.1	238.4	Baltieri et al., 2003
Diocetyl phthalate	DOP		20	-9.4	164.5	10.5	18.0	448	Baltieri et al., 2003; Wang et al., 2008
Diocetyl adipate	DOA		30	-6.9	165.3	6.2	16.1	576	
Diocetyl sebacate	DOS		30	-3.6	163.5	4.3	6.0	374	
Propylene glycol	PG	76	17		171	0.9	24.9	3,360	Råpe et al., 2015
Triethyl acetate	TEC	276	20	-30	164	2.3	15.8	1,135	Choi and Park, 2004; Råpe et al., 2015
Soybean oil	SO	920	20	-3.4	161		15		Choi and Park, 2004
Epoxidized soybean oil	ESO	975	13-20	-19	160	1.0	30	2,729	Choi and Park, 2004; Jost and Langowski, 2015; Panaitescu et al., 2017
Castor oil	CO	933	13		171	0.9	27.1	3,089	Jost and Langowski, 2015
Triethyl citrate	TC	276	30	-24	-	21	18.6	960	Råpe et al., 2015
Tributyl citrate	BTC	515	30	-23	-	32	9.4	800	Råpe et al., 2015
Acetylbutyryltriethyl citrate	ABTC	558	30	-30.7	156.8	9.7	6.1	192.7	Erceg et al., 2005; Råpe et al., 2015; Chaos et al., 2019
Salicylic acid decylester	-	-	30	-28	-	104	11.8	850	Kunze et al., 2002
Salicylic acid 2-butylloctyl ester	-	-	30	-28	-	22	13.5	810	Kunze et al., 2002
Acetylsalicylic acid hexylester	-	-	30	-14	-	126	11.8	680	Kunze et al., 2002
Ketoprofenethylester	-	-	30	-14	-	58	11.8	600	Kunze et al., 2002
polyhydroxy-butylate-hexanoate	PHI-HBX	1760	PHB-1/6	-10	102	9.8	25		Wang et al., 2008
Polyethylene glycol	PEG 1000	950-1050	50	-	170	1.0	23	2,700	Bibe et al., 1999
Linalool	L	154	20	-11.0	174	5.2	20	560	Mangeon et al., 2018
Geraniol	G	154	20	-9.0	179	5.9	21	760	Mangeon et al., 2018
Geranyl acetate	GA	196	20	-13.0	170	13.8	15	395	Mangeon et al., 2018
Dodecanol		186	10	7	155				Yoshie et al., 2000
Lauric acid	-	200	10	4	171				Yoshie et al., 2000
Tributyrin	-	302	10	1	172				Yoshie et al., 2000
Trilaurin	-	639	10	-4	173				Yoshie et al., 2000

ascribed to the variation in combining the chemical structure of the plasticizer, the molecular weight, the solubility, and compatibility with the polymer, as above discussed. Therefore, the summarized plasticizers can be discussed after their subdivision based on building block molecule: (i) glycerol, (ii) oil, (iii) citric acid, and (iv) salicylic acid. Besides these, we must also add the category of plasticizers that have structures similar to some phthalates, common plasticizers of PVC, and those of smaller natural molecules such as those of terpenes.

Yoshie et al. (2000) compared the effect of tributyrin, trilaurin, lauric acid, and dodecanol on the physical properties of PHB. All the molecules used act to reduce the T<sub>g</sub> and the cold crystallization temperature, T<sub>cc</sub>. In this trend, the best seems to be tributyrin, given its good miscibility with the polymer chains. Although there is this advantage, all additives, even in small amounts (1% by weight), promote the enzymatic degradation of the polymer.

Recently, bio-based compounds such as the terpenes have also been studied as additives for PHB, thanks to their additional beneficial properties such as antioxidant and antibacterial activities (Persico et al., 2012). Terpenes are interesting components of essential oils extracted from plants, with a chemical structure of repeating units of isoprene (C<sub>5</sub>H<sub>8</sub>). Among these, the oxygenated monoterpenes that contain alcohol have been described as having greater biological activity. Mangeon et al. (2018) studied linalool (L), geraniol (G), and geraniol acetate (GA) as PHB plasticizers. In this study, the use of terpenes led to a decrease in T<sub>g</sub> and an increase in elongation at break over 650% combined with a decrease in Young's modulus compared to pure PHB. The effect is more pronounced with GA due to the presence of the segment bearing an ester group, which increases free volume and molecular mobility. The fact that terpenes are already widely used in the chemical industry gives them real potential as a PHB plasticizer with antibacterial properties.

Salicylic acid esters and ibuprofen ketones have also been reported as suitable plasticizers of PHB. Their use, given their properties, is recommended for medical packaging (Kunze et al., 2002).

Dibutyl sebacate (DBS), dioctyl sebacate (DOS), polyethylene glycol (PEG), and Lapro1503 (L503), have also been reported in the literature as biodegradable lower molecular weight plasticizers to improve the properties of PHB. All the additives proved to be compatible with the polymer, forming monophasic mixtures up to a concentration of 15–20% by weight. For all, a decrease in  $T_g$  and an improvement and a decrease in the crystallization temperature were found (Baltieri et al., 2003; Wang et al., 2008).

Citric acid ester plasticizers are among the most important plasticizers and environment friendly because of their safety and non-toxicity. They have been approved in the United States, the European Union, and other developed countries for use in plastic products in close contact with the human body and meet high hygiene requirements (Chabrat et al., 2012). Acetyl tributyl citrate (ATBC) and tributyl citrate (TBC) are among the most studied in detail, thanks to their excellent performance. In addition, TBC has antibacterial and flame-retardant properties, which further expand its applicability (Chaos et al., 2019).

Many of these have been described as good plasticizers for PHB, improving its processability, in particular ATBC, TBC, and triethyl citrate (TC). The incorporation of plasticizers into PHB decreased TS and YM but increased the elongation at break. TBC and ATBC were the most compatible and efficient plasticizers on improving the thermal, mechanical, and barrier properties of PHB. The optimum concentration could be up to 20% depending on the desired properties of the final products (Erceg et al., 2005; Rápe et al., 2015; Chaos et al., 2019). From the study of Choi and Park (2004), triethyl citrate was the most effective plasticizer in terms of reduction in the glass transition temperature as well as in terms of improvement in the impact strength and elongation.

This result can be explained by the decrease in crystallinity and the crystalline size and in the formation of small spherulites, due to the easier penetration of the additive molecules between the polymer chains, which reduce the hydrogen bond. These data were correlated with the increase in elongation at break of the initial degradation temperature of the PHB.

Suárez Palacios et al. (2014) postponed the use of glycerol-based plasticizers and as an alternative to phthalates in the medical field. When mixed with PHB, glycerol and its derivatives showed good results due to their polarity (Jost and Langowski, 2015).

Many works in the literature point out that the use of high molecular weight plasticizers has a more pronounced effect in improving the mechanical properties. This is the case with PEG and epoxidized oils (Bibe et al., 1999). Epoxidized oils are among the most studied plasticizers of PVC, obtained by epoxidation with peracids with various oils (Turco et al., 2019b). The behavior in mixture with PHB can be explained by the higher reactivity of the epoxide group and the possibility of hydrogen bond formation (Choi and Park, 2004; Jost and Langowski, 2015; Panaiteescu et al., 2017).

The main drawback in the use of plasticizers mainly concerns the external plasticization with the migration of the plasticizer from the plasticized material. This process can occur by diffusion of the plasticizer from the bulk material to the surface (exudation) or by interface phenomena and absorption or by evaporation in the surrounding medium. This phenomenon causes a decrease in the plasticizer amount in the polymer, with loss of elasticity and ductility of the material. Additionally, the leaking plasticizer from the material can contaminate the surrounding medium (medical application problems). Several factors influence the migration of the plasticizer, the main ones with regard to the type and concentration of the plasticizer, its molecular weight, branching, and polarity. Low-molecular-weight plasticizers are more prone to migrate from the polymeric material. The more linear the plasticizer structure, the faster the extraction and migration rate will be compared to more branched plasticizers. The migration of the plasticizer is also influenced by the type of polymer, its molecular weight, and its compatibility with the plasticizer, and from the plasticization process and the homogeneity of the product.

### PHB Physical Blends and Reactive Blends

For a sustainable processing strategy, the blending with other polymers or additives represents a much more easy and cost-effective approach and, as a result, is the more frequently used technique in the industrial sector (Anna and Arrigo, 2019). In fact, following this procedure, polymeric materials with enhanced and tailored chemico-physical and mechanical properties can be obtained by opportunely regulating the weight ratio between the selected polymers. Actually, the blending of two polymeric matrices is strictly correlated to their miscibility, i.e., to their respective solubility parameters ( $\delta$ ). If they are quite similar, a good miscibility should be expected. Anyway, the miscibility between two or more polymers also depends on the processing temperature, weight ratio in the blend compositions, as well as polymer respective molecular weights and crystallinity (Arrieta et al., 2017). Among bio-based polymers, poly(lactic acid) (PLA) is the most used mainly in food packaging area because of its easy processability, high transparency, and relatively low costs. PLA is produced through fermentation of lactic acid, followed by chemical polymerization; differently from PHB, it is a compostable material mainly commercialized for single-use disposal packaging items, such as bottles, cold food cups, and trays, as well as for flexible films (Auras et al., 2004; Jamshidian et al., 2010). Blending PHB with PLA could gain mutual advantages; indeed, PLA shows low crystallinity, scarce barrier properties, low heat distortion temperature (softening above 60°C), and difficult biodegradation at ambient conditions. These drawbacks, limiting its industrial exploitation, could be improved by its melt blending with another highly crystalline biopolymer matrix with similar melting temperature, lower  $T_g$ , and suitable barrier properties and biodegradability, as in PHB (González-Ausejo et al., 2017). Hence, PHB/PLA blends have gained a great interest, since their combination allows to obtain new biopolymer based systems with enhanced properties as compared to the single components while preserving their ecosustainability (Modi et al., 2013). Nevertheless, generally, PHB and PLA do

not evidence fine miscibility although they have similar solubility parameters, ranging between 19.5 and 20.5 ( $\text{MPa}^{1/2}$ ) for PLA and between 18.5 and 20.1 ( $\text{MPa}^{1/2}$ ) for PHB. Actually, in polymer blending, several parameters should be taken in consideration. The first one is the polymer molecular weight. In their paper, Blümm and Owen found that low-molecular-weight (LMW) PLA and high-molecular-weight (HMW) PHB were melting miscible over the whole composition range, whereas a blend of HMW-PLA with LMW-PHB evidenced phase separation above PHB content of 25% (Blümm and Owen, 1995).

Similarly, Zhang and Thomas (2011) reported the formulation of PLA/PHB blends with different weight ratios (100:0, 80:20, 60:40, 40:60, and 0:100), showing that some interactions between the two polymers were established, notwithstanding their immiscibility. In particular, the blend containing 25 wt% of PHB evidenced outstandingly improved tensile properties compared with pure PLA because of the homogeneous dispersion of PHB crystals, which acted as a filler and nucleating agent in PLA. Anyway, the processing temperature can play a decisive role on PHB-PLA miscibility by providing, in some case, to melt reactive compatibilized blends. Indeed, while LMW-PLA and HMW-PHB blends obtained by solvent casting at room temperatures evidence phase separation in all compositions, the same blend melt blended at 200°C showed higher miscibility, evidenced by the lowering of both PHB melting temperature and PLA glass transition temperature. The better miscibility was ascribed to transesterification reactions occurring between PLA and PHB chains during heating, leading to the formation *in situ* of low-molecular-weight PLA-PHB block copolymers acting in the interfacial region between the two phases as enhancer of their compatibility (Zhang et al., 2012). In addition, PHB/PLA interfacial compatibilization can be improved by melt-reactive extrusion in the presence of an external compatibilizer agent. For instance, Jandas et al. (2014) used maleic anhydride (MA) as reactive compatibilizer for PLA and PHB matrices to increase their miscibility. Actually, MA chemically grafted the  $\alpha$ -carbon atom of the carbonyl group of PHB and PLA. Moreover, the presence of the reactive dicumyl peroxide was responsible of the formation of cross-linked and branched structures at their interfaces. In addition, the compatibilized blends evidenced substantial improvement of mechanical flexibility as a function of MA concentration. Passing from 1 to 9 wt%, PLA-PHB 70:30 blend changed from a brittle to a ductile material, reaching the best flexibility of more than 500% by grafting 7 wt% of MA (Jandas et al., 2014).

In order to improve PHB-PLA blends flexibility, by both increasing the polymer chain mobility and improving their processing for film manufacturing, plasticizers are frequently added to the blend. In this sense, PLA-PHB plasticization has been proven to be an effective way to enhance mechanical performance as well as to improve the compatibility between PLA and PHB biopolymers. Nowadays, the traditional plasticizers give way to natural ones due to the migration phenomenon, which could result in potential human health and environmental hazards (Harmon and Otter, 2018). Several plasticizers have been used mainly at concentrations between 10 and 30 wt% for film applications, such as glycerol (Martin and Averous, 2001),

poly(adipates) (Martino et al., 2011), PEG (Wang et al., 2008), citrate esters (Fenollar et al., 2013), and low-molecular-weight additives such as aroma compounds including D-limonene, carvacrol, and thymol (Arrieta et al., 2014). Most of them were able to decrease PLA Tg and increase polymer blend tensile strain (Arrieta et al., 2017), as previously detailed.

The blending with another natural polymers, such as thermoplastic starch (TPS), could represent a valid support to both obtain cost-effective biopolymer-based systems and enhance PHB properties without compromising environmental and carbon management benefits. Starch, a biodegradable polysaccharide produced by numerous plants, is one of the most abundant renewable feedstock resources known to man. Thanks to its biodegradability, renewability, and easy availability, starch has been extensively studied as a low-cost component of biodegradable plastic materials (Zhang et al., 2014). It is mostly composed of linear amylose and highly branched amylopectin organized in granular state due to the inherent hydrogen bonding between molecules. This native structure, providing a high crystalline material, severely hinders the dispersion of starch into a polymer matrix at a fine scale. When mixed with some water and/or plasticizers such as glycerol and following subjection to heat and shearing action, starch undergoes spontaneous destructure, provoking the breaking down of intermolecular hydrogen bonds in favor of the polymer gelatinization. A homogeneous melt known as thermoplastic starch (TPS), evidencing typical thermoplastic behavior, is thus formed (Pyshpadass et al., 2008). Hence, TPS can be obtained and formulated by means of standard equipment commonly used in industrial manufacturing of synthetic polymers (Liminana et al., 2019). However, the high hydrophilicity and hygroscopicity, the quick physical aging effect due to the retrogradation process, and the poor mechanical properties strongly affect the industrial application of neat TPS (Ortega-Toro et al., 2017). This is why blending with more hydrophobic polymers, such as PHB, could enhance its functional properties (Turco et al., 2019a).

Hence, the mixing of PHB and TPS would combine the advantages of the two polymers by synergizing their properties while preserving the complete biodegradability of the blend. In their work, Godbole et al. (2003) blended PHB and TPS at different weight ratio compositions and studied the thermal and mechanical properties of the obtained films. They found that the blends PHB/TPS with a w/w percentage ratio of 70:30 showed a consistent improvement of mechanical performances with respect to neat PHB; as an example, the blending of only 30% w/w of TPS to PHB could double and quadruple the stress and strain at break values of the polyester, respectively. Although no shifting of PHB melting temperature could be observed, thus indicating that there were no interactions at molecular level, a strong delay of PHB decomposition temperature could be highlighted passing from about 220 to 260°C; TPS could act as a thermal stabilizer of PHB.

Vice versa, by investigating the influence of PHB on TPS properties, Lai et al. (2006) studied the mechanical properties of films based on TPS doped with different amounts of PHB (1, 3, 5, and 7 wt%). They found that the mechanical properties of films increased by increasing PHB content, whereas the values of water

absorption, one of the main issues of hygroscopic TPS, decreased because of the higher PHB hydrophobicity. Actually, it is worthy to underline that, for PHB/TPS blends, there is an optimized ratio between glycerol (used to thermoplasticize starch) and PHB concentration finalized to reach a suitable compatibility between the polymers. The same authors found that, when TPS contains 25% of glycerol, the tensile strength of the blend TPS/PHB significantly increased by increasing PHB content, whereas when 33% of glycerol is used, only slight changing could be observed. This outcome could be probably due to the higher gelatinization degree, resulting in a structure more prone to water diffusion. Similar results were found by Thiré et al. (2006). In their work, the authors investigated compression-molded PHB/starch blends with starch content varying between 0 and 50%. They found that, above 30% in weight of TPS blended with PHB, higher starch contents led to the worsening of mechanical properties due to the lack of interfacial adhesion between starch and PHB, also evidenced by morphological analysis.

In order to improve the interfacial adhesion between the polymers, Zhang and Thomas (2010) prepared PHB/starch blends by melt process and investigated the properties in terms of interfacial adhesion between the polymers. Two types of maize starch, starch 1 (containing 70% amylose) and starch 2 (containing 72% amylopectin), were melt blended with PHB. The spectroscopic and morphological analyses evidenced that starch particles acted as nucleating agent for PHB crystallite formation by significantly reducing the spherulites size; moreover, the starch fillers physically interacted with PHB by means of intermolecular hydrogen bonds. This effect was particularly highlighted when the more linear and tighter structure of amylose-rich starch was used. Hydrogen bonding between the polar residues of starch (hydroxyl groups) and carbonyl residues of PHB could inhibit the chain scission degradation in PHB, thus improving its thermal stability. As a consequence, higher melt shear viscosity and better mechanical properties were observed when starch 1 was used.

### PHB Reactive Blends

Blending different polymers opens up a range of possibility for the development of novel materials with interesting properties. As previously underscored, melt compounding is one of the most effective methods to tune the polymer blending properties. This method allows preparation of new bio-based polymer blends or composites with pleasing properties. Anyway, most of the blends consist of thermodynamically immiscible polymers, and the simple physical mixing in the melt state usually leads to phase separation on the micrometer scale resulting in unfulfilling properties of the final products. To overcome the problems related to incompatibility, bio-based polymer blends and composites require a reduction in interfacial tension between the components leading to improved final properties of the materials (Muthuraj et al., 2018). Among various strategies for compatibilization, reactive blending seems to be one of the most promising and environment-friendly approaches (Raquez et al., 2008). It is a fast, solvent-free, low-cost, and environment-friendly method by which designed chemical reactions between the components in suitable processing conditions occur. Reactive blending is really versatile since it can be successfully

applied during “*in situ* polymerization” of biodegradable polymers, functionalization of natural fibers/fillers, or chemical modification of the polymer structure. Moreover, the reactive blending occurring by using the “dynamic curing” of bio-based polymers and composites is worthy of consideration in this research field. The method consists on using reactive species as organic peroxides in the melt chamber resulting in the formulation of copolymers, which act as interface compatibilizers between two (or more) polymer matrices. In the literature data, the dynamic curing of biodegradable aliphatic polyesters blends (Ma et al., 2014), aliphatic polyester/natural rubber blends (Wang et al., 2015), and, more recently, bio-composites (Luo et al., 2016) indicated that the high temperature necessary to decompose organic peroxides also induces transesterification reactions of aliphatic polyesters, responsible of polymer chain rearrangements toward soluble copolymers. This confirms that dynamic curing of bio-based polymer blends and composites can lead to the development of semi-interpenetrating networks connecting two (or more) phases, which significantly enhances their physicomechanical properties.

In their paper, Przybysz et al. (2018) used two different organic peroxides, dicumyl peroxide (DCP) and di-(2-tert-butylperoxyisopropyl)-benzene (BIB), to compatibilize polycaprolactone (PCL)/PHB blend. Polycaprolactone is a synthetic semi-crystalline linear aliphatic polyester that is biocompatible and biodegradable. It is ductile and has a significantly lower melting point than PHB at about 60°C. Blends of PCL and PHB have attracted much attention due to their inherent biodegradability and biocompatibility, although they are immiscible on the molecular scale as proven by Antunes and Felisberti (2005).

It was observed that the addition of free radical initiators to PCL/PHB blends resulted in the significant enhancement of mechanical and thermal properties in comparison to uncompatibilized blend obtained by only physical mixing. The severe improvement of PCL/PHB properties was due to the partial cross-linking and/or branching of the covalently linked blends, as evidenced by the melt flowrate. Moreover, the better efficiency of BIB due to its higher number of free radicals was responsible for a tightened final compatibilized structure (Przybysz et al., 2018).

### PHB-Based Bionanocomposites

One of the main drawbacks of PHB is the high costs correlated to the fermentation and extraction processes. As a result, several studies investigated on the preparation of PHB bio-composites by blending it with natural fibers and fillers, aiming at producing more cost-effective materials with improved properties (Delmas et al., 2011; Garcia-Garcia et al., 2016). Inspired by these considerations and in the frame of an eco-sustainable approach, Angelini et al. (2014) prepared compression-molded bio-composites employing a lignin-containing filler obtained as a by-product of the bioethanol fermentative production process, using *Arundo donax* as a biomass (Vishtal and Kraslawski, 2011). When blended with biodegradable aromatic and aliphatic polyesters, an increase in thermal stability and elastic moduli of the resulting composites was observed, not neglecting the

valid opportunity for converting an agro-food by-product into a bio-resource, aimed to improve the properties of PHB in an environment-friendly and cost-effective way (Mousavioun et al., 2010). Therefore, in order to reduce the costs of filler processing, hence the bio-composite overall cost, no pretreatments other than milling were performed on the crude lignin-containing residue filler prior to use. The biodegradation behavior of the composites, qualitatively assessed by analyzing the surface of soil buried films, evidenced a significant surface degradation of PHB-based bio-composites. The authors demonstrated that lignin positively affected the rheological behavior of the polymer melt and acted as a PHB nucleating agent (Angelini et al., 2014). In mixtures, the nucleation rate and size of the spherulite depend on the cooling rate and the nucleation density. Nucleating agents (NAs) provide polymers with homogeneous nuclei and allow more rapid crystallization during the cool-down period after the polymer melts. Indeed, it is very important to both accelerate the crystallization rate of PHB-based materials and provide the formation of small and more homogeneous spherulite sizes in order to enhance its mechanical properties. In general, adding NAs results in an increase in melt crystallization temperature and narrowing of the crystallization peak during non-isothermal melt crystallization; in other words, in the presence of NA, less degree of supercooling and shorter crystallization time occur (Shi et al., 2015).

Recently, natural fibers are increasingly being utilized as environment-friendly materials to improve polymer properties. The natural fibers can represent a valid alternative to synthetic oil-fossil-derived fibers, such as glass and carbon fibers, commonly used as reinforcements in bio-plastics due to their strong mechanical properties. The cellulose-based fibers are eco-sustainable and cost effective (Tan et al., 2015) due to their biodegradability, renewability, and availability; moreover, they have low density, competitive specific mechanical properties, and a relatively low cost (Ching et al., 2016). Generally, along with a number of benefits as reinforcements, there are some drawbacks associated with the exploitation of these natural lignocellulosic fibers. Indeed, the hydrophilicity and strong cross-linking of lignocellulosic fibers prevent the compatibility with biopolymer matrices, leading to poor interfacial adhesion and mechanical properties (Sanchez-Garcia et al., 2008). In their paper, Tănase et al. (2015), prepared new bio-composite materials based on PHB and different percentages of cellulose fibers (from 2 to 10%) in order to improve PHB physical and mechanical behavior. By increasing the cellulose fiber content, the authors evidenced a decrease in melt viscosity and melting temperature, making the composites easy to process.

The crystallinity of PHB/FC composites decreased for all samples compared to neat PHB. The decrease in the crystallinity of the tested samples could be attributed to the hindered motion of the polymer segments due to the presence of cellulose fibers in the polymer matrix. The composite showed a blocking effect in the UV light spectra region while maintaining high transparency, resulting in a suitable property for a packaging material. On the other side, the water vapor barrier was poor due to the hydrophilicity of cellulose fibers (Tănase et al., 2015).

Driven by the necessity to overcome these issues, attempts to improve bio-composite performances have been carried out by the development of bionanocomposites. Polymer nanocomposites, obtained by incorporation of nanosized particles into polymer matrices, evidenced clear improvements of PHB properties, mostly if mechanical performances are concerned. For example, studies on the effect of organoclay minerals on mechanical properties of PHAs have been performed (Ozkoc and Kemaloglu, 2009). As a matter of fact, polymer nanocomposites exhibited markedly improved properties when compared to the pure polymer. Mineral clays are the most used silicates in bionanocomposites manufacturing. Indeed, they can modify the polymer characteristics and improve their processability. As clays are naturally hydrophilic, in order to make them more compatible with hydrophobic polymer like PHB, the cations between the layers can be changed by cationic surfactants like the alkyl ammonium (Alexandre and Dubois, 2000). The modified clay becomes organophilic, its surface energy decreases, and the interbasal distance increases. The modified organo-nanosilicates are more compatible with the hydrophobic PHB nature due to the improvement of the interfacial adhesion. Furthermore, it makes possible the polymer molecules intercalating inside clay galleries, thus strongly modifying the mechanical, thermal, and barrier properties of the polymer (Bordes et al., 2009a).

Among the traditional composites, bentonite is one of the lamellar silicates most used as inorganic filler. Indeed, it is environment friendly and available in large quantities at a relatively low cost. Thus, it provides for the manufacture of bionanocomposites, preserving the biodegradability of the whole system (Bordes et al., 2009b). In their paper, Júnior et al. evaluated the thermal behavior of PHB/PEG/clay bionanocomposites. It was observed that the initial temperature of degradation of bionanocomposites increased with organobentonite content. It was also verified that clay addition to most of the systems led to an increase in crystallinity compared to the PHB matrix, which was attributed to clay nucleating action able to reduce the size of the spherulitic crystals by both decreasing the free energy barrier required for crystal growth and increasing the number of nucleation sites available for crystal growth. This effect was due to the organic modification of the bentonite able to provide suitable different interlayer structures for the bionanocomposites (Júnior et al., 2019). Actually, from the application point of view, PHBV is widely investigated in the preparation of high-performing nanocomposites to be exploited in food packaging. However, the main drawbacks needed to be overcome are its slow crystallization rate and low crystallinity responsible for the dropping down of mechanical and barrier properties. According to Zhang et al. (2017), the addition of cellulose nanocrystals (CNCs) substantially modulates the crystallization profile of the polymer, thus enhancing its mechanical property and thermal stability. In addition, finalized to bestow antibacterial properties, thus obtaining a bioactive food packaging material, the authors included bifunctional nanohybrids composed of CNCs and antibacterial agents, such as silver nanoparticles, AgNPs, in the biopolymeric matrix and found that they acted as suitable nucleating agent able to

strongly improve PHBV crystallization temperature and rate and whole crystallinity. As a consequence, also thermal stability, mechanical, barrier, and antibacterial properties of the ternary bionanocomposite significantly enhanced.

In their paper, Yu et al. (2010) performed a pioneering research about the structural and optical properties of PHBV/ZnO nanofibers fabricated by the electrospinning technique. ZnO nanoparticles (NPs), doped in the PHBV fibers, resulted in well-dispersion due to the hydrogen bonding occurring between the polar groups of ZnO and PHBV. The crystallinity and crystallization rate were lowered by adding ZnONPs.

Based on the previous research, recently, Castro-Mayorga et al. (2017b) investigated the effect of zinc oxide size, morphology, and crystalline structure on their antimicrobial activity against the foodborne pathogens *Salmonella enterica* and *Listeria monocytogenes* of PHBV for active food packaging and food contact applications. They found that ZnO particles were significantly effective when their specific surface area increased, i.e., when the hexagonal-pyramid nanoparticles (PZnO) were used. In addition, they evidence that the antibacterial properties were preserved even when they were incorporated in coating PHBV structures. Moreover, ZnO nanoparticles positively influenced the thermal stability and optical properties of PHBV active films, avoiding their browning after the thermal processing, even if they worsened the polymer mechanical and oxygen barrier properties due to the high concentration required to obtain suitable bactericide effect against *L. monocytogenes*.

In order to improve PHBV gas barrier properties, which is useful for food and electronic packaging materials, and its sensitivity to oxygen, many efforts have been performed. The introduction of nanosized fillers inside polymeric matrix attracted a great interest since their fine and homogeneous distribution inside the polymer hinders gas permeability. In their paper, Öner et al. (2016) used boron nitride crystals in hexagonal nanoplate and nanoflake due to their structural similarities to graphene. BN nanoparticles included in the PHBV matrix during the extrusion process improved the gas barrier of the polymer. Anyway, in order to enhance the physical interaction occurring between PHBV and BNPs, thus assuring a stable dispersion of BNPs, the same authors used a silane coupling agent, octyltriethoxysilane (OTES), to modify the surface of boron nitride. In their research, Öner et al. (2019) included different amounts of BNPs with different crystalline silane surfaces in PHBV, via melt compounding, and investigated their effects on the barrier properties of PHBV nanocomposites. For all the nanocomposites, the oxygen permeability decreased in comparison to the neat PHBV due to the presence of both BN nanoparticles and silane coupling agent. In particular, the physical interaction occurring between PHBV and BN were strongly enhanced in the presence of OTES, furthermore improving the barrier properties.

Similarly, Öner and İlhan (2016) investigated the chemical-physical properties of bio-composites based on PHBV and hydroxyapatite (HAP), obtained by extrusion processing. HAP is one of the bioactive and biocompatible calcium phosphates fillers widely used for polymer nanocomposites. Since both synthetic

and natural HAPs have the same chemical composition and crystallographic properties of bone joint, it is widely used as osteoconductive filler for bone regeneration (Basile et al., 2015).

The bio-composites, produced by melt extrusion of PHBV with untreated HAP and silane surface-treated HAP crystals, were investigated by structural, morphological, and thermal analyses. At high loading of unmodified HAP nanoparticles, physical agglomeration occurred, and mechanical properties dropped down, as the lack of proper adhesion between the matrix and the HAP results in insufficient stress transfer. The silane coupling agent induced a better dispersion of HAP NPs inside PHBV, as evidenced by SEM analysis; as a consequence, a good stress transfer from the matrix to the dispersed phase could be observed. Thus, surface treatment by silanization proved to be necessary to avoid a decrease in the mechanical properties of the filled biopolymer matrix (Öner and İlhan, 2016).

Finally, Ambrosio-Martin et al. (2015a,b) prepared novel nanocomposites based on PHBV and functionalized graphene nanosheets (FGS) by means of mechano-physic ball milling method. Morphological characterization evidenced proper nanofiller dispersion into the matrix, whereas DSC analysis evidenced an increased crystallinity of the polymer. Thermal stability tests revealed that FGS affected the mechanism of oxidative thermal degradation while they did not influence the thermal degradation by pyrolysis. The authors highlighted the positive influence of the homogeneous dispersion of FGS nanofiller within the polymeric matrix, for both the mechanical reinforcing effect of FGS and also gas barrier enhancement (Ambrosio-Martin et al., 2015a,b).

## CHALLENGES AND PERSPECTIVES FOR EFFECTIVE PHA EXPLOITATION

The main challenge for exploitation of PHA polymers is related to their high production costs. The costs of the raw materials and recovery process are ~10 times higher than those of conventional polymers, with the carbon sources used to feed the fermentation process accounting for more than the 50% of the total (Wang et al., 2013a; Koller et al., 2017). An estimation of the biopolymer costs is ~\$6–15/kg, almost two orders of magnitude higher than those of PE and PP (\$0.23–0.48/kg) (Reddy et al., 2003).

An important aspect related to the cost competitiveness of PHA production is the final process productivity, which in turn depends on production yield as well as on the efficiency of downstream procedure. Genome-editing and synthetic biology approaches have emerged as powerful and innovative tools to address both these aspects (Zhang et al., 2020). Ribosome-binding site (RBS) optimization, promoter engineering, and, more importantly, CRISPR-cas9-based approaches have been effective in model organisms, such as *E. coli* and non-model ones, such as *Halomonas* spp. and *Pseudomonas* spp., to boost process competitiveness (Zhang et al., 2020). Cell sizes and growth behavior are crucial targets for increasing polymer accumulation. Engineering cell size/shape or cell walls is an effective way to boost PHA accumulation within the intracellular space. CRISPR/cas9 and CRISPI methods have

polymers (physical blending and/or melt reactive blending), copolymers, and bio-composites, leading to greatly improved mechanical profiles, wider processability windows, and improved post-processed thermal stability, without neglecting that PHB compounding requires lower amounts of the neat polymer with a consequent reduction in the final material costs. These advances will improve PHB capacity to match with the practical needs in several application fields, ranging from surgical sutures, tissue engineering (Misra et al., 2010), agricultural foils, and packaging materials for the storage of food products (Bucci et al., 2005).

In this way, PHB could both shed lights on its commercial applications and enhance its penetration in wider market sectors, with a consequent reduction of its high production cost.

Nevertheless, it is expected that the PHA production will almost quadruple by 2021 with regard to 2016, as a result of a ramp-up of capacities in Asia and the USA ([www.europanbioplastics.org/market](http://www.europanbioplastics.org/market)), and thus, it seems that the costs of PHAs will decrease. This upcoming perspective is the result of an important trend, driven by the changing of consumer demands to make plastic products more efficient, eco-friendly,

and cost effective and to reduce greenhouse gas emissions and dependency on fossil-derived plastics.

## AUTHOR CONTRIBUTIONS

RT: conceptualization, writing (review and editing), and special focus on plasticizers. GS: conceptualization, writing (review and editing), special focus on blending, and bio-composites. IC: investigation and visualization. CP: conceptualization, writing (review and editing), special focus on copolymer synthesis and *in vivo* approaches, and supervision. MD: funding acquisition. All authors contributed to the article and approved the submitted version.

## FUNDING

This work was supported by grants from PRIN: PROGETTI DI RICERCA DI RILEVANTE INTERESSE NAZIONALE—Bando 2017. CARDON valorisation by InteGrated biorefinery (CARDIGAN). IC acknowledges Università degli Studi di Napoli Federico II for doctoral fellowships.

## REFERENCES

- Aeschelmann, F., and Carus, M. (2017). *Bio-Based Building Blocks and Polymers. Global Capacities*. nova-Institut GmbH. Available online at: <http://www.bio-based.eu/reports/>
- Ahmed, T., Marçal, H., Lawless, M., Wanandy, N. S., Chiu, A., and Foster, L. J. R. (2010). Polyhydroxybutyrate and its copolymer with polyhydroxyvalerate as biomaterials: influence on progression of stem cell cycle. *Biomacromolecules* 11, 2707–2715. doi: 10.1021/bm1007579
- Albuquerque, M. G. E., Concass, S., Bengtsson, S., and Reis, M. A. M. (2010). Mixed culture polyhydroxyalkanoates production from sugar molasses: the use of a 2-stage CSTR system for culture selection. *Bioresour. Technol.* 101, 7112–7122. doi: 10.1016/j.biortech.2010.04.019
- Aldor, I. S., and Keasling, J. D. (2003). Process design for microbial plastic factories: Metabolic engineering of polyhydroxyalkanoates. *Curr. Opin. Biotechnol.* 14, 475–483. doi: 10.1016/j.copbio.2003.09.002
- Alexandre, M., and Dubois, P. (2000). Polymer-layered silicate nanocomposites: preparation, properties and uses of a new class of materials. *Mater. Sci. Eng. R Rep.* 28, 1–63. doi: 10.1016/S0927-796X(00)00012-7
- Ambrosio-Martin, J., Gorrasi, G., Lopez-Rubio, A., Fabra, M. J., Mas, L. C., López-Manchado, M. A., et al. (2015a). On the use of ball milling to develop PHBV-graphene nanocomposites (I)—morphology, thermal properties, and thermal stability. *J. Appl. Polym. Sci.* 132:42101. doi: 10.1002/app.42101
- Ambrosio-Martin, J., Gorrasi, G., Lopez-Rubio, A., Fabra, M. J., Mas, L. C., López-Manchado, M. A., et al. (2015b). On the use of ball milling to develop poly(3-hydroxybutyrate-co-3-hydroxyvalerate)-graphene nanocomposites (II)—mechanical, barrier, and electrical properties. *J. Appl. Polym. Sci.* 132:42217. doi: 10.1002/app.42217
- Angelini, S., Cerruti, P., Immirzi, B., Santagata, G., Scarinzi, G., and Malinconico, M. (2014). From biowaste to bioresource: effect of a lignocellulosic filler on the properties of poly(3-hydroxybutyrate). *Int. J. Biol. Macromol.* 71, 163–173. doi: 10.1016/j.ijbiomac.2014.07.038
- Anjum, A., Zuber, M., Zia, K. M., Noreen, A., Anjum, M. N., and Tabasum, S. (2016). Microbial production of polyhydroxyalkanoates (PHAs) and its copolymers: a review of recent advancements. *Int. J. Biol. Macromol.* 89, 161–174. doi: 10.1016/j.ijbiomac.2016.04.069
- Anna, A. D., and Arrigo, R. (2019). PLA/PHB blends: biocompatibilizer effects. *Polymers* 11:1416. doi: 10.3390/polym11091416
- Antunes, M. C. M., and Felisberti, M. I. (2005). Blends of poly(hydroxybutyrate) and poly( $\epsilon$ -caprolactone) obtained from melting mixture maria. *Polymeros Cienc. e Tecnol.* 15, 134–138. doi: 10.1590/S0104-14282005000200014
- Argiz, L., Fra-Vázquez, A., del Río, Á. V., and Mosquera-Corral, A. (2020). Optimization of an enriched mixed culture to increase PHA accumulation using industrial saline complex wastewater as a substrate. *Chemosphere* 247:125873. doi: 10.1016/j.chemosphere.2020.125873
- Arikawa, H., Sato, S., Fujiki, T., and Matsumoto, K. (2016). A study on the relation between poly(3-hydroxybutyrate) depolymerases or oligomer hydrolases and molecular weight of polyhydroxyalkanoates accumulating in *Cupriavidus necator* H16. *J. Biotechnol.* 227, 94–102. doi: 10.1016/j.jbiotec.2016.04.004
- Arrieta, M. P., López, J., Hernández, A., and Rayón, E. (2014). “The potential of D(+)-limonene to improve PLA-PHB blends properties,” in *Citrus: Molecular Phylogeny, Antioxidant Properties and Medicinal Uses* (New York, NY: Nova Science Publishers), 185–197.
- Arrieta, M. P., Samper, M. D., Aldas, M., and López, J. (2017). On the use of PLA-PHB blends for sustainable food packaging applications. *Materials* 10:1008. doi: 10.3390/ma10091008
- Auras, R., Harte, B., and Selke, S. (2004). An overview of poly(lactides) as packaging materials. *Macromol. Biosci.* 4, 835–864. doi: 10.1002/mabi.200400043
- Babos, G., Ryzd, J., Kawalec, M., Klim, M., Fodor-Kardos, A., Trif, L., et al. (2020). Poly(3-Hydroxybutyrate)-based nanoparticles for sorafenib and doxorubicin anticancer drug delivery. *Int. J. Mol. Sci.* 21:7312. doi: 10.3390/ijms21197312
- Ballistreri, A., Guiffrida, M., Guglielmino, S. P. P., Carnazza, S., Ferreri, A., and Impallomeni, G. (2001). Biosynthesis and structural characterization of medium-chain-length poly(3-hydroxyalkanoates) produced by *Pseudomonas aeruginosa* from fatty acids. *Int. J. Biol. Macromol.* 29, 107–114. doi: 10.1016/S0141-8130(01)00154-4
- Baltieri, R. C., Mei, L. H. L., and Bartoli, J. (2003). Study of the influence of plasticizers on the thermal and mechanical properties of poly(3-hydroxybutyrate) compounds. *Macromol. Symp.* 197, 33–44. doi: 10.1002/masy.200350704
- Barham, P. J., Keller, A., Otun, E. L., and Holmes, P. A. (1984). Crystallization and morphology of a bacterial thermoplastic poly-3-hydroxybutyrate. *J. Mater. Sci.* 19, 2781–2794. doi: 10.1007/BF01026954
- Basile, M. A., d’Ayala, G. G., Malinconico, M., Laurienzo, P., Coudane, J., Nottelet, B., et al. (2015). Functionalized PCL/HA nanocomposites as microporous membranes for bone regeneration. *Mater. Sci. Eng. C* 48, 457–468. doi: 10.1016/j.msec.2014.12.019

been used to manipulate genes related to cell division. The deletion of fission-related genes, together with overexpression of the genes involved in the division process in *E. coli*, allows to significantly increase PHB accumulation by inducing a multiple division pattern and, consequently, the formation of a cell with increased volume (Jiang et al., 2015; Elhadi et al., 2016; Wu et al., 2016a,b). Cell shape is also an important factor influencing further cell separation from the culture broth. A convenient downstream process has been designed in engineered *Halomonas campaniensis* LS21, by deleting an *eff* operon encoding two subunits of an electron transferring flavoprotein, causing self-flocculation and an easy and rapid recovery at the bottom of the bioreactor (Ling et al., 2019; Shen et al., 2019).

Biomass feedstocks and waste materials have emerged as promising substrates for cost-effective PHA production, and their different kinds have been explored, including lignocellulosic materials and agroindustrial and food wastes (El-malek et al., 2020; Sirohi et al., 2020). Progresses in this field have been achieved through the application of *in vivo* engineering approaches. Microbial cell factories able to convert different wastes into PHA have been designed, focusing on different approaches: (i) introducing the catabolic genes required for the metabolization of waste C-sources in native PHA producers; (ii) conferring PHA-producing abilities to non-native producers endowed with advantageous metabolic/physiological features, i.e., halophilic bacteria and/or microorganisms naturally able to metabolize complex C-sources; (iii) modulating PHA composition acting on precursor-supplying pathways (Favaro et al., 2019).

Although PHA at industrial scale is currently produced by pure culture systems (wild-type or engineered microorganisms), the use of MMC is emerging as a promising strategy to reduce the intensive costs related to aeration and media and equipment sterilization (Fradinho et al., 2019; Mannina et al., 2020). A further advantage of MMC-based processes is the possibility to integrate PHA production in waste treatment plants (Kourmentza et al., 2017). In one of the most promising examples, up to 75 wt% of PHA content has been reported by MMC from fermented molasses (Albuquerque et al., 2010). It has been estimated that, by optimizing the acidogenic fermentation to get a large amount of organic acids from organic fraction of municipal solid waste (OFMSW) to be further transformed into PHA, a total gross revenue of \$7.6–16.9 billion might be achieved (Colombo et al., 2017). The feasibility of the MMC-based processes on waste substrates has been demonstrated at pilot scale, and several European projects aim at demonstrating PHA production at pilot scale have been funded (Mannina et al., 2020). Future improvements for the exploitation of MMC-based processes should address the increase in cell densities and polymer productivities (Argiz et al., 2020) as well as the improvements in the extraction technologies due to their higher resistance to cell hydrolysis with respect to pure cultures (Samori et al., 2015; Mannina et al., 2020).

Most of the reported studies focus on the successful design and optimization of the processes for PHA production from

wastes on lab-scale; however, an estimation of process costs has been reported only in few cases. In an interesting example, PHB process economics using cheese whey as the low-cost substrate was simulated on scenarios with different plant capacity. The bioprocess was found efficient at 1,000 ton/h whey feed with an estimated cost of US\$10.2/kg (Peña-Jurado et al., 2019).

Although the use of waste materials certainly allows to reduce the costs of raw material supply, the PHA production process is still not economically competitive. Exploiting microbial cell factories to obtain multiple products from the same process would enhance process competitiveness. Several examples of coproduction of PHA with other value-added products (amino acids, proteins, alcohols, hydrogen, biosurfactants, exopolysaccharides, and lipids) have been described in the recent literature (Kumar and Kim, 2018; de Jesus Assis et al., 2019). From an economical and technical point of view, the most advantageous processes are those that couple an optimized accumulation of intracellular PHA together with the recovery of extracellular products (Kumar and Kim, 2018). A further breakthrough in the same direction is represented by the implementation of “waste bio-refineries,” wherein the PHA production is integrated in an ensemble of processes aimed at the complete valorization of raw materials. A techno-economic and environmental analysis of a sugar cane bagasse biorefinery for the production of fuel ethanol, PHB, and electricity was performed by Moncada et al. (2013). An optimization procedure was applied to select the most promising process pathways for each product and to define the criteria for the selection of technologies and raw material distribution. It was demonstrated that, if considered in the frame of a multiproduct biorefinery, where all the products contribute in incomes and also share costs, instead of a separate process, the PHA production becomes a feasible process.

A similar approach was applied to evaluate the economic viability of a biorefinery for the coproduction of succinic acid, PHB, and electricity from sugarcane bagasse and trash lignocelluloses (Nieder-Heitmann et al., 2019). Different scenarios were simulated, and the most favorable configuration (where PHB was produced from 25% of the fermentable glucose stream and succinic acid from the remaining glucose together plus the hemicellulose hydrolysate) resulted in an internal rate of return (IRR) of 24.1% with a net present value of US\$477.2 million.

Although the above-described strategies of PHB production from renewable, eco-sustainable, and cost-effective biosources are ever more biotechnologically advanced and promising approaches to drastically reduce the high production cost of PHB, its commercialization is still in its early stages, even if its global production capacity is one of the fastest growing among biopolymers (Aeschelmann and Carus, 2017). This is due to the restricted areas of PHB application unavoidably associated to the lost challenge in up-front competition with the petroleum-based plastics produced on a very large scale. A valid attempt to obtain a cost-competitive material is to strongly broaden its industrial production and diffusion in bioplastics industry. A lot of progress has been recently made through the formulation of PHB with tailored additives (plasticizers, nucleating agents, organic, and inorganic fillers),

- Bhatia, S. K., Gurav, R., Choi, T. R., Jung, H. R., Yang, S. Y., Moon, Y. M., et al. (2019a). Bioconversion of plant biomass hydrolysate into bioplastic (polyhydroxyalkanoates) using *Ralstonia eutropha* 5119. *Bioresour. Technol.* 271, 306–315. doi: 10.1016/j.biortech.2018.09.122
- Bhatia, S. K., Kim, J. H., Kim, M. S., Kim, J., Hong, J. W., Hong, Y. G., et al. (2018). Production of (3-hydroxybutyrate-co-3-hydroxyhexanoate) copolymer from coffee waste oil using engineered *Ralstonia eutropha*. *Bioprocess Biosyst. Eng.* 41, 229–235. doi: 10.1007/s00449-017-1861-4
- Bhatia, S. K., Wadhwa, P., Hong, J. W., Hong, Y. G., Jeon, J. M., Lee, E. S., et al. (2019b). Lipase mediated functionalization of poly(3-hydroxybutyrate-co-3-hydroxyvalerate) with ascorbic acid into an antioxidant active biomaterial. *Int. J. Biol. Macromol.* 123, 117–123. doi: 10.1016/j.ijbiomac.2018.11.052
- Bibe, L., Tupure, V., Dz, A., and Ka, M. (1999). Improvement of the deformative characteristics of poly-β-hydroxybutyrate by plasticization. *Mech. Comp. Mater.* 35, 357–364. doi: 10.1007/BF02259726
- Blümm, E., and Owen, A. J. (1995). Miscibility, crystallization and melting of poly(3-hydroxybutyrate)/ poly(l-lactide) blends. *Polymer* 36, 4077–4081. doi: 10.1016/0032-3861(95)90987-D
- Bordes, P., Hablot, E., Pollet, E., and Avérous, L. (2009a). Effect of clay organomodifiers on degradation of polyhydroxyalkanoates. *Polym. Degrad. Stab.* 94, 789–796. doi: 10.1016/j.polydegradstab.2009.01.027
- Bordes, P., Pollet, E., and Avérous, L. (2009b). Nano-biocomposites: biodegradable polyester/nanoclay systems. *Prog. Polym. Sci.* 34, 125–155. doi: 10.1016/j.progpolymsci.2008.10.002
- Bucci, D. Z., Tavares, L. B. B., and Sell, I. (2005). PHB packaging for the storage of food products. *Polym. Test.* 24, 564–571. doi: 10.1016/j.polymertesting.2005.02.008
- Bugnicourt, E., Cinelli, P., Lazzeri, A., and Alvarez, V. (2014). Polyhydroxyalkanoate (PHA): Review of synthesis, characteristics, processing and potential applications in packaging. *Express Polym. Lett.* 8, 791–808. doi: 10.3144/expresspolymlett.2014.82
- Cai, H., and Qiu, Z. (2009). Effect of comonomer content on the crystallization kinetics and morphology of biodegradable poly(3-hydroxybutyrate-co-3-hydroxyhexanoate). *Phys. Chem. Chem. Phys.* 11, 9569–9577. doi: 10.1039/b907677h
- Castro-Mayorga, J. L., Fabra, M. J., Cabedo, L., and Lagaron, J. M. (2017a). On the use of the electrospinning coating technique to produce antimicrobial polyhydroxyalkanoate materials containing in situ-stabilized silver nanoparticles. *Nanomaterials* 7:4. doi: 10.3390/nano7010004
- Castro-Mayorga, J. L., Fabra, M. J., Pourrahimi, A. M., Olsson, R. T., and Lagaron, J. M. (2017b). The impact of zinc oxide particle morphology as an antimicrobial and when incorporated in poly(3-hydroxybutyrate-co-3-hydroxyvalerate) films for food packaging and food contact surfaces applications. *Food Bioprod. Process* 101, 32–44. doi: 10.1016/j.fbp.2016.10.007
- Cha, D., Ha, H. S., and Lee, S. K. (2020). Metabolic engineering of *Pseudomonas putida* for the production of various types of short-chain-length polyhydroxyalkanoates from levulinic acid. *Bioresour. Technol.* 309:123332. doi: 10.1016/j.biortech.2020.123332
- Chabrat, E., Abdillahi, H., Rouilly, A., and Rigal, I. (2012). Influence of citric acid and water on thermoplastic wheat flour/poly(lactic acid) blends. I: thermal, mechanical and morphological properties. *Ind. Crops Prod.* 37, 238–246. doi: 10.1016/j.indcrop.2011.11.034
- Chang, H. M., Wang, Z. H., Luo, H. N., Xu, M., Ren, X. Y., Zheng, G. X., et al. (2014). Poly(3-hydroxybutyrate-co-3-hydroxyhexanoate)-based scaffolds for tissue engineering. *Braz. J. Med. Biol. Res.* 47, 533–539. doi: 10.1590/1414-431X20143930
- Chanprateep, S., Bunsri, K., Muangwong, A., and Utiswannakul, P. (2010). Biosynthesis and biocompatibility of biodegradable poly(3-hydroxybutyrate-co-4-hydroxybutyrate). *Polym. Degrad. Stab.* 95, 2003–2012. doi: 10.1016/j.polydegradstab.2010.07.014
- Chaos, A., Sangroniz, A., Gonzalez, A., Iriarte, M., Sarasua, J. R., del Rio, J., et al. (2019). Tributyl citrate as an effective plasticizer for biodegradable polymers: effect of plasticizer on free volume and transport and mechanical properties. *Polym. Int.* 68, 125–133. doi: 10.1002/pi.5705
- Chea, V., Angellier-Coussy, H., Peyron, S., Kemmer, D., and Gontard, N. (2016). Poly(3-hydroxybutyrate-co-3-hydroxyvalerate) films for food packaging: physical-chemical and structural stability under food contact conditions. *J. Appl. Polym. Sci.* 133:41850. doi: 10.1002/app.41850
- Chen, Q., Wang, Q., Wei, G., Liang, Q., and Qi, Q. (2011). Production in *Escherichia coli* of poly(3-hydroxybutyrate-co-3-hydroxyvalerate) with differing monomer compositions from unrelated carbon sources. *Appl. Environ. Microbiol.* 77, 4886–4893. doi: 10.1128/AEM.00091-11
- Chen, Y., Chen, X. Y., Du, H. T., Zhang, X., Ma, Y. M., Chen, J. C., et al. (2019). Chromosome engineering of the TCA cycle in *Halomonas bluephagenesis* for production of copolymers of 3-hydroxybutyrate and 3-hydroxyvalerate (PHBV). *Metab. Eng.* 54, 69–82. doi: 10.1016/j.ymben.2019.03.006
- Ching, Y. C., Ershad Ali, M., Abdullah, L. C., Choo, K. W., Kuan, Y. C., Julaihi, S. J., et al. (2016). Rheological properties of cellulose nanocrystal-embedded polymer composites: a review. *Cellulose* 23, 1011–1030. doi: 10.1007/s10570-016-0868-3
- Choi, J. S., and Park, W. H. (2004). Effect of biodegradable plasticizers on thermal and mechanical properties of poly(3-hydroxybutyrate). *Polym. Test.* 23, 455–460. doi: 10.1016/j.polymertesting.2003.09.005
- Choi, M. U. N. H., Yoon, S. C., and Lenz, R. W. (1999). Production of poly(3-hydroxybutyric acid-co-4-hydroxybutyric acid) and poly(4-hydroxybutyric acid) without subsequent degradation by *Hydrogenophaga pseudoflava*. *Appl. Environ. Microbiol.* 65, 1570–1577. doi: 10.1128/AEM.65.4.1570-1577.1999
- Choi, S. Y., Rhee, M. N., Kim, H. T., Joo, J. C., Cho, I. J., Son, I., et al. (2020). Metabolic engineering for the synthesis of polyesters: a 100-year journey from polyhydroxyalkanoates to non-natural microbial polyesters. *Metab. Eng.* 58, 47–81. doi: 10.1016/j.ymben.2019.05.009
- Colombo, B., Favini, F., Scaglia, B., Sciarria, T. P., D'Imporzano, G., Pognani, M., et al. (2017). Enhanced polyhydroxyalkanoate (PHA) production from the organic fraction of municipal solid waste by using mixed microbial culture. *Biotechnol. Biofuels* 10:201. doi: 10.1186/s13068-017-0888-8
- Corrado, L., Abdalrazeq, M., Pezzella, C., Di Girolamo, R., Porta, R., Sanna, G., et al. (2021). Design and characterization of poly(3-hydroxybutyrate-co-hydroxyhexanoate) nanoparticles and their grafting in whey protein-based nanocomposites. *Food Hydrocoll.* 110:160167. doi: 10.1016/j.foodhyd.2020.106167
- Crétois, R., Chenal, J.-M., Sheibat-Othman, N., Monnier, A., Martin, C., Astruz, O., et al. (2016). Physical explanations about the improvement of polyhydroxybutyrate ductility: hidden effect of plasticizer on physical ageing. *Polymer* 102, 176–182. doi: 10.1016/j.polymer.2016.09.017
- Dai, Y., Lambert, L., Yuan, Z., and Keller, J. (2008). Microstructure of copolymers of polyhydroxyalkanoates produced by glycogen accumulating organisms with acetate as the sole carbon source. *Process Biochem.* 43, 968–977. doi: 10.1016/j.procbio.2008.04.023
- de Jesus Assis, D., Santos, J., de Jesus, C. S., de Souza, C. O., Costa, S. S., Miranda, A. L., et al. (2019). Valorization of crude glycerol based on biological processes for accumulation of lipophilic compounds. *Int. J. Biol. Macromol.* 129, 728–736. doi: 10.1016/j.ijbiomac.2019.02.077
- de Paula, F. C., de Paula, C. R. C., Gomez, J. G. C., Steinbüchel, A., and Contiero, J. (2017). Poly(3-hydroxybutyrate-co-3-hydroxyvalerate) production from biodiesel by-product and propionic acid by mutant strains of *Pandoraea sp.* *Biotechnol. Prog.* 33, 1077–1084. doi: 10.1002/btpr.2481
- de Sousa Dias, M. M., Koller, M., Puppi, D., Morelli, A., Chiellini, F., and Braunegg, G. (2017). Fed-batch synthesis of poly(3-hydroxybutyrate) and poly(3-hydroxybutyrate-co-4-hydroxybutyrate) from sucrose and 4-hydroxybutyrate precursors by *Burkholderia sacchari* strain DSM 17165. *Bioengineering* 4:36. doi: 10.3390/bioengineering4020036
- Degli Esposti, M., Chiellini, F., Bondioli, F., Morselli, D., and Fabbri, P. (2019). Highly porous PHB-based bioactive scaffolds for bone tissue engineering by *in situ* synthesis of hydroxyapatite. *Mater. Sci. Eng. C* 100, 286–296. doi: 10.1016/j.msec.2019.03.014
- Dehouche, N., Idres, C., Kaci, M., Zembouai, I., and Bruzaud, S. (2020). Effects of various surface treatments on Aloc Vera fibers used as reinforcement in poly(3-hydroxybutyrate-co-3-hydroxyhexanoate) (PHB/HHx) biocomposites. *Polym. Degrad. Stab.* 175:109131. doi: 10.1016/j.polydegradstab.2020.109131
- Delmas, G.-H., Benjelloun-Mlayah, B., Le Bigot, Y., and Delmas, M. (2011). Functionality of wheat straw lignin extracted in organic acid media. *J. Appl. Polym. Sci.* 121, 491–501. doi: 10.1002/app.33592
- Di Lorenzo, M. L., and Righetti, M. C. (2013). Effect of thermal history on the evolution of crystal and amorphous fractions of poly(l(R)-3-hydroxybutyrate) upon storage at ambient temperature. *Eur. Polym. J.* 49, 510–517. doi: 10.1016/j.eurpolymj.2012.11.004

- Doi, Y., Mukai, K., Kasuya, K., and Yamada, K. (1994). Biodegradation of biosynthetic and chemosynthetic polyhydroxyalkanoates. *Stud. Polym. Sci.* 12, 39–51. doi: 10.1016/B978-0-444-81708-2.50010-5
- dos Santos, A. J., Oliveira Dalla Valentina, L. V., Hidalgo Schulz, A. A., and Tomaz Duarte, M. A. (2017). From Obtaining to Degradation of PHB: Material Properties. Part I. *Ing. y Cienc.* 13, 269–298. doi: 10.17230/ingciencia.13.26.10
- dos Santos, A. J., Oliveira Dalla Valentina, L. V., Hidalgo Schulz, A. A., and Tomaz Duarte, M. A. (2018). From obtaining to degradation of PHB: a literature review. Part II. *Ing. y Cienc.* 14, 207–228. doi: 10.17230/ingciencia.14.27.9
- Elhadi, D., Lv, L., Jiang, X. R., Wu, H., and Chen, G. Q. (2016). CRISPR engineering *E. coli* for morphology diversification. *Metab. Eng.* 38, 358–369. doi: 10.1016/j.ymben.2016.09.001
- El-malek, F. A., Khairy, H., Farag, A., and Omar, S. (2020). The sustainability of microbial bioplastics, production and applications. *Int. J. Biol. Macromol.* 157, 319–328. doi: 10.1016/j.ijbiomac.2020.04.076
- Erceg, M., Kovačić, T., and Klarić, I. (2005). Thermal degradation of poly(3-hydroxybutyrate) plasticized with acetyl tributyl citrate. *Polym. Degrad. Stab.* 90, 313–318. doi: 10.1016/j.polydegradstab.2005.04.048
- Esposito, A., Delpouve, N., Causin, V., Dhotel, A., Delbreilh, L., and Dargent, E. (2016). From a three-phase model to a continuous description of molecular mobility in semicrystalline poly(hydroxybutyrate-co-hydroxyvalerate). *Macromolecules* 49, 4850–4861. doi: 10.1021/acs.macromol.6b00384
- Favaro, L., Basaglia, M., and Casella, S. (2019). Improving polyhydroxyalkanoate production from inexpensive carbon sources by genetic approaches: a review. *Biofuels Bioprod. Biorefining* 13, 208–227. doi: 10.1002/bbb.1944
- Fenollar, O., García-Sanoguera, D., Sanchez-Nacher, L., Boronat, T., López, J., and Balart, R. (2013). Mechanical and thermal properties of polyvinyl chloride plasticized with natural fatty acid esters. *Polym. Plast. Technol. Eng.* 52, 761–767. doi: 10.1080/03602559.2013.763352
- Figuerola-Lopez, K. J., Cabedo, L., Lagaron, J. M., and Torres-Giner, S. (2020). Development of electrospun poly(3-hydroxybutyrate-co-3-hydroxyvalerate) monolayers containing eugenol and their application in multilayer antimicrobial food packaging. *Front. Nutr.* 7:140. doi: 10.3389/fnut.2020.00140
- Follonier, S., Goyder, M. S., Silvestri, A. C., Crelier, S., Kalman, F., Riesen, R., et al. (2014). Fruit pomace and waste frying oil as sustainable resources for the bioproduction of medium-chain-length polyhydroxyalkanoates. *Int. J. Biol. Macromol.* 71, 42–52. doi: 10.1016/j.ijbiomac.2014.05.061
- Fradinho, J. C., Oehmen, A., and Reis, M. A. M. (2019). Improving polyhydroxyalkanoates production in phototrophic mixed cultures by optimizing accumulator reactor operating conditions. *Int. J. Biol. Macromol.* 126, 1085–1092. doi: 10.1016/j.ijbiomac.2018.12.270
- Gahlawat, G., and Soni, S. K. (2017). Valorization of waste glycerol for the production of poly(3-hydroxybutyrate) and poly(3-hydroxybutyrate-co-3-hydroxyvalerate) copolymer by *Cupriavidus necator* and extraction in a sustainable manner. *Bioresour. Technol.* 243, 492–501. doi: 10.1016/j.biortech.2017.06.139
- Gamal, R. F., Abdelhady, H. M., Khodair, T. A., El-Tayeb, T. S., Hassan, E. A., and Aboutaleb, K. A. (2013). Semi-scale production of PHAs from waste frying oil by *Pseudomonas fluorescens* S48. *Brazilian J. Microbiol.* 44, 539–549. doi: 10.1590/S1517-83822013000200034
- Gao, Y., Kong, L., Zhang, L., Gong, Y., Chen, G., Zhao, N., et al. (2006). Improvement of mechanical properties of poly(d,l-lactide) films by blending of poly(3-hydroxybutyrate-co-3-hydroxyhexanoate). *Eur. Polym. J.* 42, 764–775. doi: 10.1016/j.eurpolymj.2005.09.028
- García, I. L., López, J. A., Dorado, M. P., Kopschelis, N., Alexandri, M., Papanikolaou, S., et al. (2013). Evaluation of by-products from the biodiesel industry as fermentation feedstock for poly(3-hydroxybutyrate-co-3-hydroxyvalerate) production by *Cupriavidus necator*. *Bioresour. Technol.* 130, 16–22. doi: 10.1016/j.biortech.2012.11.088
- García-García, D., Ferri, J. M., Montanes, N., Lopez-Martinez, J., and Balart, R. (2016). Plasticization effects of epoxidized vegetable oils on mechanical properties of poly(3-hydroxybutyrate). *Polym. Int.* 65, 1157–1164. doi: 10.1002/pi.5164
- Godbole, S., Gote, S., Latkar, M., and Chakrabarti, T. (2003). Preparation and characterization of biodegradable poly-3-hydroxybutyrate-starch blend films. *Bioresour. Technol.* 86, 33–37. doi: 10.1016/S0960-8524(02)00110-4
- González-Ausejo, J., Sánchez-Safont, E., Lagarón, J. M., Balart, R., Cabedo, L., and Gámez-Pérez, J. (2017). Compatibilization of poly(3-hydroxybutyrate-co-3-hydroxyvalerate)-poly(lactic acid) blends with diisocyanates. *J. Appl. Polym. Sci.* 134, 1–11. doi: 10.1002/app.44806
- Gopi, S., Kontopoulou, M., Ramsay, B. A., and Ramsay, J. A. (2018). Manipulating the structure of medium-chain-length polyhydroxyalkanoate (MCL-PHA) to enhance thermal properties and crystallization kinetics. *Int. J. Biol. Macromol.* 119, 1248–1255. doi: 10.1016/j.ijbiomac.2018.08.016
- Gouveia, A. R., Freitas, E. B., Galinha, C. F., Carvalho, G., Duque, A. F., and Reis, M. A. M. (2017). Dynamic change of pH in acidogenic fermentation of cheese whey towards polyhydroxyalkanoates production: impact on performance and microbial population. *N. Biotechnol.* 37, 108–116. doi: 10.1016/j.nbt.2016.07.001
- Gras, N., Murray, E. J., and Holme, P. A. (1984). The thermal degradation of poly(-d)-β-hydroxybutyric acid: Part 1—identification and quantitative analysis of products. *Polym. Degrad. Stud.* 6, 47–61. doi: 10.1016/0141-3910(84)90016-8
- Haba, E., Vidal-Mas, J., Bassas, M., Espuny, M. J., Llorens, J., and Manresa, A. (2007). Poly 3-(hydroxyalkanoates) produced from oily substrates by *Pseudomonas aeruginosa* 4772 (NCBIM 40044): effect of nutrients and incubation temperature on polymer composition. *Biochem. Eng. J.* 35, 99–106. doi: 10.1016/j.bej.2006.11.021
- Han, J., Qiu, Y. Z., Liu, D. C., and Chen, G. Q. (2004). Engineered *Aeromonas hydrophila* for enhanced production of poly(3-hydroxybutyrate-co-3-hydroxyhexanoate) with alterable monomers composition. *FEMS Microbiol. Lett.* 239, 195–201. doi: 10.1016/j.femsle.2004.08.044
- Hao, J., Wang, X., and Wang, H. (2017). Overall process of using a valerate-dominant sludge hydrolysate to produce high-quality polyhydroxyalkanoates (PHA) in a mixed culture. *Sci. Rep.* 7:6939. doi: 10.1038/s41598-017-0154-3
- Harding, K. G., Dennis, J. S., von Blottnitz, H., and Harrison, S. T. L. (2007). Environmental analysis of plastic production processes: comparing petroleum-based polypropylene and polyethylene with biologically-based poly-β-hydroxybutyric acid using life cycle analysis. *J. Biotechnol.* 130, 57–66. doi: 10.1016/j.jbiotec.2007.02.012
- Harmon, J. P., and Otter, R. (2018). Green chemistry and the search for new plasticizers. *ACS Sustain. Chem. Eng.* 6, 2078–2085. doi: 10.1021/acsuschemeng.7b03508
- Heathman, T. R. J., Webb, W. R., Han, J., Dan, Z., Chen, G. Q., Forsyth, N. R., et al. (2014). Controlled production of poly(3-hydroxybutyrate-co-3-hydroxyhexanoate) (PHBHHx) nanoparticles for targeted and sustained drug delivery. *J. Pharm. Sci.* 103, 2498–2508. doi: 10.1002/jps.24035
- Hilliou, L., Teixeira, P. F., Machado, D., Covas, J. A., Oliveira, C. S. S., Duque, A. F., et al. (2016). Effects of fermentation residues on the melt processability and thermomechanical degradation of PHBV produced from cheese whey using mixed microbial cultures. *Polym. Degrad. Stab.* 128, 269–277. doi: 10.1016/j.polydegradstab.2016.03.031
- Huang, L., Chen, Z., Xiong, D., Wen, Q., and Ji, Y. (2018). Oriented acidification of wasted activated sludge (WAS) focused on odd-carbon volatile fatty acid (VFA): regulation strategy and microbial community dynamics. *Water Res.* 142, 256–266. doi: 10.1016/j.watres.2018.05.062
- Hufenus, R., Reifler, F. A., Fernández-Ronco, M. P., and Heuberger, M. (2015). Molecular orientation in melt-spun poly(3-hydroxybutyrate) fibers: effect of additives, drawing and stress-annealing. *Eur. Polym. J.* 71, 12–26. doi: 10.1016/j.eurpolymj.2015.07.039
- Impallomeni, G., Ballistreri, A., Carnemolla, G. M., Rizzo, M. G., Nicolò, M. S., and Guglielmino, S. P. P. (2018). Biosynthesis and structural characterization of polyhydroxyalkanoates produced by *Pseudomonas aeruginosa* ATCC 27853 from long odd-chain fatty acids. *Int. J. Biol. Macromol.* 108, 608–614. doi: 10.1016/j.ijbiomac.2017.12.037
- Insomphun, C., Kobayashi, S., Fujiki, T., and Numata, K. (2016). Biosynthesis of polyhydroxyalkanoates containing hydroxyl group from glycolate in *Escherichia coli*. *AMB Expr.* 6:29. doi: 10.1186/s13568-016-0200-5
- Ishida, K., Asakawa, N., and Inoue, Y. (2005). Structure, properties and biodegradation of some bacterial copoly(hydroxyalkanoate)s. *Macromol. Symp.* 224, 47–58. doi: 10.1002/masy.200550605
- Iwata, T. (2005). Strong fibers and films of microbial polyesters. *Macromol. Biosci.* 5, 689–701. doi: 10.1002/mabi.200500606
- Jamshidian, M., Tehrani, E. A., Imran, M., Jacquot, M., and Desobry, S. (2010). Poly-lactic acid: production, applications, nanocomposites,

- Pramanik, N., Das, R., Rath, T., and Kundu, P. P. (2014). Microbial degradation of linsseed oil-based elastomer and subsequent accumulation of poly(3-hydroxybutyrate-co-3-hydroxyvalerate) copolymer. *Appl. Biochem. Biotechnol.* 174, 1613–1630. doi: 10.1007/s12010-014-1061-5
- Przybysz, M., Marč, E., Klein, M., Saeh, M. R., and Formela, K. (2018). Structural, mechanical and thermal behavior assessments of PCL/PHB blends reactively compatibilized with organic peroxides. *Polym. Test.* 67, 513–521. doi: 10.1016/j.polymertesting.2018.03.014
- Pyshpadass, H. A., Marx, D. B., and Hanna, M. A. (2008). Effects of extrusion temperature and plasticizers on the physical and functional properties of starch films. *Starch* 60, 527–538. doi: 10.1002/star.200800713
- Qiu, Y. Z., Han, J., Guo, J. J., and Chen, G. Q. (2005). Production of poly(3-hydroxybutyrate-co-3-hydroxyhexanoate) from gluconate and glucose by recombinant *Aeromonas hydrophila* and *Pseudomonas putida*. *Biotechnol. Lett.* 27, 1381–1386. doi: 10.1007/s10529-005-3685-6
- Qu, X. H., Wu, Q., Liang, J., Zou, B., and Chen, G. Q. (2006a). Effect of 3-hydroxyhexanoate content in poly(3-hydroxybutyrate-co-3-hydroxyhexanoate) on *in vitro* growth and differentiation of smooth muscle cells. *Biomaterials* 27, 2944–2950. doi: 10.1016/j.biomaterials.2006.01.013
- Qu, X. H., Wu, Q., Zhang, K. Y., and Chen, G. Q. (2006b). *In vivo* studies of poly(3-hydroxybutyrate-co-3-hydroxyhexanoate) based polymers: biodegradation and tissue reactions. *Biomaterials* 27, 3540–3548. doi: 10.1016/j.biomaterials.2006.02.015
- Råpe, M., Darie-Nit, E., R. N., Grosu, E., Tenase, E. E., Trifoi, A. R., Pap, T., et al. (2015). Effect of plasticizers on melt processability and properties of PHB. *J. Optoelectron. Adv. Mater.* 17, 1778–1784.
- Rajan, K. P., Thomas, S. P., Gopanna, A., and Chavali, M. (2017). "Polyhydroxybutyrate (PHB): a standout biopolymer for environmental sustainability," in *Handbook of Ecomaterials*, eds L. M. T. Martinez, O. V. Kharissova, and B. I. Kharisov (Cham: Springer International Publishing), 1–23. doi: 10.1007/978-3-319-48281-1\_92-1
- Rao, U., Sridhar, R., and Sehgal, P. K. (2010). Biosynthesis and biocompatibility of poly(3-hydroxybutyrate-co-3-hydroxybutyrate) produced by *Cupriavidus necator* from spent palm oil. *Biochem. Eng. J.* 49, 13–20. doi: 10.1016/j.bej.2009.11.005
- Raquez, J. M., Narayan, R., and Dubois, P. (2008). Recent advances in reactive extrusion processing of biodegradable polymer-based compositions. *Macromol. Mater. Eng.* 293, 447–470. doi: 10.1002/mame.200700395
- Raza, Z. A., Abid, S., and Banat, I. M. (2018). Polyhydroxyalkanoates: characteristics, production, recent developments and applications. *Int. Biodeterior. Biodegrad.* 126, 45–56. doi: 10.1016/j.ibiod.2017.10.001
- Reddy, C. S. K., Ghai, R., and Kalia, V. C. (2003). Polyhydroxyalkanoates: an overview. *Bioresour. Technol.* 87, 137–146. doi: 10.1016/S0960-8524(02)00212-2
- Rivera-Briso, A. L., and Serrano-Aroca, Á. (2018). Poly(3-hydroxybutyrate-co-3-hydroxyvalerate): enhancement strategies for advanced applications. *Polymers* 10:732. doi: 10.3390/polym10070732
- Romanelli, M. G., Povoio, S., Favaro, L., Fontana, F., Basaglia, M., and Casella, S. (2014). Engineering *Delphia acidovorans* DSM39 to produce polyhydroxyalkanoates from slaughterhouse waste. *Int. J. Biol. Macromol.* 71, 21–27. doi: 10.1016/j.ijbiomac.2014.03.049
- Samori, C., Basaglia, M., Casella, S., Favaro, L., Galletti, P., Giorgini, L., et al. (2015). Dimethyl carbonate and switchable anionic surfactants: two effective tools for the extraction of polyhydroxyalkanoates from microbial biomass. *Green Chem.* 17, 1047–1056. doi: 10.1039/C4CG01821D
- Sanchez-Garcia, M. D., Gimenez, E., and Lagaron, J. M. (2008). Morphology and barrier properties of solvent cast composites of thermoplastic biopolymers and purified cellulose fibers. *Carbohydr. Polym.* 71, 235–244. doi: 10.1016/j.carbpol.2007.05.041
- Sangkhakar, K., Paichid, N., Yunu, T., and Prasertsan, P. (2020). Novel polyhydroxyalkanoate-based biocomposites obtained by solution casting and their application for bacteria removal and domestic wastewater purification. *J. Polym. Environ.* 28, 1893–1900. doi: 10.1007/s10924-020-01738-3
- Schmack, G., Gorenflo, V., and Steinbüchel, A. (1998). Biotechnological production and characterization of polyesters containing 4-hydroxyvaleric acid and medium-chain-length hydroxyalkanoic acids. *Macromolecules* 31, 644–649. doi: 10.1021/ma970864d
- Shen, R., Cai, L. W., Meng, D. C., Wu, L. P., Guo, K., Dong, G. X., et al. (2014). Benzene containing polyhydroxyalkanoates homo- and copolymers synthesized by genome edited *Pseudomonas entomophila*. *Sci. China Life Sci.* 57, 4–10. doi: 10.1007/s11427-013-4596-8
- Shen, R., Ning, Z. Y., Lan, Y. X., Chen, J. C., and Chen, G. Q. (2019). Manipulation of polyhydroxyalkanoate granular sizes in *Halomonas bluephagenesis*. *Metab. Eng.* 54, 117–126. doi: 10.1016/j.ymben.2019.03.011
- Sheu, D. S., Chen, Y. L., Jhuang, W. J., Chen, H. Y., and Jane, W. N. (2018). Cultivation temperature modulated the monomer composition and polymer properties of polyhydroxyalkanoate synthesized by *Cupriavidus* sp. 1.71 from levulinic acid as sole carbon source. *Int. J. Biol. Macromol.* 118, 1558–1564. doi: 10.1016/j.ijbiomac.2018.06.193
- Shi, X., Zhang, G., Phuon, T. V., and Lazerri, A. (2015). Synergistic effects of nucleating agents and plasticizers on the crystallization behavior of Poly(lactic acid). *Molecules* 20, 1579–1593. doi: 10.3390/molecules20011579
- Sharkman, B. P., and Razinkaya, I. N. (1983). Plasticization mechanism and structure of polymers. *Acta Polym.* 34, 514–520. doi: 10.1002/actp.1983.010340812
- Sirohi, R., Prakash Pandey, J., Kumar Gaur, V., Gnansounou, E., and Sindhu, R. (2020). Critical overview of biomass feedstocks as sustainable substrates for the production of polyhydroxybutyrate (PHB). *Bioresour. Technol.* 311:123536. doi: 10.1016/j.biortech.2020.123536
- Suárez Palacios, O. Y., Narváez Rincón, P. C., Corriou, J. P., Camargo Pardo, M., and Fonteix, C. (2014). Low-molecular-weight glycerol esters as plasticizers for poly(vinyl chloride). *J. Vinyl Addit. Technol.* 20, 65–71. doi: 10.1002/vnl.21351
- Sudesh, K., Abe, H., and Doi, Y. (2000). Synthesis, structure and properties of polyhydroxyalkanoates: Biological polyesters. *Prog. Polym. Sci.* 25, 1503–1555. doi: 10.1016/S0079-6700(00)00035-6
- Syafiq, I. M., Huong, K. H., Shantini, K., Vigneswari, S., Aziz, N. A., Amirul, A. A., et al. (2017). Synthesis of high 4-hydroxybutyrate copolymer by *Cupriavidus* sp. transformants using one-stage cultivation and mixed precursor substrates strategy. *Enzyme Microb. Technol.* 98, 1–8. doi: 10.1016/j.enzmictec.2016.11.011
- Taguchi, K., Aoyagi, Y., Matsusaki, H., Fukui, T., and Doi, Y. (1999). Co-expression of 3-ketoacyl-ACP reductase and polyhydroxyalkanoate synthase genes induces PHA production in *Escherichia coli* HB101 strain. *FEMS Microbiol. Lett.* 176, 183–190. doi: 10.1111/j.1574-6968.1999.tb13660.x
- Taguchi, S., Yamada, M., Matsumoto, K., Tajima, K., Satoh, Y., Munekata, M., et al. (2008). A microbial factory for lactate-based polyesters using a lactate-polymerizing enzyme. *Proc. Natl. Acad. Sci. U.S.A.* 105, 17323–17327. doi: 10.1073/pnas.0805653105
- Takisawa, K., Ooi, T., Matsumoto, K., Kadoya, R., and Taguchi, S. (2017). Xylose-based hydrolysate from eucalyptus extract as feedstock for poly(lactate-co-3-hydroxybutyrate) production in engineered *Escherichia coli*. *Process Biochem.* 54, 102–105. doi: 10.1016/j.procbio.2016.12.019
- Tamang, P., Banerjee, R., Köster, S., and Nogueira, R. (2019). Comparative study of polyhydroxyalkanoates production from acidified and anaerobically treated brewery wastewater using enriched mixed microbial culture. *J. Environ. Sci.* 78, 137–146. doi: 10.1016/j.jes.2018.09.001
- Tan, B. K., Ching, Y. C., Poh, S. C., Abdullah, I. C., and Gan, S. N. (2015). A review of natural fiber reinforced poly(vinyl alcohol) based composites: application and opportunity. *Polymers* 7, 2205–2222. doi: 10.3390/polym7111509
- Tan, D., Wu, Q., Chen, J. C., and Chen, G. Q. (2014a). Engineering *Halomonas* TD01 for the low-cost production of polyhydroxyalkanoates. *Metab. Eng.* 26, 34–47. doi: 10.1016/j.ymben.2014.09.001
- Tan, G. Y. A., Chen, C. L., Li, L., Ge, L., Wang, L., Razaad, I. M. N., et al. (2014b). Start a research on biopolymer polyhydroxyalkanoate (PHA): a review. *Polymers* 6, 706–754. doi: 10.3390/polym6030706
- Tanase, E. E., Popa, M. E., Răpă, M., and Popa, O. (2015). PHB/cellulose fibers based materials: physical, mechanical and barrier properties. *Agric. Agric. Sci. Procedia* 6, 608–615. doi: 10.1016/j.aaspro.2015.08.099
- Tebaldi, M. L., Maia, A. L. C., Poletto, F., de Andrade, F. V., and Soares, D. C. F. (2019). Poly(3-hydroxybutyrate-co-3-hydroxyvalerate) (PHBV): current advances in synthesis methodologies, antitumor applications and biocompatibility. *J. Drug Deliv. Sci. Technol.* 51, 115–126. doi: 10.1016/j.jddst.2019.02.007

- Martla, M., Umsakul, K., and Sudesh, K. (2018). Production and recovery of poly(3-hydroxybutyrate-co-3-hydroxyvalerate) from biodiesel liquid waste (BLW). *J. Basic Microbiol.* 58, 977–986. doi: 10.1002/jobm.201800279
- Masood, F. (2017). *Polyhydroxyalkanoates in the Food Packaging Industry*. Elsevier Inc. doi: 10.1016/B978-0-12-811942-6.00008-X
- Masood, F., Hasan, F., Ahmed, S., and Hameed, A. (2012). Biosynthesis and characterization of poly(3-hydroxybutyrate-co-3-hydroxyvalerate) from *Bacillus cereus* FA11 isolated from TNT-contaminated soil. *Ann. Microbiol.* 62, 1377–1384. doi: 10.1007/s13213-011-0386-3
- Meereboer, K. W., Misra, M., and Mohanty, A. K. (2020). Review of recent advances in the biodegradability of polyhydroxyalkanoate (PHA) bioplastics and their composites. *Green Chem.* 22, 5519–5558. doi: 10.1039/D0GC01647K
- Mekonnen, T., Mussone, P., Khalil, H., and Bressler, D. (2013). Progress in bio-based plastics and plasticizing modifications. *J. Mater. Chem. A* 1, 13379–13398. doi: 10.1039/c3ta12555f
- Meng, D. C., Shi, Z. Y., Wu, L. P., Zhou, Q., Wu, Q., Chen, J. C., et al. (2010). Production and characterization of poly(3-hydroxypropionate-co-4-hydroxybutyrate) with fully controllable structures by recombinant *Escherichia coli* containing an engineered pathway. *Metab. Eng.* 14, 317–324. doi: 10.1016/j.ymben.2010.04.003
- Michel, A. T., and Billington, S. L. (2012). Characterization of polyhydroxybutyrate films and hemp fiber reinforced composites exposed to accelerated weathering. *Polym. Degrad. Stab.* 97, 870–878. doi: 10.1016/j.polydegradstab.2012.03.040
- Misra, S. K., Ohashi, F., Valappil, S. P., Knowles, J. C., Roy, L., Silva, S. R. P., et al. (2010). Characterization of carbon nanotube (MWCNT) containing P(3HB)/bioactive glass composites for tissue engineering applications. *Acta Biomater.* 6, 735–742. doi: 10.1016/j.actbio.2009.09.023
- Modi, S., Koelling, K., and Vodovotz, Y. (2013). Assessing the mechanical, phase inversion, and rheological properties of poly-[(R)-3-hydroxybutyrate-co-(R)-3-hydroxyvalerate] (PHBV) blended with poly-(L-lactic acid) (PLA). *Eur. Polym. J.* 49, 3681–3690. doi: 10.1016/j.eurpolymj.2013.07.036
- Moita Fidalgo, R., Ortigueira, J., Freches, A., Pelica, J., Gonçalves, M., Mendes, B., et al. (2014). Bio-oil upgrading strategies to improve PHA production from selected aerobic mixed cultures. *N. Biotechnol.* 31, 297–307. doi: 10.1016/j.nbt.2013.10.009
- Moncada, J., Matallana, L. G., and Cardona, C. A. (2013). Selection of process pathways for biorefinery design using optimization tools: a colombian case for conversion of sugarcane bagasse to ethanol, poly-3-hydroxybutyrate (PHB), and energy. *Ind. Eng. Chem. Res.* 52, 4132–4145. doi: 10.1021/ie3019214
- Morse, M. C., Liao, Q., Criddle, C. S., and Frank, C. W. (2011). Anaerobic biodegradation of the microbial copolymer poly(3-hydroxybutyrate-co-3-hydroxyhexanoate): effects of comonomer content, processing history, and semi-crystalline morphology. *Polymer* 52, 547–556. doi: 10.1016/j.polymer.2010.11.024
- Mousavioun, P., Doherty, W. O. S., and George, G. (2010). Thermal stability and miscibility of poly(hydroxybutyrate) and soda lignin blends. *Ind. Crops Prod.* 32, 656–661. doi: 10.1016/j.indcrop.2010.08.001
- Muneer, F., Rasul, I., Azeem, F., Siddique, M. H., Zubair, M., and Nadeem, H. (2020). Microbial polyhydroxyalkanoates (PHAs): efficient replacement of synthetic polymers. *J. Polym. Environ.* 28, 2301–2323. doi: 10.1007/s10924-020-01772-1
- Muthuraj, R., Misra, M., and Mohanty, A. K. (2018). Biodegradable compatibilized polymer blends for packaging applications: a literature review. *J. Appl. Polym. Sci.* 135:45726. doi: 10.1002/app.45726
- Nieder-Heitmann, M., Haigh, K., and Görgens, J. F. (2019). Process design and economic evaluation of integrated, multi-product biorefineries for the co-production of bio-energy, succinic acid, and polyhydroxybutyrate (PHB) from sugarcane bagasse and trash lignocelluloses. *Biofuels Bioprod. Biorefining* 13, 599–617. doi: 10.1002/bbb.1972
- Noda, I., Lindsey, S. B., and Caraway, D. (2010). “Nodax™ class PHA copolymers: their properties and applications,” in *Plastics From Bacteria. Microbiology Monographs*, Vol. 14 (Berlin; Heidelberg: Springer). doi: 10.1007/978-3-642-03287-5\_10
- Noda, I., Green, P. R., Satkowski, M. M., and Schectman, L. A. (2005). Preparation and properties of a novel class of polyhydroxyalkanoate copolymers. *Biomacromolecules* 6, 580–586. doi: 10.1021/bm049472m
- Norhafini, H., Huong, K. H., and Amirul, A. A. (2019). High PHA density fed-batch cultivation strategies for 4HB-rich P(3HB-co-4HB) copolymer production by transformant *Cupriavidus malaysiensis* USMAA1020. *Int. J. Biol. Macromol.* 125, 1024–1032. doi: 10.1016/j.ijbiomac.2018.12.121
- Norhafini, H., Thinagaran, L., Shantini, K., Huong, K. H., Syaifiq, I. M., Bhubalan, K., et al. (2017). Synthesis of poly(3-hydroxybutyrate-co-4-hydroxybutyrate) with high 4HB composition and PHA content using 1,4-butanediol and 1,6-hexanediol for medical application. *J. Polym. Res.* 24:189. doi: 10.1007/s10965-017-1345-x
- Ntaikou, I., Valencia Peroni, C., Kourmentza, C., Ilieva, V. I., Morelli, A., Chiellini, E., et al. (2014). Microbial bio-based plastics from olive-mill wastewater: generation and properties of polyhydroxyalkanoates from mixed cultures in a two-stage pilot scale system. *J. Biotechnol.* 188, 138–147. doi: 10.1016/j.jbiotec.2014.08.015
- Obruca, S., Benesova, P., Petrik, S., Obrna, J., Prikryl, R., and Marova, I. (2014). Production of polyhydroxyalkanoates using hydrolysate of spent coffee grounds. *Process Biochem.* 49, 1409–1414. doi: 10.1016/j.procbio.2014.05.013
- Öner, M., Çöl, A. A., Pochat-Bohatier, C., and Bechelany, M. (2016). Effect of incorporation of boron nitride nanoparticles on the oxygen barrier and thermal properties of poly(3-hydroxybutyrate-co-hydroxyvalerate). *RSC Adv.* 6, 90973–90981. doi: 10.1039/C6RA19198C
- Öner, M., and İlhan, B. (2016). Fabrication of poly(3-hydroxybutyrate-co-3-hydroxyvalerate) biocomposites with reinforcement by hydroxyapatite using extrusion processing. *Mater. Sci. Eng. C* 65, 19–26. doi: 10.1016/j.msec.2016.04.024
- Öner, M., Keskin, G., Kizil, G., Pochat-Bohatier, C., and Bechelany, M. (2019). Development of poly(3-hydroxybutyrate-co-3-hydroxyvalerate)/boron nitride bionanocomposites with enhanced barrier properties. *Polym. Compos.* 40, 78–90. doi: 10.1002/pc.24603
- Ortega-Toro, R., Bonilla, J., Talens, P., and Chiralt, A. (2017). *Future of Starch-Based Materials in Food Packaging*. Elsevier Inc. doi: 10.1016/B978-0-12-809439-6.00009-1
- Ozkoc, G., and Kemalolu, S. (2009). Morphology, biodegradability, mechanical, and thermal properties of nanocomposite films based on PLA and plasticized PLA. *J. Appl. Polym. Sci.* 114, 2481–2487. doi: 10.1002/app.30772
- Panaiteșcu, D. M., Nicolae, C. A., Frone, A. N., Chiulan, I., Stancescu, P. O., Draghici, C., et al. (2017). Plasticized poly(3-hydroxybutyrate) with improved melt processing and balanced properties. *J. Appl. Polym. Sci.* 134, 1–14. doi: 10.1002/app.44810
- Park, D. H., and Kim, B. S. (2011). Production of poly(3-hydroxybutyrate) and poly(3-hydroxybutyrate-co-4-hydroxybutyrate) by *Ralstonia eutropha* from soybean oil. *N. Biotechnol.* 28, 719–724. doi: 10.1016/j.nbt.2011.01.007
- Park, S. J., Kim, T. W., Kim, M. K., Lee, S. Y., and Lim, S. C. (2012). Advanced bacterial polyhydroxyalkanoates: towards a versatile and sustainable platform for unnatural tailor-made polyesters. *Biotechnol. Adv.* 30, 1196–1206. doi: 10.1016/j.biotechadv.2011.11.007
- Peña-Jurado, E., Pérez-Vega, S., Zavala-Díaz de la Serna, F. J., Pérez-Reyes, I., Gutiérrez-Méndez, N., Vázquez-Castillo, J., et al. (2019). Production of poly(3-hydroxybutyrate) from a dairy industry wastewater using *Bacillus subtilis* EPAH18: bioprocess development and simulation. *Biochem. Eng. J.* 151:107324. doi: 10.1016/j.bej.2019.107324
- Peng, K., Wu, C., Wei, G., Jiang, J., Zhang, Z., and Sun, X. (2018). Implantable sandwich PHBHHx film for burst-free controlled delivery of thymopentin peptide. *Acta Pharm. Sin. B* 8, 432–439. doi: 10.1016/j.apsb.2018.03.003
- Peng, Q., Sun, X., Gong, T., Wu, C. Y., Zhang, T., Tan, J., et al. (2013). Injectable and biodegradable thermosensitive hydrogels loaded with PHBHHx nanoparticles for the sustained and controlled release of insulin. *Acta Biomater.* 9, 5063–5069. doi: 10.1016/j.actbio.2012.09.034
- Pereira, J. R., Araújo, D., Marques, A. C., Neves, L. A., Grandfils, C., Sevrin, C., et al. (2019). Demonstration of the adhesive properties of the medium-chain-length polyhydroxyalkanoate produced by *Pseudomonas chlororaphis* subsp. *aurantiaca* from glycerol. *Int. J. Biol. Macromol.* 122, 1144–1151. doi: 10.1016/j.ijbiomac.2018.09.064
- Persico, P., Ambrogli, V., Baroni, A., Santagata, G., Carfagna, C., Malinconico, M., et al. (2012). Enhancement of poly(3-hydroxybutyrate) thermal and processing stability using a bio-waste derived additive. *Int. J. Biol. Macromol.* 51, 1151–1158. doi: 10.1016/j.ijbiomac.2012.08.036

- and release studies. *Compr. Rev. Food Sci. Food Saf.* 9, 552–571. doi: 10.1111/j.1541-4337.2010.00126.x
- Jandas, P. J., Mohanty, S., and Nayak, S. K. (2014). Morphology and thermal properties of renewable resource-based polymer blend nanocomposites influenced by a reactive compatibilizer. *ACS Sustain. Chem. Eng.* 2, 377–386. doi: 10.1021/sc400395s
- Jiang, X. R., Wang, H., Shen, R., and Chen, G. Q. (2015). Engineering the bacterial shapes for enhanced inclusion bodies accumulation. *Metab. Eng.* 29, 227–237. doi: 10.1016/j.ymben.2015.03.017
- Jost, V., and Langowski, H. C. (2015). Effect of different plasticisers on the mechanical and barrier properties of extruded cast PHBV films. *Eur. Polym. J.* 68, 302–312. doi: 10.1016/j.eurpolymj.2015.04.012
- Júnior, R. M. S., de Oliveira, T. A., Araque, L. M., Alves, T. S., De Carvalho, L. H., and Barbosa, R. (2019). Thermal behavior of biodegradable bionanocomposites: influence of bentonite and vermiculite clays. *J. Mater. Res. Technol.* 8, 3234–3243. doi: 10.1016/j.jmrt.2019.05.011
- Keen, I., Raggatt, L. J., Cool, S. M., Nurcombe, V., Fredericks, P., Trau, M., et al. (2007). Investigations into poly(3-hydroxybutyrate-co-3-hydroxyvalerate) surface properties causing delayed osteoblast growth. *J. Biomater. Sci. Polym. Ed.* 18, 1101–1123. doi: 10.1163/156856207781554046
- Keskin, G., Kizil, G., Bechelany, M., Pochat-Bohatier, C., and Öner, M. (2017). Potential of polyhydroxyalkanoate (PHA) polymers family as substitutes of petroleum based polymers for packaging applications and solutions brought by their composites to form barrier materials. *Pure Appl. Chem.* 89, 1841–1848. doi: 10.1515/pac-2017-0401
- Kim, J., Kim, Y.-J., Choi, S. Y., Lee, S. Y., and Kim, K.-J. (2017). Crystal structure of *Ralstonia eutropha* polyhydroxyalkanoate synthase C-terminal domain and reaction mechanisms. *Biotechnol. J.* 12:1600648. doi: 10.1002/biot.201600648
- Koller, M., Maršálek, L., de Sousa Dias, M. M., and Braunnegg, G. (2017). Producing microbial polyhydroxyalkanoate (PHA) polyesters in a sustainable manner. *N. Biotechnol.* 37, 24–38. doi: 10.1016/j.nbt.2016.05.001
- Koller, M., Salerno, A., Strohmeier, K., Schober, S., Mittelbach, M., Illieva, V., et al. (2014). Novel precursors for production of 3-hydroxyvalerate-containing poly[(R)-hydroxyalkanoate]s. *Biocatal. Biotransformation* 32, 161–167. doi: 10.3109/10242422.2014.913580
- Kourmentza, C., Plácido, J., Venetsaneas, N., Burniol-Figols, A., Varrone, C., Gavala, H. N., et al. (2017). Recent advances and challenges towards sustainable polyhydroxyalkanoate (PHA) production. *Bioengineering* 4:55. doi: 10.3390/bioengineering4020055
- Kumar, P., and Kim, B. S. (2018). Valorization of polyhydroxyalkanoates production process by co-synthesis of value-added products. *Bioresour. Technol.* 269, 544–556. doi: 10.1016/j.biortech.2018.08.120
- Kunze, C., Freier, T., Kramer, S., and Schmitz, K. P. (2002). Anti-inflammatory prodrugs as plasticizers for biodegradable implant materials based on poly(3-hydroxybutyrate). *J. Mater. Sci. Mater. Med.* 13, 1051–1055. doi: 10.1023/A:1020392606225
- Lai, S. M., Don, T. M., and Huang, Y. C. (2006). Preparation and properties of biodegradable thermoplastic starch/poly(hydroxy butyrate) blends. *J. Appl. Polym. Sci.* 100, 2371–2379. doi: 10.1002/app.23085
- Lee, W. H., Azizan, M. N. M., and Sudesh, K. (2004). Effects of culture conditions on the composition of poly(3-hydroxybutyrate-co-4-hydroxybutyrate) synthesized by *Comamonas acidovorans*. *Polym. Degrad. Stab.* 84, 129–134. doi: 10.1016/j.polydegradstab.2003.10.003
- Li, D., Lv, L., Chen, J. C., and Chen, G. Q. (2017). Controlling microbial PHB synthesis via CRISPRi. *Appl. Microbiol. Biotechnol.* 101, 5861–5867. doi: 10.1007/s00253-017-8374-6
- Li, J., Yun, H., Gong, Y., Zhao, N., and Zhang, X. (2005). Effects of surface modification of poly(3-hydroxybutyrate-co-3-hydroxyhexanoate) (PHBHHx) on physicochemical properties and on interactions with MC3T3-E1 cells. *J. Biomed. Mater. Res. Part A* 75, 985–998. doi: 10.1002/jbm.a.30504
- Li, L., Huang, W., Wang, B., Wei, W., Gu, Q., and Chen, P. (2015a). Properties and structure of polylactide/poly(3-hydroxybutyrate-co-3-hydroxyvalerate) (PLA/PHBV) blend fibers. *Polymer* 68, 183–194. doi: 10.1016/j.polymer.2015.05.024
- Li, S., Cai, L., Wu, L., Zeng, G., Chen, J., Wu, Q., et al. (2014). Microbial synthesis of functional homo-, random, and block polyhydroxyalkanoates by  $\beta$ -oxidation deleted *Pseudomonas entomophila*. *Biomacromolecules* 15, 2310–2319. doi: 10.1021/bm500669s
- Li, X., Chang, H., Luo, H., Wang, Z., Zheng, G., Lu, X., et al. (2015b). Poly(3-hydroxybutyrate-co-3-hydroxyhexanoate) scaffolds coated with PhaP-RGD fusion protein promotes the proliferation and chondrogenic differentiation of human umbilical cord mesenchymal stem cells *in vitro*. *J. Biomed. Mater. Res. Part A* 103, 1169–1175. doi: 10.1002/jbm.a.35265
- Li, Z. J., Shi, Z. Y., Jian, J., Guo, Y. Y., Wu, Q., and Chen, G. Q. (2010). Production of poly(3-hydroxybutyrate-co-4-hydroxybutyrate) from unrelated carbon sources by metabolically engineered *Escherichia coli*. *Metab. Eng.* 12, 352–359. doi: 10.1016/j.ymben.2010.03.003
- Lim, J. S., Park, K., Il, C., G. S., and Kim, J. H. (2013). Effect of composition ratio on the thermal and physical properties of semicrystalline PLA/PHB-HHx composites. *Mater. Sci. Eng. C* 33, 2131–2137. doi: 10.1016/j.msec.2013.01.030
- Liminana, P., Garcia-Sanoguera, D., Quiles-Carrillo, L., Balart, R., and Montanes, N. (2019). Optimization of maleinized linseed oil loading as a bio-based compatibilizer in poly(Butylene Succinate) composites with almond shell flour. *Materials* 12:685. doi: 10.3390/ma12050685
- Ling, C., Qiao, G. Q., Shuai, B. W., Song, K. N., Yao, W. X., Jiang, X. R., et al. (2019). Engineering self-flocculating *Halomonas campaniensis* for wastewaterless open and continuous fermentation. *Biotechnol. Bioeng.* 116, 805–815. doi: 10.1002/bit.26897
- Liu, F., Jian, J., Shen, X., Chung, A., Chen, J., and Chen, G. Q. (2011a). Metabolic engineering of *Aeromonas hydrophila* 4A4K4 for production of copolymers of 3-hydroxybutyrate and medium-chain-length 3-hydroxyalkanoate. *Bioresour. Technol.* 102, 8123–8129. doi: 10.1016/j.biortech.2011.05.074
- Liu, Q., Luo, G., Zhou, X. R., and Chen, G. Q. (2011b). Biosynthesis of poly(3-hydroxydecanoate) and 3-hydroxydodecanoate dominating polyhydroxyalkanoates by  $\beta$ -oxidation pathway inhibited *Pseudomonas putida*. *Metab. Eng.* 13, 11–17. doi: 10.1016/j.ymben.2010.10.004
- Lu, X., Zhang, J., Wu, Q., and Chen, G. Q. (2003). Enhanced production of poly(3-hydroxybutyrate-co-3-hydroxyhexanoate) via manipulating the fatty acid  $\beta$ -oxidation pathway in *E. coli*. *FEMS Microbiol. Lett.* 221, 97–101. doi: 10.1016/S0378-1097(03)00173-3
- Lu, X. Y., Wu, Q., and Chen, G. Q. (2004). Production of poly(3-hydroxybutyrate-co-3-hydroxyhexanoate) with flexible 3-hydroxyhexanoate content in *Aeromonas hydrophila* CGMCC 0911. *Appl. Microbiol. Biotechnol.* 64, 41–45. doi: 10.1007/s00253-003-1417-1
- Lukasiewicz, B., Basnett, P., Nigmatullin, R., Matharu, R., Knowles, J. C., and Roy, I. (2018). Binary polyhydroxyalkanoate systems for soft tissue engineering. *Acta Biomater.* 71, 225–234. doi: 10.1016/j.actbio.2018.02.027
- Luo, S., Cao, J., and McDonald, A. G. (2016). Interfacial improvements in a green biopolymer alloy of poly(3-hydroxybutyrate-co-3-hydroxyvalerate) and lignin via *in situ* reactive extrusion. *ACS Sustain. Chem. Eng.* 4, 3465–3476. doi: 10.1021/acssuschemeng.6b00495
- Ma, P., Cai, X., Zhang, Y., Wang, S., Dong, W., Chen, M., et al. (2014). *In-situ* compatibilization of poly(lactic acid) and poly(butylene adipate-co-terephthalate) blends by using dicumyl peroxide as a free-radical initiator. *Polym. Degrad. Stab.* 102, 145–151. doi: 10.1016/j.polydegradstab.2014.01.025
- Madden, L. A., Anderson, A. J., and Asrar, J. (1998). Synthesis and characterization of poly(3-hydroxybutyrate) and poly(3-hydroxybutyrate-co-3-hydroxyvalerate) polymer mixtures produced in high-density fed-batch cultures of *Ralstonia eutropha* (*Alcaligenes eutrophus*). *Macromolecules* 31, 5660–5667. doi: 10.1021/ma980606w
- Mangeon, C., Michely, L., Rios De Anda, A., Theveniau, F., Renard, E., and Langlois, V. (2018). Natural terpenes used as plasticizers for Poly(3-hydroxybutyrate). *ACS Sustain. Chem. Eng.* 6, 16160–16168. doi: 10.1021/acssuschemeng.8b02896
- Mannina, G., Presti, D., Montiel-Jarillo, G., Carrera, J., and Suárez-Ojeda, M. E. (2020). Recovery of polyhydroxyalkanoates (PHAs) from wastewater: a review. *Bioresour. Technol.* 297:122478. doi: 10.1016/j.biortech.2019.122478
- Markl, E. (2018). PHB - bio based and biodegradable replacement for PP: a review. *Nov. Tech. Nutr. Food Sci.* 2, 206–209. doi: 10.31031/NTNF.2018.02.000546
- Martin, O., and Averous, L. (2001). Poly(lactic acid): plasticization and properties of biodegradable multiphase systems. *Polymer* 42, 6209–6219. doi: 10.1016/S0032-3861(01)00086-6
- Martino, V. P., Jiménez, A., Ruscakate, R. A., and Averous, L. (2011). Structure and properties of clay nano-biocomposites based on poly(lactic acid) plasticized with polyadipates. *Polym. Adv. Technol.* 22, 2206–2213. doi: 10.1002/pat.1747

- Thiré, R. M. S. M., Ribeiro, T. A. A., and Andrade, C. T. (2006). Effect of starch addition on compression-molded poly(3-hydroxybutyrate)/ starch blends. *J. Appl. Polym. Sci.* 100, 4338–4347. doi: 10.1002/app.23215
- Tian, S. J., Lai, W. J., Zheng, Z., Wang, H. X., and Chen, G. Q. (2005). Effect of over-expression of phasin gene from *Aeromonas hydrophila* on biosynthesis of copolymers of 3-hydroxybutyrate and 3-hydroxyhexanoate. *FEMS Microbiol. Lett.* 244, 19–25. doi: 10.1016/j.femsle.2005.01.020
- Tripathi, L., Wu, L. P., Dechuan, M., Chen, J., Wu, Q., and Chen, G. Q. (2013a). *Pseudomonas putida* KT2442 as a platform for the biosynthesis of polyhydroxyalkanoates with adjustable monomer contents and compositions. *Bioresour. Technol.* 142, 225–231. doi: 10.1016/j.biortech.2013.05.027
- Tripathi, L., Wu, L. P., Meng, D., Chen, J., and Chen, G. Q. (2013b). Biosynthesis and characterization of diblock copolymer of P(3-hydroxypropionate)-block-P(4-hydroxybutyrate) from recombinant *Escherichia coli*. *Biomacromolecules* 14, 862–870. doi: 10.1021/bm3019517
- Tsuge, T. (2016). Fundamental factors determining the molecular weight of polyhydroxyalkanoate during biosynthesis. *Polym. J.* 48, 1051–1057. doi: 10.1038/pj.2016.78
- Turco, R., Ortega-Toro, R., Tesser, R., Mallardo, S., Collazo-Bigliardi, S., Boix, A. C., et al. (2019a). Poly(lactic acid)/thermoplastic starch films: effect of cardoon seed epoxidized oil on their chemico-physical, mechanical, and barrier properties. *Coatings* 9, 574. doi: 10.3390/coatings9090574
- Turco, R., Tesser, R., Cucciolito, M. E., Fagnano, M., Ottaiano, L., Mallardo, S., et al. (2019b). *Cynara cardunculus* biomass recovery: an eco-sustainable, nonedible resource of vegetable oil for the production of poly(lactic acid) bioplasticizers. *ACS Sustain. Chem. Eng.* 7, 4069–4077. doi: 10.1021/acssuschemeng.8b05519
- Vandewijngaerden, J., Murariu, M., Dubois, P., Carleer, R., Yperman, J., D'Haen, J., et al. (2016). Effect of ultrafine talc on crystallization and end-use properties of poly(3-hydroxybutyrate-co-3-hydroxyhexanoate). *J. Appl. Polym. Sci.* 133:43808. doi: 10.1002/app.43808
- Vandewijngaerden, J., Murariu, M., Dubois, P., Carleer, R., Yperman, J., Adriaensens, P., et al. (2014). Gas permeability properties of poly(3-hydroxybutyrate-co-3-hydroxyhexanoate). *J. Polym. Environ.* 22, 501–507. doi: 10.1007/s10924-014-0688-1
- Vastano, M., Corrado, I., Sanna, G., Solaiman, D. K. Y., and Pezzella, C. (2019). Conversion of no/low value waste frying oils into biodiesel and polyhydroxyalkanoates. *Sci. Rep.* 9:13751. doi: 10.1038/s41598-019-50278-x
- Vastano, M., Pellis, A., Immirzi, B., Dal Poggetto, G., Malinconico, M., Sanna, G., et al. (2017). Enzymatic production of clickable and PEGylated recombinant polyhydroxyalkanoates. *Green Chem.* 19, 5494–5504. doi: 10.1039/C7GC01872J
- Verlinden, R. A. J., Hill, D. J., Kenward, M. A., Williams, C. D., and Radecka, I. (2007). Bacterial synthesis of biodegradable polyhydroxyalkanoates. *J. Appl. Microbiol.* 102, 1437–1449. doi: 10.1111/j.1365-2672.2007.03335.x
- Vidéki, B., Klébert, S., and Pukánszky, B. (2007). External and internal plasticization of cellulose acetate with caprolactone: structure and properties. *J. Polym. Sci. Part B Polym. Phys.* 45, 873–883. doi: 10.1002/polb.21121
- Vieira, M. G. A., Da Silva, M. A., Dos Santos, L. O., and Beppu, M. M. (2011). Natural-based plasticizers and biopolymer films: a review. *Eur. Polym. J.* 47, 254–263. doi: 10.1016/j.eurpolymj.2010.12.011
- Vieira, M. G. A., Da Silva, M. A., Maçamoto, A. C. G., Dos Santos, L. O., and Beppu, M. M. (2014). Synthesis and application of natural polymeric plasticizer obtained through polyesterification of rice fatty acid. *Mater. Res.* 17, 386–391. doi: 10.1590/S1516-14392014005000017
- Vishtal, A., and Kraslawski, A. (2011). Challenges in industrial applications of technical lignins. *BioResources* 6, 3547–3568. doi: 10.15376/biores.6.3.3547-3568
- Vroman, I., and Tighzert, L. (2009). Biodegradable polymers. *Materials* 2, 307–344. doi: 10.3390/ma2020307
- Wang, B., Sharma-Shivappa, R. R., Olson, J. W., and Khan, S. A. (2013a). Production of polyhydroxybutyrate (PHB) by *Alcaligenes latus* using sugarbeet juice. *Ind. Crops Prod.* 43, 802–811. doi: 10.1016/j.indcrop.2012.08.011
- Wang, H. H., Zhou, X. R., Liu, Q., and Chen, G. Q. (2011). Biosynthesis of polyhydroxyalkanoate homopolymers by *Pseudomonas putida*. *Appl. Microbiol. Biotechnol.* 89, 1497–1507. doi: 10.1007/s00253-010-2964-x
- Wang, L., Yang, Z., Fan, F., Sun, S., Wu, X., Lu, H., et al. (2019). PHBHHx facilitated the residence, survival and stemness maintain of transplanted neural stem cells in traumatic brain injury rats. *Biomacromolecules* 20, 3294–3302. doi: 10.1021/acs.biomac.9b00408
- Wang, L., Zhu, W., Wang, X., Chen, X., Chen, G.-Q., and Xu, K. (2008). Processability modifications of poly(3-hydroxybutyrate) by plasticizing, blending, and stabilizing. *J. Appl. Polym. Sci.* 107, 166–173. doi: 10.1002/app.27004
- Wang, S., Chen, W., Xiang, H., Yang, J., Zhou, Z., and Zhu, M. (2016). Modification and potential application of short-chain-length polyhydroxyalkanoate (SCL-PHA). *Polymers* 8:273. doi: 10.3390/polym8080273
- Wang, Y., Chen, K., Xu, C., and Chen, Y. (2015). Supertoughened biobased poly(lactic acid)-epoxidized natural rubber thermoplastic vulcanizates: fabrication, co-continuous phase structure, interfacial *in situ* compatibilization, and toughening mechanism. *J. Phys. Chem. B* 119, 12138–12146. doi: 10.1021/acs.jpcc.5b06244
- Wang, Y., Chen, R., Cai, J. Y., Liu, Z., Zheng, Y., Wang, H., et al. (2013b). Biosynthesis and thermal properties of PHBV produced from levulinic acid by *Ralstonia eutropha*. *PLoS ONE* 8:e0060318. doi: 10.1371/journal.pone.0060318
- Wang, Y., Wu, H., Jiang, X., and Chen, G. Q. (2014). Engineering *Escherichia coli* for enhanced production of poly(3-hydroxybutyrate-co-4-hydroxybutyrate) in larger cellular space. *Metab. Eng.* 25, 183–193. doi: 10.1016/j.ymben.2014.07.010
- Wijeyekoon, S., Carere, C. R., West, M., Nath, S., and Gapes, D. (2018). Mixed culture polyhydroxyalkanoate (PHA) synthesis from nutrient rich wet oxidation liquors. *Water Res.* 140, 1–11. doi: 10.1016/j.watres.2018.04.017
- Wu, H., Chen, J., and Chen, G. Q. (2016a). Engineering the growth pattern and cell morphology for enhanced PHB production by *Escherichia coli*. *Appl. Microbiol. Biotechnol.* 100, 9907–9916. doi: 10.1007/s00253-016-7715-1
- Wu, H., Fan, Z., Jiang, X., Chen, J., and Chen, G. Q. (2016b). Enhanced production of polyhydroxybutyrate by multiple dividing *E. coli*. *Microb. Cell Fact.* 15:128. doi: 10.1186/s12934-016-0531-6
- Yang, J. E., Choi, Y. J., Lee, S. J., Kang, K. H., Lee, H., Oh, Y. H., et al. (2014). Metabolic engineering of *Escherichia coli* for biosynthesis of poly(3-hydroxybutyrate-co-3-hydroxyvalerate) from glucose. *Appl. Microbiol. Biotechnol.* 98, 95–104. doi: 10.1007/s00253-013-5285-z
- Ye, H. M., Wang, Z., Wang, H. H., Chen, G. Q., and Xu, J. (2010). Different thermal behaviors of microbial polyesters poly(3-hydroxybutyrate-co-3-hydroxyvalerate-co-3-hydroxyhexanoate) and poly(3-hydroxybutyrate-co-3-hydroxyhexanoate). *Polymer* 51, 6037–6046. doi: 10.1016/j.polymer.2010.10.030
- Ye, J., Hu, D., Che, X., Jiang, X., Li, T., Chen, J., et al. (2018). Engineering of *Halomonas bluephagenesis* for low cost production of poly(3-hydroxybutyrate-co-4-hydroxybutyrate) from glucose. *Metab. Eng.* 47, 143–152. doi: 10.1016/j.ymben.2018.03.013
- Yeo, J. C. C., Muiruri, J. K., Thitsartarn, W., Li, Z., and He, C. (2018). Recent advances in the development of biodegradable PHB-based toughening materials: approaches, advantages and applications. *Mater. Sci. Eng. C* 92, 1092–1116. doi: 10.1016/j.msec.2017.11.006
- Yoshie, N., Nakasato, K., Fujiwara, M., Kasuya, K., Abe, H., Doi, Y., et al. (2000). Effect of low molecular weight additives on enzymatic degradation of poly(3-hydroxybutyrate). *Polymer* 41, 3227–3234. doi: 10.1016/S0032-3861(99)00547-9
- Yu, W., Lan, C.-H., Wang, S.-J., Fang, P.-F., and Sun, Y.-M. (2010). Influence of zinc oxide nanoparticles on the crystallization behavior of electrospun poly(3-hydroxybutyrate-co-3-hydroxyvalerate) nanofibers. *Polymer* 51, 2403–2409. doi: 10.1016/j.polymer.2010.03.024
- Zhang, H., Yu, H.-Y., Wang, C., and Yao, J. (2017). Effect of silver contents in cellulose nanocrystal/silver nanohybrids on PHBV crystallization and property improvements. *Carbohydr. Polym.* 173, 7–16. doi: 10.1016/j.carbpol.2017.05.064
- Zhang, H. F., Ma, L., Wang, Z. H., and Chen, G. Q. (2009). Biosynthesis and characterization of 3-hydroxyalkanoate terpolyesters with adjustable properties by *Aeromonas hydrophila*. *Biotechnol. Bioeng.* 104, 582–589. doi: 10.1002/bit.22409
- Zhang, K., Mohanty, A. K., and Misra, M. (2012). Fully biodegradable and biorenewable ternary blends from polylactide, poly(3-hydroxybutyrate-co-hydroxyvalerate) and poly(butylene succinate) with balanced properties. *ACS Appl. Mater. Interfaces* 4, 3091–3101. doi: 10.1021/am3004522
- Zhang, M., and Thomas, N. L. (2010). Preparation and properties of polyhydroxybutyrate blended with different types of starch. *J. Appl. Polym. Sci.* 116, 688–694. doi: 10.1002/app.30991

- Zhang, M., and Thomas, N. L. (2011). Blending polylactic acid with polyhydroxybutyrate: the effect on thermal, mechanical, and biodegradation properties. *Adv. Polym. Technol.* 30, 67–79. doi: 10.1002/adv.20235
- Zhang, X., Lin, Y., Wu, Q., Wang, Y., and Chen, G. Q. (2020). Synthetic biology and genome-editing tools for improving PHA metabolic engineering. *Trends Biotechnol.* 38, 689–700. doi: 10.1016/j.tibtech.2019.10.006
- Zhang, Y., Rempel, C., and Liu, Q. (2014). Thermoplastic starch processing and characteristics—a review. *Crit. Rev. Food Sci. Nutr.* 54, 1353–1370. doi: 10.1080/10408398.2011.636156
- Zhila, N., and Shishatskaya, E. (2018). Properties of PHA bi-, ter-, and quarter-polymers containing 4-hydroxybutyrate monomer units. *Int. J. Biol. Macromol.* 111, 1019–1026. doi: 10.1016/j.ijbiomac.2018.01.130
- Zinn, M., Weilenmann, H.-U., Hany, R., Schmid, M., and Egli, T. (2003). Tailored synthesis of Poly([R]-3-hydroxybutyrate-co-3-hydroxyvalerate) (PHB/HV) in *Ralstonia eutropha* DSM 428. *Acta Biotechnol.* 23, 309–316. doi: 10.1002/abio.200390039
- Conflict of Interest:** The authors declare that the research was conducted in the absence of any commercial or financial relationships that could be construed as a potential conflict of interest.
- Copyright © 2021 Turco, Santagata, Corrado, Pezzella and Di Serio. This is an open-access article distributed under the terms of the Creative Commons Attribution License (CC BY). The use, distribution or reproduction in other forums is permitted, provided the original author(s) and the copyright owner(s) are credited and that the original publication in this journal is cited, in accordance with accepted academic practice. No use, distribution or reproduction is permitted which does not comply with these terms.



## Turning Wastes into Resources: Exploiting Microbial Potential for the Conversion of Food Wastes into Polyhydroxyalkanoates

# 6

Iolanda Corrado, Marco Vastano, Nicoletta Cascelli, Giovanni Sannia, and Cinzia Pezzella

### Abstract

Polyhydroxyalkanoates (PHA) are microbial polyesters produced by a wide range of microorganisms as storage materials. Besides displaying material properties similar to those of petroleum-based plastics, their intrinsic biodegradability makes them “green” candidates for solving plastic pollution issues. The PHA diversity, determined by monomer size as well as by polymer structure, translates into a wide range of material properties finding applications in different sectors. This tunability is due to the complex metabolic network that drives PHA biosynthesis *in vivo*, which makes every microorganism unique in its producing abilities. Despite such potentialities, the production of PHAs at large scale is hindered by the high cost of carbon substrate necessary to feed PHA producing microbes. In this regard, the use of food wastes as starting feedstock for microbial fermentation would represent a cost-effective way to boost PHA exploitation. This chapter examines the state of the art of food wastes conversion into PHAs, focusing on the strategies applied to develop microbial strains for producing PHAs with tailored properties and high yield. Examples of PHA production based on natural or engineered strains will be examined, and prospects and challenges for the effective exploitation of the processes will be presented.

### Keywords

Polyhydroxyalkanoates (PHA) · Biorefinery · Strain engineering · Waste valorization

I. Corrado · M. Vastano · N. Cascelli · G. Sannia  
Department of Chemical Sciences, University Federico II, Naples, Italy

C. Pezzella (✉)  
Department of Agricultural Sciences, University Federico II, Naples, Italy  
e-mail: [cpezzella@umina.it](mailto:cpezzella@umina.it)

© Springer Nature Singapore Pte Ltd. 2021  
S. Shah et al. (eds.), *Bio-valorization of Waste*, Environmental and Microbial Biotechnology, [https://doi.org/10.1007/978-981-15-9696-4\\_6](https://doi.org/10.1007/978-981-15-9696-4_6)

133

## 6.1 Introduction

The exploitation of fossil resources to satisfy the current demand for plastic materials is a serious threat for the environment, with consequences in terms of global warming, human health risks, and ecosystem toxicity (Harding et al. 2007). Since their introduction in human everyday life, petro-plastics, due to their intrinsic resistance to microbial degradation, have accumulated in the environment, generating a real pollution emergency. European policies in relation to waste management, emission reduction, and sustainable development strongly encourage the search for new green solutions to the plastic issue (Directive 2008/98/EC on waste).

Polyhydroxyalkanoates (PHAs) are biodegradable and naturally synthesized polyesters, accumulated by various microorganisms as carbon, energy and redox storage material, in response to stressful/unbalanced growth conditions. In the last decade, PHAs have been emerging as “green” candidates for solving plastic pollution issues due to their spectrum of properties, very close to those of petroleum-based plastics.

Since the first identification of PHA accumulation in *Bacillus megaterium* by Lemoigne in 1926, over 90 PHA producing species and about 150 (R)-hydroxyalkanoic acids, as monomer constituents of natural PHAs, have been discovered (Ojumu et al. 2004). According to monomer chain length, PHAs have been classified in two main categories: short chain length (scl)-PHA (C4 and C5) and medium chain length (mcl)-PHA (C ≥ 6). Polyhydroxybutyrate (PHB), a scl-PHA, is by far the most well-studied PHA polymer, accumulated to up to 80% of cell dry weight by native as well as recombinant microorganisms (Aldor and Keasling 2003). Due to its thermoplastic properties, similar to those of polypropylene, PHB has found application in food packaging as well as in agricultural purposes (Reddy et al. 2003). On the other hand, mcl-PHAs characterized by high elasticity and low crystallinity emerged as suitable materials for novel applications in cosmetics, paint formulations, medical devices, and tissue engineering (Vastano et al. 2017).

Three main pathways regulate PHA biosynthesis *in vivo*. The biosynthetic routes to PHA monomers, which are strictly interconnected with the central metabolic pathways, compete with and/or rely on tricarboxylic acid (TCA) cycle, fatty acid biosynthesis and degradation, and are based on central metabolites and cofactors, i.e. acetyl-CoA and NADPH (Fig. 6.1).

The complex metabolic network that drives PHA biosynthesis *in vivo* makes every microorganism unique in its producing abilities. PHA composition and properties are strictly influenced by the supplied carbon source, the activated pathway, the properties of the enzymes involved, as well as by growth and operating conditions. The term “PHAome” was coined to describe the diverse and dynamic modifications the PHA spectrum undergoes within the cell (Chen and Hajnal 2015). Beside monomer composition, these modifications also reflect in the diversity of polymer structure (homopolymers, random or block-copolymers) and molecular weights, resulting from controlling operative culture conditions and/or external substrate feeding (Aldor and Keasling 2003; Chen and Hajnal 2015).

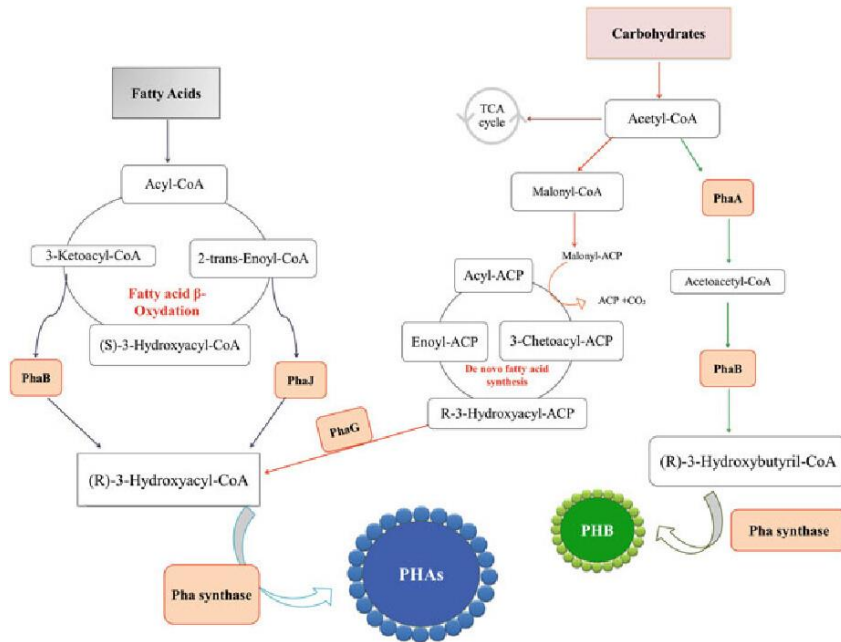


**Fig. 6.1** Schematic representation of the main metabolic pathways involved in PHA synthesis. (Note: *PhaA*  $\beta$ -ketothiolase, *PhaB* ketoacyl-CoA reductase, *PhaG* transacylase, *PhaJ* enoyl-CoA hydratase, *TCA cycle* tricarboxylic acid cycle)

This scenario left room to metabolic engineering to channel precursors into preferred routes in order to control PHA composition (Chen and Jiang 2017; Lee et al. 2019). At the same time, since the incorporation of specific precursors is linked to the substrate specificity of the PHA synthetic enzymes, protein engineering was applied to PHA biosynthetic enzymes, especially to the PHA synthase (*PhaC*), to modulate the abundance of a specific monomer into the synthesized polymers (Lee et al. 2019).

PHA heterogeneity gives rise to a wide range of materials, from thermoplastic polymers, to elastomers or even sticky resins. This feature, coupled to the intrinsic biodegradability and the renewable origin, confers an enormous potential to PHAs exploitation. It has been estimated that PHA production can save on average 2 kg CO<sub>2</sub> emitted (about 30 MJ of fossil resources) for 1 kg PHA produced, compared to fossil-derived plastics (Essel and Carus 2012). However, PHA production reached industrial scale only in few examples (Pakalapati et al. 2018), with production capacities from 1000 tonnes/year (Biomer, Germany; Kaneka Corporation, Japan) to 10,000 tonnes/year (Tianjin GreenBio Materials, PR China). The main obstacle to effective PHA application is the cost associated with the substrates used to feed the microbial process that was estimated to account for more than 50% of the production

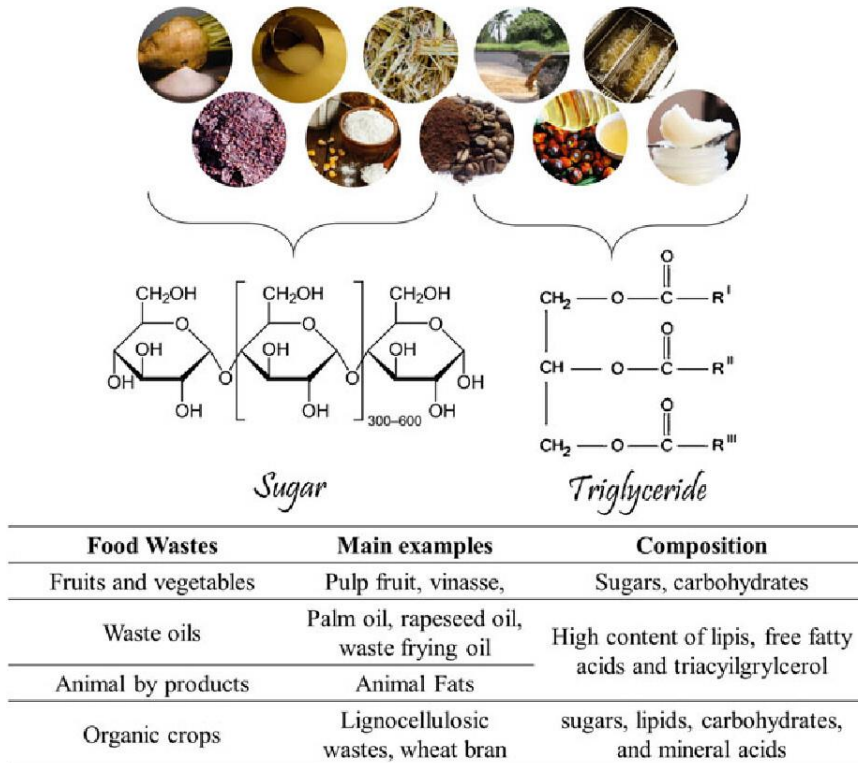


**Fig. 6.2** Main examples of food wastes and their principal components

costs (Koller et al. 2017). This makes the whole process not cost-efficient when compared with petroleum-based plastics and has encouraged the use of inexpensive waste biomasses to reduce the economic impact of the raw material (Sabapathy et al. 2017). In addition, the use of edible carbohydrates like glucose or lipids of nutritional value would provoke the “plate-versus-plastics” controversy, adding ethics concerns about bioplastic exploitation.

To be sustainable, PHA production processes should encompass aspects of economic, environmental protection, optimized engineering, and ethics (Koller 2019). A possible solution is to directly link the food production sector with biopolymer production, by using carbon-rich waste streams of food and feed production as raw materials for biopolymer manufacturing (Nielsen et al. 2017). The valorization of these wastes through a microbial process would also represent a solution to their disposal. About  $10^{12}$  kg of food is discarded per year (Kwan et al. 2018), and many carbon-rich food waste streams are produced from different productive sectors: from the cheese industry, to food companies producing waste

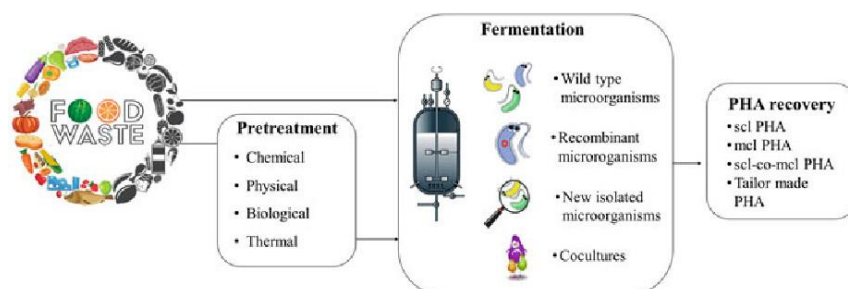


**Fig. 6.3** Main steps of PHA production from food wastes

frying oils; from waste animal fats from slaughterhouse to lignocellulosic wastes from different agro-sectors (Fig. 6.2).

Several studies explored the use of these waste materials as substrate for microbial PHA production. A survey of the scientific literature (Scopus search) published over the past 35 years reveals an increasing trend in the number of articles containing the keyword “PHA”, with a positive correlation with those resulting from the search for “PHA and waste”. In the published papers, different aspects have been addressed: the effect of waste composition on microbial metabolism and, consequently, the choice of proper PHA producer for the selected waste; the presence of readily metabolizable C-sources or the need for a pretreatment step to hydrolyse complex substrates into small convertible compounds; the necessity to detoxify the hydrolysates to remove inhibiting compounds.

This chapter covers the research carried out in the last decade on the exploitation of food waste materials for PHA production, focusing on the different strategies applied to optimize and customize biopolymer production processes (Fig. 6.3).

## 6.2 Exploring PHA Production from Pure Cultures and New Microbial Isolates

Bacterial strains able to produce PHAs are generally classified into two groups: (1) microorganisms that accumulate PHAs under limitation of some nutrients like oxygen, nitrogen or phosphorous in presence of C-sources excess; (2) microorganisms which do not require nutrient limitation for PHA biosynthesis, because polymer production is associated with growth (Kourmentza et al. 2017).

Microbial PHA production from food wastes was thoroughly investigated in order to reduce the production costs. In this section, the state of the art of food waste conversion into PHAs is discussed, focusing on the most abundant wastes worldwide and on the most relevant microbial processes in terms of PHA production yield, costs and innovation (Tables 6.1 and 6.2).

**Table 6.1** Examples of PHA production from lipid-rich waste by pure cultures

Waste source	Microorganism	Fermentation strategy	% PHA (w/w)	Monomeric composition	References
Waste frying oil	<i>Pseudomonas fluorescens</i> S48	Batch flask	12	PHB	Gamal et al. (2011)
Waste frying oil	<i>Pseudomonas fluorescens</i> S48	One-stage bioreactor	30	PHB	Gamal et al. (2012)
		Two-stage bioreactor	47		
		Fed-batch bioreactor	50		
Waste frying oil	<i>Pseudomonas fluorescens</i> S48	High cell density fed-batch culture in bioreactor	55	PHB	Gamal et al. (2013)
Waste frying oil	<i>Pseudomonas resinovorans</i>	Batch flask	28	mcl-PHA	Cruz et al. (2016)
Olive oil distillate	<i>Pseudomonas resinovorans</i>	Batch flask	31	mcl-PHA	
Olive oil distillate	<i>Cupriavidus necator</i>	Batch flask	62	PHB	
Two-phase olive mill waste	<i>Azotobacter chroococcum</i> H23	Batch flask	44	PHB	Cerrone et al. (2010)
	<i>Azotobacter vinelandii</i> UWD		33		
Two-phase olive mill waste	<i>Haloferax mediterranei</i>	Batch flask	43	P(3HB-co-3HV)	Alsafadi and Al-Mashaqbeh (2017)
Waste palm oil	<i>Pseudomonas</i> sp. GI01	Batch bioreactor	43	mcl-PHA	Możejko and Ciesielski (2013)
Waste rapeseed oil	<i>Pseudomonas</i> sp. GI01	Batch bioreactor	20	mcl-PHA	Możejko et al. (2011)
Waste rapeseed oil	<i>Pseudomonas</i> sp. GI01	Fed-batch bioreactor	44	mcl-PHA	Możejko and Ciesielski (2014)
Waste animal fats	<i>Ralstonia eutropha</i>	Batch bioreactor	70	PHB	Riedel et al. (2015)

Note: 3HB 3-hydroxybutyrate, 3HV 3-hydroxyvalerate

**Table 6.2** Examples of PHA production from food and agro-industrial wastes by pure microbial cultures

Waste source	Microorganism	Pretreatment	Fermentation strategy	Monomeric composition	%PHA (w/w)	References
Spent coffee grounds	<i>Cupriavidus necator</i> H16	Solvent oil extraction	Fed-batch bioreactor	PHB	89	Obruca et al. (2014a)
	<i>Burkholderia cepacia</i>	Solvent oil extraction and detoxification	Batch flask	P(3HB-co-3HV)	55	Obruca et al. (2014a)
Sugarcane molasses	<i>Cupriavidus necator</i> DSM 428	seCO <sub>2</sub> oil extraction	Fed-batch bioreactor	PHB	78	Cruz et al. (2014)
	<i>Bacillus megaterium</i> BA-019	–	Fed-batch bioreactor	PHB	42	Kulpreecha et al. (2009)
Molasses	<i>Pseudomonas</i> sp.	–	Batch flask	PHB	21	Chaudhry et al. (2011)
	<i>Bacillus megaterium</i> uyuni S29	–	Batch bioreactor	PHB	55	Schmid et al. (2019)
Desugared sugar molasses	<i>Haloferax mediterranei</i>	Adsorption of phenolic compounds with activated carbon	Batch flask	P(3HB-co-3HV)	70	Bhattacharya et al. (2014)
Cassava starch wastewater	<i>Haloarcula marismortui</i>	–	–	PHB	30	Pramanik et al. (2012)
	<i>Cupriavidus</i> sp. KKU38	Enzymatic saccharification	Batch flask	PHB	62	Poomipuk et al. (2014)
Starch	<i>Haloferax mediterranei</i>	Enzymatic saccharification	Fed-batch bioreactor	P(3HB-co-3HV)	51	Chen et al. (2006)
	<i>Bacillus cereus</i> CFR06	–	Batch flask	PHB	40	Halami (2008)
	<i>Bacillus thuringiensis</i>	–	Batch flask	PHB	73	Gowda and Shivakumar (2014)
	<i>Azotobacter chroococcum</i>	–	Batch flask	PHB	46	Kim (2000)

(continued)

Table 6.2 (continued)

Waste source	Microorganism	Pretreatment	Fermentation strategy	Monomeric composition	%PHA (w/w)	References
	<i>Bacillus megaterium</i> PHB29	–	Batch flask	PHB	73	Aneesh et al. (2016)
	<i>Halogeometricum borinquense</i> E3	–	Batch flask	P(3HB-co-3HV)	45	Salgaonkar et al. (2019)
White grapes pomace	<i>Pseudomonas resinovorans</i>	Enzymatic saccharification	Two-stage batch bioreactor	mcl-PHA	23	Follonier et al. (2014)
Apple pomace	<i>Pseudomonas putida</i> KT2440	–	Batch flask	mcl-PHA	25	Urbina et al. (2018)
Apple pulp	<i>Pseudomonas citronellolis</i> NRLL B2504	–	Batch bioreactor	mcl-PHA	30	Rebocho et al. (2019)
Pineapple peel	<i>Ralstonia eutropha</i> ATCC 17697	Acidic hydrolysis	Batch flask	P(3HB-co-3HV)	45	Vega-Castro et al. (2016)
Orange and passion fruit wastes	<i>Cupriavidus necator</i>	Polygalacturonases (pectinases)	Batch flask	N.D.	N.D.	Locatelli et al. (2019)
Lignocellulosic material	<i>Pandoraea</i> sp. B-6	–	Batch flask	PHB	25	Liu et al. (2019)
Wheat straw (lignin)	<i>Burkholderia sacchari</i> DSM 17165	AFEX-pre-treatment and enzymatic saccharification	Fed-batch bioreactor	PHB	72	Cesário et al. (2014)
	<i>Ralstonia eutropha</i> NCIMB 11599	Enzymatic saccharification	Batch flask	PHB	62	Annamalai and Sivakumar (2016)
Bagasse (lignin)	<i>Ralstonia eutropha</i>	Acidic hydrolysis	Batch flask	PHB	60	Yu and Stahl (2008)
Industrial oil products	<i>Pseudomonas aeruginosa</i> 42A2	–	Batch flask	ND	25	Rodríguez-Carmona et al. (2012)

Dairy waste, rice bran and brackish water	<i>Bacillus megaterium</i> sp.	–		Two step fed-batch bioreactor	PHB	ND	RamKumar Pandian et al. (2010)
Soybean effluent	<i>Halomonas</i> sp. SF 2003	–		Batch bioreactor	P(3HB-co-3HV)	23	Lemechko et al. (2019)
Rice mill effluent	<i>Acinetobacter junii</i> BP25	–		Batch flask	PHB	92	Sabapathy et al. (2019)
Rice-based ethanol stillage	<i>Haloflex mediterranei</i>			Batch flask	P(3HB-co-3HV)	71	Bhattacharyya et al. (2014)
MSW (municipal solid wastes)	<i>Rhodospirillum rubrum</i>	MIP		Batch flask	PHB	16	Revelles et al. (2017)
Whey	<i>Pseudomonas hydrogenovora</i>	–		Fed-batch bioreactor	P(3HB-co-3HV)	12	Koller et al. (2008)
	<i>Bacillus megaterium</i>	–		Batch flask	PHB	37	Obruca et al. (2011)
	<i>Caulobacter segnis</i> DSM 29236	–		Batch bioreactor	PHB	37	Bustamante et al. (2019)
	<i>Haloflex mediterranei</i>	–		Batch bioreactor	PHB	50	Koller et al. (2007)
Digestate liquor	<i>Cupriavidus necator</i>	–		Fed-batch bioreactor	PHB	90	Passanha et al. (2013)
Fish solid extract	<i>Bacillus subtilis</i> KP17 2548	–		Batch flask	PHB	70	Mohapatra et al. (2017)

Note: PHB-HV poly 3-hydroxybutyrate-co-3-hydroxyvalerate, AFEX ammonia fibre expansion, MIP microwave induced pyrolysis, SsCO<sub>2</sub> supercritical fluid extraction

### 6.2.1 Fatty Wastes

Vegetable oils were studied as possible candidates for PHA production. Due to their composition in medium and long chain fatty acids, oil-containing substrates can act as precursor for PHA with medium/long-monomer length (Table 6.1).

Waste frying oils (WFO) from food industry are mainly composed of triglycerides, containing long fatty acids (FFAs) with saturated and/or unsaturated bonds. Despite their common reuse in biodiesel industry, WFO were also tested as substrates for PHA production. Compared to pure vegetable oil, WFO provide components that improve growth and PHA accumulation such as food residues, readily available nitrogen compounds, peroxides, and short chain compound formed during heating (Verlinden et al. 2011). An example of WFO exploitation as carbon source at industrial scale was developed using *P. fluorescens* S48. Different strategies were investigated. With a continuous WFO feeding at 0.55 mL/L/h, the authors obtained a PHA content of 55.34% (w/w) and 0.64 g/L cell dry weight (cdw) after 54 h (Gamal et al. 2013). When operated in fed batch, with WFO supplying, a higher cell dry weight (3.46 g/L) and 49.71% polymer content (w/w) were achieved in a shorter time (48 h) (Gamal et al. 2012). In both cases, the feeding of carbon source improved its solubility and availability for bacteria.

Olive oil distillate (OOD) is a by-product from olive refining industry representing 0.05–0.1% of total processed oil. It is mainly composed of free fatty acids (>50 wt.%) with a lower concentration in triglycerides, diglycerides, and monoglycerides than WFO (less than 10 wt.%). As for WFO, the concentration of saturated fatty acids is lower than that of unsaturated FFA (Cruz et al. 2016). Using OOD as substrate for PHA production, up to 62% of PHB (w/w) was obtained using *C. necator*, and 31% (w/w) with *P. resinovorans* (Cruz et al. 2016). In the latter case, the polymer was mainly composed of 3-hydroxyoctanoate (3HO) and 3-hydroxydecanoate (3HD) with smaller amount of 3hydroxyhexanoate (3HHx).

An interesting bioprocess, combining anaerobic and aerobic steps, was reported by Cerrone and co-authors using the Two-Phase Olive Mill Waste (TPOMW), a semisolid waste generated in the olive mill industry by the two-phase extraction system (Cerrone et al. 2010). This waste is characterized by a high concentration of organic matter and elevated hydro-soluble carbohydrate content (Dionisi et al. 2005). The first biological anaerobic treatment transformed TPOMW, during the hydrolytic and acidogenic phases, into propionic, butyric or valeric acids; these were then used as precursors for the synthesis of 3-hydroxybutyric (3HB) and 3-hydroxyvaleric (3HV) in the subsequent aerobic step. Nevertheless, despite the capability of *A. chroococcum* H23 and *A. vinelandii* UWD to grow on this pretreated waste, they produced only homopolymers of PHB (*A. chroococcum* 44% (w/w), *A. vinelandii* 33% (w/w)); according to the authors this is due to the high concentration of carbohydrates (10 g/L) with respect to that of volatile fatty acids (30 mg/L) within the medium.

Alsafadi and Al-Mashaqbeh (2017) proposed a one-stage cultivation step on WFO, by exploiting extremophilic organisms, which exhibits tolerance to a range of environmental stressors. As a fact, *H. mediterranei* is able to incorporate

3HV units in the synthesized polymer, using Olive Mill Waste (OMW) as carbon source, without the need of a fermentation step or any additional feeding with costly 3HV-related precursors. *H. mediterranei* cultivation conditions were optimized in medium containing 15% OMW by investigating several parameters affecting PHA production. High salt concentration inhibits PHA biosynthetic pathway activating an osmotic balance response (Vega-Castro et al. 2016). The highest PHA content (43% (w/w)) was achieved at 37 °C, 170 rpm and 22% salt concentration.

Song, Haba and co-workers reported the synthesis of mcl-PHA by *Pseudomonas* species using waste palm oil (WPO) as carbon source (Song et al. 2008; Haba et al. 2007). *Pseudomonas* sp. GI01 strain was not able to grow on WPO in its original form, and a preliminary saponification step to break down the triglycerides into free fatty acids was required. After this pretreatment, up to 43% of mcl-PHA (w/w) after 17 h was produced (Mozejko and Ciesielski 2013). Interestingly, nitrogen limitation is unnecessary for stimulating biopolymer synthesis. *Pseudomonas* sp. GI01 was also reported to produce mcl-PHA from waste rapeseed oil as carbon source (Mozejko et al. 2011). In this case, oxygen concentration plays a crucial role, with lower oxygen supply being responsible for higher PHAs accumulation. In addition, the authors proposed a pulsed feeding strategy as more favourable approach for mcl-PHA production, reaching 44% (w/w) at 41 h of fermentation (Mozejko and Ciesielski 2014).

In addition to vegetable oils, waste animal lipids from the food processing and slaughtering industries have a huge potential as carbon feedstock for PHA production. There are many examples of PHA production from tallow; however, its low availability to microorganisms renders the addition of an emulsifying agent mandatory. Riedel et al. (2015) achieved a total production of 70% of PHB (w/w) by *R. eutropha* using a pre-emulsified tallow (mechanical mixing of tallow with arabic gum before inoculation). To increase the yield, they investigated the possibility to feed liquefied (by heat treatment) tallow during the fermentation in a fed-batch process. However, in this condition a lower polymer accumulation (63% (w/w)) with respect to the batch process was achieved (Riedel et al. 2015).

### 6.2.2 Spent Coffee Grounds (SCG)

SCG is a solid residue derived from coffee processing and consumption. Coffee is one of the world's most common beverages and its consumption has grown in the last 150 years: about 6.0 million ton of SCG are estimated to be produced worldwide and disposed as solid wastes (Tokimoto et al. 2005). Apart from coffee oils (about 15% weight), SCG contains carbohydrates, especially hemicelluloses (37% weight) and cellulose (9% weight), proteins (13% weight), and lignin (29% weight). Many studies showed SCG potentiality for PHA production as a low-cost oil-containing waste. When compared to other waste oils (rapeseed, palm, sunflower), oils extracted from SCG (by using *n*-hexane) assured the highest PHB accumulation and biomass recovery (70.3% PHA (w/w) and 14.2 g/L cell dry weight, cdw), in shake-flasks experiments using *C. necator* H16 (Obruca et al. 2014b). The authors

attributed the superior properties of coffee oil to its high content of free fatty acids, easily utilized by the bacterial culture. When scaled up in fed-batch mode, a productivity of 0.82 g PHA per g of oil was achieved. Furthermore, the addition of pure plant oils or recycled ones was also found effective to solve the difficulty related to the natural foaming effect of SCG, because they act as antifoaming agent. Since oil extraction reduces the calorific value of SCG by only 9%, the residual SCG can be used as fuel to partially cover heat and energy demands of the fermentation process, thus improving the economic feasibility of the PHA producing process.

Valorization of residual SCG after oil extraction was also pursued by Obruca et al. (2014b). A detoxification step, aimed at extracting SCG polyphenols, was applied before SCG hydrolysis to improve the fermentability of the hydrolysate (SCGH). *B. cepacia* was able to utilize the SCGH and produced a PHB-co-HV copolymer up to 51.6% (w/w). Levulinic acid present in the SCGH acted as precursor for 3HV monomer. The introduction of a polyphenol extraction step before the acidic hydrolysis enhanced PHA yields of about 25% (w/w) and allowed also to recover these important side products with potential high market value.

In order to avoid the use of hazardous organic solvents like *n*-hexane, Cruz et al. (2014) extracted SCG oil by supercritical fluid extraction with CO<sub>2</sub> obtaining a yield higher than 90% (w/w). The oils were directly fed to *C. necator* DSM 428 in fed-batch mode. The culture reached a 16.7 g/L cdw, with a PHB content of 78.4% (w/w) (13.1 g/L). In contrast, batch mode operation produced lower amounts of PHB (55% (w/w), 6 g/L) (Cruz et al. 2014).

### 6.2.3 Sugar Industry Waste

Several processes have been studied using molasses for PHA production. Sugarcane molasses is a by-product of sugar industry, rich in nutrients, growth factors and minerals, sucrose and glucose residues, not suitable for food. The absence of the proper enzymes (i.e.  $\alpha$ -galactosidases and  $\beta$ -furanosidases) required to metabolize the major carbohydrates components of molasses (sucrose, stachyose and raffinose) has limited the exploitation of this waste to few classes of microorganisms. *Pseudomonas* species have been considered for a long time the best microorganisms to produce PHAs by molasses, accumulating up to 20.6% of PHB (w/w) (Chaudhry et al. 2011). Recently, in a promising study by Kulpreecha et al. (2009), sugarcane molasses was used as C-source by *B. megaterium* BA-019 achieving a cdw of 72.7 g/L and a PHB content of 42% (w/w) (Kulpreecha et al. 2009). Schmid et al. (2019) on the other hand, recently investigated the potential of the halophilic bacterium *B. megaterium uyuni* S29 in accumulating PHB by desugared sugar beet molasses, a saline by-product of fractionation of beet molasses obtained from the separation of the sugar, betaine, and the refined fraction, which has a lower economic value than regular sugar beet molasses and is currently used as fertilizer and as nutrient additive for animal feed (Schmid et al. 2019). Fermentation of sugarcane molasses and other linked by-products led to a prevalent synthesis of the homopolymer PHB (Table 6.2).

Another significant sugar industry waste is vinasse, an acidic compost with a pH of 3.5–5.0, rich of organic and water-soluble components. It is the major by-product of ethanol production by molasses, left after alcohol distillation from the fermentation broth. Recent research on using it as a C-source for PHA production focused on extremely halophilic species like *H. marismortui* and *H. mediterranei*, notable for their ability to produce P(3HB-co-3HV) without the addition of organic acids (Pramanik et al. 2012; Bhattacharyya et al. 2014). Halophilic organisms have also the advantage of reducing the risk of microbial contamination even in a not rigidly sterile environment, due to the high salinity of the fermentation broth. The inhibitory effects of polyphenols into vinasse and the accumulation of salts after fermentations are two of the possible side effects in using them. While the second issue is affordable using two-stage desalination of spent medium to reuse salts, pretreatments like adsorption on activated carbon, at certain pH ranges, can reduce phenols allowing the usage of vinasse as C-source above the concentration of 10% wt. After this pretreatment, *H. mediterranei* was able to produce up to 19.7 g/L of P(3HB-co-3HV) (70% of polymer (w/w)), from a vinasse concentrations of up to 50% weight, while *H. marismortui* accumulated 4.5 g/L PHB, corresponding to 30% (w/w) of production, starting from 100% of vinasse.

#### 6.2.4 Starch

Starch is a polysaccharide found in many wastes, like food (cereals, fruits, tubers, legume) and agricultural ones (roots). Worldwide, scientists tried to use this renewable carbon source for the production of different value-added products, i.e. bioethanol and maltose syrup (Keshavarz and Roy 2010; Lareo et al. 2013). There are only few reports about the use of starch directly by bacteria: most of microorganisms do not have the metabolic apparatus for its metabolization, thus a preliminary hydrolysis (chemical or enzymatic) step is required. Poomipuk et al. (2014) isolated a new *Cupriavidus* sp. K KU38 from cassava starch wastewater and tested it for PHAs production using hydrolysed cassava starch as C-source, under selected conditions and nitrogen starvation (Poomipuk et al. 2014). A PHB content of 5.9 g/L corresponding to 61.6% (w/w) was reported. Interestingly, *H. mediterranei* (Chen et al. 2006) produced P(3HB-co-3HV) copolymer from salt medium supplemented with previously hydrolysed starch.

In order to skip substrates pretreatment, and consequently reduce the overall process cost, more attention has been paid to microorganisms with the ability to metabolize starch and simultaneously produce PHA. Halami (2008) found that the isolated *B. cereus* CFR06 secretes the enzyme amylase for substrate hydrolysis and produces 0.48 g/L of PHB (48.0% (w/w) and 1.0 g/L cdw) (Halami 2008). *B. thuringiensis* is also able to produce approximately 60–72% of PHB (w/w) with a cdw of 3.6 g/L (Gowda and Shivakumar 2014). A production of 25 g/L of PHB (46% (w/w)) was reported when soluble starch was utilized as a carbon source by *A. chroococcum* in batch mode with oxygen limitation (Kim 2000). Aneesh et al. (2016) focused on PHB production by a new environmental isolate *B. megaterium*

PHB29 with 73.46% of PHB (w/w) accumulation (Aneesh et al. 2016). Salgaonkar et al. (2019) explored the interesting potential of the Archaea *H. boriquense* E3 strain to produce copolymers P(3HB-co-3HV) from cassava starch wastes with a 44.7% (w/w) of accumulation (Salgaonkar et al. 2019).

### 6.2.5 Pomaces

Pomaces are fruit residues obtained by the pressing of grapes and distillation of fruits like apricots and cherries. They are constituted by fruit skins, pulp and seeds, and are considered as no-value wastes, usually subjected to landfill disposal, incineration or composting. Due to their high polysaccharide content (cellulose, hemicellulose, starch and pectin), pomaces have been used for the production of enzymes, organic acids, fuels and also PHA. In their interesting work, Follonier et al. (2014) investigated the production of mcl-PHA by the native PHA producer *P. resinovorans* carrying out a two-step process (Follonier et al. 2014). Nine types of fruit pomaces including apricots, cherries and red/white grapes were used as C-source for biomass growth in the first step. All these wastes underwent a preliminary enzymatic hydrolysis to produce fermentable sugars, otherwise inaccessible to *P. resinovorans*. WFO were added in the second step of a batch fermentation to sustain PHA synthesis. All fruit pomaces hydrolysates were assayed for the presence of possible growth inhibitors like phenols and tannins. The best PHA production was achieved by White Solaris grapes reaching 6.1 g/L of cdw, 21.3 g/(L<sub>pomace</sub>) of PHA and 23.3% of mcl-PHA accumulation (w/w) (Fig. 6.4).

Urbina et al. (2018) used apple pomace (cider and apple juice by-products), rich of a heterogeneous mixture of sugars like fructose, glucose, xylose and sucrose, directly as substrate for mcl-PHA production by *P. putida* KT2440 (Urbina et al. 2018). A PHA concentration of 1.1 g/L with a 25.5% PHA (w/w) and 4.3 g/L cdw was achieved employing the fed-batch strategy. Compared to the Follonier's two-step process, despite the comparable production yields, the process reported by Urbina is more economically sustainable because no saccharification step of fruit residues are needed and no fatty acids were supplemented during the fermentation process.

Untreated apple pulp wastes gained the attention of Rebocho research group who produced about 30% mcl-PHA (w/w) using *P. citronellolis* NRLL B-2504 (Rebocho et al. 2019). The authors succeeded in obtaining mcl-films by solvent casting and characterized them. The films display enhanced hydrophobicity, presenting a lower permeability to CO<sub>2</sub> and O<sub>2</sub> than silicone rubber, are less rigid and even less resistant to deformations than other natural polyesters as PHB, P(3HB-co-3HV), P(3-HB-co-3HHx) and polylactic acid (PLA), thus they turned out interesting for applications in food packaging and biomedical fields.

Among fruit pomaces attracting recent attention, pineapple peel wastes, particularly abundant in Colombia agro-industries, were tested as cheap C-source for scl-PHA (containing 3HV, prevalently) production by *R. eutropha* ATCC 17697 with a maximum of 44.8% (w/w) accumulation (Vega-Castro et al. 2016).

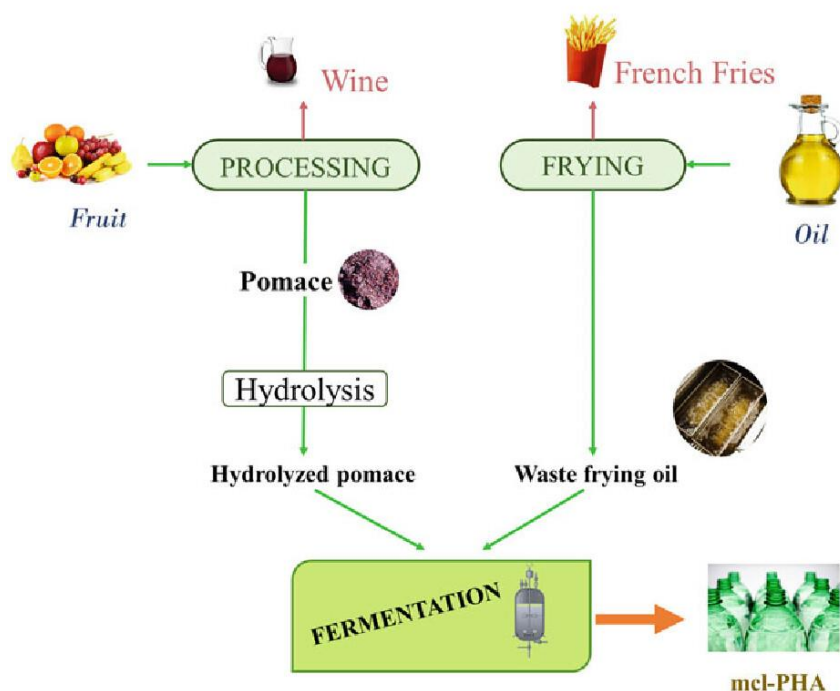


**Fig. 6.4** Overview of the production process of mcl-PHA using *P. resinovorans* grown on pomaces as C-source and WFO as mcl-PHA precursor (Follonier et al. 2014)

### 6.2.6 Lignocellulosic Wastes

Lignocellulosic biomasses are plant residues obtained from different manufacturing processes, made of hemicelluloses, cellulose, pectin and lignin. To be used as C-sources for microbial processes, these materials need to be hydrolysed and often detoxified to remove growth-inhibiting compounds. Lignocellulosic residues from wheat straw (Cesário et al. 2014), bagasse (Yu and Stahl 2008), and wheat bran (Annamalai and Sivakumar 2016) were investigated for PHA production, testing different pretreatment methods, in which lignin depolymerization is always the limiting step. Laccases, lignin peroxidases and other extracellular oxidative enzymes, from fungi and bacteria, were applied as enzymatic pretreatment, reaching similar production yields (as shown in Table 6.2).

Liu et al. (2019) very recently reported an interesting direct bioconversion system of lignin into PHA by *Pandoraea* sp. B-6 (Liu et al. 2019) without any pretreatment. From the genome analysis of the isolated microorganisms, putative genes coding for lignin depolymerases like laccases, peroxidases and Fenton-reaction enzymes were individuated. Even if they are far from setting an ideal production process in terms of

PHA content in both cases, the authors built the bases for the lignin bioconversion into PHAs in one step, reducing the overall costs of the process and opening up new perspectives in this field.

### 6.2.7 Dairy Industry Wastes

The dairy industry embraces several production sectors, milk, cheese, butter, milk powder or condensate, each of them producing different kind of wastes. Dairy industry wastes are characterized by high BOD and COD content, representing polluting materials with high disposal costs. Ramkumar Pandian et al. (2010) analysed a new potential PHB producer, *B. megaterium* sp. isolated from brackish water. They optimized the production medium made of a mixture of dairy wastes, rice bran and sea water as sources using RSM methodology, thus obtaining a maximum of 11.3 g/L of PHB (RamKumar Pandian et al. 2010).

Whey is the main by-product from cheese manufacture. It is rich in fermentable nutrients such as lactose, soluble proteins vitamins and mineral salts. About 50% of whey is recycled as animal feed, the remaining part usually destined for disposal. Whey can be considered a cheap source for microbial fermentation aimed at PHA production. Generally, whey does not require any extensive pretreatment before fermentation: the only limit is the bacterial strain ability of using lactose directly for their growth. Many microorganisms are reported to produce PHB directly from whey, some of the most interesting in terms of production yields being *B. megaterium* (Obruca et al. 2011), *H. mediterranei* and *P. hydrogenovora* (Koller et al. 2008). In their recent work, Bustamante et al. (2019) found a new PHA producer by cheese way, *C. segnis* DSM 29236, using an in silico screening approach (Bustamante et al. 2019). They achieved 37% of PHB (w/w) reaching up to 9.2 g/L, the highest concentration reported to date for a wild-type microorganism capable of converting lactose from whey into PHA.

### 6.2.8 Other Wastes

The treatment of wastewaters, comprising liquid wastes discharged by domestic or commercial residences and agricultural activities, was also coupled to the conversion into PHAs. Lemechko et al. (2019) recently reported the production of a P(3HB-co-3HV) copolymer using soybean industry effluents with the addition of valeric acid for tuning the proportion of 3HV into the chains (Lemechko et al. 2019). In a recent study, PHA production was investigated using different microbial strains pre-isolated from sludge collected by different processes and fed with raw wastewaters mainly containing milk, soybean and fruit juice residues (Lam et al. 2017). Despite the low PHA yields achieved by both single and mixed strains cultures, due to the inhibitory effects of the high organic loading, this approach succeeded in reducing drastically COD and BOD of the wastewater. Higher yields of PHB production were, on the other hand, achieved by *A. junii* BP 25 using rice mill

effluent supplemented with some nutrients after a statistical medium optimization using PB and RSM technique (Table 6.2) (Sabapathy et al. 2019).

Waste rice-based ethanol stillage, a distillery spent wash, was proved to be a good substrate for PHA production. It does not contain antibacterial substances like phenolic residues, thus no pretreatment is required, making the process costly competitive. Bhattacharyya et al. (2014) produced and characterized the copolymer P(3HB-co-3HV) obtained by the halophilic strain *H. mediterranei* grown on this waste, obtaining a polymer accumulation of 71% (w/w) and optimizing the recovery and the reuse of the spent saline production medium, which is a possible solution for solving the major bottleneck in the industrial production of PHA by halophilic strains (Bhattacharyya et al. 2014).

Syngas obtained from pyrolysis and gasification of solid municipal wastes was efficiently introduced in chemical platforms for the production of PHA by using microorganisms able to metabolize this gas as C-source and/or energy for growth (Sahoo et al. 2021). Revelles et al. (2017) verified the PHA production from syngas by the photosynthetic microorganism *R. rubrum*, using the microwave-induced pyrolysis (MIP) as an eco-friendly and productive alternative to the standard thermal conversion of solid wastes. The principal by-product of MIP is the carbonaceous solid fraction (char) that can be used as solid fuel or amendment for carbon sequestration according to the biorefinery concept (Revelles et al. 2017).

The anaerobic digestion of solid organic wastes is a pretreatment process which degrades and stabilizes these wastes producing, at the same time, renewable energy in the form of methane and hydrogen. The digestate resulting as by-product of the process, rich of residual nutrients, is usually used as plant fertilizer. An interesting valorization of the digested liquors is their use as feedstock for PHA production. Passanha et al. (2013) set up different growth experiments of *C. necator* on different microfiltered digestates (Passanha et al. 2013). They achieved a major PHA accumulation yield than that obtained in rich media (12 g/L, 90% (w/w)) and they also demonstrated the reusability of the residual media after appropriate removal of biomass and complementation of the consumed nutrients. Another significant example of solid organic wastes revaluation is provided by Mohapatra et al. (2017). They tested for the first time the bioconversion of fish solid waste extract into PHB by using *B. subtilis* (KP172548), in one stage of batch cultivation at industrial scale (Table 6.2).

### 6.3 PHA Production from Mixed Microbial Cultures (MMCs)

In recent years, PHA production by MMCs gained increasing attention due to its inherent advantages. It is a cost-effective strategy, since sterilization of culture media is not required, and control and process operation are facilitated. Moreover, the presence of multiple species broadens the choice of possible feedstocks, as the consortium tends gradually to adapt itself to the carbon source provided each time. Preliminary studies, based on life cycle analysis, revealed that MMCs PHA

production may be more favourable than pure culture in economic as well as environmental terms (Gurieff and Lant 2007).

The MMCs based process for PHA production requires three essential stages: (1) selection of suitable feedstocks; (2) enrichment of MMCs with biopolymer producing microorganisms; (3) PHA production. The most significant examples of MMCs applied to PHA production are reported in Table 6.3.

Unlike most pure cultures, MMCs tend to accumulate glycogen as storing reserve instead of PHA. Therefore, PHA production from food wastes requires a previous transformation of complex organic compounds into short chain volatile fatty acids (VFA), which can be effectively stored as PHA by mixed microbial cultures (Albuquerque et al. 2010a, b). In most cases, VFA production is obtained by an anaerobic acidogenic fermentation and, according to the specific raw materials, different parameters should be taken into account to maximize VFA yields such as pH, temperature, hydraulic retention time, sludge retention time, and organic loading rate (Strazzer et al. 2018). Recently, Luo and co-workers reviewed the possible strategies for enhancing VFA production from waste activated sludge derived from wastewater treatment, including the co-digestion with different substrates and the mechanical, chemical-physical and biological pretreatments. They concluded that the VFA production performances vary considerably with sludge characteristics, thus process parameters should be optimized for each specific co-substrate (Luo et al. 2019). Lee et al. (2014) studied the influence of temperature (30, 40 and 55 °C) on acidogenic fermentation of palm oil mill effluent (POME). Mesophilic conditions (30 and 40 °C) considerably outperformed thermophilic condition (55 °C) revealing acidification degrees of 48% and 7%, respectively (Lee et al. 2014).

Besides influencing the production yield, the anaerobic fermentation conditions also affect the composition of the synthesized polymer. Gouveia et al. (2017) focused on the possibility of tailoring PHA by controlling the acidogenic reactor operating conditions, namely pH, using cheese whey as model feedstock (Gouveia et al. 2017). They operated the acidogenic reactor under dynamic pH change conditions in the range 4.5–7. The variation imposed on pH led to different monomer precursor profiles, which resulted in PHA copolymer with different compositions. Using the same feedstock, through the manipulation of the acidogenic reactor conditions, it was possible to produce PHA with composition in terms of 3HB and 3HV percentage of 70/30, 83/17 and 95/5 at pH values 6, 5 and 4.5, respectively (Gouveia et al. 2017). Similarly, Huang et al. studied the effect of pH and the concentrations of  $\beta$ -cyclodextrin and glycerol on the anaerobic digestion of wasted activated sludge in order to increase the abundance of odd-carbon VFA (Huang et al. 2018).

Although less explored, there are also alternative strategies to acidogenic fermentation for monomer precursor fuelling. Moita Fidalgo et al. (2014) compared the PHAs production performances of MMC from bio-oil, the liquid fraction resulting from pyrolysis processes (Moita Fidalgo et al. 2014). Two strategies for bio-oil upgrade were applied, anaerobic fermentation and vacuum distillation, and the resulting liquid streams were tested for PHA production. The first one was rich in VFA, the second mainly in phenolic and long chain fatty acids. The vacuum distilled

**Table 6.3** PHA production using MMCs

Sludge	Type of fermentation	Waste material	Type of polymer	References
Anaerobic wastewater treatment plant	CSTR subjected to a dynamic pH change	Cheese whey	P (3HB-co-3HV)	Gouveia et al. (2017)
Wasted activated sludge	Batch and semi-continuous reactors	Wasted activated sludge	P (3HB-co-3HV)	Huang et al. (2018)
Activated sludge from wastewater treatment plant	Sequencing batch reactors	Bio-oil (liquid fraction from pyrolysis processes)	P (3HB-co-3HV)	Moita Fidalgo et al. (2014)
Biological nutrient removal (Bardenpho process) sludge	Sequencing batch reactors	Hydrothermal liquors	P (3HB-co-3HV)	Wijeyekoon et al. (2018)
Activated sludge from the municipal wastewater treatment plant	Sequencing batch reactors with pulse and batch feed	Brewery wastewater	P (3HB-co-3HV)	Tamang et al. (2019)
Mixed consortia of <i>Pseudomonas</i> sp.	Sequencing batch reactors	Oil mill wastewater	P (3HB-co-3HO)	Ntaikou et al. (2014)
PHA-accumulating mixed culture acclimatized to the fermented molasses feedstock	CSTR system (acidogenic fermentation) and sequencing batch reactors	Sugar molasses	P (3HB-co-3HV)	Albuquerque et al. (2010b)
Sludge from a full-scale anaerobic digester operated in continuous mode under anaerobic conditions for a period of over 2 years	2-stage CSTR system (acidogenic fermentation and culture enrichment); batch reactor (PHA production)	Sugar molasses	P (3HB-co-3HV)	Albuquerque et al. (2010a)
Activated sludge from the "Roma Nord" (Italy) full-scale municipal treatment plant	<i>Sequencing batch reactors</i>	Olive oil mill wastewater	P (3HB-co-3HV)	Campanari et al. (2014)
Activated sludge taken from a long-term operating parent SBR	Sequencing batch reactors	Food waste fermentation leachate	P (3HB-co-3HV)	Wen et al. (2018)
Heterotrophic aerobic bacterium from a facultative anaerobic pond of POME and sludge from a waste stabilization pond	Bio-PORec <sup>®</sup>	Palm oil mill effluent	P3HB	Md Din et al. (2012)

(continued)

**Table 6.3** (continued)

Sludge	Type of fermentation	Waste material	Type of polymer	References
Aerobic consortia acquired from an operating activated sludge process (ASP) treating ten MLD of composite wastewater from domestic and industrial processes	Sequencing batch reactors under aerobic and anoxic microenvironments	Food waste and effluent from acidogenic biohydrogen production process	P (3HB-co-3HV)	Venkateswar Reddy and Venkata Mohan (2012)
Phototrophic mixed cultures	CSTR system (acidogenic fermentation), phototrophic selector reactor (MMC selection), batch reactor (PHA production)	Fermented cheese whey	P (3HB-co-3HV)	Fradinho et al. (2019)
Activate sludge	CSTR system (acidogenic fermentation), sequencing batch reactors (MMC selection), fed batch (PHA production)	Cheese whey and sugarcane molasses	P (3HB-co-3HV)	Duque et al. (2014)

bio-oil was not as effective as the digested one since it favoured growth instead of PHA production (Moita Fidalgo et al. 2014).

Wijeyekoon et al. (2018) tested, for the first time, the oxidative hydrothermal liquors from wet oxidation of organic residues for PHA production. They selected two sources of organic biomass, municipal wastewater sludge and food waste to subject to sub-critical wet oxidation to convert organic material into VFA, particularly acetic acid (Wijeyekoon et al. 2018). The enriched culture produced up to 41% of a PHA copolymer (77% Polyhydroxybutyrate (PHB) and 23% Polyhydroxyvalerate (PHV)) (w/w). Similarly, Tamang et al. (2019) investigated the potentiality of acidified brewery wastewater, compared to the anaerobically treated one, as carbon source for PHA production by an enriched MMC. They reported a similar maximum of PHA production in optimized conditions for both wastewaters (45% (w/w)), in spite of the higher VFA concentration in acidified brewery wastewaters (Tamang et al. 2019). Ntaikou et al. (2014) applied a clarification step, based on aluminium sulphate to induce flocculation and precipitation of solids, to the acidified oil mill wastewater. The treated waste was then tested for PHA production from a *Pseudomonas* sp. enriched culture. Although

clarification had no direct effect on the profile of the produced VFA, it positively affected PHA production, altering the values of total suspended solids and total chemical oxygen demand (Ntaikou et al. 2014).

The most common approach for enriching a mixed culture with the PHA-storing phenotype was through an aerobic dynamic feeding (ADF), called “Feast and Famine”: this process configuration originates periods of excess (Feast) and lack (Famine) of external carbon substrate, resulting in the selection of microbial populations with an enhanced capacity to store PHA.

In the MMC-based process, culture selection/enrichment and PHA production occur in different Sequencing Batch Reactors (SBR), operated independently (different optimum conditions—namely different nutrient concentrations—were shown to favour each step). Through optimization of the culture enrichment stage, Albuquerque et al. (2010b) were able to achieve 74% PHA content (w/w) in batch production stage using fermented molasses as feedstock fermentation (Albuquerque et al. 2010a, b). The same research group also investigated the possibility to operate the culture enrichment in a 2-stage continuous stirred tank reactor (CSTR) under feast and famine conditions. The effect of inlet VFA concentration and hydraulic retention times (HRT) of the first and second reactors on system’s selection efficiency was tested. It was shown that the feast reactor residual substrate concentration affected the selective pressure for PHA storage (Albuquerque et al. 2010a).

Once the starting inoculum was enriched with a consortium with high PHA-storing capacity, according to the selected feedstock, process parameters have been optimized for biopolymer production. Campanari et al. (2014) studied the effect of organic loading rates (OLR) ranging from 2.40 to 8.40 gCOD/(Ld) in MMC PHA production using dephenolized OMW (Campanari et al. 2014). Wen et al. (2018) reported the effect of sodium chloride concentration on PHA production from food waste fermentation leachate under different (OLR) (1.35–8.43 gCOD/(Ld) (Wen et al. 2018). Also, the micro-environment aeration is crucial for PHA yield as reported by Md Din et al. (2012) for production of PHA from POME and Venkateswar Reddy and Venkata Mohan (2012) for production of PHA from food waste and effluent from acidogenic biohydrogen production process (Md Din et al. 2012; Venkateswar Reddy and Venkata Mohan 2012).

PHA production with MMCs enriched by ADF limits the exploitability to only aerobic organisms, while the diversity of bacterial species that can produce and accumulate PHA is much wider. Fradinho et al. (2019) developed a different enrichment strategy based on an anaerobic permanent feast. In anaerobic conditions, the organisms must activate internal mechanisms to oxidize reduced molecules produced during cell metabolism (like NADH, NADPH). One of these mechanisms is based on the accumulation of PHA that requires the reduction of monomer precursors during its synthesis (Fig. 6.1). Therefore, the permanent feast strategy allowed the selection of microorganisms able to regulate internal reducing power via PHA production. The authors tested the selected Phototrophic Mixed Culture (PMC) for PHA production from fermented cheese whey and obtained a biopolymer with a 3HV content of 12%. Interestingly, the used light intensities (20 W/L) opened up the

possibility for direct sunlight illumination for processes carried out in sunny regions (Fradinho et al. 2019).

A common problem to all MMC process from wastes or by-product is the seasonal availability of the feedstock. Duque et al. (2014) developed a system operating with two feedstocks with different annual availability (cheese whey and sugarcane molasses). The two raw materials induce different VFA profile during biological conversion. By mixing the two feedstocks in defined volume proportions, polymers with target compositions were achieved (Duque et al. 2014).

## 6.4 Engineered Strains for PHA Production

Genetic approaches have been widely applied to improve the performance of microorganisms potentially exploitable for PHA production process (Favaro et al. 2018). A huge of examples have been described in the last decade, focusing on different aspects: (1) optimizing PHA yield in native PHA producers, through host cell genome manipulation and/or recombinant gene expression; (2) introducing catabolic operons to allow metabolization of new C-sources in native PHA producers; (3) conferring PHA producing abilities to non-native producers endowed with advantageous metabolic/physiological features, i.e. halophilic bacteria, microorganisms naturally able to metabolize complex C-sources; (4) modulating PHA composition acting on precursors supplying pathways (Favaro et al. 2018). Engineering strategies were also adopted to design microbial factories able to convert different food wastes into PHAs (Table 6.4).

Cheese whey is a potential carbon source for PHA production, being rich in lactose, lipids and soluble proteins. However, only a limited number of wild-type microorganisms is able to metabolize lactose: among them, *Escherichia coli* has been the main object of genetic manipulation. This host is also attractive due to the absence of enzymes for PHA degradation and the easiness of polymer downstream processing (Reddy et al. 2003). *E. coli* was engineered to efficiently produce PHB from cheese whey by recombinant expression of the PHA biosynthetic operon from *Alcaligenes latus* (Lee et al. 1997; Woo Suk Ahn et al. 2000) and *C. necator* (Pais et al. 2014). In the latter example, implementation of PHB production was achieved by generating *E. coli* mutants with reduced organic acid production capacity with the aim to direct the strain's metabolism towards biopolymer synthesis. The selected mutant displayed the highest reduction in organic acid synthesis coupled to an almost threefold increase of PHB yield with respect to the original *E. coli* strain (Pais et al. 2014).

Among natural PHA producers, *C. necator* was engineered with the *E. coli lac* operon to allow lactose utilization using cheese whey as carbon feedstock. Interestingly, the *lac* genes were introduced within an intracellular depolymerase coding gene (*phaZ1*) achieving its inactivation. Disruption of *phaZ1* ensured lower PHB degradation and higher polymer yield compared to the wild-type strain (Povolo et al. 2010).

**Table 6.4** Engineering strategies for waste valorization into PHA

Strain	Engineering/gene targets	Waste material	Type of polymer	References
<i>C. necator</i> DSM 545	<i>phaZ</i> depolymerase inactivation Insertion of <i>E. coli lacZ</i> , <i>lacI</i> , <i>lacO</i> genes for lactose utilization	Cheese whey	PHB	Povolo et al. (2010)
<i>C. necator</i> H16	Replacement of endogenous <i>phaC</i> with <i>Aeromonas caviae phaC</i>	Waste cooking oils	P (3HB-co-3HHx)	Kamilah et al. (2013)
<i>C. necator</i> H16	Improved activities of enzymes involved in oxidative stress response	Waste frying oils	P (3HB-co-3HV)	Obruca et al. (2013)
<i>E. coli</i> CML3-1	Recombinant expression of <i>C. necator phaABC</i> operon Reduced synthesis of organic acids	Cheese whey	PHB	Pais et al. (2014)
<i>Delftia acidovorans</i> DSM39	Recombinant expression of <i>Pseudomonas stutzeri</i> BT3 lipase genes <i>lipC</i> and <i>lipH</i>	Agricultural fatty by-products	P (3HB-co-4HB)	Romanelli et al. (2014)
<i>E. coli</i> SKB99	Recombinant expression of: <i>Panibacillus</i> sp. amylase coding gene and <i>R. eutropha phaABC</i> operon	Starch	PHB	Bhatia et al. (2015)
<i>R. eutropha</i> H16	Recombinant expression of: <i>scl-mcl</i> -PHA synthase from <i>Rhodococcus aetherivorans</i> and <i>P. aeruginosa phaJ</i>	Waste animal fats and waste frying oils	P (3HB-co-3HHx)	Riedel et al. (2015)
<i>R. eutropha</i> NCIMB11599	Recombinant expression of <i>E. coli xylA</i> (xylose isomerase) and <i>xylB</i> (xylulokinase)	Hydrolysate solution of sunflower stalk	PHB	Kim et al. (2016)
<i>E. coli</i>	Recombinant expression of: mutated <i>Pseudomonas</i> sp.61-3 <i>phaCIPs</i> (ST/QK) (lactic acid polymerizing enzyme); <i>Megasphaera elsdenii</i> propionyl-CoA-transferase; <i>R. eutropha phaA</i> and <i>phaB</i>	Lignocellulosic waste (hydrolysate from woody extract)	P(LA-co-3HB)	Takisawa et al. (2017)
<i>Burkholderia sacchari</i>	Recombinant expression of endogenous <i>xylA</i> (xylose isomerase) and <i>xylB</i> (xylulokinase)	Xylose	PHB	Guamán et al. (2018)
<i>R. eutropha</i> Re2133/pCB81	Deletion of endogenous <i>phaB</i> Replacement of endogenous <i>phaC</i> with <i>Rhodococcus aetherivorans phaC2</i>	Food waste ferment	P (3HB-co-3HHx)	Bhatia et al. (2019)
<i>Pseudomonas putida</i> KT2440	Deletion of <i>tctA</i> (tricarboxylate transporter coding gene)	Waste vegetable oil	mcl-PHA	Borrero-de Acuña et al. (2019)

Similar approaches were applied to design microbial strains able to utilize carbon sources potentially derivable from food wastes (Bhatia et al. 2015; Takisawa et al. 2017; Kim et al. 2016; Guamán et al. 2018). Starch, for example, is a renewable carbon source, available in large quantities in waste bread or mixed domestic wastes (Tsang et al. 2019). An *E. coli* strain expressing the PHB synthetic genes from *R. eutropha* was transformed with a functional amylase coding gene from *Panibacillus* sp. to achieve PHB accumulation utilizing starch as the sole carbon source (Bhatia et al. 2015). Lignocellulosic wastes are the most abundant resources on earth, representing a promising substrate for PHA producing platforms. Xylose is the major components of the hydrolysed lignocellulose, thus engineering approaches were applied to transfer the *E. coli* xylose catabolic genes *xylAB* (coding for xylose isomerase and xylulokinase) to a native PHA producer, such as *R. eutropha* (Kim et al. 2016). The recombinant strain accumulated PHB from both xylose and glucose/xylose containing media and achieved high biopolymer yields when tested on the hydrolysate solution of sunflower stalks, as a model lignocellulosic biomass. Similarly, overexpression of the endogenous xylose assimilation operon in *B. sacchari*, a non-model bacterium with high capacity for PHB accumulation, proved to be an effective strategy to improve both xylose utilization and PHB yield (Guamán et al. 2018).

An important target of strain engineering is the modulation of polymer composition, aimed at the incorporation of mcl monomers in the synthesized PHA. In fact, the incorporation of mcl units within scl-mcl copolymer was shown to positively affect material properties, reducing stiffness and brittleness which characterize PHB polymers. Two main approaches were pursued: (1) altering the specificity of PHA synthetic enzymes towards mcl-precursors; (2) engineering metabolic routes promoting the activation of the pathways fuelling mcl-precursors ( $\beta$ -oxidation and synthesis of fatty acids). These strategies, either individually or in combination, were applied to bioprocesses fed with different wastes. In particular, WFOs, a source of fatty acids, cheap and widely available, were investigated by many authors as a starting feedstock for PHA producing bioprocesses. In one of the early examples, Kamilah and co-workers engineered *C. necator* by replacing the endogenous scl-specific PhaC synthase with a PHA synthase gene of *A. caviae* endowed with different specificity. When the recombinant strain was fed with WFOs and a properly selected nitrogen source, it produced a P(3HB-co-3HHx) copolymer, while the wild type accumulated only PHB (Kamilah et al. 2013). A similar approach was applied to construct a *R. eutropha* mutant expressing a scl/mcl-PHA<sub>1</sub> synthase from *R. aetherivorans*, favouring the synthesis of P(HB-co-3HHx), together with an enoyl-CoA hydratase gene (*phaI*) from *P. aeruginosa*. The combination of both genetic modifications allowed to boost the incorporation of HHx moieties in the copolymer synthesized using waste animal fats as inexpensive raw material (Riedel et al. 2015). On the other hand, a random chemical mutagenesis was applied to *C. necator* to select for the variants with the best producing performances from waste frying oils. The selected mutant displayed not only the ability to produce polymer with improved yields, but also an increased incorporation of 3HV in the final copolymer (Obruca et al. 2013). The authors characterized some phenotypic traits

of the mutant, coming to the hypotheses that the increased NADPH/NADP levels observed in the mutant may support polymer accumulation, the highest activity of malic enzyme may reduce the availability of oxaloacetate for the utilization of propionyl-CoA in 2-methylcitrate cycle, thus resulting in more propionyl-CoA available for incorporation into the copolymer (Obruca et al. 2013).

More recently, implementation of PHA production yield from waste vegetable oils was achieved in a natural mcl-PHA producer, *P. putida* KT2440, by knocking out the *tctA* (tricarboxylate transporter) gene, coding for the key transport enzyme of carboxylic acids. The inactivation of the transport systems for these preferred carbon sources resulted in a nearly twofold increment in the mcl-PHA volumetric productivity with respect to the wild-type strain (Borrero-de Acuña et al. 2019). In order to combine the native ability of *D. acidovorans* DSM39 to incorporate 4-hydroxybutyrate (4HB) monomer with the valorization of agricultural fatty by-products (udder, lard and tallow), this strain, unable to grow on fatty substrates, was engineered with *lip* genes from *P. stutzeri* BT3. The recombinant strain proved to be able to accumulate P3HB-P4HB copolymer directly from slaughterhouse residues without the supplementation of any precursor (Romanelli et al. 2014).

Furthermore, examples of copolymers synthesized from non-fatty wastes were reported. Taking advantage of the *E. coli* abilities to metabolize both xylose and galactose derived from woody-extract hemicellulosic hydrolysate, Takisawa et al. designed a microbial cell factory for the production of P(LA-co-3HB) copolymer from lignocellulosic feedstock (Takisawa et al. 2017). To this aim, the authors carried out a fine *E. coli* engineering, developing a recombinant strain that expressed, besides *PhaA* and *PhaB* from *R. eutropha*, a propionyl-CoA transferase (PCT) from *Megasphaera elsdenii* able to catalyse Coenzyme A addition to lactic acid, and a mutated PHA synthase from *Pseudomonas* sp. 61-3 endowed with the ability to polymerize lactoyl-CoA precursor (Yang et al. 2011). In another example, Bhatia et al. (2019) applied a tailor-made designed *R. eutropha* strain to the production of P(3HB-co-3HHx) copolymer from anaerobically digested food waste derived volatile fatty acids (Bhatia et al. 2019). The strain was engineered with a deletion of the acetoacetyl-CoA reductase (*PhaB*) and a replacement of the native PHA synthase with *phaC2* from *R. aetherivorans*, characterized by a high specificity towards mcl-PHA precursors (Jeon et al. 2014). A response surface design study showed that in mixtures, butyrate is the main organic acid involved in PHA production, acting as precursor for 3HHx monomer (Bhatia et al. 2019), without the addition of any additional precursor for mcl-monomer units.

## 6.5 Biorefinery-Inspired Approaches for PHA Production

Despite the huge attempts made over the past decades to design sustainable and cost-competitive PHA-based bioprocess, large-scale production of PHA is still limited due to the cost of substrates and of recovery processes (Rodriguez-Perez et al. 2018). The use of agro-food wastes was estimated to reduce PHA production cost up to 50%, and several attempts in this direction have been discussed in this chapter. In

**Table 6.5** Examples of waste valorization processes for co-production of PHA with other compounds

Strain	Co-product	Waste material	References
<i>P. aeruginosa</i> IFO3924	Rhamnolipid	Palm oil	Marsudi et al. (2008)
<i>Rhodobacter sphaeroides</i> O.U.001	Biohydrogen	Olive mill wastewater (OMW)	Eroğlu et al. (2008)
<i>P. aeruginosa</i> L2-1	Rhamnolipid	Cassava wastewater/waste cooking oil	Costa et al. (2009)
<i>P. aeruginosa</i> 7a	Rhamnolipid	Waste cooking oil	Costa et al. (2009)
<i>Sinorhizobium meliloti</i> MTCC100	EPS	Rice bran hydrolysate	Saranya Devi et al. (2012)
<i>Bacillus</i> sp. CFR-67	$\alpha$ -amylase	Wheat and rice bran hydrolysates	Shamala et al. (2012)
<i>Bacillus</i> sp. CFR-67	$\alpha$ -amylase	Wheat and rice bran hydrolysates	Sreekanth et al. (2013)
<i>Bacillus thuringiensis</i> IAM 12077	$\alpha$ -amylase	Nine agriculture/food wastes	Gowda and Shivakumar (2014)
<i>Bacillus cereus</i> EGU43	Biohydrogen	Pea shell slurry	Patel et al. (2015)
<i>Rhodopseudomonas palustris</i> sp.	Biohydrogen	Olive mill wastewater (OMW)	Padovani et al. (2016)
<i>Rhodobacter capsulatus</i> ATCC17015	Biohydrogen	Fruit/vegetable wastes	Montiel Corona et al. (2017)
<i>Burkholderia thailandensis</i>	Rhamnolipid	Used cooked oil	Kourmentza et al. (2018)
<i>Paracoccus</i> sp. LL1	Astaxanthin	Waste cooking oil	Kumar and Kim (2019)
MMC	Biohydrogen	Dairy waste streams	Colombo et al. (2019)
Recombinant <i>E. coli</i> <i>Pseudomonas resinovorans</i>	Biodiesel	Waste frying oils	Vastano et al. (2019)

view of a zero-waste policy, the efficient exploitation of resources is crucial to support the sustainability of the process. In this regard, designing systems for the production of multiple products would boost process competitiveness by further lowering manufacturing costs and assuring a more efficient utilization of raw materials (Li et al. 2017). Several examples of co-production of PHA with other value-added products (amino acids, proteins, alcohols, hydrogen, biosurfactants, exopolysaccharides) have been described in the recent literature (Kumar et al. 2018). It is worth to note that PHA synthesis is strictly related to energy and carbon metabolism, thus it was shown to positively affect the production of other cellular metabolites, i.e. amino acids, or more generally, all the products connected with cellular oxidation/reduction balance (Li et al. 2017). From an economical and technical point of view, the most advantageous processes are those which couple an optimized accumulation of intracellular PHA together with the recovery of extracellular products.

Few examples of multi-product processes starting from agro-food wastes were reported (Table 6.5). The simultaneous production of PHA and biosurfactants, amphiphilic compounds able to decrease surface tension, was achieved in several bioprocess fed with waste oils. Among biosurfactants, rhamnolipids have attracted interests since they are produced in large quantities by microbial fermentation, especially in the presence of hydrophobic substrates, as a strategy to enhance bioavailability of the C-source (Kourmentza et al. 2018). In addition, their recovery as extracellular products are relatively easy, thus increasing process feasibility. Different *P. aeruginosa* strains displayed a wide range of PHA and rhamnolipids yields when grown in the presence of various raw materials (waste oils, cassava wastewater and palm oil). However, the use of these opportunistic pathogens represents a limiting factor for the process. More recently, Kourmentza et al. (2018) isolated a non-pathogenic strain of *Burkholderia thailandensis*, able to co-produce high yields of PHB and rhamnolipids using waste cooking oil as low-cost carbon source (Kourmentza et al. 2018).

Exopolysaccharides (EPS) are polymers secreted by several bacteria under stress conditions, with the aim to protect the cells and provide energy source under adverse conditions. The concurrent synthesis of both PHA and EPS polymers was observed in many microorganisms, since their accumulation is triggered by quite similar environmental stimuli (Kumar and Kim 2018). Supplementation of growth medium with rice bran hydrolysate was found to enhance the co-production of both PHA and EPS in *S. meliloti* MTCC100 (Saranya Devi et al. 2012).

In a PHA production process coupled to the synthesis of a co-product, the higher market value the co-product has, the more economically attractive will be the process. This is the case of compounds belonging to carotenoids such as adonixanthin, astaxanthin,  $\beta$ -carotene, etc., characterized by very high market value (about US\$2000/kg). Few photosynthetic and dark-fermentative bacteria were reported to produce pigments together with PHA and/or  $H_2$  (Kumar et al. 2018). *R. sphaeroides*, grown on oil mill wastewater (OMW) produced  $H_2$ , coupled to both PHA and carotenoids (Eroğlu et al. 2008). When fed with waste cooking oil as substrate, the halophilic strain of *Paracoccus* sp. LL1 co-generated the copolymer P(3HB-co-HV) together with high yields of astaxanthin-rich carotenoids. Additionally, these co-products were secreted in the form of vesicles, with a further advantage to the recovery process (Kumar and Kim 2019; Kumar et al. 2018).

Process sustainability is also encouraged when inexpensive waste feedstocks are used to support the co-generation of PHA with bioproducts characterized by high large-scale production costs, i.e. microbial enzymes. Besides accumulating a P(3HB-co-HV) copolymer, *Bacillus* sp. CFR-67 was found to produce high titres of  $\alpha$ -amylase, an industrially relevant enzyme, when grown on a mixture of wheat bran and/or rice bran hydrolysates supplemented with corn starch and ammonium acetate (Shamala et al. 2012; Sreekanth et al. 2013). On the other hand, the intrinsic  $\alpha$ -amylase production by *B. thuringiensis* IAM 12077 was explored to support the hydrolysis of nine different agriculture and food wastes (rice husk, wheat bran, ragi husk, jowar husk, jackfruit seed powder, mango peel, potato peel, bagasse and straw). The enzymatically treated substrates promoted PHB accumulation at levels

comparable to that of the acid-hydrolysed ones, thus supporting the one-step biomass pretreatment and PHB production process (Gowda and Shivakumar 2014).

Several native isolates, mainly photosynthetic and dark-fermentative bacteria, were reported to co-produce biohydrogen and PHA in response to different culture conditions (Padovani et al. 2016; Montiel Corona et al. 2015, 2017; Patel et al. 2015). A dark-fermentation effluent from fruit and vegetable wastes was tested as substrate for the simultaneous production of H<sub>2</sub> and PHA (Montiel Corona et al. 2017). Among the tested microorganisms, *R. capsulatus* achieved an increase in PHB production and H<sub>2</sub>, when light-dark cycles were applied in alternative to continuous illumination, with also a benefit in terms of saved energy (Montiel Corona et al. 2017). A more advantageous process to couple PHA with H<sub>2</sub> production was achieved through a two-step system employing mixed microbial cultures (MMC) and two dairy waste streams coming from cheese whey deproteinization. During the first step, dark fermentation of the sugar content of the wastes resulted in high daily H<sub>2</sub> volume, together with production of organic acids. The latter were used in the second step, as substrates for aerobic PHA production, reaching high conversion yields and PHA accumulation for both the fermented dairy streams (Colombo et al. 2019).

Finally, an original example of waste frying oil conversion into two added-value products, i.e. PHA and biodiesel, was recently reported by Vastano et al. (2019). The authors used a WFO with a high content of free fatty acids (FFAs), unsuitable for direct transesterification into biodiesel, to design a process aimed at (1) reducing the FFAs content allowing its conversion into biodiesel and (2) simultaneously producing PHA. The bioprocess was verified using both recombinant (*E. coli*) and native (*P. resinovorans*) PHAs producing cell factories. Proper strain designing and process optimization allowed to address the FFAs into PHA metabolism, achieving up to 1.5 g L<sup>-1</sup> of mcl-PHAs, together with an efficient conversion (80% (w/w) yield) of the treated WFO into biodiesel (Vastano et al. 2019).

---

## 6.6 Conclusion and Perspectives

The current state of the art about “food waste conversion to PHA” depicted in this chapter highlights the main strengths and weaknesses of the process. The principal hurdles to waste exploitation are related to their availability and/or to the necessity to store them properly, anticipating their seasonal shortage. Furthermore, the variability in waste composition may influence process productivity as well as polymer recovery. In this regard, monitoring the quality of the wastes and how it impacts on process performances would be useful to define the crucial process variables and to develop strategies to cope with them.

Although representing a green alternative to petroleum-derived plastics, PHA exploitation is still limited by the high costs related to its large-scale production. The use of waste materials allows to reduce the overall cost, but the production process is still not economically competitive. A winning strategy seems to be to design processes, which combine the production of PHA with that of other added-value

compounds. PHA synthetic pathway is centred on acetyl-CoA, a connecting link of the majority of the biomolecule synthetic pathways, thus co-production of any metabolite with PHA must balance the overall cellular metabolic flux. This implies a strict optimization of process conditions and subtle strain designing, in order to avoid competition for the main substrate. Protein engineering together with mathematical model analyses will represent powerful tools to get insight into the metabolic fluxes underlying multi-products processes, and to identify the main targets for performance improvement.

In conclusion, the conversion of food wastes into PHA represents a very promising possibility to face both waste disposal and biopolymer production from renewable sources. The future in this field will rely on the integration of polymer production within a “Waste Biorefinery” aimed at valorizing wastes as renewable feedstocks to recover biobased products and energy, in line with the concept of circular economy-based process.

## References

- Ahn WS, Park SJ, Lee SY (2000) Production of poly(3-hydroxybutyrate) by fed-batch culture of recombinant *Escherichia Coli* with a highly concentrated whey solution. *Appl Environ Microbiol* 66(8):3624–3627. <https://doi.org/10.1128/AEM.66.8.3624-3627.2000>
- Albuquerque MGE, Concas S, Bengtsson S, Reis MAM (2010a) Mixed culture Polyhydroxyalkanoates production from sugar molasses: the use of a 2-stage CSTR system for culture selection. *Bioresour Technol* 101(18):7112–7122. <https://doi.org/10.1016/j.biortech.2010.04.019>
- Albuquerque MGE, Torres CAV, Reis MAM (2010b) Polyhydroxyalkanoate (PHA) production by a mixed microbial culture using sugar molasses: effect of the influent substrate concentration on culture selection. *Water Res* 44(11):3419–3433. <https://doi.org/10.1016/j.watres.2010.03.021>
- Aldor IS, Keasling JD (2003) Process design for microbial plastic factories: metabolic engineering of Polyhydroxyalkanoates. *Curr Opin Biotechnol* 14(5):475–483. <https://doi.org/10.1016/j.copbio.2003.09.002>
- Alsafadi D, Al-Mashaqbeh O (2017) A one-stage cultivation process for the production of poly-3-(hydroxybutyrate-co-hydroxyvalerate) from olive mill wastewater by *Haloflex mediterranei*. *New Biotechnol* 34:47–53. <https://doi.org/10.1016/j.nbt.2016.05.003>
- Aneesh BP, Arjun JK, Kavitha T, Harikrishnan K (2016) Production of short chain length polyhydroxyalkanoates by *Bacillus megaterium* PHB29 from starch feed stock. *Int J Curr Microbiol App Sci* 5(7):816–823. <https://doi.org/10.20546/ijcmas.2016.507.094>
- Annamalai N, Sivakumar N (2016) Production of polyhydroxybutyrate from wheat bran hydrolysate using *Ralstonia eutropha* through microbial fermentation. *J Biotechnol* 237:13–17. <https://doi.org/10.1016/j.jbiotec.2016.09.001>
- Bhatia SK, Shim YH, Jeon JM, Brigham CJ, Kim YH, Kim HJ, Seo HM et al (2015) Starch based polyhydroxybutyrate production in engineered *Escherichia coli*. *Bioprocess Biosyst Eng* 38(8):1479–1484. <https://doi.org/10.1007/s00449-015-1390-y>
- Bhatia SK, Gurav R, Choi TR, Jung HR, Yang SY, Song HS, Jeon JM, Kim JS, Lee YK, Yang YH (2019) Poly(3-hydroxybutyrate-co-3-hydroxyhexanoate) production from engineered *Ralstonia eutropha* using synthetic and anaerobically digested food waste derived volatile fatty acids. *Int J Biol Macromol* 133:1–10. <https://doi.org/10.1016/j.ijbiomac.2019.04.083>
- Bhattacharyya A, Saha J, Haldar S, Bhowmic A, Mukhopadhyay UK, Mukherjee J (2014) Production of poly-3-(hydroxybutyrate-co-hydroxyvalerate) by *Haloflex mediterranei* using

- rice-based ethanol stillage with simultaneous recovery and re-use of medium salts. *Extremophiles* 18(2):463–470. <https://doi.org/10.1007/s00792-013-0622-9>
- Borrero-de Acuña J, Aravena-Carrasco C, Gutierrez-Urrutia I, Duchens D, Poblete-Castro I (2019) Enhanced synthesis of medium-chain-length poly(3-hydroxyalkanoates) by inactivating the tricarboxylate transport system of *Pseudomonas putida* KT2440 and process development using waste vegetable oil. *Process Biochem* 77:23–30. <https://doi.org/10.1016/j.procbio.2018.10.012>
- Bustamante D, Segarra S, Tortajada M, Ramón D, del Cerro C, Auxiliadora Prieto M, Iglesias JR, Rojas A (2019) In silico prospection of microorganisms to produce polyhydroxyalkanoate from whey: *Caulobacter segnis* DSM 29236 as a suitable industrial strain. *Microb Biotechnol* 12(3):487–501. <https://doi.org/10.1111/1751-7915.13371>
- Campanari S, Silva FAE, Bertin L, Villano M, Majone M (2014) Effect of the organic loading rate on the production of Polyhydroxyalkanoates in a multi-stage process aimed at the valorization of olive oil mill wastewater. *Int J Biol Macromol* 71:34–41. <https://doi.org/10.1016/j.ijbiomac.2014.06.006>
- Cerrone F, Sánchez-Peinado M d M, Juárez-Jimenez B, González-López J, Pozo C (2010) Biological treatment of two-phase olive mill wastewater (TPOMW, Alpeorujo): polyhydroxyalkanoates (PHAs) production by *Azotobacter* strains. *J Microbiol Biotechnol* 20(3):594–601. <https://doi.org/10.4014/jmb.0906.06037>
- Cesário MT, Raposo RS, de Almeida MCMD, van Keulen F, Ferreira BS, da Fonseca MMR (2014) Enhanced bioproduction of poly-3-hydroxybutyrate from wheat straw lignocellulosic hydrolysates. *New Biotechnol* 31(1):104–113. <https://doi.org/10.1016/j.nbt.2013.10.004>
- Chaudhry WN, Jamil N, Ali I, Ayaz MH, Hasnain S (2011) Screening for polyhydroxyalkanoate (PHA)-producing bacterial strains and comparison of PHA production from various inexpensive carbon sources. *Ann Microbiol* 61(3):623–629. <https://doi.org/10.1007/s13213-010-0181-6>
- Chen G, Hajnal I (2015) The ‘PHAome’. *Trends Biotechnol* 33(10):559–564. <https://doi.org/10.1016/j.tibtech.2015.07.006>
- Chen GQ, Jiang XR (2017) Engineering bacteria for enhanced polyhydroxyalkanoates (PHA) biosynthesis. *Synth Syst Biotechnol* 2(3):192–197. <https://doi.org/10.1016/j.synbio.2017.09.001>
- Chen CW, Don TM, Yen HF (2006) Enzymatic extruded starch as a carbon source for the production of poly(3-hydroxybutyrate-co-3-hydroxyvalerate) by *Haloferax mediterranei*. *Process Biochem* 41(11):2289–2296. <https://doi.org/10.1016/j.procbio.2006.05.026>
- Colombo B, Calvo MV, Sciarria TP, Scaglia B, Kizito SS, D’Imporzano G, Adani F (2019) Biohydrogen and polyhydroxyalkanoates (PHA) as products of a two-steps bioprocess from deproteinized dairy wastes. *Waste Manag* 95:22–31. <https://doi.org/10.1016/j.wasman.2019.05.052>
- Costa SGVAO, Lépina F, Milot S, Déziel E, Nitschke M, Contiero J (2009) Cassava wastewater as a substrate for the simultaneous production of rhamnolipids and polyhydroxyalkanoates by *Pseudomonas aeruginosa*. *J Ind Microbiol Biotechnol* 36(8):1063–1072. <https://doi.org/10.1007/s10295-009-0590-3>
- Cruz MV, Paiva A, Lisboa P, Freitas F, Alves VD, Simões P, Barreiros S, Reis MAM (2014) Production of polyhydroxyalkanoates from spent coffee grounds oil obtained by supercritical fluid extraction technology. *Bioresour Technol* 157:360–363. <https://doi.org/10.1016/j.biortech.2014.02.013>
- Cruz MV, Freitas F, Paiva A, Mano F, Dionísio M, Ramos AM, Reis MAM (2016) Valorization of fatty acids-containing wastes and byproducts into short- and medium-chain length polyhydroxyalkanoates. *New Biotechnol* 33(1):206–215. <https://doi.org/10.1016/j.nbt.2015.05.005>
- Dionisi D, Carucci G, Papini MP, Riccardi C, Majone M, Carrasco F (2005) Olive oil mill effluents as a feedstock for production of biodegradable polymers. *Water Res* 39(10):2076–2084. <https://doi.org/10.1016/j.watres.2005.03.011>
- Duque AF, Oliveira CSS, Carmo ITD, Gouveia AR, Pardelha F, Ramos AM, Reis MAM (2014) Response of a three-stage process for PHA production by mixed microbial cultures to feedstock

- shift: impact on polymer composition. *New Biotechnol* 31(4):276–288. <https://doi.org/10.1016/j.nbt.2013.10.010>
- Eroğlu I, Tabanoğlu A, Gündüz U, Eroğlu E, Yücel M (2008) Hydrogen production by *Rhodobacter sphaeroides* O.U.001 in a flat plate solar bioreactor. *Int J Hydrog Energy* 33(2):531–541. <https://doi.org/10.1016/j.ijhydene.2007.09.025>
- Essel R, Carus M (2012) Meta-analysis of 30 LCAs. *Bioplastics Magazine* 7(2):46–49. <https://doi.org/10.1186/1742-6405-6-12>
- Favaro L, Basaglia M, Casella S (2018) Improving polyhydroxyalkanoate production from inexpensive carbon sources by genetic approaches: a review. *Biofuels Bioprod Biorefin* 13:208–227. <https://doi.org/10.1002/bbb.1944>
- Follonier S, Goyder MS, Silvestri AC, Crelier S, Kalman F, Riesen R, Zinn M (2014) Fruit pomace and waste frying oil as sustainable resources for the bioproduction of medium-chain-length polyhydroxyalkanoates. *Int J Biol Macromol* 71:42–52. <https://doi.org/10.1016/j.ijbiomac.2014.05.061>
- Fradinho JC, Oehmen A, Reis MAM (2019) Improving polyhydroxyalkanoates production in phototrophic mixed cultures by optimizing accumulator reactor operating conditions. *Int J Biol Macromol* 126:1085–1092. <https://doi.org/10.1016/j.ijbiomac.2018.12.270>
- Gamal RF, Hassan E, El-tayeb T, Abou-taleb K (2011) Production of polyhydroxyalkanoate (PHAs) and copolymer [P(HB-co-HV)] by soil bacterial isolates in batch and two-stage batch cultures. *Egypt J Microbiol* 46(1):109–123. <https://doi.org/10.21608/ejm.2011.266>
- Gamal RF, Hassan EA, El-tayeb TS, Abou-taleb KA (2012) Production of PHAs from waste frying oil by *Pseudomonas fluorescens* S48 using different bioreactor feeding strategies. *Egypt J Microbiol* 47(1):1–15. <https://doi.org/10.21608/ejm.2012.249>
- Gamal RF, Abdelhady HM, Khodair TA, El-Tayeb TS, Hassan EA, Aboutaleb KA (2013) Semi-scale production of PHAs from waste frying oil by *Pseudomonas fluorescens* S48. *Braz J Microbiol* 44(2):539–549. <https://doi.org/10.1590/S1517-83822013000200034>
- Gouveia AR, Freitas EB, Galinha CF, Carvalho G, Duque AF, Reis MAM (2017) Dynamic change of PH in acidogenic fermentation of cheese whey towards polyhydroxyalkanoates production: impact on performance and microbial population. *New Biotechnol* 37:108–116. <https://doi.org/10.1016/j.nbt.2016.07.001>
- Gowda V, Shivakumar S (2014) Agrowaste-based polyhydroxyalkanoate (PHA) production using hydrolytic potential of *Bacillus Thuringiensis* IAM 12077. *Braz Arch Biol Technol* 57(1):55–61. <https://doi.org/10.1590/S1516-89132014000100009>
- Guamán LP, Oliveira-Filho ER, Barba-Ostria C, Gomez JGC, Taciro MK, da Silva LF (2018) XylA and XylB overexpression as a successful strategy for improving xylose utilization and poly-3-hydroxybutyrate production in *Burkholderia Sacchari*. *J Ind Microbiol Biotechnol* 45(3):165–173. <https://doi.org/10.1007/s10295-018-2007-7>
- Gurieff N, Lant P (2007) Comparative life cycle assessment and financial analysis of mixed culture polyhydroxyalkanoate production. *Bioresour Technol* 98(17):3393–3403. <https://doi.org/10.1016/j.biortech.2006.10.046>
- Haba E, Vidal-Mas J, Bassas M, Espuny MJ, Llorens J, Manresa A (2007) Poly 3-(hydroxyalkanoates) produced from oily substrates by *Pseudomonas Aeruginosa* 47T2 (NCBIM 40044): effect of nutrients and incubation temperature on polymer composition. *Biochem Eng J* 35(2):99–106. <https://doi.org/10.1016/j.bej.2006.11.021>
- Halami P (2008) Production of polyhydroxyalkanoate from starch by the native isolate *Bacillus cereus* CFR06. *World J Microbiol Biotechnol* 24:805–812. <https://doi.org/10.1007/s11274-007-9543-z>
- Harding KG, Dennis JS, von Blottnitz H, Harrison STL (2007) Environmental analysis of plastic production processes: comparing petroleum-based polypropylene and polyethylene with biologically-based poly- $\beta$ -hydroxybutyric acid using life cycle analysis. *J Biotechnol* 130(1):57–66. <https://doi.org/10.1016/j.jbiotec.2007.02.012>
- Huang L, Chen Z, Xiong D, Wen Q, Ji Y (2018) Oriented acidification of wasted activated sludge (WAS) focused on odd-carbon volatile fatty acid (VFA): regulation strategy and microbial community dynamics. *Water Res* 142:256–266. <https://doi.org/10.1016/j.watres.2018.05.062>

- Jeon JM, Brigham CJ, Kim YH, Kim HJ, Yi DH, Kim H, Rha CK, Sinskey AJ, Yang YH (2014) Biosynthesis of poly(3-hydroxybutyrate-co-3-hydroxyhexanoate) (P(HB-co-HHx)) from butyrate using engineered *Ralstonia eutropha*. *Appl Microbiol Biotechnol* 98(12):5461–5469. <https://doi.org/10.1007/s00253-014-5617-7>
- Kamilah H, Tsuge T, Yang TA, Sudesh K (2013) Waste cooking oil as substrate for biosynthesis of poly(3-hydroxybutyrate) and poly(3-hydroxybutyrate-co-3-hydroxyhexanoate): turning waste into a value-added product. *Malays J Microbiol* 9(1):51–59. <https://doi.org/10.21161/mjm.45012>
- Keshavarz T, Roy I (2010) Polyhydroxyalkanoates: bioplastics with a green agenda. *Curr Opin Microbiol* 13(3):321–326. <https://doi.org/10.1016/j.mib.2010.02.006>
- Kim B (2000) Production of poly(3-hydroxybutyrate) from inexpensive substrates. *Enzym Microb Technol* 27:774–777. [https://doi.org/10.1016/s0141-0229\(00\)00299-4](https://doi.org/10.1016/s0141-0229(00)00299-4)
- Kim HS, Oh YH, Jang YA, Kang KH, David Y, Ju Hyun Y, Song BK et al (2016) Recombinant *Ralstonia eutropha* engineered to utilize xylose and its use for the production of poly(3-hydroxybutyrate) from sunflower stalk hydrolysate solution. *Microb Cell Factories* 15(1):1–13. <https://doi.org/10.1186/s12934-016-0495-6>
- Koller M (2019) Biopolyesters from agro-industrial by-products for securing food safety. *Appl Food Biotechnol* 6:1–6
- Koller M, Hesse P, Bona R, Kutschera C, Atlić A, BrauneGG G (2007) Biosynthesis of high quality polyhydroxyalkanoate co- and terpolyesters for potential medical application by the archaeon *Haloferax mediterranei*. *Macromol Symp* 253:33–39. <https://doi.org/10.1002/masy.200750704>
- Koller M, Bona R, Chiellini E, Fernandes EG, Horvat P, Kutschera C, Hesse P, BrauneGG G (2008) Polyhydroxyalkanoate production from whey by *Pseudomonas hydrogenovora*. *Bioresour Technol* 99(11):4854–4863. <https://doi.org/10.1016/j.biortech.2007.09.049>
- Koller M, Maršálek L, de Sousa Dias MM, BrauneGG G (2017) Producing microbial polyhydroxyalkanoate (PHA) biopolyesters in a sustainable manner. *New Biotechnol* 37:24–38. <https://doi.org/10.1016/j.nbt.2016.05.001>
- Kourmentza C, Plácido J, Venetsaneas N, Burniol-Figols A, Varrone C, Gavala H, Reis M (2017) Recent advances and challenges towards sustainable polyhydroxyalkanoate (PHA) production. *Bioengineering* 4(2):1–43. <https://doi.org/10.3390/bioengineering4020055>
- Kourmentza C, Costa J, Azevedo Z, Servin C, Grandfils C, De Freitas V, Reis MAM (2018) *Burkholderia thailandensis* as a microbial cell factory for the bioconversion of used cooking oil to polyhydroxyalkanoates and rhamnolipids. *Bioresour Technol* 247:829–837. <https://doi.org/10.1016/j.biortech.2017.09.138>
- Kulpreecha S, Boonruangthavorn A, Meksiriporn B, Thongchul N (2009) Inexpensive fed-batch cultivation for high poly(3-hydroxybutyrate) production by a new isolate of *Bacillus megaterium*. *J Biosci Bioeng* 107(3):240–245. <https://doi.org/10.1016/j.jbiosc.2008.10.006>
- Kumar P, Kim B (2018) Valorization of polyhydroxyalkanoates production process by co-synthesis of value-added products. *Bioresour Technol* 269:544–556. <https://doi.org/10.1016/j.biortech.2018.08.120>
- Kumar P, Kim B (2019) *Paracoccus* sp. strain LL1 as a single cell factory for the conversion of waste cooking oil to polyhydroxyalkanoates and carotenoids. *Appl Food Biotechnol* 6(1):53–60. <https://doi.org/10.22037/afb.v6i1.21628>
- Kumar P, Jun HB, Kim BS (2018) Co-production of polyhydroxyalkanoates and carotenoids through bioconversion of glycerol by *Paracoccus* sp. strain LL1. *Int J Biol Macromol* 107:2552–2558. <https://doi.org/10.1016/j.ijbiomac.2017.10.147>
- Kwan TH, Hu Y, Lin CSK (2018) Techno-economic analysis of a food waste valorisation process for lactic acid, lactide and poly(lactic acid) production. *J Clean Prod* 181:72–87. <https://doi.org/10.1016/j.jclepro.2018.01.179>
- Lam W, Wang Y, Chan PL, Chan SW, Tsang YF, Chua H, Yu PHF (2017) Production of polyhydroxyalkanoates (PHA) using sludge from different wastewater treatment processes and the potential for medical and pharmaceutical applications. *Environ Technol* 38(13–14):1779–1791. <https://doi.org/10.1080/09593330.2017.1316316>

- Możejko J, Ciesielski S (2013) Saponified waste palm oil as an attractive renewable resource for mcl-polyhydroxyalkanoate synthesis. *J Biosci Bioeng* 116:485–492. <https://doi.org/10.1016/j.jbiosc.2013.04.014>
- Możejko J, Ciesielski S (2014) Pulsed feeding strategy is more favorable to medium-chain-length polyhydroxyalkanoates production from waste rapeseed oil. *Biotechnol Prog* 30(5):1243–1246. <https://doi.org/10.1002/btpr.1914>
- Możejko J, Przybyłek G, Ciesielski S (2011) Waste rapeseed oil as a substrate for medium-chain-length polyhydroxyalkanoates production. *Eur J Lipid Sci Technol* 113(12):1550–1557. <https://doi.org/10.1002/ejlt.201100148>
- Nielsen C, Rahman A, Rehman AU, Walsh MK, Miller CD (2017) Food waste conversion to microbial polyhydroxyalkanoates. *Microb Biotechnol* 10(6):1338–1352. <https://doi.org/10.1111/1751-7915.12776>
- Ntaikou I, Valencia Peroni C, Kourmentza C, Ilieva VI, Morelli A, Chiellini E, Lyberatos G (2014) Microbial bio-based plastics from olive-mill wastewater: generation and properties of polyhydroxyalkanoates from mixed cultures in a two-stage pilot scale system. *J Biotechnol* 188:138–147. <https://doi.org/10.1016/j.jbiotec.2014.08.015>
- Obruca S, Marova I, Melusova S, Mravcova L (2011) Production of polyhydroxyalkanoates from cheese whey employing *Bacillus megaterium* CCM 2037. *Ann Microbiol* 61(4):947–953. <https://doi.org/10.1007/s13213-011-0218-5>
- Obruca S, Snajdar O, Svoboda Z, Marova I (2013) Application of random mutagenesis to enhance the production of polyhydroxyalkanoates by *Cupriavidus necator* H16 on waste frying oil. *World J Microbiol Biotechnol* 29(12):2417–2428. <https://doi.org/10.1007/s11274-013-1410-5>
- Obruca S, Benesova P, Petrik S, Oborna J, Prikryl R, Marova I (2014a) Production of polyhydroxyalkanoates using hydrolysate of spent coffee grounds. *Process Biochem* 49(9):1409–1414. <https://doi.org/10.1016/j.procbio.2014.05.013>
- Obruca S, Petrik S, Benesova P, Svoboda Z, Eremka L, Marova I (2014b) Utilization of oil extracted from spent coffee grounds for sustainable production of polyhydroxyalkanoates. *Appl Microbiol Biotechnol* 98(13):5883–5890. <https://doi.org/10.1007/s00253-014-5653-3>
- Ojumu TV, Yu J, Solomon BO (2004) Production of polyhydroxyalkanoates, a bacterial biodegradable polymer. *Afr J Biotechnol* 3(1):18–24. <https://doi.org/10.5897/AJB2004.000-2004>
- Padovani G, Carozzi P, Seggiani M, Cinelli P, Vitolo S, Lazzeri A (2016) PHB-rich biomass and BioH2 production by means of photosynthetic microorganisms. *Chem Eng Trans* 49:55–60. <https://doi.org/10.3303/CET1649010>
- Pais J, Farinha I, Freitas F, Serafim LS, Martínez V, Martínez JC, Arévalo-Rodríguez M, Auxiliadora Prieto M, Reis MAM (2014) Improvement on the yield of polyhydroxyalkanoates production from cheese whey by a recombinant *Escherichia coli* strain using the proton suicide methodology. *Enzym Microb Technol* 55:151–158. <https://doi.org/10.1016/j.enzmictec.2013.11.004>
- Pakalapati H, Chang CK, Show PL, Arumugasamy SK, Lan JCW (2018) Development of polyhydroxyalkanoates production from waste feedstocks and applications. *J Biosci Bioeng* 126(3):282–292. <https://doi.org/10.1016/j.jbiosc.2018.03.016>
- Passanha P, Esteves SR, Kedia G, Dinsdale RM, Guwy AJ (2013) Increasing polyhydroxyalkanoate (PHA) yields from *Cupriavidus necator* by using filtered digestate liquors. *Bioresour Technol* 147:345–352. <https://doi.org/10.1016/j.biortech.2013.08.050>
- Patel SKS, Kumar P, Singh M, Lee JK, Kalia VC (2015) Integrative approach to produce hydrogen and polyhydroxybutyrate from biowaste using defined bacterial cultures. *Bioresour Technol* 176:136–141. <https://doi.org/10.1016/j.biortech.2014.11.029>
- Poomipuk N, Reungsang A, Plangklang P (2014) Poly- $\beta$ -hydroxyalkanoates production from cassava starch hydrolysate by *Cupriavidus* sp. KKU38. *Int J Biol Macromol* 65:51–64. <https://doi.org/10.1016/j.ijbiomac.2014.01.002>
- Povolo S, Toffano P, Basaglia M, Casella S (2010) Polyhydroxyalkanoates production by engineered *Cupriavidus necator* from waste material containing lactose. *Bioresour Technol* 101(20):7902–7907. <https://doi.org/10.1016/j.biortech.2010.05.029>
- Pramanik A, Mitra A, Arumugam M, Bhattacharyya A, Sadhukhan S, Ray A, Haldar S, Mukhopadhyay UK, Mukherjee J (2012) Utilization of vinasse for the production of

- Lareo C, Ferrari MD, Guigou M, Fajardo L, Larnaudie V, Ramírez MB, Martínez-Garreiro J (2013) Evaluation of sweet potato for fuel bioethanol production: hydrolysis and fermentation. *Springerplus* 2(1):1–11. <https://doi.org/10.1186/2193-1801-2-493>
- Lee SY, Middelberg APJ, Lee YK (1997) Poly(3-hydroxybutyrate) production from whey using recombinant *Escherichia coli*. *Biotechnol Lett* 19(10):1033–1035. <https://doi.org/10.1023/A:1018411820580>
- Lee WS, Chua ASM, Yeoh HK, Ngho GC (2014) Influence of temperature on the bioconversion of palm oil mill effluent into volatile fatty acids as precursor to the production of polyhydroxyalkanoates. *J Chem Technol Biotechnol* 89(7):1038–1043. <https://doi.org/10.1002/jctb.4197>
- Lee Y, Cho IJ, Choi SY, Lee SY (2019) Systems metabolic engineering strategies for non-natural microbial polyester production. *Biotechnol J* 14(9):1800426. <https://doi.org/10.1002/biot.201800426>
- Lemehko P, Le Fellic M, Bruzard S (2019) Production of poly(3-hydroxybutyrate-co-3-hydroxyvalerate) using agro-industrial effluents with tunable proportion of 3-hydroxyvalerate monomer units. *Int J Biol Macromol* 128:429–434. <https://doi.org/10.1016/j.ijbiomac.2019.01.170>
- Li T, Elhadi D, Chen GQ (2017) Co-production of microbial polyhydroxyalkanoates with other chemicals. *Metab Eng* 43:29–36. <https://doi.org/10.1016/j.ymben.2017.07.007>
- Liu D, Yan X, Si M, Deng X, Min X, Shi Y, Chai L (2019) Bioconversion of lignin into bioplastics by *Pandoraea* sp. B-6: molecular mechanism. *Environ Sci Pollut Res* 26(3):2761–2770. <https://doi.org/10.1007/s11356-018-3785-1>
- Locatelli GO, Finkler L, Finkler CLL (2019) Orange and passion fruit wastes characterization, substrate hydrolysis and cell growth of *Cupriavidus necator*, as proposal to converting of residues in high value added product. *Anais Da Academia Brasileira de Ciencias* 91(1):1–9. <https://doi.org/10.1590/0001-3765201920180058>
- Luo K, Pang Y, Yang Q, Wang D, Li X, Lei M, Huang Q (2019) A critical review of volatile fatty acids produced from waste activated sludge: enhanced strategies and its applications. *Environ Sci Pollut Res* 26:13984–13998. <https://doi.org/10.1007/s11356-019-04798-8>
- Marsudi S, Unno H, Hori K (2008) Palm oil utilization for the simultaneous production of polyhydroxyalkanoates and rhamnolipids by *Pseudomonas aeruginosa*. *Appl Microbiol Biotechnol* 78:955–961. <https://doi.org/10.1007/s00253-008-1388-3>
- Md Din M, Mohanadoss P, Ujang Z, van Loosdrecht M, Yunus S, Chelliapan S, Zambare V, Olsson G (2012) Development of Bio-PORec® system for polyhydroxyalkanoates (PHA) production and its storage in mixed cultures of palm oil mill effluent (POME). *Bioresour Technol* 124:208–216. <https://doi.org/10.1016/j.biortech.2012.08.036>
- Mohapatra S, Sarkar B, Samantaray DP, Daware A, Maity S, Pattnaik S, Bhattacharjee S (2017) Bioconversion of fish solid waste into PHB using *Bacillus subtilis* based submerged fermentation process. *Environ Technol* 38(24):3201–3208. <https://doi.org/10.1080/09593330.2017.1291759>
- Moita Fidalgo R, Ortigueira J, Freches A, Pelica J, Gonçalves M, Mendes B, Lemos P (2014) Bio-oil upgrading strategies to improve PHA production from selected aerobic mixed cultures. *New Biotechnol* 31:297–307. <https://doi.org/10.1016/j.nbt.2013.10.009>
- Montiel Corona V, Revah S, Morales M (2015) Hydrogen production by an enriched photoheterotrophic culture using dark fermentation effluent as substrate: effect of flushing method, bicarbonate addition, and outdoor–indoor conditions. *Int J Hydrog Energy* 40:9096–9105. <https://doi.org/10.1016/j.ijhydene.2015.05.067>
- Montiel Corona V, Le Borgne S, Revah S, Morales M (2017) Effect of light-dark cycles on hydrogen and poly- $\beta$ -hydroxybutyrate production by a photoheterotrophic culture and *Rhodobacter capsulatus* using a dark fermentation effluent as substrate. *Bioresour Technol* 226:238–246. <https://doi.org/10.1016/j.biortech.2016.12.021>

- polyhydroxybutyrate by *Haloarcula marismortui*. *Folia Microbiol* 57(1):71–79. <https://doi.org/10.1007/s12223-011-0092-3>
- RamKumar Pandian S, Deepak V, Kalishwaralal K, Rameshkumar N, Jeyaraj M, Gurunathan S (2010) Optimization and fed-batch production of PHB utilizing dairy waste and sea water as nutrient sources by *Bacillus megaterium* SRKP-3. *Bioresour Technol* 101(2):705–711. <https://doi.org/10.1016/j.biortech.2009.08.040>
- Rebocho AT, Pereira JR, Freitas F, Neves LA, Alves VD, Sevrin C, Grandfils C, Reis MAM (2019) Production of medium-chain length polyhydroxyalkanoates by *Pseudomonas citronellolis* grown in apple pulp waste. *Appl Food Biotechnol* 6(1):71–82. <https://doi.org/10.22037/afb.v6i1.21793>
- Reddy CSK, Ghai R, Rashmi, Kalia VC (2003) Polyhydroxyalkanoates: an overview. *Bioresour Technol* 87(2):137–146. [https://doi.org/10.1016/S0960-8524\(02\)00212-2](https://doi.org/10.1016/S0960-8524(02)00212-2)
- Revelles O, Beneroso D, Menéndez JA, Arenillas A, García JL, Prieto MA (2017) Syngas obtained by microwave pyrolysis of household wastes as feedstock for polyhydroxyalkanoate production in *Rhodospirillum rubrum*. *Microb Biotechnol* 10(6):1412–1417. <https://doi.org/10.1111/1751-7915.12411>
- Riedel SL, Jahns S, Koenig S, Bock MCE, Brigham CJ, Bader J, Stahl U (2015) Polyhydroxyalkanoates production with *Ralstonia eutropha* from low quality waste animal fats. *J Biotechnol* 214:119–127. <https://doi.org/10.1016/j.jbiotec.2015.09.002>
- Rodríguez-Carmona E, Bastida J, Manresa A (2012) Utilization of agro-industrial residues for poly(3-hydroxyalkanoate) production by *Pseudomonas aeruginosa* 42A2 (NCIMB 40045): optimization of culture medium. *J Am Oil Chem Soc* 89(1):111–122. <https://doi.org/10.1007/s11746-011-1897-6>
- Rodríguez-Perez S, Serrano A, Pantión AA, Alonso-Fariñas B (2018) Challenges of scaling-up PHA production from waste streams. A review. *J Environ Manag* 205:215–230. <https://doi.org/10.1016/j.jenvman.2017.09.083>
- Romanelli MG, Povoio S, Favaro L, Fontana F, Basaglia M, Casella S (2014) Engineering *Delftia acidovorans* DSM39 to produce polyhydroxyalkanoates from slaughterhouse waste. *Int J Biol Macromol* 71:21–27. <https://doi.org/10.1016/j.ijbiomac.2014.03.049>
- Sabapathy PC, Devaraj S, Kathirvel P (2017) *Parthenium hysterophorus*: low cost substrate for the production of polyhydroxyalkanoates. *Curr Sci* 112(10):2106–2111. <https://doi.org/10.18520/cs/v112/i10/2106-2111>
- Sabapathy PC, Devaraj S, Parthipan A, Kathirvel P (2019) Polyhydroxyalkanoate production from statistically optimized media using rice mill effluent as sustainable substrate with an analysis on the biopolymer's degradation potential. *Int J Biol Macromol* 126:977–986. <https://doi.org/10.1016/j.ijbiomac.2019.01.003>
- Sahoo J, Patil P, Verma A, Lodh A, Khanna N, Prasad R, Pandit S, Fosso-Kankeu E (2021) Biochemical aspects of syngas fermentation. In: Prasad R, Singh J, Kumar V, Upadhyay CP (eds) Recent developments in microbial technologies. Springer Nature, Singapore, pp 395–424
- Salgaonkar BB, Mani K, Bragança JM (2019) Sustainable bioconversion of cassava waste to poly(3-hydroxybutyrate-co-3-hydroxyvalerate) by Halogeometricum borinquense strain E3. *J Polym Environ* 27(2):299–308. <https://doi.org/10.1007/s10924-018-1346-9>
- Saranya Devi E, Vijayendra SVN, Shamala TR (2012) Exploration of rice bran, an agro-industry residue, for the production of intra- and extra-cellular polymers by *Sinorhizobium meliloti* MTCC 100. *Biocatal Agric Biotechnol* 1(1):80–84. <https://doi.org/10.1016/j.bcab.2011.08.014>
- Schmid MT, Song H, Raschbauer M, Emerstorfer F, Omann M, Stelzer F, Neureiter M (2019) Utilization of desugared sugar beet molasses for the production of poly(3-hydroxybutyrate) by halophilic *Bacillus megaterium* uyuni S29. *Process Biochem* 86:9–15. <https://doi.org/10.1016/j.procbio.2019.08.001>
- Shamala TR, Vijayendra SVN, Joshi GJ (2012) Agro-industrial residues and starch for growth and co-production of polyhydroxyalkanoate copolymer and  $\alpha$ -amylase by *Bacillus* sp. CFR-67. *Braz J Microbiol* 43(3):1094–1102. <https://doi.org/10.1590/S1517-83822012000300036>
- Song JH, Jeon CO, Choi MH, Yoon SC, Park W (2008) Polyhydroxyalkanoate (PHA) production using waste vegetable oil by *Pseudomonas* sp. strain DR2. *J Microbiol Biotechnol* 18(8):1408–1415

- Sreekanth MS, Vijayendra SVN, Joshi GJ, Shamala TR (2013) Effect of carbon and nitrogen sources on simultaneous production of  $\alpha$ -amylase and green food packaging polymer by *Bacillus* sp. CFR 67. *J Food Sci Technol* 50(2):404–408. <https://doi.org/10.1007/s13197-012-0639-6>
- Strazzerza G, Battista F, Garcia NH, Frison N, Bolzonella D (2018) Volatile fatty acids production from food wastes for biorefinery platforms: a review. *J Environ Manag* 226:278–288. <https://doi.org/10.1016/j.jenvman.2018.08.039>
- Takisawa K, Ooi T, Matsumoto K'i, Kadoya R, Taguchi S (2017) Xylose-based hydrolysate from eucalyptus extract as feedstock for poly(lactate-co-3-hydroxybutyrate) production in engineered *Escherichia coli*. *Process Biochem* 54:102–105. <https://doi.org/10.1016/j.procbio.2016.12.019>
- Tamang P, Banerjee R, Köster S, Nogueira R (2019) Comparative study of polyhydroxyalkanoates production from acidified and anaerobically treated brewery wastewater using enriched mixed microbial culture. *J Environ Sci (China)* 78:137–146. <https://doi.org/10.1016/j.jes.2018.09.001>
- Tokimoto T, Kawasaki N, Nakamura T, Akutagawa J, Tanada S (2005) Removal of lead ions in drinking water by coffee grounds as vegetable biomass. *J Colloid Interface Sci* 281(1):56–61. <https://doi.org/10.1016/j.jcis.2004.08.083>
- Tsang YF, Kumar V, Samadar P, Yang Y, Lee J, Ok YS, Song H, Kim KH, Kwon EE, Jeon YJ (2019) Production of bioplastic through food waste valorization. *Environ Int* 127:625–644. <https://doi.org/10.1016/j.envint.2019.03.076>
- Urbina L, Wongsirichot P, Corcuera MÁ, Gabilondo N, Eceiza A, Winterburn J, Retegi A (2018) Application of cider by-products for medium chain length polyhydroxyalkanoate production by *Pseudomonas putida* KT2440. *Eur Polym J* 108:1–9. <https://doi.org/10.1016/j.eurpolymj.2018.08.020>
- Vastano M, Pellis A, Immirzi B, Dal Poggetto G, Malinconico M, Sannia G, Guebitz GM, Pezzella C (2017) Enzymatic production of clickable and PEGylated recombinant polyhydroxyalkanoates. *Green Chem* 19(22):5494–5504. <https://doi.org/10.1039/c7gc01872j>
- Vastano M, Corrado I, Sannia G, Solaiman DKY, Pezzella C (2019) Conversion of no/low value waste frying oils into biodiesel and polyhydroxyalkanoates. *Sci Rep* 9(1):1–8. <https://doi.org/10.1038/s41598-019-50278-x>
- Vega-Castro O, Contreras-Calderon J, León E, Segura A, Arias M, Pérez L, Sobral PJA (2016) Characterization of a polyhydroxyalkanoate obtained from pineapple peel waste using *Ralstonia eutropha*. *J Biotechnol* 231:232–238. <https://doi.org/10.1016/j.biotech.2016.06.018>
- Venkateswar Reddy M, Venkata Mohan S (2012) Influence of aerobic and anoxic microenvironments on polyhydroxyalkanoates (PHA) production from food waste and acidogenic effluents using aerobic consortia. *Bioresour Technol* 103(1):313–321. <https://doi.org/10.1016/j.biortech.2011.09.040>
- Verlinden RAJ, Hill DJ, Kenward MA, Williams CD, Piotrowska-Seget Z, Radecka IK (2011) Production of polyhydroxyalkanoates from waste frying oil by *Cupriavidus necator*. *AMB Express* 1(1):1–8. <https://doi.org/10.1186/2191-0855-1-11>
- Wen Q, Ji Y, Hao Y, Huang L, Chen Z, Sposob M (2018) Effect of sodium chloride on polyhydroxyalkanoate production from food waste fermentation leachate under different organic loading rate. *Bioresour Technol* 267:133–140. <https://doi.org/10.1016/j.biortech.2018.07.036>
- Wijeyekoon S, Carere CR, West M, Nath S, Gapes D (2018) Mixed culture polyhydroxyalkanoate (PHA) synthesis from nutrient rich wet oxidation liquors. *Water Res* 140:1–11. <https://doi.org/10.1016/j.watres.2018.04.017>
- Yang TH, Jung YK, Kang HO, Kim TW, Park SJ, Lee SY (2011) Tailor-made type II *Pseudomonas* PHA synthases and their use for the biosynthesis of polylactic acid and its copolymer in recombinant *Escherichia coli*. *Appl Microbiol Biotechnol* 90(2):603–614. <https://doi.org/10.1007/s00253-010-3077-2>
- Yu J, Stahl H (2008) Microbial utilization and biopolyester synthesis of bagasse hydrolysates. *Bioresour Technol* 99(17):8042–8048. <https://doi.org/10.1016/j.biortech.2008.03.071>